Progress in the Chemistry of Organic Natural Products

A. Douglas Kinghorn · Heinz Falk · Simon Gibbons · Yoshinori Asakawa · Ji-Kai Liu · Verena M. Dirsch *Editors*

116

Progress in the Chemistry of Organic Natural Products

Springer

Progress in the Chemistry of Organic Natural Products

Alvaro Viljoen, Department of Pharmaceutical Sciences, Tshwane University of Technology, Pretoria, South Africa

Yang Ye, State Key Laboratory of Drug Research and Natural Products Chemistry Department, Shanghai Institute of Materia Medical, Shanghai, China

The volumes of this classic series, now referred to simply as "Zechmeister" after its founder, Laszlo Zechmeister, have appeared under the Springer Imprint ever since the series' inauguration in 1938. It is therefore not really surprising to find out that the list of contributing authors, who were awarded a Nobel Prize, is quite long: Kurt Alder, Derek H.R. Barton, George Wells Beadle, Dorothy Crowfoot-Hodgkin, Otto Diels, Hans von Euler-Chelpin, Paul Karrer, Luis Federico Leloir, Linus Pauling, Vladimir Prelog, with Walter Norman Haworth and Adolf F.J. Butenandt serving as members of the editorial board.

The volumes contain contributions on various topics related to the origin, distribution, chemistry, synthesis, biochemistry, function or use of various classes of naturally occurring substances ranging from small molecules to biopolymers.

Each contribution is written by a recognized authority in the field and provides a comprehensive and up-to-date review of the topic in question. Addressed to biologists, technologists, and chemists alike, the series can be used by the expert as a source of information and literature citations and by the non-expert as a means of orientation in a rapidly developing discipline.

All contributions are listed in PubMed.

More information about this series at http://www.springer.com/series/10169

A. Douglas Kinghorn · Heinz Falk ·
Simon Gibbons · Yoshinori Asakawa · Ji-Kai Liu ·
Verena M. Dirsch
Editors

Progress in the Chemistry of Organic Natural Products

Volume 116

With contributions by

Maggie M. Reddy · Laurence Jennings · Olivier P. Thomas

Karina L. Silva-Brandão · André V. L. Freitas ·
Márcio Zikán Cardoso · Rodrigo Cogni ·
Ana Beatriz Barros de Morais

René Escobedo-González · Pablo Mendoza · María Inés Nicolás-Vázquez · Maricarmen Hernández-Rodríguez · Joel Martínez · René Miranda Ruvalcaba

Nguyen Thi Thuy Linh · Ninh The Son ·
Nguyen Thi Thu Ha · Nguyen Thanh Tra · Le Thi Tu Anh ·
Sibao Chen · Nguyen Van Tuyen

Nguyen Thi Thuy Linh · Ninh The Son

Springer

Editors
A. Douglas Kinghorn
College of Pharmacy
Ohio State University
Columbus, OH, USA

Heinz Falk
Institute of Organic Chemistry
Johannes Kepler University
Linz, Austria

Simon Gibbons
School of Pharmacy
University of East Anglia
Norwich, UK

Yoshinori Asakawa
Faculty of Pharmaceutical Sciences
Tokushima Bunri University
Tokushima, Japan

Ji-Kai Liu
School of Pharmaceutical Sciences
South-Central University for Nationalities
Wuhan, China

Verena M. Dirsch
Department of Pharmaceutical Sciences
University of Vienna
Vienna, Wien, Austria

ISSN 2191-7043 ISSN 2192-4309 (electronic)
Progress in the Chemistry of Organic Natural Products
ISBN 978-3-030-80559-3 ISBN 978-3-030-80560-9 (eBook)
https://doi.org/10.1007/978-3-030-80560-9

This Springer imprint is published by the registered company Springer Nature Switzerland AG
The registered company address is: Gewerbestrasse 11, 6330 Cham, Switzerland

Contents

Marine Biodiscovery in a Changing World

Maggie M. Reddy, Laurence Jennings, and Olivier P. Thomas

Contents

M. M. Reddy · L. Jennings · O. P. Thomas (✉)
Marine Biodiscovery, School of Chemistry and Ryan Institute, NUI Galway, University Road, Galway H91TK33, Ireland
e-mail: olivier.thomas@nuigalway.ie

M. M. Reddy
e-mail: mageshneem.reddy@nuigalway.ie

L. Jennings
e-mail: laurence.jennings@nuigalway.ie

A. D. Kinghorn, H. Falk, S. Gibbons, Y. Asakawa, J.-K. Liu, V. M. Dirsch (eds.),
Progress in the Chemistry of Organic Natural Products 116,
https://doi.org/10.1007/978-3-030-80560-9_1

1 Introduction

The marine environment represents an untapped reservoir of bioresources that play an increasing role in the wellbeing of our societies as stated in the emerging field of Blue Growth [1]. Several maritime countries have identified the potential of marine bioresources for the development of their societies. Together with the exploration of our oceans, the most lucrative application was soon identified as drug discovery and the term "marine pharmacology" was used in the late 1960s [2]. At around the same time, the term "bioprospecting," also known as "biodiversity prospecting," was used to describe the exploration of natural resources in the search for biomolecules of commercial value.

The term "biodiscovery" was only defined later in the early 2000s and used specifically in Australia and New Zealand, where it replaced "bioprospecting," as this term was often associated with biopiracy. The creation of a biodiscovery act in 2004 in Australia, Queensland, set the scene for a broader use of this term, especially, for marine exploration. Investigations in this area quickly extended to other maritime countries including but not limited to South Korea, Japan, Italy, Norway, Germany, and the United Kingdom (Scotland). Significant academic national efforts in China, the USA, and Europe, coupled with private initiatives like Pharmamar in Spain have contributed to the collection of marine macro- and microorganisms from several regions around the world. The main objective was to discover new and high-value drugs from these organisms, with a special focus on anticancer agents [3–5]. Marine biodiscovery has focused largely on marine invertebrates, but this has recently shifted toward microorganisms that represent a much more diverse group, and thus opening new avenues for biotechnology and an efficient producer of bioactive metabolites [6].

Some lessons have been learnt from the early development of this field, and some recent changes should prompt us to propose new directions in the field of marine biodiscovery:

- the decreasing rate of discovery of new chemical entities among marine natural products;
- the decreasing number of taxonomists specializing in marine organisms;
- climate change especially affecting the oceans;
- accelerated loss in biodiversity;
- increasing inequalities, especially for developing countries, which are often the richest in terms of marine biodiversity; and
- the emergence of new pandemics in the context of public health.

In this contribution, we will detail the construction of a National Marine Biodiscovery Laboratory in Ireland that has been developed, by considering some or all of these changes. Key modifications have been applied to our first initiative to take into account most of the abovementioned changes [7, 8]. First, the construction of regional marine biomaterial repositories can mitigate some of these recent changes. Then, the development of new technologies for the screening and dereplication of

the biomaterials will also contribute to address some of the other issues. Finally, we will propose some important changes that could make the term marine biodiscovery more inclusive and central for the development of the three pillars of sustainability: the blue economy, environmental challenges, and also social impacts.

2 Exploration of Marine Biodiversity and Establishing Biomaterial Repositories

All key indicators point to an unequivocal global decline in biodiversity across most terrestrial [9] and marine [10, 11] organisms. Anthropogenic activities, such as over-population and habitat destruction, are the leading factors responsible for this unprecedented loss of biodiversity. This is heightened further by unsustainable resource use and climate change [12]. The overall negative trend in biodiversity has gained momentum over the past few decades and is projected to continue in a downward trajectory [13] in the absence of global intervention. Drastic changes in current agricultural practices and fishing methods or ambitious conservation efforts are urgently needed if humanity is to reverse current biodiversity trends by 2050 [9]. However, further mitigation strategies are also needed and will require innovative solutions and synergistic efforts from industries, governments, and scientists.

Safeguarding against biodiversity loss goes beyond immediate conservation goals and human benefit, but may also be important for tackling future climate-related challenges [14–16]. Biodiversity consistently has represented a source of food, fertilizer, medicine, cosmetics, and textiles for human society. For example, traditional medicine was integral to ancient societies and was used to treat various ailments and disease [17, 18]. Interestingly, naturally inspired drugs remain important today and have greatly benefitted from advances in natural product chemistry and drug discovery, including from the marine environment [5].

Bioactive compounds originating from the ocean are opening new avenues for the bioeconomy due to their unique structures and bioactivities. Similar to terrestrial plants, marine macro- and especially microorganisms, have been shown to produce highly diverse biomolecules usually absent in the terrestrial environment [19, 20]. However, despite several decades of exploration in marine biodiscovery, only a few groups of interest are well studied, such as bacteria, fungi, sponges, tunicates, and octocorals, and even fewer (Porifera, Chordata, Mollusca) account for marine-derived or marine-inspired drugs available in the market today [21]. Interestingly, marine-derived drugs have exponentially grown in the last 15 years, showing potential for future research in this field. Although it may be possible to discover new compounds with new applications from the same organism [22], or through the application of new methods, exploration of novel biodiversity ecoregions or targeting non-model organisms will more likely result in the discovery of new natural products.

Expanding chemical and biological screening efforts beyond model organisms, however, will depend on access to a wide range of biodiversity samples that can be

difficult, costly, and time consuming, especially for marine organisms [6]. Research expeditions typically focus on specific groups of interest [23], and those investing in wider sampling efforts are understandably confined to specific geographic regions. The wealth of biodiversity samples collected during these costly research expeditions are then retained in university-based or private biodiversity collections and are only used to address specific research questions locally. Another major drawback of one-off research expeditions is the possibility of overlooking transient or rare species with potentially new chemical compounds. Taken together, and on considering additional limitations, such as stricter permit regulations, limited funding for exploratory research missions, and a lack of research visibility, it is imperative that we rethink our current approach for the collection, storage, and utilization of biodiversity samples for marine biodiscovery.

2.1 Definitions and Examples

Biodiversity collections broadly encompass preserved, living, or digital biodiversity collections and may focus on specific taxa or specific geographic regions and represent publicly accessible or private collections. Natural History Collections (NHC), Biorepositories or Biobanks, and university-based or private collections exist within the broad concept of biodiversity collections. Natural History Collections are probably the best-known example of a biodiversity collection and comprise preserved collections such as those housed in herbariums and museums, and living collections such as botanical gardens, zoos, aquaria, and tissue/culture collections [24]. The recent emergence of digital repositories also adds to the broader concept of NHCs and may be associated with physical specimens, e.g., NMNH Biorepository, GBIF [25], and IDigBio [26], or based on observational data (e.g., INaturalist), and may account for global inventories, e.g., GBIF, inventories for specific groups, e.g., AlgaeBase or The World Porifera Database or regional inventories (e.g., NIST). In general, biodiversity collections have gained far more visibility from digitization, reaching a much wider user base than previously imagined [15].

Historically, natural history collections, such as herbariums and museums, primarily have housed "type specimens" and served as a record of both extant and extinct biodiversity. However, associated specimen details have since been used to address a broad range of biological, ecological, biogeography, and evolutionary questions [24]. It has also been used to assess changes in biodiversity patterns over time or to detect and track invasive species [27]. Natural History Collections contain a wealth of knowledge that has more recently been disseminated through public outreach and educational programs [28]. However, the main purpose of NHCs remains the collection and storage of biodiversity specimens. Although voucher specimens may be available on loan, access to such specimens is usually difficult and often require non-invasive utilization of samples, which usually are not suitably preserved for applied research such as genomic, biotechnological/bioprospecting, or biomedical research.

Biorepositories essentially extend the function of NHCs and are involved mainly in the collection, processing, storage, and distribution of biospecimens or derived biomaterials for scientific research, with a large focus on applied research. Biorepositories were developed over the last few decades in response to a rising demand for high-quality samples for "-omic" sciences [29, 30]. Although the terms "biobanks" and "biorepositories" are often used interchangeably, it is important to note that a biobank is a type of biorepository. Biobanks were developed with a central focus on human-derived samples and associated information for biomedical research [31]. There are numerous different types of biobanks, each designed for a specific application, e.g., cancer or HIV/AIDS research and generally covering a broad geographic range. Even though the term biobank is largely reserved for human-derived samples, it also has been adopted for plant (seed banks), animal, microbial, and environmental collections.

More commonly, however, plant, animal (excluding humans), or microbial biospecimens and derived biomaterials are typically held in biorepositories and may comprise preserved (e.g., NIST) or living collections (Roscoff Culture Collection). Biorepositories either target a broad range of taxa from a specific geographic region (e.g., GEC BioRepository) or habitat (e.g., MarBank), or focus on a particular group (e.g., microorganisms: Rosscoff Culture Collection). More recently, there has been a major focus on building marine genomic biorepositories, mostly in North and Central America to ensure the preservation of biodiversity in the face of a rapidly changing world. Examples of these include the GEC BioRepository in Guam, the Ocean Genome Legacy Center, the NIST Biorepository, Genomic Biorepository of Coastal Marine Species in Estero Padre Ramos and Estero Real, Nicaragua [32], the Smithsonian, MarBank in Norway [33], and the NEON Biorepository at Arizona State University. In all cases, biorepositories operate at a national level and cater to specific research needs, e.g., genomic studies. Despite the huge benefits associated with these biorepositories, in some cases, a lack of funding and support, especially in developing countries, has limited their continuation [31].

2.2 Access and Benefit Sharing

Biodiversity is overwhelmingly concentrated in tropical regions of the world, which also corresponds with the locations of many developing nations. Furthermore, the marine environment of several maritime developing nations remains relatively unexplored. There is of course enormous potential for marine biodiversity and biodiscovery research in these regions, as they often host a wide range of undocumented taxonomic diversity, and hence an untapped source of potential new natural products [6].

All coastal countries have sovereignty and exclusive access to marine resources within 200 nautical miles of their coastline, regions referred to as their "Exclusive

Economic Zone." Access and utilization of samples, particularly in coastal developing nations, raises an ethical concern for access and benefit sharing. The "Convention on Biological Diversity" later supplemented by the "Nagoya Protocol on Access to Genetic Resources and the Fair and Equitable Sharing of Benefits Arising from their Utilization" were drafted to address concerns regarding the misappropriation of marine and other genetic resources. The resultant Nagoya Protocol was implemented in 2014 and is a legally binding agreement signed by 128 member states as of 2020. In cases where requirements for the "United Nations Convention on the Law of the Sea" (350 nautical miles) and the Nagoya Protocol (250 nautical miles) overlap, both conventions come into effect.

In summary, access and benefit sharing broadly encourage fair access and utilization of resources between nations, with a strong focus on shared benefits among developing and developed nations. In addition to monetary benefits, non-monetary benefits which may include traditional knowledge, research outputs, or building research capacity and transferring technology within providing countries are also considered [15]. Interestingly, Schindel and Cook [15] also discuss shared risks in addition to shared benefits. There are two main but different aspects of the Nagoya Protocol, which permits for (1) access and (2) utilization of samples [34]. Collection and access to samples typically involve local partners and traditional knowledge and begin with "Mutually Agreed Terms" negotiated between "providers" and "users." It outlines detailed access and benefit sharing, "Material Transfer Agreements," and third-party access granted for interested parties not originally involved in the mutually agreed terms agreement. Material Transfer Agreements (MTAs) should be approached in two phases, first, by agreement on research terms, and then, subsequent agreement terms for commercialization. Material Transfer Agreements are required before users request a "Prior Informed Consent" which is typically granted by competent authorities of individual member states, for example, the Ministry of Fisheries. It is the joint responsibility of "providers" and "users" to ensure that all necessary domestic permits are obtained, and national regulations respected. Additionally, coastal countries need to be informed of planned marine research activities 6 months in advance. The resultant "Prior Informed Consent" is proof that resources were obtained legally [35]. Although not yet widely implemented, correctly performed "Prior Informed Consent" may become a requirement for scientific publication in the future [34]. Non-compliance with access and benefit sharing may result in fines or interruption and even cessation of research and commercialization.

2.3 Field Identification and Taxonomy

A major challenge in collecting, characterizing, and utilizing biodiversity samples is the identification of specimens. Species names are tags and as such contain important biological, ecological, and evolutionary information. The accurate identification of specimens is therefore fundamental to subsequent research but depends on available taxonomic information and expertise. New species are defined (species delimitation)

based on the available information and the application of available methods or tools [36–38], and assigned names (nomenclature) following various naming conventions. As a result, taxa are commonly re-assigned to more appropriate groups as new information becomes available. Species names and their classification are therefore in a constant flux and continue to evolve, as do the species themselves.

It is important to remember that species identification and species characterization are fundamentally different. Species are characterized based on shared traits or similarity and identifiable by a set of diagnostic traits using different species concepts as working hypotheses. The Morphological Species Concept, Reproductive Species Concept, and more recently, the Evolutionary or Phylogenetic Species Concept are among the most widely applied, each relying on different types of data and subject to various advantages and limitations [39]. Most taxonomists today generally apply a unified species concept. Different species concepts are still widely debated and this has been referred to as "the species problem" by Ernest Mayr. This long-standing debate reflects the notorious difficulty associated with certain species.

A broad spectrum of diagnostic traits is found commonly among individuals of a single species and therefore species boundaries (species delimitation) needs to be carefully considered. New species are discovered against this background and are described when sufficient evidence supports their placement as distinct entities. Although there are no rules in taxonomy, there are rules when naming (nomenclature) a species. In recent years, there has been a strong move toward integrative taxonomy, which is intended to reduce the subjectivity often involved with species delimitation. For this approach, multiple lines of evidence, such as morphology/anatomy, ecological/biological, DNA, and DNA-based algorithms, commonly are used more than a single method. More recently, metabolomics, which provides a unique metabolic fingerprint, has also been used as an additional line of evidence in integrative taxonomy and has been successful in identifying taxonomic ambiguities [40, 41] and defining species [42].

Taxonomy is fundamental in terms of subsequent species identification. However, this may be challenging for a large majority of marine organisms as they often represent understudied groups. Species identification may be even more challenging when blurred species boundaries, such as overlapping diagnostic traits or cryptic taxa, are encountered. The problem of proper species identification is hampered further when field identifications are confused with species identification. Field names are commonly assigned to taxa based on visual inspection of the overall gross morphology and distinctiveness. However, field identifications based on morphology can be misleading, and typically require further verification using microscopy or DNA [43]. This is particularly true for sister species of structurally less complex organisms, such as seaweeds or sponges, which superficially resemble one another.

Deoxyribonucleic acid barcoding was developed as a fast, cost-effective, and standardized method for species identification [44]. The cytochrome oxidase subunit I is utilized commonly as the marker of choice for barcoding, but different DNA barcodes or a set of DNA barcodes may be preferred for different groups. Reliable identification based on DNA barcoding depends on comprehensive reference libraries against which unknown specimens are identified based on similarity [45]. Although not

intended for this purpose, DNA barcoding has also been used for species discovery. It is important to remember that even though DNA barcoding may expedite the identification of new species, it does not replace alpha taxonomy and taxonomic expertise that are essential for species descriptions.

Accurate identification of taxa is fundamental to marine biodiscovery/natural product chemistry for several reasons [6]. First, it may be informative for prioritizing taxa for marine biodiscovery, as similar taxa are known to produce similar chemical analogs [46]. Accurate species identification is also critical at the early stages of drug discovery, as recollections of species may be required for further testing. Although chemical synthesis of products may limit the need for recollections thereafter, this procedure cannot be used routinely to synthesize complex chemical structures [47] of alginates for example. Last, misapplied names and hidden diversity could lead to misleading species distributions and mask potentially interesting regions for marine biodiscovery exploration.

In addition to accurate identification of taxa, fully understanding the biology and ecology of species is also important for marine biodiscovery and natural product chemistry. While shared common metabolic pathways can be a more significant predictor at higher order phylogenetic ranks, habitat or ecological diversity are believed to evoke certain secondary metabolic pathways and account for similar bioactivity among similar genera or species [19].

2.4 The Irish Marine Biomaterial Repository

The Irish coast extends for roughly 3,000 km, bounded by the Irish Sea to the east and the north-east Atlantic Ocean to the west. This dynamic coastline is richly diverse in marine life and has a long history of marine exploitation with seaweed utilization dating back to the Middle Ages. However, the exploitation and use of marine resources have remained largely unchanged since then, despite enormous potential applications.

The Irish Marine Biomaterial Repository (IMBR) has been developed recently, with the aim of bridging the gap between research, industry, and conservation. The central tenet of the biorepository is to provide a focal point for shared bioresources. The IMBR focuses on, but is not limited to, the collection, processing, storage, and distribution of coastal macro-marine organisms with a main priority on the preparation of chromatographic fractions ready to be used for biological and chemical screening. It is organized according to a data management plan centered around a web database that allow the recording and tracking of all the data present in the IMBR [48]. Voucher specimens associated with subsamples for DNA, microscopy, and biomass are prepared following best practices [31] (Fig. 1). Careful characterization of morphological, genetic, and chemical profiles are generated as a baseline for future comparison purposes.

The IMBR endeavors to provide accurate species identification from a combined morphological and DNA approach by working with taxonomic experts, especially

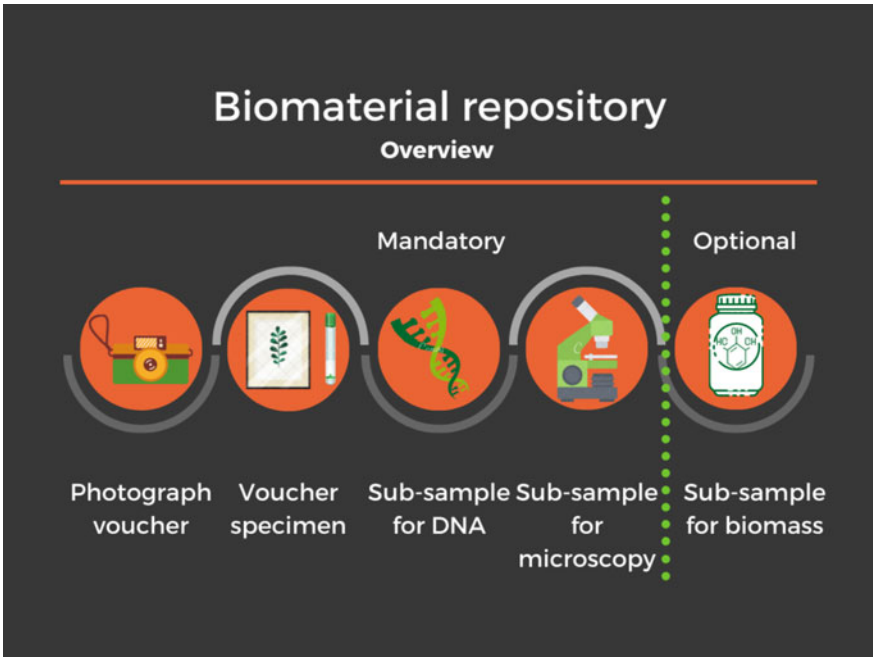

Fig. 1 The Irish Marine Biomaterial Repository (IMBR)

when cryptic taxa are encountered. Proper taxonomic identification of species may also reveal related organisms of interest and will aid in prioritizing taxa for marine biodiscovery. The need for accurate species identification is crucial to all research and is particularly important for marine biodiscovery research, as a growing body of evidence suggests that different species may produce structurally different bioactive compounds with different applications [22]. However, as mentioned earlier, accurate identification depends on the available taxonomic information, which is often poorly documented for the large majority of marine organisms, particularly in understudied regions. For this reason, voucher specimens will remain permanently in the collection and will be revised continually to reflect updated taxonomic changes. All specimens will also be associated with a DNA barcode that will facilitate the process and may be used as a unique identifier until taxonomic research on specific groups is carried out. This will avoid the waiting time for species to be described as new, which may take a few decades in some cases [49]. Taxonomic changes will be made and communicated with end-users of the IMBR. All available specimens and associated metadata, including in situ and field photographs, are available online in a standardized and open access format. Future developments such as providing access of subsamples to interested users (researchers or the industry) for further study remain to be developed, as does testing the viability of chromatographic fractions or extracts of organisms for long-term storage. Although some challenges and additional future work remain,

this pilot-scale project offers enormous opportunities for future development when applied to different regions of the world.

2.5 Challenges and Opportunities for Biorepositories

In terms of the cost and benefit of biorepositories, it is recognized that establishing and maintaining a biorepository will require initial capital investment (facilities), capacity (staff), and time (curation). However, investing in these costs today may yield better returns for the future and could mean a trade-off between costly research expeditions and maintaining redundant collections. Below, are discussed important benefits that the authors believe marine biorepositories provide, and hence may further justify the costs and risks associated with maintaining such biodiversity collections.

Marine biorepositories, such as the IMBR initiative, are intended to foster collaboration between research sectors (academia, industries) that would otherwise work in isolation or in parallel. For academic researchers, access to a broad range of samples may be highly beneficial for students and postdoctoral fellows working on time-limited projects, which require extensive spatial and temporal comparisons. As a result, it may also lead to achieving broader study aims or guide a better study design. Furthermore, linking data (DNA, morphology, chemistry) originating from a single specimen will promote robust and accurate results, especially considering the rampant misidentification of specimens and the misapplication of species names. Another major benefit of marine biorepositories is extending the longevity and value of samples beyond immediate study goals. Specimen donations from previous projects or from private or university-based biodiversity collections are at risk of being lost when researchers relocate or retire. These collections could add to a growing and comprehensive knowledge base and promote easy access to samples and wider availability of associated information if donated to open access biorepositories.

2.5.1 Working with Natural History Collections

Biorepositories should be viewed as being auxiliary rather than a substitute for natural history collections, as each biodiversity collection functions with different but complementary goals. For example, long-term or baseline data from natural history collections may be supplemented with new collections from biorepositories. In some instances, natural history collections have recognized the changing needs of modern-day research, including host museum-based biorepositories, e.g., the Smithsonian [30]. Clearly, similar efforts will benefit greatly natural history collections at large, but these are unlikely to be achieved for many natural history collections due to escalating challenges related to limited funding and lack of personnel. Given the complementary functions of natural history collections and biorepositories, it is

believed that it could be mutually beneficial for these facilities to work together for shared funding, expertise, and facilities.

The value of natural history collections and biorepositories has received considerable attention recently in the light of emerging infectious diseases. Holistic sampling is the collection of either host and parasite collections, or extended specimen details, which are among the eminent changes needed for the next generation of biodiversity collections [15]. This, complemented with a range of chromatographic fractions ready-to-be tested against new infectious diseases, could prevent or alleviate the damaging social and economic losses incurred by infectious diseases such as the current COVID-19 pandemic. However, these chemical and biological libraries can also be used to resolve other biodiversity-related issues. The impact of plastic pollution is well documented in the literature, but far fewer studies propose solutions to this growing problem. The utilization and convenience of single-use products is so pervasive today that changing the mindset of society may take time. However, finding alternative natural sources to plastics, such as biopolymers, could be an effective intermediate solution until drastic paradigm shifts in societal attitudes occur.

2.5.2 Biodiscovery and Conservation

If biodiversity is required as a source of biomolecules to cope with future challenges, then intuitively our future initiatives should be developed with sustainability in mind. In the short term, this could be achieved by targeting species with high biomasses and not at risk of extinction or species amenable to aquaculture (see the species prioritization list below). Wild-harvested species with commercial applications should also be coupled with monitoring and environmental impact assessments. Identifying regions of high biodiversity and potential application could also be used to advise in marine-protected areas for planning purposes and to encourage the integration of such data from biodiscovery. Planning in marine-protected areas will therefore not only consider environmental and social sustainability goals but also include economic sustainability.

2.5.3 Addressing Social Challenges

Bioproperty and shared derived benefits from bioresources remain a major concern today. At present, marine biodiscovery may be carried out with little to no involvement by participants from the providing member states where the samples are collected, typically in developing nations. This is understandable as the availability of facilities and expertise are largely concentrated in the developed world. However, more rudimentary stages of marine biodiscovery that involve less technical equipment and requirements should focus on building local capacities. For example, establishing and maintaining marine biorepositories could have a strong social impact on developing nations. This has the potential to build and support research capacity and add value to resources. Other future directions may include developing “green” and

sustainable extraction processes in-state using renewable and accessible resources, thereby diversifying the use of resources rather than depending on a single resource. It is also needed to focus on more diverse applications of the biomolecules, such as exploring alternatives for current animal feed that is often protein fit for human consumption, or tackling other food security issues even though this may be less potentially profitable than drug discovery.

In a changing world, scientific research may be propelled into new and unpredictable directions. As biorepositories extend the function of natural history collections, new research methods may require new preservation methods or sample requirements. Biodiversity collections therefore need to be dynamic and able to meet the ever-changing needs of research and development. The combination of this approach with new tools in drug discovery described below has the potential to address many of the new challenges of our present century.

3 New Chemical Entities from Marine Bioresources

The identification of new bioactive chemicals from marine organisms traditionally has been conducted through the use of conventional biological screening, liquid chromatographic separation, and nuclear magnetic resonance (NMR) structural elucidation. However, over the last two decades, the development of highly sensitive robotic hyphenated methods has led to alternate approaches to marine natural product isolation. This has increased significantly the ability to produce large libraries of extracts and chromatographic fractions, as well as chemically and biologically screen a large number of samples so as to focus on the directed isolation of new natural products. Therefore, the contemporary marine biodiscovery workflow typically now includes an initial chemical analysis and dereplication stage utilizing these modern techniques. These methods are usually coupled with updated natural product databases and calculated chemical data, so that specimens can be prioritized rapidly for the isolation of new natural products.

These modern methods can be further utilized for the fast and semi-automated isolation and structural elucidation of compounds. Additionally, the significant increase in resolution and the sensitivity of traditional methods has led to a greater ability to characterize new molecules using extremely low nanomolar quantities. These modern procedures have had a significant impact on the field of marine natural products research over the last 20 years, leading to a substantial increase in the number of marine natural products reported in the scientific literature each year.

This section will cover the typical contemporary workflow employed by marine natural product chemists, starting from the use of samples present in a marine biorepository to the identification of a bioactive molecule, focusing mainly on new developments. This includes chemical screening and dereplication stages, biological screening, and the isolation and identification of natural products.

3.1 Chemical Screening: Dereplication

With over 35,000 marine natural products isolated, it has now become standard practice in marine natural products chemistry to use high-throughput chemical screening and dereplication methods to prioritize isolation from unknown specimens. Normally, it is preferable to screen chemically and biologically fractionated extracts, as more complex crude extracts may confound screening results [50]. While the use of fractions can provide better screening efficiency, this greatly increases the quantity of samples that need to be evaluated. However, more recent high-throughput technology has allowed for the development of methods that can be used to screen thousands of samples.

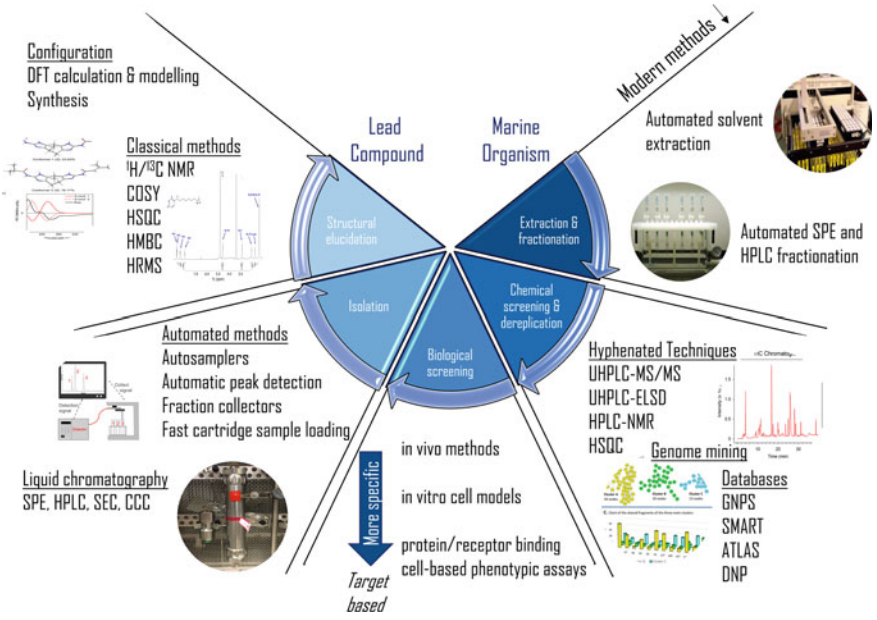

Fig. 2 The marine biodiscovery workflow from a biomaterial repository to the isolation of bioactive compounds. This process includes five major steps including extraction and fractionation, chemical screening and dereplication, biological screening, purification, and finally, structure elucidation. This schematic highlights the most important modern methods that increase the efficiency and outcomes of this process. Abbreviations: DFT (Density Functional Theory); NMR (Nuclear Magnetic Resonance), COSY (COrrelation SpectroscopY), HSQC (Heteronuclear single quantum coherence), HMBC (Heteronuclear Multiple Bond Correlation); HRMS (High Resolution Mass Spectroscopy); SPE (Solid Phase Extraction); HPLC (High Performance Liquid Chromatography); SEC (Size Exclusion Chromatography); CCC (CounterCurrent Chromatography); UHPLC (Ultra High Performance Liquid Chromatography); MS (Mass Spectroscopy); GNPS (Global Natural Product Social Molecular Networking); SMART (Small Molecule Accurate Recognition Technology); DNP (Dictionary of Natural Products).

Over the last two decades, a number of new hyphenated methods have become highly popular for the dereplication of known natural products. The standard combination is an analytical chromatographic separation procedure coupled with an analytical detector. These methods include high-performance liquid chromatography-MS, high-performance liquid chromatography-evaporative light scattering detection, and high-performance liquid chromatography-NMR spectroscopy. These results then are compared to dedicated databases containing chemical data from known natural products (Fig. 2).

3.1.1 Chemical Structure Databases

The process of dereplication can be defined as the identification of already known natural products through the comparison of experimental data with pre-existing analytical information. Therefore, over the last 20 years, publicly available databases have been developed that contain continuously updated lists of known natural products as well as analytical data related to each compound. Many of these databases are now being designed specifically for dereplication purposes to contain appropriate search tools including structural and analytical data searches, as well as bioactivity and taxonomy searches. The latter is extremely important in marine natural product chemistry as the efficiency of dereplication can be improved substantially if the taxonomy of a given marine organism is known. While a number of general chemical databases are available, more recently, more specialized marine natural product databases have been developed.

A number of common chemical and natural product databases are typically used in marine natural products for dereplication. General chemical databases (synthetic and natural molecules) typically used for this purpose include SciFinder [51], PubChem [52], ChemSpider [53], ChEBI [54], ChEMBL [55], and REAXYS [56]. These databases all contain comprehensive records of new chemical entities that can be inspected readily using structural data and search terms. While these databases all contain broad levels of data, the search results obtained can often be confusing due to the number of synthetic products also included. As such, a number of databases specific for natural products have been developed, including the "Dictionary of Natural Products" (DNP) [57], among others [58]. The "Dictionary of Natural Products," in particular, is regarded widely as the most comprehensive database of natural products, and in addition to structural and keyword based searches, it also offers researchers an ability to search for marine natural products based on biological activity and taxonomy.

However, with over 300,000 reported natural products thus far, more specialized databases are becoming ever more common in marine natural product chemistry [59]. These databases include Antimarin, MarinLit [60], ATLAS [61], CyanoMet [62], and StreptomeDB [62]. The latter three databases have been designed specifically for microbial natural products and contain information regarding the gene sequences of some species. However, for the last two decades, the database that has become most popular within marine natural products chemistry is the MarinLit

database. MarinLit was established in the 1970s by Professors John Blunt and Murray Munro to specifically record marine-derived natural products. Today, it is hosted by the Royal Society of Chemistry and contains >35,000 compounds. This database has become very popular among marine natural product chemists due to its unique tailored searches. These are separated into searches for compounds (structure, NMR chemical shift data, exact mass, molecular formula, or UV), taxonomy (phyla through to species), prior literature, and geographic location. A comprehensive compilation of all these data make this an important tool for modern marine natural product dereplication methods.

3.1.2 Analytical Separation Methods

Over the last 20 years, liquid chromatography-based separation techniques have become the most frequently used for the screening of marine extracts and fractions. Typically, these methods include the use of high-performance liquid chromatography, though this has begun to change in recent years with the introduction of the more efficient ultra-high-performance liquid chromatography (UHPLC). This method utilizes higher pressure systems (up to 1200 bar) with lower diameter, smaller particle size columns to allow separations with rapid run times and high resolution [64]. This is performed typically using reversed-phase columns, which are more appropriate for dealing with the polarity of most drug-like bioactive marine natural products [65]. Currently, it is becoming common for laboratories to include in-house dereplication databases that can also incorporate retention times of metabolites for the specific systems used.

Other common separation methods for the isolation of marine products include size-exclusion chromatography, countercurrent chromatography, and capillary electrophoresis. These additional methods are useful typically when separating highly polar materials due the high quantity of ocean salts in marine extracts that can hinder chemical analysis.

3.1.3 Mass Spectrometric Screening

Undoubtedly, mass spectroscopy (MS) has become the most highly utilized detection method in marine biodiscovery over the last two decades, due to the significant improvement in both resolution and sensitivity of modern time-of-flight spectrometers (ToF) and the development of newer mass spectrometers (e.g., Orbitrap™) [66]. Mass spectrometric data allow researchers to determine unequivocally the molecular formula of natural products even at nanomolar concentration levels. Furthermore, the ability to fragment metabolites through tandem mass spectroscopy (MS/MS) with no additional time involvement has made this method of chemical screening vastly popular. Additionally, with a wide variety of commercial ionization methods, including ESI (Electrospray Ionization), FAB (Fast Atom Bombardment), APCI (Atmospheric-Pressure Chemical Ionization), DESI (Desorption Electrospray

Ionization), and MALDI (Matrix-Assisted Laser Desorption Ionization), users now have the ability to obtain greater sensitivity for a wider range of different biological samples. Ionization methods such as DESI and MALDI allow the direct MS detection on solid samples of marine organisms without the need for extraction and other preparation processes [67, 68].

Mass spectrometric data usually can then be evaluated with the molecular databases described above to identify rapidly known compounds and can provide the exact mass and molecular formula. However, more recently, new resources have become available to allow for the automated dereplication of MS/MS data. Most notably, for marine biodiscovery, is the recent development of the Global Natural Products Social molecular networking resource (GNPS) [69]. This resource contains MS/MS databases populated and curated by the natural products community and allows for the visualization of clusters of structurally similar natural products. The software compares the experimental data to the database and returns fragmentation similarities between two molecules. Furthermore, it is becoming more common in marine biodiscovery to use the feature-based molecular networking tool for dereplicated metabolites and to identify potential new analogs [70]. While this is a useful tool for dereplication, some aspects of this approach can be highly laborious if conducting large-scale chemical screening. However, the GNPS feature-based molecular networking procedure has been widely adopted by the marine natural products community, with there being a rising number of marine natural products reported each year utilizing this tool [71]. Some recent examples of new natural products identified through molecular networking include lamellarin sulfates from the ascidian *Didemnum ternerratum* [72], microcolin lipopeptides from the cyanobacterium *Moorea producens* [73], and new chlorinated polyketides from a *Smenospongia* sp. sponge [74].

Other new MS/MS dereplication methods include the use of in silico fragmentation algorithms so that experimental fragmentation can be compared to computationally calculated fragmentation patterns of molecules matching the exact mass. These in silico packages include but are not limited to CFM-ID [75], MetFrag [76], and CSI:FingerID [77]. These can be highly useful resources, as a majority of published natural products do not have MS/MS data reported. These packages can be utilized to produce in silico fragmented assemblies of compounds and marine natural products to be compared to experimental data. Additionally, the use of moiety and pharmacophore in silico fragmentation has been employed for identified substructures within a molecule to target subsequently bioactive metabolites using MS/MS [78].

A primary limitation of MS methods is that the data obtained are not able to be used to confidently assign the definite structure of a natural product, especially for regio- and stereoisomers. Another limitation of MS is the ionization efficiency of natural products for detection. While a number of useful ionization methods are commercially available, issues can still arise from molecules that cannot be easily ionized or that form a plethora of different adduct ions that may complicate the analysis. Problems can also arise from highly instable compounds that can readily fragment with low ionization energies, hindering the identification of the exact mass of a given molecule.

3.1.4 Nuclear Magnetic Resonance Spectroscopic Screening

While mass spectroscopy has become highly popular due to its easy use in hyphenated setups, Nuclear Magnetic Resonance (NMR) spectroscopy provides far superior data for organic compound structural determination. For example, where MS cannot, NMR spectroscopy can be used to identify the different isomers from a change in the chemical shifts. Furthermore, the non-destructive nature of NMR spectroscopy is a major benefit over other dereplication methods, especially due to the low quantities of material typically available in marine natural product studies. Nuclear magnetic resonance spectroscopy has only recently become a more commonly used dereplication method, as a result of the recent developments in NMR spectroscopy automation including auto-sampling and auto-acquisition. ^{1}H NMR experiments are rapid experiments and can be used to quickly obtain proton chemical shift data. However, due to the complex mixtures of compounds in marine natural product screening, overlapping signals with just a one-dimensional NMR experiment can hinder a dereplication process. With the increase in resolution and sensitivity of modern high-field NMR instruments, it has become more common to use rapid two-dimensional experiments including COSY (Correlation Spectroscopy), DOSY (Diffusion Ordered Spectroscopy), HSQC (Heteronuclear Single Quantum Correlation), and TOCSY (Total Correlation Spectroscopy) for chemical screening [79, 80]. This allows overlapping signals in one-dimensional NMR data to be identified and assigned. More recently, other NMR experiments have been designed to address these issues including the use of hyphenated NMR procedures. Modern hyphenated NMR techniques that have been described for the identification of marine natural products include high-performance liquid chromatography-NMR [81] and high-performance liquid chromatography-solid-phase-extraction (SPE)-NMR [82]. These methods can be used for the acquisition of NMR spectra using small amounts of crude material. Such hyphenated methods have been used previously for the identification of a number of known natural products from marine organisms including sponges, brown alga, and red alga [81, 83, 84]. An example of the importance of HPLC-NMR is the isolation of plocamenone and iso-plocamenone from the red alga, *Plocamium angustum* [83]. The NMR detection method was highly important as the use of other methods would have not allowed the discrimination of these isomers.

As NMR data has been an essential requirement for the publication of new molecules, since the late 1980s, a considerable amount of NMR data is available for known natural products. Therefore, a direct comparison of published and experimental data can be used to confidently identify known structures. A number of databases including MarinLit and DEREP-NP [85] are utilized in marine biodiscovery to allow searches of chemical shifts and NMR features, respectively, for rapid dereplication work. The most recent NMR dereplication resource is the SMART NMR database [80]. This resource offers an automated dereplication through comparison of an experimental HSQC spectrum with the SMART database. The first compound to be reported following the use of the SMART dereplication was symplocolide A, a maritime natural product from the marine cyanobacteria *Symploca* sp. [86].

The current limitations of NMR spectroscopy are due primarily to the cost of buying and running this equipment. Costs associated with the preparation of samples for analysis are also typically expensive in requiring special glassware and deuterated solvents. Also, for an exact match between two sets of experimental data, NMR experiments must sometimes be conducted in the same solvent and in some cases at the same pH. This can make the selection of a solvent for screening mixtures of natural products complicated when weighing up the solubility and data availability.

3.1.5 Molecular Genomics Screening

With the development of new cheaper and faster DNA sequencing methods, it has become much more efficient to sequence and identify biosynthetic gene clusters. This, therefore, has become a useful tool for the identification of biosynthetic genes encoding for the production of natural products. The sequencing and analysis of these "biosynthetic gene clusters" can reveal a range of information including the precursor metabolites, the biosynthetic intermediates, and also the structure of the metabolites present. For this reason, researchers have begun to investigate this approach as a potential dereplication tool. The genomic investigation of organisms for the proposition of new natural products has been coined "genome mining" [87, 88]. This method is now becoming a more standard approach among groups with a strong focus on microbial-derived products. With the significant rise in marine microorganism natural products being discovered, this has become more popular in marine biodiscovery in recent years.

A number of new databases currently are used in marine biodiscovery for the rapid identification of biosynthetic gene cluster sequences. These include the MIBiG repository [89], the taxon-specific Prospect (fungal genes) [90], and ActDES (Actinomycetes genes) [91] databases as well as the computationally predicted gene databases antiSMASH [92] and IMG-ABC [93]. After identification of biosynthetic genes, it is then necessary to identify the structures or structural features for which these genes encode, to dereplicate natural products. With recent developments in machine learning, tools have been developed to use the identified genes to predict chemical structures. These tools include PRISM [94], SBSPKS v3 [95], and Adenyl-Pred [96] for the chemical structure prediction of predominately polyketides and nonribosomal peptides. Currently, a number of these tools have been tailored towards bacterial metabolites and gene sequences, although with the recent focus in marine biodiscovery on the isolation of fungal natural products, it is highly likely that there will be a shift towards fungal biosynthetic genes in the coming years [21].

There are some pitfalls to the use of genome mining that need to be addressed. The first issue is that this method is, currently, mainly applicable for the identification of polyketide and nonribosomal peptide sequences. This limits the use of genome mining for marine natural products due to the significant number of unique marine-derived terpene, alkaloid, and polyaromatic metabolites. Additionally, the structures of these natural products cannot be identified based solely on the genomic data. Unknown genetic transformations or spontaneous reactions of a natural product

may not be predicted confidently as the molecule encoded by the genes may not match the final product. Another limitation is that a number of natural products are produced by multiple organisms and that some moieties may be incorporated into a molecule through an organism's diet [97, 98]. While this method will likely improve in the future, currently, there is still a need for this genomic approach to be used in conjunction with chemical methods to confirm molecular structures.

3.2 Biological Screening

Over the past 60 years, marine organisms have been a rich source of unique bioactive compounds with activities including antitumor, antibacterial, antifungal, antiinflammatory, antiviral, antiparasitic, and antioxidant activities, useful for a broad range of applications, but mainly for drug discovery. High-throughput screening methods of the twenty-first century have transformed the field of drug discovery from marine sources. The use of methods utilizing high-throughput automated liquid handlers, plate readers, and 384/1,534-well assay plates have increased throughput to a point where thousands of marine samples can be screened over a few days. Traditional assay methods utilize in vivo whole organisms and in vitro organism-derived cell lines. The screening of natural product extracts in cell line assays can often lead to non-specific hits and false positives that typically are not advantageous for development as lead compounds. However, more recently, bioassays have shifted to more specific phenotypic cellular function assays and protein/receptor binding assays [99]. These highly specialized assays can be useful for the identification of target specific compounds that may then be classified as lead compounds.

Cell line models are still the most common biological assays used for screening marine natural product extracts. This is due to the primary targets for drug discovery being traditionally antitumor and antimicrobial compounds. Cell-based assays have been used significantly in cancer research due to the availability of tumor cell lines. Similarly, microbial cell cultures are very common and can be screened with relative ease. Furthermore, a number of other more specific phenotypic genetically modified cell lines have become common when screening for antiinflammatory, antiviral, and antiparasitic activities. Cellular assays are very common due to their development as high-throughput assays in microwell plates with robotic liquid handlers. A major problem with cell-based assays is that they often use established and immortalized cell lines that are vastly different from cells of in vivo systems [100]. However, typically this is a trade-off that is made to achieve higher throughput results.

Biological assays in marine biodiscovery are shifting slowly from these in vitro cell assays to more specific cell-free protein biochemical assays [99]. With a goal of obtaining natural products with more specific activity, target-based receptor binding assays have become more common primarily due to their increased specificity. Additionally, these offer the ability for multiple different methods of analysis so that not only drug targets can be identified but also diagnostic tools. An enzyme substrate can be used to identify if the activity is inhibited, and fluorescent dyes can be used

to bind to the protein–ligand complex, and more recently, in marine biodiscovery, native MS can be used to identify protein–ligand complexes [101, 102]. In particular, the protein–ligand native MS assay has been of interest in marine biodiscovery due to its ability to obtain the MS data for unknown active compounds allowing a mass-guided purification as opposed to a bioassay-guided study. However, these assays further trade cellular mechanisms and similarities to in vivo systems, to achieve higher throughput, higher specificity, and often false results.

Bioassay-guided purification is probably the most widely utilized method when conducting natural product drug discovery projects. This process is very appealing as the bioactivity at each purification step can target only bioactive components. However, difficulties can include inactivity due to false positives [103]. This is a common occurrence, especially when starting with crude extracts instead of less complex fractions. The use of more modern receptor binding assays led to some success for complex mixtures of natural products in overcoming this issue [100]. As such, receptor binding assays have become more common for bioassay-guided purification of active samples [101]. These methods are also advantageous due to the microscale of the assays in requiring smaller quantities of material. However, due to the common possibility of false positives when screening marine organism extracts, it is becoming more common to rely less on the biological screening results and more on chemical data. Furthermore, methods that integrate the chemical screening with biological screening can help in the identification of false results and also point to potential molecules within fractions that may be responsible for activity [104, 105]. We suggest that the use of both target-based receptor binding assays and chemical screening on marine fractions followed by cell-based and in vivo models would be the most beneficial process.

3.3 Ireland's National Marine Biodiscovery Approach

In Ireland, a major focus of the National Marine Biodiscovery Laboratory is the large-scale chemical screening and dereplication of known metabolites, and targeting unknown metabolite identification. This dereplication method utilizes a library of fractions produced through the organic extraction and fractionation using reversed-phase solid-phase extraction and storage in the biomaterial repository described above. These fractions are then subjected to chemical screening using two hyphenated methods; UHPLC-MS/MS for dereplication using the MarinLit database and the GNPS molecular networking tool as discussed above, as well as UHPLC-ELSD (evaporative light-scattering detection) to identify relative quantities of compounds within a sample for prioritization. This screening is performed utilizing the same ultra-high-performance liquid chromatography methods and columns so that the MS data and ELSD data can be compared. This ELSD dataset is important, as a large proportion of peaks that are identified using MS data are typically compounds that are strongly ionized and are present at low nano- and picogram quantities. This can

be problematic if samples containing new natural products obtained in quantities too low for isolation are prioritized. The ELSD data allows researchers to identify the relative quantity of material available in an extract so that time is not wasted purifying samples that will not yield compounds that can be analyzed by NMR spectroscopy. Additionally, if only a small amount of biomass is available, this can be prioritized for recollection so that minor compounds of interest can be isolated. On the other hand, compounds that display high quantities of natural products in the ELSD but do not display ions in the MS/MS can be prioritized for alternative methods of screening such as NMR analysis.

This dereplication method was used successfully to identify known bisindole alkaloids from the sponge *Spongosorites calcicola* and also identify two minor unknown brominated metabolites, the calcicamides, for isolation [106]. The feature-based molecular networking using GNPS was also used for the identification of a new family of highly branched thiolane derivatives, the nebulosins, from the marine annelid *Eupolymnia nebulosa.* The screening displayed three clusters of unknown natural products that constituted the major metabolites of this annelid [107].

While both types of analysis use high-throughput autosamplers, this method can be improved in the future through the addition of a splitter unit between the UHPLC and detectors to obtain results in a single run. It would also be advantageous to integrate the ELSD data with feature-based molecular networking to better understand clusters and the production of natural products.

In terms of bioassays, the choice was made in Ireland to outsource the necessary biological screening, for several reasons:

- expertise in pharmacology is usually required to develop robust bioassays;
- biological screening is more efficient when using expensive automated robots;
- automatic robots require maintenance and dedicated space as usually available in companies; and
- as new targets appear, it would not be possible to embrace the full range of potential bioactivities targeted.

Our group therefore established a collaboration with Fundacion Medina in Spain, leaders in Europe in the biological screening of metabolites of natural origin, especially for rapid antimicrobial and cytotoxicity assessments.

3.4 Prioritization Strategies

Due to the high number of samples present in collections or biorepositories, a prioritization strategy is a key component of a successful process in marine biodiscovery. When thousands of samples are present in collections, a decision has to be made about where to start, and the biological assay should not be the only criterion taken into account. We decided to develop a prioritization strategy on each targeted bioassay (application) based on weights and scores assigned for (Fig. 3):

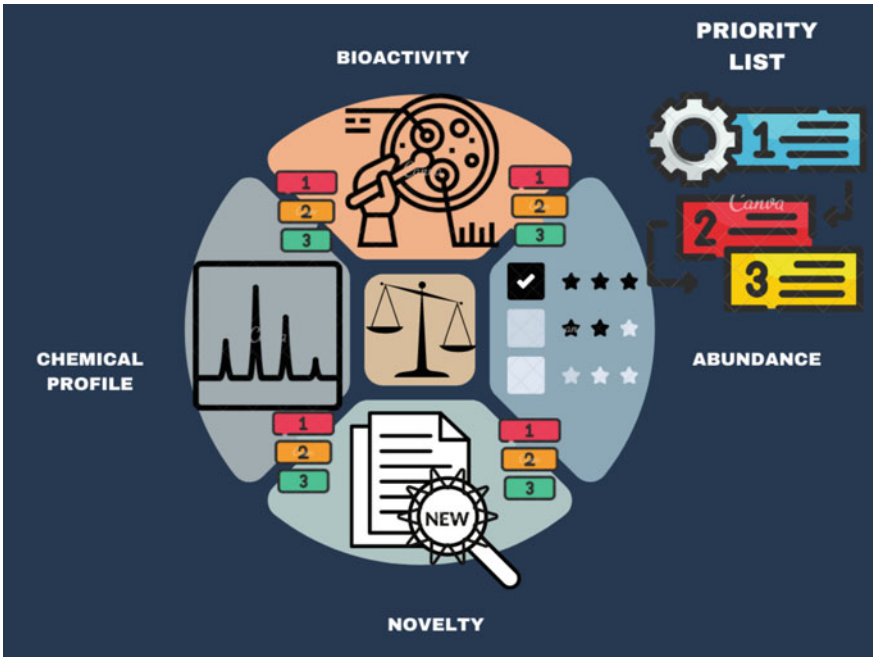

Fig. 3 Prioritization strategy for marine biodiscovery

- the availability of the sample (biomass in Nature);
- new metabolites following chemical screening (dereplication) but also new species following taxonomy;
- ease of purification using chemical profiling; and
- biological activities evident.

The use of prioritization is very flexible, and the weights applied will depend on the main question addressed. Importantly, this strategy can only be based on the discovery of new species and chemical entities for the construction of repositories and advances of knowledge. In this case, the weight of novelty and chemical profile should be the highest. For more commercial applications, several options can be envisaged. Indeed, for a company working on the production of low-value products, the most important will be the availability of the resource and therefore the abundance (wild or cultured) will have the highest weight. Conversely, for a pharmaceutical company, the novelty and the bioactivity will have the highest weights. In the case of the IMBR, we gave very similar weights to the four different factors, as our main goal was to find bioactive natural products from a diverse range of species and that were easy to purify for metabolites (chemical profile).

At this point, it is important to extend the concept of marine biodiscovery beyond drug discovery. This high risk and long-term research question should not only correspond to one aspect of marine biodiscovery. Short-term applications of the extracts or

fractions as fertilizers or other agricultural application would contribute significantly to the blue economy. Applications requiring large biomass of the marine resource will be assigned the highest weights for prioritization.

This strategy has streamlined the selection of promising species for the identification of new bioactive marine natural products.

3.5 Natural Product Chemistry

The purification and structural elucidation of marine natural products is the most time-consuming and expensive process of the marine biodiscovery pipeline. A large biomass is needed for isolation of active metabolite at a level that can facilitate the subsequent structure elucidation procedure. The presence of a highly potent minor metabolite in trace amounts can further complicate the isolation and structure determination process. However, recent technological advancements and the availability of higher field NMR spectrometers now mean that even natural products available in only sub-milligram quantities can be isolated and identified. This also means that smaller quantities of biomass (<10 g) can also undergo purification. These are especially important developments for marine biodiscovery for species obtained with a natural low biomass. Typically, the isolation and structure elucidation of marine natural products utilizes similar methodologies to terrestrial compounds, but with a fractionation process using a reversed-phase material such as vacuum-liquid chromatography.

3.5.1 Purification of Marine Natural Products

The complex and unique nature of marine organism extracts can make the isolation of the associated natural products difficult and highly time consuming. Moreover, most chemists consider the purification of natural products to be the most arduous part of the marine natural products pipeline. Therefore, samples are prioritized using their chemical and biological screening results, so that only the specimens that contain unknown metabolites and exhibit bioactivity undergo this laborious process. As unknown compounds are the target of most natural product isolations, there is no set procedure for purification and often multiple different subsequent methods must be used. However, the chemical profile and dereplication data obtained should aid in the selection of isolation methods. A usual purification process follows a process of large-scale, low-pressure fractionation, followed by subsequent small-scale, high-pressure HPLC separations of these fractions.

These large-scale fractionation methods include solid-phase extraction, vacuum-liquid chromatography, column chromatography, and liquid–liquid partitioning. These methods can utilize a variety of solid phases depending on the targeted molecules including a reversed phase (polar to non-polar molecules), normal phase (non-polar molecules), ion-exchange resins (ionic molecules), and size-exclusion

gels (polymers and water-soluble molecules). The primary aim of this first large-scale step in marine biodiscovery is to separate the secondary metabolites of interest from the bulk primary metabolites and ocean salts.

Subsequent smaller scale steps usually include higher resolution separation methods including column chromatography, thin-layer chromatography, high-performance liquid chromatography (HPLC), size-exclusion chromatography, and countercurrent chromatography. The primary aim of the high-resolution purification step is to obtain pure natural products of interest for chemical characterization. In marine natural product chemistry, preparative high-performance liquid chromatography utilizing a reversed phase (typically C_{18} or phenyl bonded silica) is the most common and possibly the most useful method for isolating secondary metabolites.

Most modern preparative high-performance liquid chromatography systems are connected in series with a UV or a diode array detector to identify compounds eluting from the column and also a fraction collector for automated sample collection. Additionally, a number of new technologies for an increase in speed and automation of purification are now being incorporated into marine biodiscovery workflows. These include active high-performance liquid chromatography splitters in conjunction with other detectors (MS, ELSD) that can be used to purify compounds without a UV chromophore. Stop-flow high-performance liquid chromatography-NMR can be used to acquire sets of NMR data on compounds throughout a high-performance liquid chromatography purification [81], while peak-detecting fraction collectors that automatically collect compounds as they are detected eluting from the column are available.

While the processes used in marine biodiscovery closely match terrestrial methods, the difficulties inherent can differ slightly. Two main difficulties that may occur during the purification of marine extracts are the isolation of water-soluble small molecules, as the separation of these molecules from salts can often be difficult [108], and that marine natural products can be unstable and contain extremely labile functional groups (sulfates, polyenes).

3.5.2 Structure Elucidation

The most significant technological improvement in natural products chemistry has been the development of two-dimensional NMR spectroscopic experiments from the mid-1970s to mid-1980s. With the invention of 2D-NMR experiments, the time to elucidate structures of compounds decreased from years to days, and the quantity of product required decreased from hundreds of milligrams to just a few milligrams. Now, with modern NMR spectrometers, 2D-NMR data can be acquired on sub-milligram quantities of molecules. However, since the development of 2D-NMR pulse sequences, little has changed in the approach to determining the planar structure of marine natural products. Typically, planar structural elucidation is still performed through manual interpretation of ^{1}H NMR, ^{13}C NMR, COSY, HSQC, and HMBC data as well as the exact mass of a molecule. While NMR spectroscopy made the assignment of the planar structure “relatively” straight forward, the complete stereo

chemical assignments of marine natural products is still a challenging task. Traditionally, relative configurational assignments have been made through the use of coupling constants and nuclear Overhauser effect NMR experiments. In turn, absolute configurational assignments have been conducted using degradation and derivatization procedures, and X-ray crystallography. With the exception of NMR experiments, these methods often require quite large quantities of isolated compounds and can often be destructive to the sample.

More recently, a number of new computational tools have become more widely utilized for the structural assignment of marine natural products. These include computer-assisted structure elucidation and quantum chemical calculation of chiroptical properties and NMR spectra. In a large number of circumstances, a compound structural assignment using NMR spectroscopy is relatively straight forward, but there are instances when NMR assignments can be complicated, usually when a molecule has a low H:C ratio. In these situations, either the use of computer-assisted structure elucidation to generate a structure or the calculation of NMR spectrometric parameters to support structures are useful methods. Computer-assisted structure elucidation tools typically generate a number of different structures and give each structure a relative probability [109]. Common computer-assisted structure elucidation tools include ACD Structure Elucidator, Bruker CMC-se, and MNova Structure Elucidation. Currently, only a limited number of published marine natural products report the use of computer-assisted structure elucidation steps in their structural determination. However, assignments made using Gauge independent atomic orbital calculated NMR has become a popular method in marine natural products to support structural assignments [110].

Over the last 10 years, there has been a considerable shift in the methods used for configurational assignments in marine natural products. More recently, the use of time-dependent density functional theory for predicted electronic circular dichroism and Gauge independent atomic orbital NMR has dominated such assignments [111]. These time-dependent density functional theory methods have become popular in marine biodiscovery as a result of advancements in high performance computation early in the twenty-first century. These methods facilitate the reliable and fast prediction of both chiroptical properties (electronic circular dichroism, vibrational circular dichroism, and optical rotation) for absolute configuration and NMR for relative configuration [112]. The predicted data can be compared to experimental data on sub-milligrams of compounds to allow structural assignments. Statistical approaches including DP4 and its upgrades have become commonly used in marine biodiscovery for the calculation of a relative configuration with calculated NMR shifts or coupling constants [113–115]. A new tool, DP4-AI, recently has become available and combines both the automated computer-assisted structure elucidation 2D structure elucidation and NMR predicted relative configuration [116]. This method merging computer-assisted structure elucidation and DP4 is a significant improvement that is likely to make automated marine natural products assignment to the point of relative configuration more common.

One other technique that has recently been developed and has so far been exclusively used for marine natural products structural elucidation is the crystalline sponge

X-ray crystallographic method [117]. This method allows X-ray crystallography to be performed on non-crystalline compounds by allowing them to form a complex with a host crystal. This method so far has been used to identify the structure of nanogram amounts of several red algal terpenoids. The limitations of this method are that only non-polar compounds can be absorbed by current crystals in non-polar solvents such as hexane. However, this procedure offers great promise for a new and robust method of absolute structural elucidation on sub-milligrams of sample.

3.5.3 Bioactive Natural Products from Irish Waters

During the last 5 years, the application of the workflow for marine biodiscovery in Ireland has led to a number of interesting compounds and five main publications (Fig. 4).

The first original aromatic urea derivatives were isolated from the intertidal lichen *Lichina pygmaea* [118]. Still in the intertidal area of the western coast of Ireland, the chemical study of the marine worm *Eupolymnia nebulosa* led to the discovery of an entire family of sulfur-containing metabolites [107]. These discoveries demonstrate the potential of overlooked marine organisms for marine biodiscovery that has been often restricted to sponges or tunicates. Then, the chemical studies of the subtidal sponges *Clathria strepsitoxa* and *Spongosorites calcicola* provided some interesting

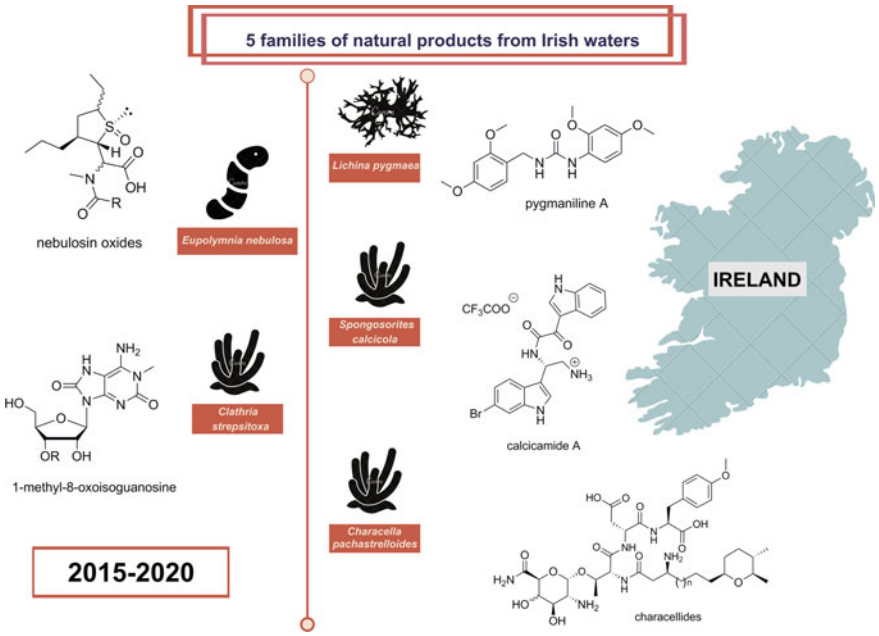

Fig. 4 Main families of natural products identified from Irish waters using the newly developed marine biodiscovery workflow

bioactive alkaloids [105, 119]. Finally, in the context of a program dedicated to the exploration of a deep-sea hotspot of bio- and chemodiversity, a new family of characellides was identified from the sponge *Chracella pachastrelloides* [120].

4 Concluding Remarks

Throughout this chapter, we have highlighted the importance of the construction of marine biomaterial repositories, especially in regions of the world with high marine biodiscovery potential, i.e., maritime developing nations. A number of advantages associated with the establishment and maintenance of such facilities have been detailed above. We believe that the Irish Marine Biomaterial Repository (MBR), which recently has been developed, can serve as an example for developing nations to follow, using best practices and data management systems already implemented over the past 5 years at the IMBR. A marine biomaterial repository requires a minimum investment from local authorities and can provide the following benefits:

- a marine biorepository represents the biological and chemical patrimony present in local species over time, and may be used to track changes in species distributions due to global change;
- it will contribute to building capacity in developing countries, especially in research areas such as taxonomy, where specialists are lacking;
- actions are available to quickly assess the potential of local marine bioresources against emerging pathogens or targets (e.g., SARS-COVID-2);
- it will provide new opportunities in the field of the blue economy for local communities through intellectual property associated with the genetic material stored; and
- it may also provide job opportunities and capacity building through training and technology transfer in member states or developing maritime nations.

Overall, the approach developed above contributes to the three pillars of sustainability as outlined below (Fig. 5).

The environmental impact of developing local marine biorepositories may be envisioned to be positive overall, as vouchers will be stored and processed at local facilities. Furthermore, local scientists will be consulted when access to samples is required and will be kept up-to-date on research and development being performed on local marine bioresources. Changes in the distribution of some species could lead to their protection by local and also international agencies. As only small quantities of samples are required for chemical and biological screening, local populations are not likely to be affected by initial bioprospecting collections. Subsequent collections of larger biomasses, however, will need to be carefully monitored by local authorities and communities so as to prevent population declines and possible extinction. It is important to include all the marine diversity present in the different coastal habitats, and not only focus on common groups such as sponges or tunicates. Some annelids or mollusks can also be promising in the marine biodiscovery workflow.

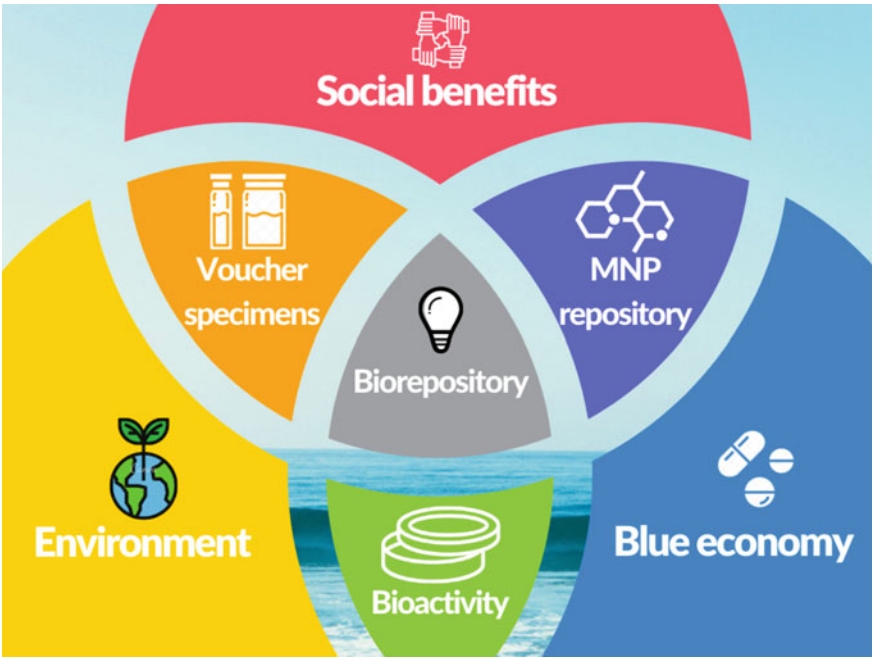

Fig. 5 A sustainable marine biodiscovery approach

Finally, the possible economic value associated with some bioactive species has the potential to influence decision makers with regard to marine spatial planning and the establishment of special areas of conservation.

The presence of voucher specimens hosted by local entities ensures not only a positive social impact through capacity building and training of young scientists, but also interactions with worldwide experts and developing taxonomic skills in different groups of marine organisms. Members of the younger generation will have a better understanding of their rich marine biodiversity. On the other hand, the presence of chemical ensembles and regulations on access and benefit sharing could provide some positive economic inputs to the communities. Indeed, economic benefits will be shared between the industrial companies and the local communities through royalties on the licenses of the new biomolecules developed.

Finally, this type of marine organism organization will clearly contribute positively to the blue economy. The biomaterials produced are easily available for screening and the discovery of new applications is clearly accelerated. We recommend that marine biodiscovery should be more inclusive and cover both biological and biochemical discovery. The repositories should also integrate the large array of species available in an ecoregion and not only the most emblematic species like corals, sponges, and seaweeds. The future of marine biodiscovery will be bright if researchers in the field start building capacities in all regions of the world. The global trends that led us

from invertebrates to microbes and now a large investment in the seaweeds can be dangerous if a strong foundation is not built for the next generation of researchers.

Acknowledgments This project is financed by the Irish Government and the European Maritime and Fisheries Fund (EMFF) 2014–2020, Blue Growth & Marine Spatial Planning Scheme (SERV-20-MEFS-044), and also by the Marine Institute (Grant PDOC/19/02/01). We also acknowledge some fruitful discussions with colleagues of the Interreg project EBB.

References

1. Eikeset AM, Mazzarella AB, Davíðsdóttir B, Klinger DH, Levin SA, Rovenskaya E, Stenseth NC (2018) What is blue growth? The semantics of "Sustainable Development" of marine environments. Mar Policy 87:177
2. Baslow MH (1969) Marine pharmacology. A study of toxins and other biologically active substances of marine origin. The Williams and Wilkins Company, Baltimore, USA
3. Molinski TF, Dalisay DS, Lievens SL, Saludes JP (2009) Drug development from marine natural products. Nat Rev Drug Discov 8:69
4. Gerwick WH, Moore BS (2012) Lessons from the past and charting the future of marine natural products drug discovery and chemical biology. Chem Biol 19:1631
5. Jaspars M, De Pascale D, Andersen JH, Reyes F, Crawford AD, Ianora A (2016) The marine biodiscovery pipeline and ocean medicines of tomorrow. J Mar Biol Assoc UK 96:151
6. Sigwart JD, Blasiak R, Jaspars M, Jouffray J-B, Tasdemir D (2021) Unlocking the potential of marine biodiscovery. Nat Prod Rep. https://doi.org/10.1039/D1030NP00067A
7. Rae M, Folch H, Moniz MBJ, Wolff CW, McCormack GP, Rindi F, Johnson MP (2013) Marine bioactivity in Irish waters. Phytochem Rev 12:555
8. Firsova D, Mahajan N, Solanki H, Morrow C, Thomas OP (2017) Current status and perspectives in marine biodiscovery. In: Paterson R, Lima N (eds) Bioprospecting: success, potential and constraints, vol 16. Topics in biodiversity and conservation. Springer, Cham, Switzerland, p 29
9. Leclère D, Obersteiner M, Barrett M, Butchart SHM, Chaudhary A, De Palma A, DeClerck FAJ, Di Marco M, Doelman JC, Dürauer M, Freeman R, Harfoot M, Hasegawa T, Hellweg S, Hilbers JP, Hill SLL, Humpenöder F, Jennings N, Krisztin T, Mace GM, Ohashi H, Popp A, Purvis A, Schipper AM, Tabeau A, Valin H, van Meijl H, van Zeist WJ, Visconti P, Alkemade R, Almond R, Bunting G, Burgess ND, Cornell SE, Di Fulvio F, Ferrier S, Fritz S, Fujimori S, Grooten M, Harwood T, Havlík P, Herrero M, Hoskins AJ, Jung M, Kram T, Lotze-Campen H, Matsui T, Meyer C, Nel D, Newbold T, Schmidt-Traub G, Stehfest E, Strassburg BBN, van Vuuren DP, Ware C, Watson JEM, Wu W, Young L (2020) Bending the curve of terrestrial biodiversity needs an integrated strategy. Nature 585:551
10. Blasiak R, Wynberg R, Grorud-Colvert K, Thambisetty S (2020) The ocean genome: conservation and the fair, equitable and sustainable use of marine genetic resources. World Resources Institute, Washington, DC, USA
11. Hillebrand H, Brey T, Gutt J, Hagen W, Metfies K, Meyer B, Lewandowska A (2018) Climate change: warming impacts on marine biodiversity. Handbook on marine environment protection, p 353
12. Di Marco M, Harwood TD, Hoskins AJ, Ware C, Hill SLL, Ferrier S (2019) Projecting impacts of global climate and land-use scenarios on plant biodiversity using compositional-turnover modelling. Glob Change Biol 25:2763
13. Ledger S (2020) Living planet report 2020 - bending the curve of biodiversity loss. WWF, Gland, Switzerland

14. Colella, JP, Agwanda BR, Khan FAA, Bates J,Carrión Bonilla CA, de la Sancha N, Dunnum JL, Ferguson AW, Greiman SW, Kiswele PK, Lessa EP, Soltis P, Thompson CW, Vanhove MPM, Webala PW, Weksler M, Joseph A (2020) Build international biorepository capacity. Science 370:773
15. Schindel DE, Cook JA (2018) The next generation of natural history collections. PLoS Biol 16:1
16. Thompson CW, Phelps KL, Allard MW, Cook JA, Dunnum JL, Ferguson AW, Gelang M, Khan FAA, Paul DL, Reeder DM, Simmons NB, Vanhove MPM, Webala PW, Weksler M, Kilpatrick CW (2021) Preserve a voucher specimen! The critical need for integrating natural history collections in infectious disease studies. mBio 12:1
17. Dias DA, Urban S, Roessner U (2012) A historical overview of natural products in drug discovery. Metabolites 2:303
18. Pérez-Lloréns JL, Mouritsen OG, Rhatigan P, Cornish ML, Critchley AT (2020) Seaweeds in mythology, folklore, poetry, and life. J Appl Phycol 32:3157
19. Evans-Illidge EA, Logan M, Doyle J, Fromont J, Battershill CN, Ericson G, Wolff CW, Muirhead A, Kearns P, Abdo D, Kininmonth S, Llewellyn L (2013) Phylogeny drives large scale patterns in Australian marine bioactivity and provides a new chemical ecology rationale for future biodiscovery. PLoS One 8:1
20. Mühling M, Joint I, Willetts AJ (2013) The biodiscovery potential of marine bacteria: an investigation of phylogeny and function. Microb Biotechnol 6:361
21. Carroll AR, Copp BR, Davis RA, Keyzers RA, Prinsep MR (2021) Marine natural products. Nat Prod Rep 38:362
22. Bergmann W, Feeney RJ (1951) Contributions to the study of marine products. XXXII. The nucleosides of sponges. I. J Org Chem 16:981
23. Planes S, Allemand D, Agostini S, Banaigs B, Boissin E, Boss E, Bourdin G, Bowler C, Douville E, Flores JM, Forcioli D, Furla P, Galand PE, Ghiglione J-F, Gilson E, Lombard F, Moulin C, Pesant S, Poulain J, Reynaud S, Romac S, Sullivan MB, Sunagawa S, Thomas OP, Troublé R, de Vargas C, Vega Thurber R, Voolstra CR, Wincker P, Zoccola D (2019) The Tara Pacific expedition—a pan-ecosystemic approach of the "-omics" complexity of coral reef holobionts across the Pacific Ocean. PLoS Biol 17:e3000483
24. Miller SE, Barrow LN, Ehlman SM, Goodheart JA, Greiman SE, Lutz HL, Misiewicz TM, Smith SM, Tan M, Thawley CJ, Cook JA, Light JE (2020) Building natural history collections for the twenty-first century and beyond. Bioscience 70:674
25. Edwards JL, Lane MA, Nielsen ES (2000) Interoperability of biodiversity databases: biodiversity information on every desktop. Science 289:2312
26. Page LM, Macfadden BJ, Fortes JA, Soltis PS, Riccardi G (2015) Digitization of biodiversity collections reveals biggest data on biodiversity. Bioscience 65:841
27. Lavoie C (2013) Biological collections in an ever changing world: herbaria as tools for biogeographical and environmental studies. Perspect Plant Ecol Evol Syst 15:68
28. Hedrick BP, Heberling JM, Meineke EK, Turner KG, Grassa CJ, Park DS, Kennedy J, Clarke JA, Cook JA, Blackburn DC, Edwards SV, Davis CC (2020) Digitization and the future of natural history collections. Bioscience 70:243
29. Day JG, Stacey GN (2008) Biobanking. Mol Biotechnol 40:202
30. Funk VA, Gostel M, Devine A, Kelloff CL, Wurdack K, Tuccinardi C, Radosavljevic A, Peters M, Coddington J (2017) Guidelines for collecting vouchers and tissues intended for genomic work (Smithsonian Institution): botany best practices. Biodivers Data J 5:e11625
31. De Souza YG, Greenspan JS (2013) Biobanking past, present and future: responsibilities and benefits. AIDS 27:303
32. Huete-Pérez JA, Mendoza-Ramírez EN (2012) Genomic biorepository of coastal marine species in Estero Padre Ramos and Estero Real Nicaragua. Encuentro 93:6
33. Gabrielsen KL (2012) Marbank – a biobank of arctic marine organisms. Planta Med 78:PL18
34. Lallier LE, McMeel O, Greiber T, Vanagt T, Dobson ADW, Jaspars M (2014) Access to and use of marine genetic resources: understanding the legal framework. Nat Prod Rep 31:612

35. Morgera E, Tsioumani E, Buck M (2014) Unraveling the Nagoya Protocol: a commentary on the Nagoya Protocol on access and benefit-sharing to the Convention on Biological Diversity. Brill & Nijhoff, Leiden, The Netherlands.https://doi.org/10.1163/9789004217188
36. Pons J, Barraclough TG, Gomez-Zurita J, Cardoso A, Duran DP, Hazell S, Kamoun S, Sumlin WD, Vogler AP (2006) Sequence-based species delimitation for the DNA taxonomy of undescribed insects. Syst Biol 55:595
37. Puillandre N, Lambert A, Brouillet S, Achaz G (2012) ABGD, Automatic barcode gap discovery for primary species delimitation. Mol Ecol 21:1864
38. Zhang J, Kapli P, Pavlidis P, Stamatakis A (2013) A general species delimitation method with applications to phylogenetic placements. Bioinformatics 29:2869
39. De Queiroz K (2007) Species concepts and species delimitation. Syst Biol 56:879
40. Cachet N, Genta-Jouve G, Ivanisevic J, Chevaldonné P, Sinniger F, Culioli G, Pérez T, Thomas OP (2015) Metabolomic profiling reveals deep chemical divergence between two morphotypes of the zoanthid *Parazoanthus axinellae*. Sci Rep 5:1
41. Villamor A, Signorini LF, Costantini F, Terzin M, Abbiati M (2020) Evidence of genetic isolation between two Mediterranean morphotypes of *Parazoanthus axinellae*. Sci Rep 10:1
42. Ruiz C, Ivanišević J, Chevaldonné P, Ereskovsky AV, Boury-Esnault N, Vacelet J, Thomas OP, Pérez T (2015) Integrative taxonomic description of *Plakina kanaky*, a new polychromatic sponge species from New Caledonia (Porifera: Homoscleromorpha). Mar Ecol 36:1129
43. Reddy MM, De Clerck O, Leliaert F, Anderson RJ, Bolton JJ (2020) An appraisal of the genus *Pyropia* (Bangiales, Rhodophyta) from southern Africa based on a multi-gene phylogeny, morphology and ecology, including the description of *Pyropia meridionalis* sp. nov. SAfr J Bot 131:18
44. Hebert PDN, Penton EH, Burns JM, Janzen DH, Hallwachs W (2004) Ten species in one: DNA barcoding reveals cryptic species in the neotropical skipper butterfly *Astraptes fulgerator*. Proc Natl Acad Sci USA 101:14812
45. Hebert PDN, Gregory TR (2005) The promise of DNA barcoding for taxonomy. Syst Biol 54:852
46. Rutz A, Dounoue-Kubo M, Ollivier S, Bisson J, Bagheri M, Saesong T, Ebrahimi SN, Ingkaninan K, Wolfender JL, Allard PM (2019) Taxonomically informed scoring enhances confidence in natural products annotation. Front Plant Sci 10:1
47. Hirata UD (1986) Halichondrins—antitumor polyether macrolides from a marine sponge. Pure Appl Chem 58:701
48. Marine Biodiscovery Ireland (2018) http://www.imbd.ie/. Accessed 14 March 2021
49. D'Archino R, Nelson WA, Sutherland JE (2020) Unnamed for over 30 years: *Gigartina falshawiae* sp. nov. (Gigartinaceae, Rhodophyta) and its confusion with *Iridaea tuberculosa* in New Zealand. Phycologia 59:45
50. Camp D, Davis RA, Campitelli M, Ebdon J, Quinn RJ (2012) Drug-like properties: guiding principles for the design of natural product libraries. J Nat Prod 75:72
51. SciFinder American Chemical Society. https://scifinder.cas.org/scifinder/view/scifinder/scifinderExplore.jsf
52. PubChem National Library of Medicine, National Institutes of Health. https://pubchem.ncbi.nlm.nih.gov/
53. ChemSpider Royal Society of Chemistry. https://www.chemspider.com/
54. Chemical Entities of Biological Interest (ChEBI) European Molecular Biology Laboratory. https://www.ebi.ac.uk/chebi/
55. Davies M, Nowotka M, Papadatos G, Dedman N, Gaulton A, Atkinson F, Bellis L, Overington JP (2015) ChEMBL web services: streamlining access to drug discovery data and utilities. Nucl Acids Res 43:W612
56. Reaxys Elsevier Life Sciences IP Limited. https://www.reaxys.com
57. Dictionary of Natural Products 29.2. CRC Press, Taylor & Francis Group. http://dnp.chemnetbase.com

58. Sorokina M, Steinbeck C (2020) Review on natural products databases: where to find data in 2020. J Cheminformat 12:20
59. Blunt J, Munro M, Upjohn M (2012) The role of databases in marine natural products research. In: Fattorusso E, Gerwick WH, Taglialatela-Scafati O (eds) Handbook of marine natural products. Springer, Netherlands, Dordrecht, p 389
60. MarinLit. Royal Society of Chemistry. http://pubs.rsc.org/marinlit/
61. van Santen JA, Jacob G, Singh AL, Aniebok V, Balunas MJ, Bunsko D, Neto FC, Castaño-Espriu L, Chang C, Clark TN, Cleary Little JL, Delgadillo DA, Dorrestein PC, Duncan KR, Egan JM, Galey MM, Haeckl FPJ, Hua A, Hughes AH, Iskakova D, Khadilkar A, Lee J-H, Lee S, LeGrow N, Liu DY, Macho JM, McCaughey CS, Medema MH, Neupane RP, O'Donnell TJ, Paula JS, Sanchez LM, Shaikh AF, Soldatou S, Terlouw BR, Tran TA, Valentine M, van der Hooft JJJ, Vo DA, Wang M, Wilson D, Zink KE, Linington RG (2019) The Natural Products Atlas: an open access knowledge base for microbial natural products discovery. ACS Cent Sci 5:1824
62. Jones MR, Pinto E, Torres MA, Dörr F, Mazur-Marzec H, Szubert K, Tartaglione L, Dell'Aversano C, Miles CO, Beach DG, McCarron P, Sivonen K, Fewer DP, Jokela J, Janssen EM-L (2020) Comprehensive database of secondary metabolites from cyanobacteria. BioRxiv:2020.2004.2016.038703
63. Moumbock AFA, Gao M, Qaseem A, Li J, Kirchner Pascal A, Ndingkokhar B, Bekono BD, Simoben CV, Babiaka Smith B, Malange YI, Sauter F, Zierep P, Ntie-Kang F, Günther S (2020) StreptomeDB 3.0: an updated compendium of Streptomycetes natural products. Nucl Acids Res 49:D600
64. Fekete S, Schappler J, Veuthey J-L, Guillarme D (2014) Current and future trends in UHPLC. TrAC, Trends Anal Chem 63:2
65. Blunt JW, Copp BR, Keyzers RA, Munro MHG, Prinsep MR (2012) Marine natural products. Nat Prod Rep 29:144
66. Seger C, Sturm S, Stuppner H (2013) Mass spectrometry and NMR spectroscopy: modern high-end detectors for high resolution separation techniques–state of the art in natural product HPLC-MS, HPLC-NMR, and CE-MS hyphenations. Nat Prod Rep 30:970
67. Esquenazi E, Dorrestein PC, Gerwick WH (2009) Probing marine natural product defenses with DESI-imaging mass spectrometry. 106:7269
68. Yarnold JE, Hamilton BR, Welsh DT, Pool GF, Venter DJ, Carroll AR (2012) High resolution spatial mapping of brominated pyrrole-2-aminoimidazole alkaloids distributions in the marine sponge *Stylissa flabellata* via MALDI-mass spectrometry imaging. Mol Biosyst 8:2249
69. Wang M, Carver JJ, Phelan VV, Sanchez LM, Garg N, Peng Y, Nguyen DD, Watrous J, Kapono CA, Luzzatto-Knaan T, Porto C, Bouslimani A, Melnik AV, Meehan MJ, Liu W-T, Crüsemann M, Boudreau PD, Esquenazi E, Sandoval-Calderón M, Kersten RD, Pace LA, Quinn RA, Duncan KR, Hsu C-C, Floros DJ, Gavilan RG, Kleigrewe K, Northen T, Dutton RJ, Parrot D, Carlson EE, Aigle B, Michelsen CF, Jelsbak L, Sohlenkamp C, Pevzner P, Edlund A, McLean J, Piel J, Murphy BT, Gerwick L, Liaw C-C, Yang Y-L, Humpf H-U, Maansson M, Keyzers RA, Sims AC, Johnson AR, Sidebottom AM, Sedio BE, Klitgaard A, Larson CB, Boya PCA, Torres-Mendoza D, Gonzalez DJ, Silva DB, Marques LM, Demarque DP, Pociute E, O'Neill EC, Briand E, Helfrich EJN, Granatosky EA, Glukhov E, Ryffel F, Houson H, Mohimani H, Kharbush JJ, Zeng Y, Vorholt JA, Kurita KL, Charusanti P, McPhail KL, Nielsen KF, Vuong L, Elfeki M, Traxler MF, Engene N, Koyama N, Vining OB, Baric R, Silva RR, Mascuch SJ, Tomasi S, Jenkins S, Macherla V, Hoffman T, Agarwal V, Williams PG, Dai J, Neupane R, Gurr J, Rodríguez AMC, Lamsa A, Zhang C, Dorrestein K, Duggan BM, Almaliti J, Allard P-M, Phapale P, Nothias L-F, Alexandrov T, Litaudon M, Wolfender J-L, Kyle JE, Metz TO, Peryea T, Nguyen D-T, VanLeer D, Shinn P, Jadhav A, Müller R, Waters KM, Shi W, Liu X, Zhang L, Knight R, Jensen PR, Palsson BØ, Pogliano K, Linington RG, Gutiérrez M, Lopes NP, Gerwick WH, Moore BS, Dorrestein PC, Bandeira N (2016) Sharing and community curation of mass spectrometry data with global natural products social molecular networking. Nat Biotechnol 34:828

70. Yang JY, Sanchez LM, Rath CM, Liu X, Boudreau PD, Bruns N, Glukhov E, Wodtke A, de Felicio R, Fenner A, Wong WR, Linington RG, Zhang L, Debonsi HM, Gerwick WH, Dorrestein PC (2013) Molecular networking as a dereplication strategy. J Nat Prod 76:1686
71. Nothias L-F, Petras D, Schmid R, Dührkop K, Rainer J, Sarvepalli A, Protsyuk I, Ernst M, Tsugawa H, Fleischauer M, Aicheler F, Aksenov AA, Alka O, Allard P-M, Barsch A, Cachet X, Caraballo-Rodriguez AM, Da Silva RR, Dang T, Garg N, Gauglitz JM, Gurevich A, Isaac G, Jarmusch AK, Kameník Z, Kang KB, Kessler N, Koester I, Korf A, Le Gouellec A, Ludwig M, Martin HC, McCall L-I, McSayles J, Meyer SW, Mohimani H, Morsy M, Moyne O, Neumann S, Neuweger H, Nguyen NH, Nothias-Esposito M, Paolini J, Phelan VV, Pluskal T, Quinn RA, Rogers S, Shrestha B, Tripathi A, van der Hooft JJJ, Vargas F, Weldon KC, Witting M, Yang H, Zhang Z, Zubeil F, Kohlbacher O, Böcker S, Alexandrov T, Bandeira N, Wang M, Dorrestein PC (2020) Feature-based molecular networking in the GNPS analysis environment. Nat Methods 17:905
72. Bracegirdle J, Robertson LP, Hume PA, Page MJ, Sharrock AV, Ackerley DF, Carroll AR, Keyzers RA (2019) Lamellarin sulfates from the Pacific tunicate *Didemnum ternerratum.* J Nat Prod 82:2000
73. Yu H-B, Glukhov E, Li Y, Iwasaki A, Gerwick L, Dorrestein PC, Jiao B-H, Gerwick WH (2019) Cytotoxic microcolin lipopeptides from the marine cyanobacterium *Moorea producens*. J Nat Prod 82:2608
74. Teta R, Della Sala G, Esposito G, Via CW, Mazzoccoli C, Piccoli C, Bertin MJ, Costantino V, Mangoni A (2019) A joint molecular networking study of a *Smenospongia* sponge and a cyanobacterial bloom revealed new antiproliferative chlorinated polyketides. Org Chem Front 6:1762
75. Djoumbou-Feunang Y, Pon A, Karu N, Zheng J, Li C, Arndt D, Gautam M, Allen F, Wishart DS (2019) CFM-ID 3.0: Significantly improved ESI-MS/MS prediction and compound identification. Metabolites 9:72
76. Wolf S, Schmidt S, Müller-Hannemann M, Neumann S (2010) In silico fragmentation for computer assisted identification of metabolite mass spectra. BMC Bioinformat 11:148
77. Dührkop K, Shen H, Meusel M, Rousu J, Böcker S (2015) Searching molecular structure databases with tandem mass spectra using CSI:FingerID. Proc Natl Acad Sci USA 112:12580
78. Deyon-Jung L, Morice C, Chéry F, Gay J, Langer T, Frantz M-C, Rozot R, Dalko-Csiba M (2016) Fragment pharmacophore-based in silico screening: a powerful approach for efficient lead discovery. MedChemComm 7:506
79. Buedenbender L, Habener LJ, Grkovic T, Kurtböke Dİ, Duffy S, Avery VM, Carroll AR (2018) HSQC–TOCSY Fingerprinting for prioritization of polyketide- and peptide-producing microbial isolates. J Nat Prod 81:957
80. Zhang C, Idelbayev Y, Roberts N, Tao Y, Nannapaneni Y, Duggan BM, Min J, Lin EC, Gerwick EC, Cottrell GW, Gerwick WH (2017) Small molecule accurate recognition technology (SMART) to enhance natural products research. Sci Rep 7:14243
81. Dias DA, Urban SJJoss (2009) Application of HPLC-NMR for the rapid chemical profiling of a southern Australian sponge, *Dactylospongia* sp. 32:542
82. Jaroszewski JW (2005) Hyphenated NMR methods in natural products research, 2: HPLC-SPE-NMR and other new trends in NMR hyphenation. Planta Med 71:795
83. Timmers MA, Dias DA, Urban S (2012) Application of HPLC-NMR in the identification of plocamenone and isoplocamenone from the marine red alga *Plocamium angustum.* Mar Drugs 10:2089
84. Urban S, Timmers M (2013) HPLC-NMR Chemical profiling and dereplication studies of the marine brown alga, *Cystophora torulosa.* Nat Prod Commun 8:715
85. Zani CL, Carroll AR (2017) Database for rapid dereplication of known natural products using data from MS and fast NMR experiments. J Nat Prod 80:1758

86. Reher R, Kim HW, Zhang C, Mao HH, Wang M, Nothias L-F, Caraballo-Rodriguez AM, Glukhov E, Teke B, Leao T, Alexander KL, Duggan BM, Van Everbroeck EL, Dorrestein PC, Cottrell GW, Gerwick WH (2020) A convolutional neural network-based approach for the rapid annotation of molecularly diverse natural products. J Am Chem Soc 142:4114
87. Mohimani H, Pevzner PA (2016) Dereplication, sequencing and identification of peptidic natural products: from genome mining to peptidogenomics to spectral networks. Nat Prod Rep 33:73
88. Udwary DW, Zeigler L, Asolkar RN, Singan V, Lapidus A, Fenical W, Jensen PR, Moore BS (2007) Genome sequencing reveals complex secondary metabolome in the marine actinomycete *Salinispora tropica.* Proc Natl Acad Sci USA 104:10376
89. Kautsar SA, Blin K, Shaw S, Navarro-Muñoz JC, Terlouw BR, van der Hooft JJJ, van Santen JA, Tracanna V, Suarez Duran HG, Pascal Andreu V, Selem-Mojica N, Alanjary M, Robinson SL, Lund G, Epstein SC, Sisto AC, Charkoudian LK, Collemare J, Linington RG, Weber T, Medema MH (2020) MIBiG 2.0: a repository for biosynthetic gene clusters of known function. Nucl Acids Res 48:D454
90. Robey MT, Caesar LK, Drott MT, Keller NP, Kelleher NL (2020) An interpreted atlas of biosynthetic gene clusters from 1000 fungal genomes. BioRxiv 2020.2009.2021.307157
91. Schniete JK, Selem-Mojica N, Birke AS, Cruz-Morales P, Hunter IS, Barona-Gomez F, Hoskisson PA (2021) ActDES – a curated actinobacterial database for evolutionary studies. Microb Genom 7:498
92. Blin K, Shaw S, Kautsar SA, Medema MH, Weber T (2020) The antiSMASH database version 3: increased taxonomic coverage and new query features for modular enzymes. Nucl Acids Res 49:D639
93. Palaniappan K, Chen I-MA, Chu K, Ratner A, Seshadri R, Kyrpides NC, Ivanova NN, Mouncey NJ (2019) IMG-ABC v.5.0: an update to the IMG/atlas of biosynthetic gene clusters knowledgebase. Nucl Acids Res 48:D422
94. Skinnider MA, Johnston CW, Gunabalasingam M, Merwin NJ, Kieliszek AM, MacLellan RJ, Li H, Ranieri MRM, Webster ALH, Cao MPT, Pfeifle A, Spencer N, To QH, Wallace DP, Dejong CA, Magarvey NA (2020) Comprehensive prediction of secondary metabolite structure and biological activity from microbial genome sequences. Nat Commun 11:6058
95. Agrawal P, Mohanty D (2020) A machine learning-based method for prediction of macrocyclization patterns of polyketides and non-ribosomal peptides. Bioinformatics Oct3, btaa851
96. Robinson SL, Terlouw BR, Smith MD, Pidot SJ, Stinear TP, Medema MH, Wackett LP (2020) Global analysis of adenylate-forming enzymes reveals lactone biosynthesis pathway in pathogenic *Nocardia.* J Biol Chem 295:14826
97. Saporito RA, Donnelly MA, Norton RA, Garraffo HM, Spande TF, Daly JW (2007) Oribatid mites as a major dietary source for alkaloids in poison frogs. Proc Natl Acad Sci USA 104:8885
98. Fahey SJ, Garson MJ (2002) Geographic variation of natural products of tropical nudibranch *Asteronotus cespitosus.* J Chem Ecol 28:1773
99. Swinney DC, Anthony J (2011) How were new medicines discovered? Nat Rev Drug Disc 10:507
100. Wilson BAP, Thornburg CC, Henrich CJ, Grkovic T, O'Keefe BR (2020) Creating and screening natural product libraries. Nat Prod Rep 37:893
101. Futamura Y, Muroi M, Osada H (2013) Target identification of small molecules based on chemical biology approaches. Mol Biosyst 9:897
102. Liu M, Van Voorhis WC, Quinn RJ (2021) Development of a target identification approach using native mass spectrometry. Sci Rep 11:2387
103. Strömstedt AA, Felth J, Bohlin L (2014) Bioassays in natural product research – strategies and methods in the search for anti-inflammatory and antimicrobial activity. Phytochem Anal 25:13
104. Nothias L-F, Nothias-Esposito M, da Silva R, Wang M, Protsyuk I, Zhang Z, Sarvepalli A, Leyssen P, Touboul D, Costa J, Paolini J, Alexandrov T, Litaudon M, Dorrestein PC (2018) Bioactivity-based molecular networking for the discovery of drug leads in natural product bioassay-guided fractionation. J Nat Prod 81:758

105. Wolfender J-L, Litaudon M, Touboul D, Queiroz EF (2019) Innovative omics-based approaches for prioritisation and targeted isolation of natural products – new strategies for drug discovery. Nat Prod Rep 36:855
106. Jennings LK, Khan NMD, Kaur N, Rodrigues D, Morrow C, Boyd A, Thomas OP (2019) Brominated bisindole alkaloids from the Celtic sea sponge *Spongosorites calcicola*. Molecules 24:3890
107. Calabro K, Jennings LK, Lasserre P, Doohan R, Rodrigues D, Reyes F, Ramos C, Thomas OP (2020) Nebulosins: trisubstituted thiolane natural products from the northeastern Atlantic annelid *Eupolymnia nebulosa*. J Org Chem 85:14026
108. Sarker SD, Latif Z, Gray AI (eds) (2006) Natural products isolation, 2 edn. (Methods in Biotechnology, vol 20). Humana Press Inc., Totowa, NJ, USA
109. Burns DC, Mazzola EP, Reynolds WF (2019) The role of computer-assisted structure elucidation (CASE) programs in the structure elucidation of complex natural products. Nat Prod Rep 36:919
110. Guillen PO, Jaramillo KB, Genta-Jouve G, Sinniger F, Rodriguez J, Thomas OP (2017) Terrazoanthines, 2-aminoimidazole alkaloids from the tropical eastern Pacific zoantharian *Terrazoanthus onoi*. Org Lett 19:1558
111. Carroll AR, Copp BR, Davis RA, Keyzers RA, Prinsep MR (2020) Marine natural products. Nat Prod Rep 37:175
112. Mándi A, Kurtán T (2019) Applications of OR/ECD/VCD to the structure elucidation of natural products. Nat Prod Rep 36:889
113. Smith SG, Goodman JM (2010) Assigning stereochemistry to single diastereoisomers by GIAO NMR calculation: the DP4 probability. J Am Chem Soc 132:12946
114. Grimblat N, Zanardi MM, Sarotti AM (2015) Beyond DP4: an improved probability for the stereochemical assignment of isomeric compounds using quantum chemical calculations of NMR shifts. J Org Chem 80:12526
115. Grimblat N, Gavín JA, Hernández Daranas A, Sarotti AM (2019) Combining the power of *J* coupling and DP4 analysis on stereochemical assignments: the *J*-DP4 Methods. Org Lett 21:4003
116. Howarth A, Ermanis K, Goodman JM (2020) DP4-AI automated NMR data analysis: straight from spectrometer to structure. Chem Sci 11:4351
117. Kersten RD, Lee S, Fujita D, Pluskal T, Kram S, Smith JE, Iwai T, Noel JP, Fujita M, Weng J-K (2017) A red algal bourbonane sesquiterpene synthase defined by microgram-scale NMR-coupled crystalline sponge X-ray diffraction analysis. J Am Chem Soc 139:16838
118. Mahajan N, Chadda R, Calabro K, Solanki H, O' Connell E, Murphy PV, Thomas OP (2017) Isolation and synthesis of pygmanilines, phenylurea derivatives from the northeastern Atlantic lichen *Lichina pygmaea*. Tetrahedron Lett 58:1237
119. Firsova D, Calabro K, Lasserre P, Reyes F, Thomas OP (2017) Isoguanosine derivatives from the northeastern Atlantic sponge *Clathria* (*Microciona*) *strepsitoxa*. Tetrahedron Lett 58:4652
120. Afoullouss S, Calabro K, Genta-Jouve G, Gegunde S, Alfonso A, Nesbitt R, Morrow C, Alonso E, Botana LM, Allcock AL, Thomas OP (2019) Treasures from the deep: Characellides as anti-inflammatory lipoglycotripeptides from the sponge *Characella pachastrelloides*. Org Lett 21:246

Maggie M. Reddy is a postdoctoral researcher at the National University of Galway, Ireland. Her passion for the sea began as a little girl exploring the seashores of southern KwaZulu-Natal. She graduated with a Ph.D. degree in Marine Biology from the University of Cape Town in South Africa working in collaboration with the University of Ghent in Belgium. Her doctoral research revealed extensive species diversity including new and cryptic species in the Bangiales, an economically valuable group of seaweeds. Her main research focuses on marine biodiversity, taxonomy and molecular systematics. She has extensive experience in marine biodiversity collections having sampled much of the southern African coast from southern Mozambique to southern Angola.

Laurence Jennings obtained a Bachelor of Marine Science degree from Griffith University, Gold Coast, Australia. He then continued his studies completing a Ph.D. degree in marine natural products chemistry under the supervision of Prof. Anthony R. Carroll. Since 2018 he has held a postdoctoral research position at the National University of Ireland Galway within the group of Prof Olivier P. Thomas. This postdoctoral position, funded by the Marine Institute, has focused on the development of a biodiscovery laboratory and the investigation of secondary metabolites with pharmacological properties from Irish coastal organisms. His main research interests are the isolation and identification of bioactive marine natural products. He has a particular interest in the structural elucidation of complex natural products using NMR spectroscopic and computational methods.

Olivier P. Thomas has an Established Chair in Marine Biodiscovery at the National University of Ireland, Galway (NUIG). In 2002, he obtained a Ph.D. degree in medicinal chemistry from the University of René Descartes Paris. After two years as a post-doctoral researcher in biochemistry at the CEA Saclay in France, he was recruited as a lecturer in marine natural product chemistry at the University of Côte d'Azur, France. Following his passion for the oceans and their hidden treasures, he moved to the island of Ireland where he is leading the marine biodiversity group at NUIG. The research focus of the laboratory is the chemistry of marine metabolites with an emphasis on drug discovery but also biotoxins and chemical ecology through the use of environmental metabolomics.

The Chemistry and Chemical Ecology of Lepidopterans as Investigated in Brazil

Karina L. Silva-Brandão, André V. L. Freitas, Márcio Zikán Cardoso, Rodrigo Cogni, and Ana Beatriz Barros de Morais

Contents

K. L. Silva-Brandão (✉)
Centro de Biologia Molecular e Engenharia Genética, Universidade Estadual de Campinas, Av. Candido Rondom, 400, Campinas, SP, Brazil
e-mail: klsilva@gmail.com

A. V. L. Freitas
Departamento de Biologia Animal and Museu da Diversidade Biológica, Instituto de Biologia, Universidade Estadual de Campinas, Rua Monteiro Lobato, 255, Campinas, SP, Brazil
e-mail: baku@unicamp.br

M. Z. Cardoso
Departamento de Ecologia, Universidade Federal do Rio de Janeiro, Av. Carlos Chagas Filho, 373, Rio de Janeiro, RJ CEP 21941-902, Brazil
e-mail: marciozikan@gmail.com

R. Cogni
Departamento de Ecologia, Instituto de Biociências, Universidade de São Paulo, Rua do Matão, 321, São Paulo, SP CEP 05508-090, Brazil
e-mail: rodrigocogni@gmail.com

A. B. B. de Morais
Rua Major Duarte 855 ap 1002, Santa Maria, RS, Brazil
e-mail: abbdemorais@gmail.com

A. D. Kinghorn, H. Falk, S. Gibbons, Y. Asakawa, J.-K. Liu, V. M. Dirsch (eds.),
Progress in the Chemistry of Organic Natural Products 116,
https://doi.org/10.1007/978-3-030-80560-9_2

1 Introduction

The investigation of chemical communication among species and the identification of the chemical compounds involved in such interactions is within the field of chemical ecology. This includes the elucidation of the chemical substances involved in insect–plant interactions. According to Ref. [1], the roots of chemical ecology reach back as far as 300 BCE (revised in [2]), but much more time passed before the first studies on insect communication were conducted. One of the earliest descriptions of the role of chemicals compounds in mediating these interactions dates back to 1959 with the identification of the sex pheromone bombykol of the female silkworm *Bombyx mori* by A. Butenandt [3]. The first studies on chemical ecology in Brazil were conducted in the decades of the 1950s and 1960s at the Instituto de Química Agrícola of the Federal University of Rio de Janeiro (UFRJ). The main researchers involved included Walter Mors, Otto Gottlieb, Benjamin Gilbert, and Bernard Tursch [3]. The interdisciplinary field of chemical ecology in Brazil is currently followed by groups that emerged from the pioneering studies of Keith Spalding Brown Jr. and José Tércio Barbosa Ferreira (who established the area of total synthesis of insect pheromones at the Universidade Federal de São Carlos) [4], although the field is currently dominated by applied agricultural studies. The following subsections will provide accounts of the work of two towering representatives of Brazilian chemical ecology research, Keith S. Brown Jr. and José Roberto Trigo.

1.1 Keith S. Brown Jr.

Keith S. Brown Jr. (born in 1938) (Fig. 1) graduated from California Institute of Technology (Caltech) with a major in Chemistry in 1959, having obtained a scholarship from the Alfred P. Sloan Foundation. During his junior year, he spent three months on a mission to the Philippines, which he described to DuPont, the chemical company that financed his mission as "of such importance to my future that it must be realized" (his emphasis). Clearly, this experience, which included both religious and scientific activities (the study of traditional medicines), was a turning point and helped shape Brown's future career decisions, including the choice of his Ph.D. degree topic (alkaloids of the boxwood plant) at the University of Wisconsin–Madison, and the later decision to move abroad. After completing his Ph.D. degree under the direction of Prof. S. Morris Kupchan in Organic and Pharmaceutical Chemistry in 1962, funded by an NSF grant, he proceeded to carry out research in the chemistry of natural and pharmaceutical products (particularly alkaloids) in Prof. Carl Djerassi's laboratory at Stanford University, with a NIH fellowship. In 1964, after already having decided to move to Pakistan to work at the Forman Christian College together with his wife, he received an offer to continue his research on the chemistry of natural products at the "Centro de Pesquisas de Produtos Naturais" of the Pharmacy and Biochemistry

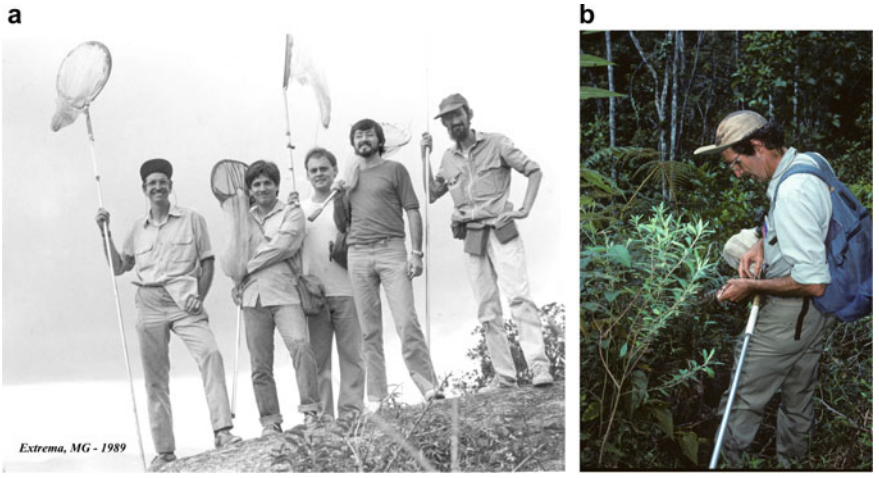

Fig. 1 **a** Professor Keith Brown Jr. with his students in an expedition to collect butterflies in Extrema, Minas Gerais, SE Brazil, in 1989. From left to right: Keith Brown, André V. L. Freitas, Clécio F. Klitzke, Paulo C. Motta, and Ronaldo B. Francini (Photo courtesy by Ronaldo B. Francini); **b** Keith Brown collecting butterflies in Santa Teresa, Espírito Santo, Brazil, in April 1988

Faculty of the Federal University of Rio de Janeiro (UFRJ). By that time, the chemistry of natural products in Brazil was greatly boosted by the work of Walter Mors and his supervisor, Carl Djerassi. Djerassi, with the American Chemical Society, recommended some ex-students to work with Mors in Rio de Janeiro as part of a joint research and training program of Stanford University and UFRJ. Professor Benjamin Gilbert came first to conduct postdoctoral research with Djerassi. Brown arrived as a postdoctoral fellow and moved with his family to Brazil in late July 1964. He immediately began teaching and developing laboratory and field work in the forests surrounding Rio de Janeiro. As a legacy of his interest in natural history, bird watching and collecting butterflies, Keith Brown started to do a series of collecting trips in the surroundings of Rio de Janeiro, including the large forest area of "Floresta da Tijuca", the nearby mountains of Petrópolis and Teresópolis, and some lowland forest areas in the region of the former State of Guanabara (now part of Rio de Janeiro). Using collected material from these initial collecting trips, Brown published his first study on Lepidoptera, describing a new L-α-amino acid, 3-hydroxykynurenine, from the light yellow pigmented areas of the wings and bodies of Ithomiini and Heliconiini butterflies [5]. During these first years in Brazil, the indications that Brown's career would eventually change to butterfly ecology and natural history became clearer, but during the succeeding years his contribution to the chemical ecology of Neotropical butterflies were enormous, and his publications served as the foundations for several research lines in Brazil and abroad. Moreover, Keith Brown Jr. had a notable capacity for combining research areas, and this was clear with his publication associating the presence of 3-hydroxykynurenine with butterfly systematics [6] and from another

study suggesting that aposematic butterflies could serve as indicators of plants that exhibit active and potentially interesting pharmacological substances [7].

After working for nearly ten years on soft money at UFRJ, mainly from research grants and fellowships obtained from the USA (Rockefeller Foundation, Mellon Foundation), Brown accepted a permanent teaching/research position at the University of Campinas (UNICAMP) in 1973. During his career, Brown's main contributions in chemical ecology included studies on several groups of aposematic butterflies, including Troidini swallowtails (Papilionidae) and the clearwing butterflies in the Danainae tribe Ithomiini (Nymphalidae). Other less-studied groups included the Nymphalidae tribes Acraeini (Heliconiinae), Danaini and Tellervini (Danainae), and tiger moths (Erebidae: Arctiinae).

1.2 José Roberto Trigo

After his undergraduate degree in Biology at the University of São Paulo, José Roberto Trigo (1956–2017) (Fig. 2) worked for his Master's thesis in Ecology between 1984 and 1988 under Keith Brown's supervision studying the interaction between Ithomiini butterflies and their host plants that are mediated by pyrrolizidine alkaloids (PAs). This was the beginning of the lifetime work of Trigo on plant secondary metabolites and insect defense interactions, including the publication of ca. of 80 scientific papers and book chapters and the supervision of more than 30 students. Whereas Brown moved from chemistry to natural history, biology, and systematics of butterflies—although he had frequently combined the theory and practice of both areas in his studies—Trigo followed in the opposite direction and carried out his doctoral studies in chemistry at the UNICAMP, under the supervision of Dr.

Fig. 2 José Roberto Trigo (Photo courtesy by Gustavo Shimizu)

Lauro E. Soares Barata, in collaboration with Brown [8]. His degree in chemistry, followed by a postdoctoral position in Thomas Hartmann's laboratory at the Technische Universität Braunschweig, Germany, in the 1990s, allowed Trigo to apply a strong chemical approach to answer ecological and behavioral questions in insect–host plant interaction mediated by plant secondary compounds (infochemicals) [9], mainly pyrrolizidine alkaloids. In 1997, Trigo became a lecturer at UNICAMP and leader of the Chemical Ecology Laboratory, following Brown's retirement, who was the former head of this laboratory [8].

The combined influence of Keith Brown Jr. and José R. Trigo to the chemical ecology field in Brazil is indisputable. Herein, are presented an overview of their contributions to insect–plant interactions as mediated by plant natural products, an area where both these scientist–teachers dominated and contributed to the development of several younger professional colleagues throughout their lifetimes.

2 Pyrrolizidine Alkaloids

Brown's first contributions on alkaloids included several publications on the extraction, purification, and structural characterization of steroidal, bisbenzylisoquinoline, indole, and lactone alkaloids, mainly from the shrub *Buxus sempervirens* (boxwood; Buxaceae), a plant used in ethnomedicine to treat malaria and other diseases [10]. Also, other plants containing alkaloids were investigated in the decades of the 1960s and 1970s [11–19]. The statement that "Alkaloids hold many secrets of life" [20] summarizes succinctly the importance of these compounds both for plants and animals. Alkaloids are organic compounds derived from amino acids of L-configuration (proteinaceous amino acids) and from non-proteinaceous amino acids such as ornithine [21]. They are found in Nature in the leaves, fruits, roots, and stems of plants as secondary metabolites [22], as well as in some animals and microorganisms [23]. Alkaloids usually have a basic nitrogen atom or atoms in a heterocyclic ring system and are classified according to their different rings and chemical structures, biological activities, and biosynthesis pathways [23]. The pH-neutral compounds of this type may be found in plant tissues as water-soluble salts of organic and inorganic acids and esters, or combined with tannins or sugars, and their free bases are generally soluble in nonpolar organic solvents, such as chloroform, methylene chloride, and diethyl ether [23]. More than 27,000 alkaloids are currently known [22, 23].

The bitter taste associated with alkaloids in plants suggests that they are protective from attacks by herbivory animals and these compounds indeed provide a general plant defense mechanism [22, 24–26]. Due to their intimate role of mediating plant–insects associations, alkaloids are believed to perform a central role in the evolution of these interactions since the sequestration of plant alkaloids by insects might provide defense against predation and have key roles in their own metabolism and life cycle [20, 26]. They may also have key roles in the life processes of some invertebrates as pheromones, inducers of sexual behavior, and in reproduction [26]. Additionally,

alkaloids may act as growth stimulators and inhibitors in plants and as storage reservoirs of nitrogen [20, 24]. These compounds are also of great human interest due to their activities as anti-inflammatory, antibacterial, antimitotic, analgesic, anesthetic, hypnotic, psychotropic, and antitumor metabolites [22]. Morphine, a strong analgesic, was the first alkaloid to be isolated from opium poppies [22, 25].

In an important revision about this subject, Brown and Trigo reviewed several questions on the dynamics of the in vivo activity of alkaloids in ecosystems [27]. They focused on several alkaloid-related questions in this publication, such as the variation of alkaloid structures and storage in different parts of organisms and among individuals, populations, species, genera, families and higher taxa; the differential production and accumulation of different types of alkaloids; their qualitative and quantitative variation in plants; the role of alkaloids in communication and chemical defense in microorganisms, plants, and animals; the importance of alkaloids in intraspecific communication; and the multiple activities and roles of alkaloids in Nature and their use by humankind. They also presented several ecological activities reported for the different structural classes of alkaloids.

Brown's, and later Trigo's studies with pyrrolizidine alkaloids were by far their main contributions to the area of chemical ecology, and mainly concerned the role of pyrrolizidine alkaloids in mediating associations among insects and plants. These elegant studies approached both chemical techniques applied to the extraction and characterization of pyrrolizidine alkaloids and chemically mediated ecological questions. Pyrrolizidine alkaloids originate from the amino acids L-ornithine or L-arginine and occur as the esters of 1-hydroxymethylpyrrolizidines (necines) and necic acids [23]. They are structurally characterized by two five-membered rings with a bridgehead nitrogen atom and can be categorized into three major types: as derivatives of retronecine (e.g., senecionine (**1**)), heliotrine (e.g., heliotridine (**2**)), and otonecine (e.g., senkirkine (**3**)) [23] (Fig. 3). Pyrrolizidine alkaloids are found in insects and in the seeds, leaves, and flowering parts of plants of the families Asteraceae, Boraginaceae, and Fabaceae, as well as in 15 other plant families [28], where they are often accumulated as *N*-oxides (except for the otonecine type of pyrrolizidine alkaloids) [23, 27–29]. The genera *Crotalaria* (Fabaceae) and *Senecio* (Asteraceae) are particularly rich in pyrrolizidine alkaloids [21]. Culvenor [30] classified pyrrolizidine alkaloids into three major classes (Fig. 3):

(a) aliphatic monocarboxylic esters (found in plants of the family Boraginaceae);
(b) aromatic and aralkyl esters (Orchidaceae);
(c) macrocyclic diesters (Asteraceae and Fabaceae).

Ratmanova and collaborators [31] reviewed the innumerable strategic approaches to the synthesis of pyrrolizidine alkaloids. More than 350 different pyrrolizidine alkaloids have been identified so far and they are known for causing variable adverse effects in animals and humans [23].

In one of the most fascinating insect–plant chemically-mediated interactions, pyrrolizidine alkaloids are sequestered from host plants by specialized insects, such as nymphalid butterflies of the tribes Danaini and Ithomiini (subfamily Danainae) and Arctiinae moths (Erebidae), and used as a form of chemical defense against

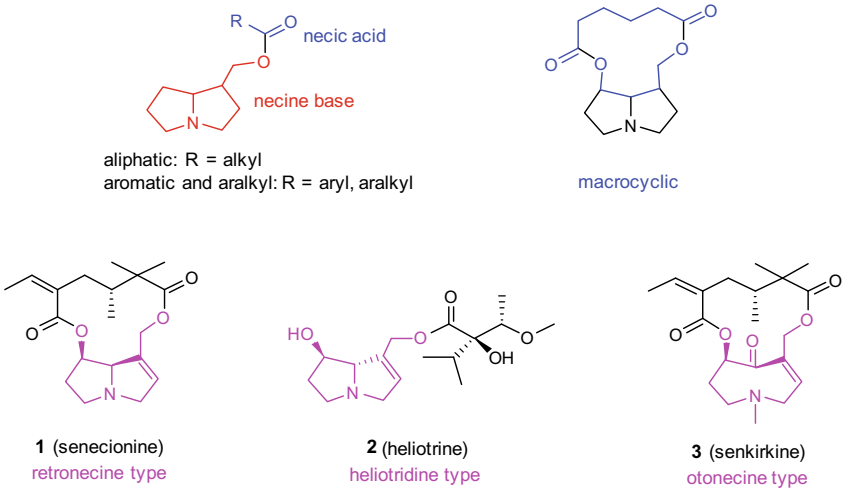

Fig. 3 Major classes and types of pyrrolizidine alkaloids

their predators (Fig. 4). Moths of the species *Tyria jacobaeae* (family Erebidae), for instance, are able to detoxify pyrrolizidine alkaloids from their host plant, *Senecio jacobaea* (Asteraceae) and use the highly toxic pyrrole moieties present in their gut against predators [25]. Additionally, butterflies of the genus *Danaus* (tribe Danaini) sequester and accumulate pyrrolizidine alkaloids throughout their adulthood and use them as pheromone precursors in a well-characterized association [26]. Other pyrrolizidine alkaloids derivatives (**4**–**18**) were also identified in Ithomiini butterflies (Fig. 5) [32].

Pyrrolizidine alkaloids can protect pyrrolizidine alkaloid-feeding insects from both invertebrate and vertebrate predators: the pure pyrrolizidine alkaloid monocrotaline (**19**) (mainly found in plants of the genus *Crotalaria*) (Fig. 6) is indeed unpalatable to the pileated finch, *Coryphospingus pileatus* (Emberizidae), and the birds were even able to recognize subsequent prey as unpalatable items after their experience in previous encounters [33].

Brown's first contributions to the field of chemical ecology focused on the sequestration of pyrrolizidine alkaloids by Lepidoptera and were published in the decade of the 1980s [34, 35]. These publications discussed the role of pyrrolizidine alkaloids in the protection of butterflies against golden orb-weaving spiders *Trichonephila clavipes* (previously known as *Nephila clavipes*) (Araneidae, Tetragnathinae), a model predator that became used recurrently in pyrrolizidine alkaloid bioassays in later years [36–40] (Fig. 7; Box 1). *Trichonephila clavipes* and other species within the genus *Nephila* show very specific types of predatory behavior toward their prey, with the most conspicuous being to cut unpalatable items of prey out of its web, and then to release them unharmed [41]. Ithomiini and some Danaini butterflies (which have pyrrolizidine alkaloids), for instance, are almost always released unharmed from *T. clavipes*' webs after the spider touches (with the tarsi) and palpates (with

Fig. 4 Species of Lepidoptera involved in pyrrolizidine alkaloid-mediated interactions. **a** *Aeria olena olena*; **b** *Tithorea harmonia pseudethra* (Photo courtesy: Ricardo Costa); **c**, **d** Grouped aposematic larvae and an adult of *Placidina euryanassa* feeding on a pyrrolizidine alkaloid-rich nectar source, *Adenostemma* sp. (Asteraceae), respectively; **e** *Mechanitis polymnia casabranca* (Nymphalidae: Danainae: Ithomiini); **f** Larva of *Utetheisa ornatrix* (Erebidae: Arctiinae) feeding on a fruit of *Crotalaria* sp. (Fabaceae) (Photos: A.V.L.F.)

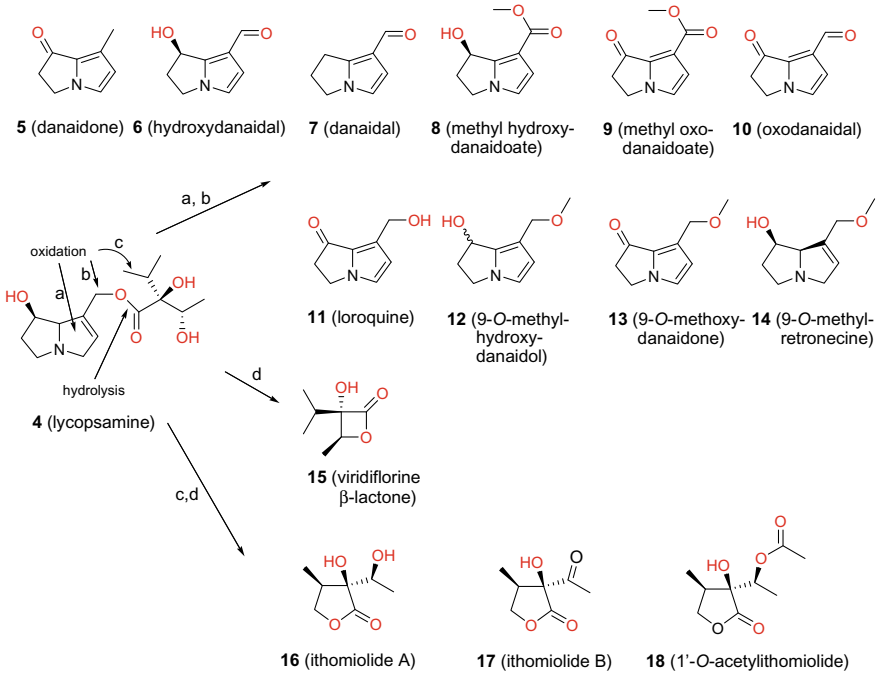

Fig. 5 Pyrrolizidine alkaloid derivatives (Modified from [32])

Fig. 6 Pyrrolizidine alkaloid used in assays with a vertebrate predator [33]

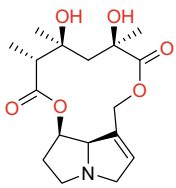

19 (monocrotaline)

the pedipalps) any part of their body or wings, while other pyrrolizidine alkaloid-free butterflies are usually subjected to predation [42]. Moreover, Brown was the first to show unequivocally that contrary to "common sense", ithomiines sequester those pyrrolizidine alkaloids used for their protection from adult nectar sources, and not from their larval host plants [34, 36]. Later on, Brown, Trigo, and collaborators showed that in some cases, ithomiines can sequester protective substances from their host plants (see below), including pyrrolizidine alkaloids (in some apocynaceous feeding species) and tropane alkaloids in *Placidina euryanassa*, of which the larvae are also aposematic [43] (Fig. 4).

Brown and Trigo published their first study together focusing on the pyrrolizidine alkaloid-mediated interactions between Ithomiini butterflies and their host plants

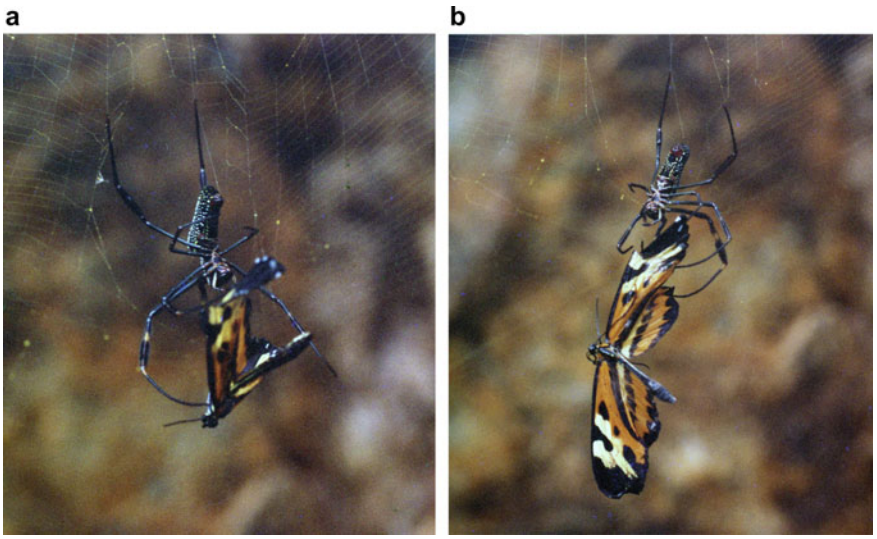

Fig. 7 *Trichonephila clavipes* typical behavior toward unpalatable butterflies. **a** When the Ithomiini butterfly of the species *Mechanitis polymnia* falls on the web of *T. clavipes* the spider touches (with the tarsi) and palpates (with the pedipalps) the butterfly. If the prey is considered unacceptable, it is cut off from the web; **b** The unacceptable adult butterfly is then released unharmed from the web (Photos: K.L.S.-B.)

[44]. In this study, they presented Trigo's dissertation research work results on differences in patterns of pyrrolizidine alkaloid content in three species of Ithomiini over several months, pointing out that such differences must be due to the dynamics of pyrrolizidine alkaloid incorporation in these species. They considered that this quantitative variation is dependent on pyrrolizidine alkaloid sources, such as larval food plants, nectar, or adult food resources. In a following publication, they reported the evolutionary implications of pyrrolizidine alkaloid assimilation by the larval forms of Danaini and Ithomiini butterflies and suggested that such assimilation is maintained by selective pressures on the adults, such as predation and sexual selection [45]. Trigo and Motta [45] were able to show that larvae of danaine and ithomiine butterflies can assimilate purified pyrrolizidine alkaloids painted on their larval host plants.

Trigo pursued this line of inquiry during his Ph.D. degree work in chemistry under Dr. Lauro Barata's supervision in Brazil and Dr. Thomas Hartmann's in Germany, by quantitatively and qualitatively characterizing pyrrolizidine alkaloids in lepidopterans. One of the models investigated was the arctiid moth *Hyalurga syma* (Erebidae: Arctiinae: Pericopinae), which sequesters pyrrolizidine alkaloids from its larval food plant *Heliotropium transalpinum* (Boraginaceae) and is still capable of modifying plant-derived pyrrolizidine alkaloids [37]. Some species were also shown to be able to perform stereochemical inversion of pyrrolizidine alkaloids from (7*S*)-OH to (7*R*)-OH, such as the Ithomiini butterfly *Mechanitis polyminia*

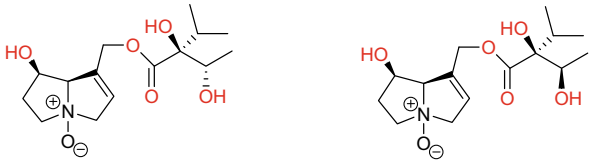

20 (lycopsamine *N*-oxide) **21** (intermedine *N*-oxide)

Fig. 8 Principal pyrrolizidine alkaloid structures found in 40 species in 38 genera of Ithomiini, stored as their *N*-oxide derivatives [47]

[46] (Fig. 4). Following this, a further 40 species in 38 genera of Ithomiini were assessed for their pyrrolizidine alkaloid content by gas chromatography-mass spectrometry (GC–MS) and the principal compounds found in them were the epimers lycopsamine (**20**) and intermedine (**21**), stored as the corresponding *N*-oxides [47] (Fig. 8). The larval and adult feeding strategies of Ithomiini butterflies were investigated in other two species in addition to *M. polyminia*, namely, *Tithorea harmonia* and *Aeria olena* [35] (Fig. 5), with each showing variable feeding habits. Larvae of *M. polyminia* feed on several pyrrolizidine alkaloid-free *Solanum* species, while adult males sequester pyrrolizidine alkaloids from various plant sources. *Tithorea harmonia* sequesters pyrrolizidine alkaloids from their larval food plant *Prestonia acutifolia* (Apocynaceae: Echitoideae) and adults may also obtain these compounds from plant sources. Finally, larvae of *A. olena* feed on *Prestonia coalita*, a plant that biosynthesizes pyrrolizidine alkaloids. The concentration of pyrrolizidine alkaloids found in freshly emerged adults of these species was also shown to be associated with the protection efficiency against *T. clavipes*.

The characterization of several different structures of pyrrolizidine alkaloids was reported for other Ithomiini butterflies throughout several of Trigo's collaborative publications with colleagues and students, as in two species that feed on *Brugmansia suaveolens* as larvae, *Placidina euryanassa* (which sequesters tropane alkaloids from its larval host plant) (Fig. 4) and *Pagyris cymothoe* [43]. The same approach was applied to investigate qualitatively larvae and adults of the Ithomiini *Tellervo zoilus*, which sequesters pyrrolizidine alkaloids from its larval food plant, the apocynaceous vine *Parsonsia straminea*, and stores them in all life cycle stages, mainly as *N*-oxides [48].

An elegant experiment with radioactively-labeled pyrrolizidine alkaloids, using [^{14}C]rinderine (**22**) (free base) and [^{14}C]senecioylretronecine (free base) (**23**) (Fig. 9), was developed by Trigo and Bruckman [49] to investigate the specificity and mechanisms of uptake, metabolism, and storage of pyrrolizidine alkaloids in alkaloid-sequestering ithomiine butterflies. They fed adults of *Mechanitis polymnia* butterflies with the tracers dissolved in a saturated sugar solution (Fig. 10). After recovering the labeled pyrrolizidine alkaloids, they confirmed that the labeled rinderine was efficiently N-oxidized. Senecioylretronecine (**23**), however, is metabolized in a different manner. The authors were able to show the capability of these butterflies to sequester

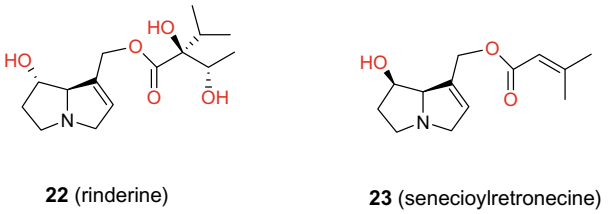

22 (rinderine) **23** (senecioylretronecine)

Fig. 9 Radioactively labeled pyrrolizidine alkaloids [49]

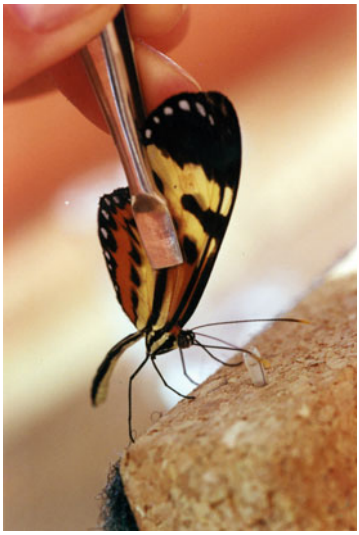

Fig. 10 *Mechanitis polymnia* fed on a saturated sugar solution. (Photo: K.L.S.-B.)

and partly N-oxidize labeled pyrrolizidine alkaloids, as well their inefficiency in storing them.

The association among different pyrrolizidine alkaloid structures at variable concentrations and their defensive role against *T. clavipes* was investigated by testing both the free base and *N*-oxide forms of six pyrrolizidine alkaloids [39]. Methanolic solutions of these different pyrrolizidine alkaloids at specific concentrations were applied to dead bees, which subsequently were offered to *T. clavipes* (Fig. 11). The capture/release typical response of *T. clavipes* spiders toward their prey was indeed associated with both to the pyrrolizidine alkaloid structure and concentration.

The association between the arctiid "ornate bella" moth *Utetheisa ornatrix* and their host plants of the genus *Crotalaria* (Fabaceae), beautifully described by Thomas Eisner [50], was explored largely by Trigo's research group. Pyrrolizidine alkaloids are sequestered from *Crotalaria* spp. by *U. ornatrix*, mainly from unripe seeds (which show a higher concentration of pyrrolizidine alkaloids when compared to plant leaves) (Fig. 4), and were also suggested to protect the moths against predation by *T. clavipes*, although they are unprotected from predation by two ant species [40].

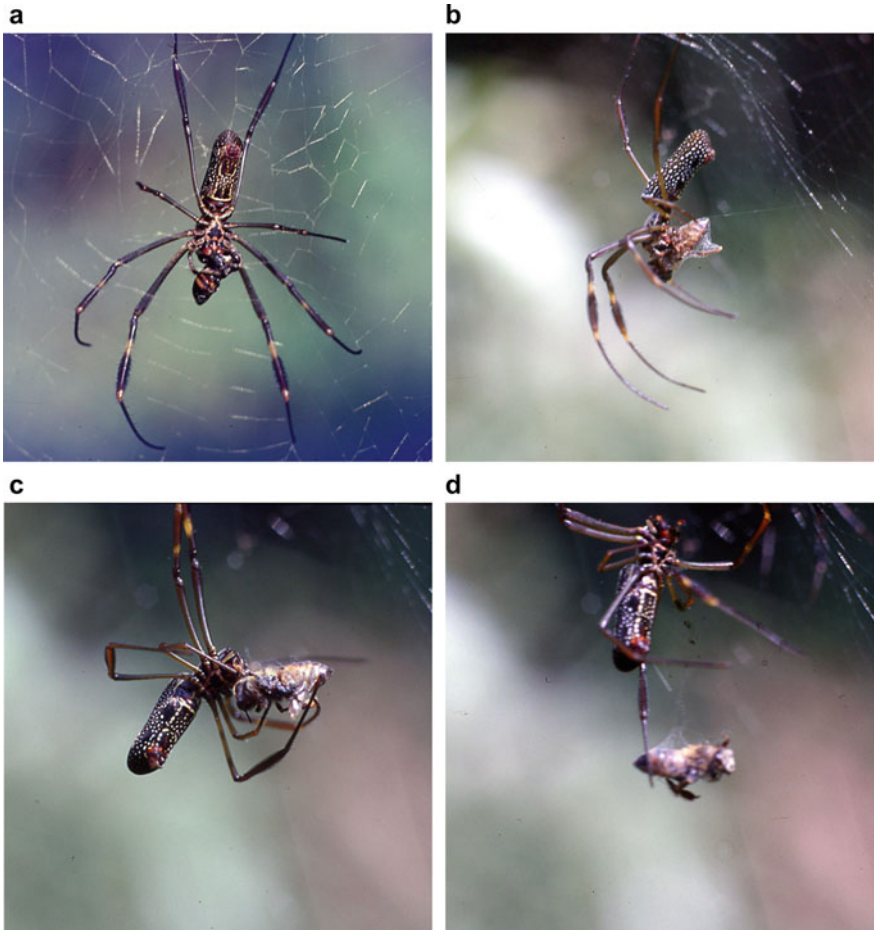

Fig. 11 Behavior of *Trichonephila clavipes* toward methanolic solutions of different pyrrolizidine alkaloid structures at specific concentrations applied to dead bees. **a** A dead bee is thrown on to the *T. clavipes* web; **b–c** If the prey is accepted it is carried to the center of the web and handled by the spider; **d** Otherwise, if the prey is unacceptable, it is released from the web (Photos: K.L.S.-B.)

The defensive mechanism against *T. clavipes* is dose-dependent and *U. ornatrix* also shows an exclusive insect pyrrolizidine alkaloid biosynthesized from the necine base retronecine from its host plant [51].

Trigo and colleagues also explored how pyrrolizidine alkaloids can affect the interaction between *U. ornatrix* and its host plants. *Crotalaria pallida*, one of the most common *U. ornatrix* hostplants, has a broad distribution in the New World, from the southeastern United States to Argentina. When populations from Florida and southeastern Brazil were compared, *U. ornatrix* showed local adaptions to its host plant, but no evidence of local adaptation was observed when three populations in southeastern Brazil that were ca. 150 km apart were compared [52]. These

results motivated the quantification of pyrrolizidine alkaloids in *C. pallida* from different populations. Intriguingly, the patterns of pyrrolizidine alkaloid variation among populations did not explain the patterns of local adaptation, suggesting that another yet unknown chemical defense mechanism in the host may be responsible [53]. This approach was later extended to include a much larger number of populations and the non-specialist herbivore *Etiella zinckenella* (Lepidoptera: Pyralidae), in addition to the specialist *U. ornatrix*. There was a great variation among populations in attack rates by the two herbivores and in the concentrations of the plant pyrrolizidine alkaloids. However, herbivore attack rates were not correlated with the concentration of pyrrolizidine alkaloids in the local host population [54].

To better understand the relationship between the concentration of pyrrolizidine alkaloids in the host plant and herbivore performance, a series of controlled laboratory experiments was carried out in which pyrrolizidine alkaloids were extracted from host plants and added at different concentrations to an artificial diet. *Utetheisa ornatrix* showed a plastic pyrrolizidine alkaloid-feeding preference [55]. When fed on low pyrrolizidine alkaloid concentration diets, the larvae showed a strong subsequent preference for diets with high pyrrolizidine alkaloid concentrations; however, when larvae were fed on a high pyrrolizidine alkaloid concentration diet, they subsequently they did not discriminate between diets with high and low pyrrolizidine alkaloid concentrations. Interestingly, *U. ornatrix* was able to sequester extremely high amounts of pyrrolizidine alkaloids with no fitness cost [56]. These results imply that *U. ornatrix* may act as a selection agent that can decrease the concentration of pyrrolizidine alkaloids in natural host plant populations. In Nature, larvae may regulate the amount of ingested pyrrolizidine alkaloid by choosing between eating leaves, which have lower pyrrolizidine alkaloid concentrations, and seeds that present higher concentrations of pyrrolizidine alkaloids. This may be complicated by the fact that some *Crotalaria* species have extrafloral nectaries near their fruits that attract predatory ants [57]. The feeding habit of *U. ornatrix* larvae seems to be a plastic response dependent both on the presence or absence of extrafloral nectaries and pyrrolizidine alkaloid concentrations of their host plants [58]. Even though *U. ornatrix* may choose plants with higher concentrations of pyrrolizidine alkaloids, the opposite is true for non-adapted generalist herbivores. For example, pyrrolizidine alkaloids caused high larval mortality in *Heliothis virescens* (Lepidoptera: Noctuidae) [59]. Therefore, the contrasting pattern between *U. ornatrix* and non-adapted generalist herbivores, and the interaction with other defense traits such as extrafloral nectaries, may explain the complex pattern of variation in pyrrolizidine alkaloid concentration and herbivore abundance in field populations [54].

Trigo and collaborators also investigated *U. ornatrix* performance on different *Crotalaria* species by comparing native and introduced species and how pyrrolizidine alkaloids may explain the differences in performance. Initially, they reported that *U. ornatrix* showed oviposition preference and higher fitness for the introduced host *C. pallida* than for the native host *C. incana* [60]. Trigo et al. [61] compared *U. ornatrix* performance using two native (*C. micans* and *C. paulina*) and two introduced (*C. pallida* and *C. juncea*) *Crotalaria* species and observed higher performances for the native when compared to the introduced species. The performance on the introduced

C. pallida, however, was similar to those of the two native species. The investigators discovered similar patterns of higher *U. ornatrix* performance on the native species when comparing twelve *Crotalaria* species (five native and seven introduced). The differences in performance among the different host species was not explained by variations in either the concentration of pyrrolizidine alkaloids or the nutritional quality (measured as lipids, sugar, and protein concentrations) [61].

For *U. ornatrix* moths, pyrrolizidine alkaloids were also suggested to protect the specialist pericopine moth *Scearctia figulina* (Erebidae: Arctiinae) from predation by the spiders *T. clavipes* and *Lycosa erythrognatha* (Lycosidae) [62]. The moth *Scearctia figulina* (Erebidae: Arctiinae) also sequesters pyrrolizidine alkaloids from its larval host plants, *Heliotropium transalpinum* (Boraginaceae), and both pyrrolizidine alkaloid structures and the mechanisms of pyrrolizidine alkaloid incorporation, as well as the biosynthesis of the alkaloids from necine bases, were described for this moth [62].

Hair pencils are pheromone-signaling structures found in the males of Lepidoptera that are used in courtship and copulation behaviors toward females. An investigation of compounds found on the hair pencils of 54 species in 30 genera of Ithomiini butterflies described 13 volatile compounds formed by hydrolysis, oxidation, lactonizationand/or methylation of both the necic acid and pyrrolizidine base portions of the pyrrolizidine alkaloid lycopsamine (**4**) (Fig. 5), a structure probably originating from the ingestion of food plant resources by these butterflies [32].

The chemical characterization of pyrrolizidine alkaloids sequestered by specialized insects included the investigation of the structural stabilities of the retronecine and heliotridine molecules, which represent the necine bases occurring in almost all 1,2-unsaturated pyrrolizidine alkaloids, using different ab initio, semiempirical, and molecular mechanics methods [63].

The sequestration of pyrrolizidine alkaloids from host plants were also characterized in other insects besides lepidopterans by Trigo and his colleagues including the hemipteran *Largus ruxpennis* (Largidae) and the coleopteran *Chauliog-nathus fallax* (Cantharidae), two species that feed on *Senecio brasiliensis* (Asteraceae) [64].

In a noteworthy publication, Trigo reviewed the ecological and evolutionary mechanisms behind the interactions among pyrrolizidine alkaloid-specialized lepidopterans and their predators mediated by pyrrolizidine alkaloids from their host plants, which he named as "different trophic levels" [65]. All of these notable interactions involving pyrrolizidine alkaloid-specialist insects began with the capacity of the insects to feed on plants with pyrrolizidine alkaloids. In this case, the term "capacity" includes the presence of digestive and detoxification enzymes in the insects to overcome the chemical defense of these plants. During evolutionary time, these insects would become capable of sequestering those secondary compounds from their host plants, incorporating them in their body parts. As a result, secondary compounds in insects may work directly against predation, or may be used as precursors for the biosynthesis of an insect's defensive or mating pheromone compounds.

3 Aristolochic Acids

Aristolochic acids (AAs) (Fig. 12) are natural products with a very restricted distribution in plants that have been described only in plants of the genera *Aristolochia* and *Asarum*, both belonging to the family Aristolochiaceae [66]. They are nitrophenanthrenes derived biosynthetically from the aporphine alkaloids [67] and more than 178 aristolochic acid analogs have been isolated so far [68]. The biosynthesis of aristolochic acids studied in *Aristolochia sipho* involves tyrosine, DOPA, dopamine, and noradrenaline as specific precursors [69]. Additionally, Attaluri and collaborators [70] presented a versatile approach to the synthesis of aristolochic acids and their major metabolites based primarily on a Suzuki–Miyaura coupling reaction. Several aristolochic acids have medical implications associated mainly with their renal toxicity and carcinogenicity [66, 71]. Plants within the Aristolochiaceae also contain other secondary compounds including benzylisoquinoline alkaloids, aristolactams, and terpenoids (Fig. 12) [72, 73].

Caterpillars of the neotropical swallowtail butterflies of the tribe Troidini (Papilionidae: Papilioninae) (Fig. 13), which figure among the most popular insect taxa and have greatly contributed to studies of ecology, behavior and evolution in insects [74], feed only on plants in the family Aristolochiaceae and sequester the chemical compounds present in their host plants [75]. These compounds are believed to cause the unpalatability of these butterflies to possible predators [76–78].

One of Keith Brown's first studies with aristolochic acids focused on the natural history of several species of Troidini swallowtail butterflies from southeastern Brazil and their relationships with host plants in the genus *Aristolochia* [79]. In this study, Brown and colleagues suggested that the chemical features of the species of *Aristolochia* may influence the patterns of host plant use, as well as the identification of

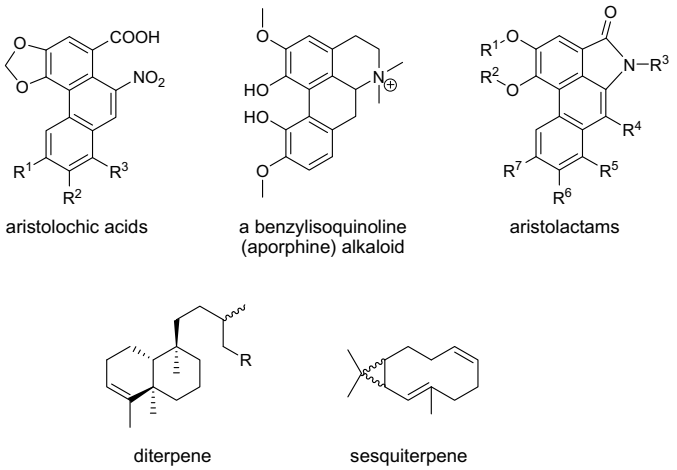

Fig. 12 Examples of compounds present in *Aristolochia* species

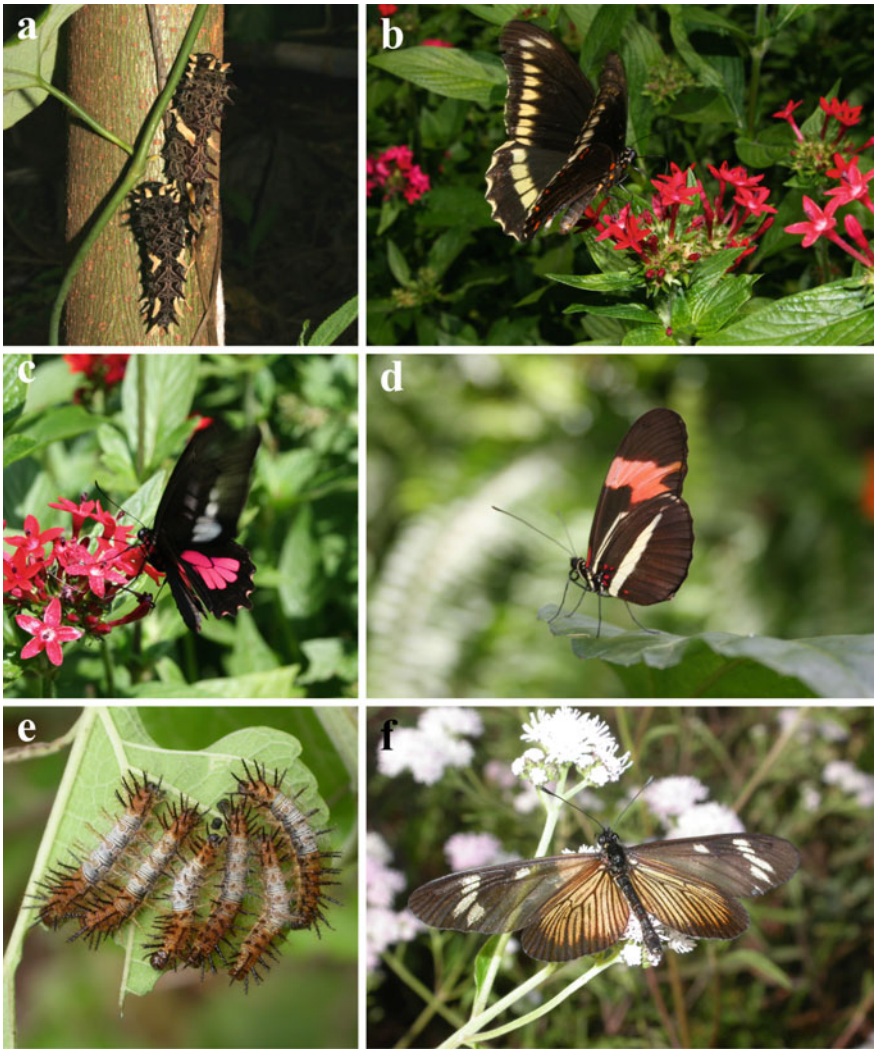

Fig. 13 Examples of other butterfly groups studied by Brown and Trigo. **a**, **b** Two larvae and an adult of *Battus polydamas* (Papilionidae: Troidini), respectively; **c** *Parides neophilus eurybates* (Papilionidae: Troidini); **d** *Heliconius erato phyllis* (Nymphalidae: Heliconiinae: Heliconiini); **e** Grouped larvae of *Actinote pellenea pellenea*; **f** *Actinote genitrix genitrix* (Nymphalidae: Heliconiinae: Acraeini) (Photos: A.V.L.F.)

suitable plants, by Troidini butterflies [79]. Bioassays with five species of Troidini showed that they do not oviposit equally on all species of the available host plants. Additionally, there is evidence that the caterpillars of Troidini react differently to the available host plants [80, 81].

Clécio Klitzke [80], under Brown's supervision, classified plants within the genus *Aristolochia* used as host plants by Troidini butterflies into three groups, according to their chemical characteristics: (1) species with aristolochic acids in the leaves (*A. sessilifolia, A. melastoma, A. rumicifolia, A. arcuata, A. macroura* and *A. triangularis*), (2) species without both aristolochic acids and labdanoic acids (Fig. 12) in the leaves (*A. odora* and *A. elegans*), and (3) species without aristolochic acids and with labdanoic acids in the leaves (*A. esperanzae, A. cymbifera* and *A. galeata*). He then associated the presence and absence of these compounds to the use of host plants by the different species of Troidini. Later, the presence of aristolochic acids was described in all 17 troidine species evaluated, in variable concentrations [82].

The role of aristolochic acids for the chemical protection of Troidini caterpillars against invertebrate natural enemies (an ichneumonid wasp specialist parasitoid, and ant and bug generalist predators) both in field and laboratory conditions was investigated under Trigo's first Ph.D. student supervision [83]. The tritrophic system was studied in the association among *Aristolochia arcuata* and *Battus polydamas* (Fig. 13) and the natural enemies of the latter species in a fragment of a neotropical semi-deciduous forest in southeastern Brazil. The investigators conducted natural field mortality observations and laboratory bioassays associated with the chemical extractions of both the host plant leaves and larvae. Later, additional laboratory and field predation trials with young chicks and carpenter ants were carried out and these were followed by bioassays to assess the anti-predation activity of a mixture of commercial aristolochic acids I and II applied topically on palatable baits [84]. However, despite the results of differential predation of immature *B. polydamas* associated with larval developmental stage, the aristolochic acids I and II mixture failed to show activity and the baits were consumed both in the laboratory and in field bioassays [84]. As *Aristolochia* plants contain additional chemical compounds (other alkaloids and aristolactams, already mentioned, and mono-, sesqui-, di-, and triterpenes, among others (Fig. 12)) they could be sequestered and act, individually or synergistically, as deterrents against predators. Further studies of the immature Troidini defensive chemistry remain to be developed.

The relationships between troidine butterflies and their host plants are extremely important in terms of understanding the evolution of this group within the Papilioninae. With this in mind, a hypothesis of mutually evolved relationships between *Aristolochia* and neotropical troidines was proposed [85]. According to this hypothesis, species in the earlier derived clades within *Parides*, such as *P. proneus*, are able to feed on host plants without aristolochic acids and sequester terpenes for defense, whereas larvae of the remaining clades could sequester aristolochic acids from their host plants. However, posterior studies using phylogenetic approaches and chemical characterization to elucidate the relationships between Troidini butterflies and their host plants did not corroborate the above-mentioned hypothesis [86, 87]. In fact, the current pattern of host plant use by troidine butterflies is suggested not to be constrained by the phylogeny of their food plants, nor indeed by the secondary chemicals in these plants or by their geographical similarity. Instead, troidine butterflies may be opportunistic in the use of host plants [87].

4 Cyanogenic Compounds

Cyanogenic glucosides (cyanoglucosides) are bioactive plant products derived from amino acids that carry a cyanide moiety that is released upon their breakdown [88, 89]. Structurally, they are characterized as α-hydroxynitriles (cyanohydrins) that are stabilized by glucosylation [89]. Glealdow and Møller [89] precisely described the biosynthesis of these compounds: "Cyanogenic glucosides are synthesized from specific amino acids in a series of reactions catalyzed by two multifunctional, membrane-bound cytochrome P450s (P450aa and P450ox) and a soluble UDP-glucosyl-transferase, with an oxime and an α-hydroxynitrile (cyanohydrin) as key intermediates. Cyanogenesis occurs when the β-glucosidic linkage is hydrolyzed by a specific β-glycosidase to form an unstable α-hydroxynitrile (cyanohydrin) that dissociates into hydrogen cyanide (HCN) and a ketone either spontaneously at high pH or catalyzed by an α-hydroxynitrilase".

Diverse in form and structure, cyanoglucosides are present in many plant families, being notably diverse in the Passifloraceae [90]. Among animals, aromatic cyanoglucosides are found in arthropods such as millipedes and centipedes (Myriapoda), while aliphatic cyanogenic glucosides are found in butterflies (Nymphalidae: Heliconiini) and *Zygaena* moths (Zygaenidae) [91, 92]. More complex, cyclopentenoid cyanogens are also found in Heliconiini butterflies [93] (Fig. 14).

Acraeini butterflies (Nymphalidae: Heliconiinae) are unpalatable or unpleasant to potential predators [94] and it is assumed that their unpalatability is due to cyanogenic glucosides secreted from their thoracic glands. African Acraeini sequester cyanoglucosides from their host plants (in the families Passifloraceae, Turneraceae and Flacourtiaceae [95]) and are also able to biosynthesize them de novo [96]. New World Acraeini, on the other hand, feed exclusively on pyrrolizidine alkaloid-rich plants in the Asteraceae family (e.g., *Eupatorium* spp. and *Mikania* spp.) and there are no records of cyanogenic host plants for these species. Brown and Francini [94] investigated whether New World Acraeini (*Actinote* and *Altinote*) (Fig. 13) sequester

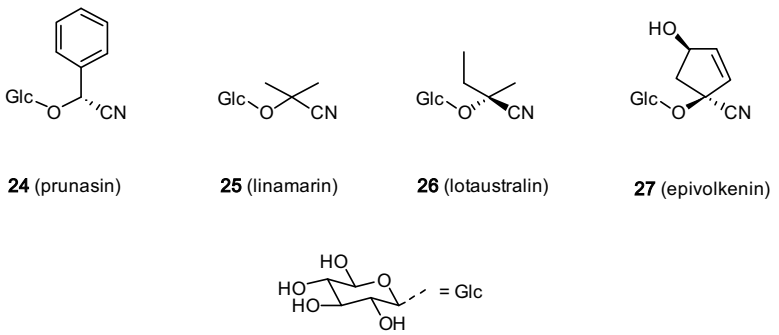

24 (prunasin) **25** (linamarin) **26** (lotaustralin) **27** (epivolkenin)

Fig. 14 Types of cyanogenic glycoside structures

pyrrolizidine alkaloids from their host plants or, as in the case of their African counterparts, accumulate cyanogenic glycosides from de novo biosynthesis. By testing all life stages of *Actinote* and *Altinote* species, they did not find evidence of pyrrolizidine alkaloid storage, except for minute quantities in larval guts, probably derived from feeding activities. On the other hand, all life stages, including the eggs, tested positive for cyanogenic glucosides. Chemical extraction and further analyses showed that the most common cyanogenic glucoside was linamarin (**25**), followed by other minor cyanoglucosides that were not identified at the time. Thus, New World Acraeini also synthesize their own defenses via storage of aliphatic linamarin (**25**) (Fig. 14).

The aliphatic cyanogenic glucosides linamarin (**25**) and lotaustralin (**26**), derived from leucine and isoleucine, respectively, are the most common cyanogenic glucosides in butterflies and moths [88]. Most cyanogenic glucosides are derived from de novo synthesis but some are due also to sequestration, notably in the case of *Zygaena* larvae feeding on cyanogenic host plants that contain linamarin (**25**) and lotaustralin (**26**) [97]. Sequestration from cyanogenic host plants allows the accumulation of cyanogenic glycosides other than **25** and **26**, as observed in African *Acraea* and American *Heliconius* species [93, 98] (Fig. 13). Brown and Francini's [94] investigation is the only study that examined the chemical profile of New World Acraeini. Their discovery that these butterflies do not sequester pyrrolizidine alkaloids from hosts and favor cyanogenic glucosides is relevant to our present understanding of the evolutionary implication of biochemical evolution of chemical defense.

In order to understand the role of cyanoglucosides in butterfly chemical defense, Trigo and Cardoso [99] collaborated on the investigation of the efficacy of cyanogenic glucosides as predator deterrent. The tests were carried with naïve chicks and aimed to evaluate the effect of the cyanoglucosides and their breakdown products. The

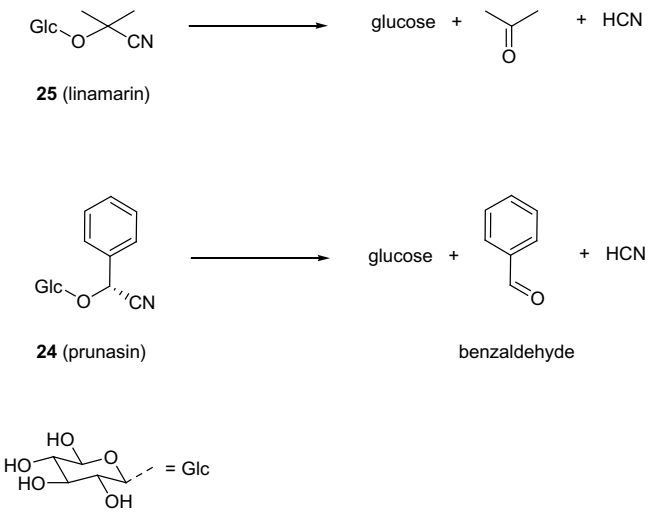

Fig. 15 Breakdown of cyanogenic glycosides

experiments tested an aromatic cyanogenic glucoside (prunasin) and an aliphatic cyanoglucoside (linamarin). The tests indicated that not only can cyanide reduce predation by chicks, but also the other non-toxic, volatile breakdown products, such as benzaldehyde and acetone can also do so (Fig. 15). The dual effect suggests that predators may learn to associate chemical defense and smell. It was also surprising to find that the effects, although significant, were not strong. These results may explain why in some *Heliconius* species the ability to sequester other types of cyanogenic glycosides has evolved [100].

5 Conclusions

The interdisciplinary area of chemical ecology is undoubtedly fascinating. It permits the exploration of complementary layers of knowledge, with each one being challenging and unexpected due the large number of newly unanswered questions, not only in chemistry and biology, but also in evolution and related disciplines. So, it is not by chance that Keith Brown Jr. and José Roberto Trigo stood out in the area: they both had unique personalities and combined hard work and dedication in their research and teaching activities. Most of what is currently known of the chemical ecology of Neotropical butterflies came from their studies—and from the efforts of their students afterward. Certainly, extra chapters would be needed to fully describe Keith Brown's contribution on natural history, biology, and systematics of butterflies and José Roberto Trigo's work with plant secondary metabolites and other insects. Hopefully, the present contribution may at least partly acknowledge their major contributions to the Brazilian chemical ecology field and stimulate future students to pursue new studies on the chemical ecology of butterflies and moths.

Box 1 (Personal memories of Márcio Zikán Cardoso)

I met Dr. Keith Brown Jr. in a national conference in 1983. I was in my second-year majoring in Biology and attended this big panel meeting on biotic diversification in the neotropics, where he was one of the speakers. He circulated a sign-up list for those who were interested in receiving his professorship thesis [100]. By the time the list arrived in my hands there was barely any space left—I had to write my name and address at the corner, next to the paper margin thinking I would never receive the document. I had heard of him, of course, back in Rio de Janeiro, from some of my older colleagues, who spoke of him with reverence. We were surprised and elated when he appeared at our poster session and read our paper on the fauna of tank bromeliads. In addition to the traditional information, we had added a small leaflet with a note about habitat loss and its consequences for endemic species that were found in our study site. He was particularly happy to see that note and congratulated us on it. Dr. Brown was also presenting a poster there. When I saw his poster, I

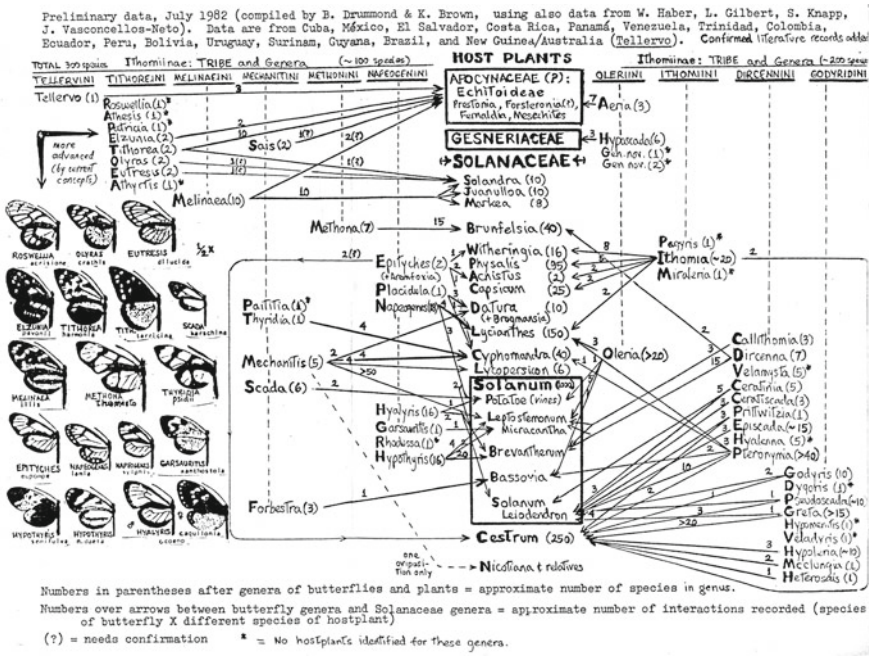

Fig. 16 Example of a drawing of Keith Brown's

could not understand a thing. It was so different in design that it baffled me. Then he began to explain it: intricate drawings, arrows, hand-written text and many, many connections (both real and metaphorical). And it all made sense (an example of such drawings is shown in Fig. 16). He then turned on a small Super-8 projector and showed this fascinating video movie about orb-weaving spiders releasing butterflies from their web. I was hooked! I could not foresee, but this was the beginning of my interest in chemical ecology and the fantastic butterflies that Keith Brown introduced me to. Sometime after returning home and back to my school work, I received Dr. Brown's dissertation in the mail. I was too young to realize I had a masterpiece, a tour-de-force, in my hands. Almost forty years later I often see myself in awe at the breadth of that work, and really thankful that Keith Brown came through with the promise at the panel and made me one of the lucky few who has a hardcopy of that work.

In 1984, Keith published a paper in "Nature" [35] showing the work that he had been doing with pyrrolizidine alkaloid-storing butterflies. In that same year, I met him in Campinas for the first time and began a long-lasting relationship that culminated in me attending the University of Campinas for my master's degree. It was also an opportunity to join the International Society of Chemical Ecology, which had been recently created. I was happy to be one of

the founding members, together with Keith Brown and José Roberto Trigo. The annual meetings were opportunities to learn more about this amazing interdisciplinary field. It was always an exciting moment when Keith returned from these meetings and would show us the material he gathered and the notes he had taken there. Because we did not have money to travel, this was our way of being in contact with first-rate science. Keith´s note taking ability amazed me and I now see how much this influenced my own note taking. It is said that people sometimes teach by their actions. His "bag full of treats" (notes and other materials from conferences) always taught me about the value of good science, note taking, and sharing.

I do not remember when I first met Trigo, but I am sure it must have been in Keith's lab sometime before 1986, the year I moved to Campinas. He was older than me and was the senior student in chemical ecology. We were to become good friends during my years in Campinas.

The main activities in the lab were primarily directed toward the study of chemical defenses in Ithomiini butterflies. Keith had laid down the groundwork by showing that adult butterflies sequestered the compounds from the nectar of their adult feeding plants rather than sequestering from the larval host plant, which was the "expected" mode of acquiring defenses from toxic host plants. Keith showed convincingly that freshly emerged individuals were palatable to the giant orb weaver spide *Trichonephila clavipes.* Yet, when treated with PA extracts on their surface, these butterflies were readily rejected by the same spiders. This became the "*T. clavipes* bioassay" that was to become a staple for not only Keith´s work, but also for Trigo and his students when he later became a professor after Keith vacated the lab. Apparently, this bioassay was developed by Eisner in Florida, testing pyrrolizidine alkaloid-storing bella moths (*Utetheisa ornatrix*), and saw much use in Keith´s lab. Many field demonstrations have used this bioassay to illustrate predator behavior. In my early days in the lab, I thought naïvely that the spiders refused all sorts of chemically defended prey and was very frustrated when I tossed a hapless *Heliconius* spp. on a *T. clavipes* web only to see it being happily accepted by the spider. Trigo would later speculate as to why the spiders would only respond to pyrrolizidine alkaloids. Although Trigo would go on to explore many details of the chemical ecology of pyrrolizidine alkaloid insects, many of the avenues paved by Keith in his "Nature" paper and in a more detailed study published in the "Brazilian Journal of Biology" still need to be fully explored. Sexual selection is one such theme. Together with *Danaus* and *Utetheisa*, ithomiines use their pyrrolizidine alkaloids to synthesize sexual pheromones. For instance, males could be selected by females based on their potential contribution for offspring defense via donation of protective chemicals in their spermatophore. Would females mate multiple times to replenish their pyrrolizidine alkaloid content? Will males compete to access to females? These are unanswered questions.

Keith Brown has left a remarkable legacy in butterfly ecology and conservation and I gather his contributions are more recognized in these two fields than in chemical ecology. His work in chemical ecology was pivotal for some years of his decades-long scientific career. He definitely saw Trigo as his successor and left the door open for him.

Acknowledgments We thank the following colleagues: Roberto G. S. Berlinck, for inviting us to write the present chapter; George G. Brown, Keith Brown's son, for providing valuable information and helping with text revision and organization in the introductory section, Ricardo Costa, for kindly providing us with a photo of *Tithorea harmonia pseudethra*, and Clécio Klitzke for insights on Keith Brown's early work in Brazil. We also acknowledge all colleagues and co-workers of the "Laboratório de Ecologia Química" in UNICAMP. Karina L. Silva-Brandão thanks FAPESP (grant 1998/0764-9) for a graduate fellowship during her Master's degree dissertation. André V. L. Freitas acknowledges support from FAPESP (Biota-Fapesp - grants 2011/50225-3, 2014/50316-7) and from the Brazilian Research Council – CNPq (303834/2015-3). Márcio Zikán Cardoso thanks FAPESP for graduate and postdoctoral fellowships that allowed his research work with K. Brown and J.R. Trigo, and CNPq for support (Proc 400242/2014-1, 306985/2013-6). This publication is part of the RedeLep "Rede Nacional de Pesquisa e Conservação de Lepidópteros" SISBIOTA-Brasil/CNPq (563332/2010-7). The butterfly species are registered in the SISGEN (# ADF1F75; A0E7804; A3F4F61).

References

1. Feeny P (1992) The evolution of chemical ecology: contributions from the study of herbivorous insects. In: Rosenthal GA, Berenbaum MR (eds) Herbivores: their interactions with secondary plant metabolites, vol 2, 2nd edn. Academic Press, San Diego, p 1
2. Trigo JR, Bittrich V, Amaral Md C, Marsaioli AJ (2000) Ecologia química. Revista Chemkeys:1
3. Pilli RA, Zarbin PHG (2000) Editorial. J Brazil Chem Soc 11(6):0
4. Pinto AC, Rezende CM, Garcez FR, Epifanio RdA (2003) Um olhar holístico sobre a química de produtos naturais brasileira. Quim Nova 26:966
5. Brown Jr KS (1965) A new L-α-amino acid from Lepidoptera. J Am Chem Soc 87:4202
6. Brown Jr KS (1967) Chemotaxonomy and chemomimicry: the case of 3-hydroxykynurenine. Syst Biol 16:213
7. Brown Jr KS (1980) A review of the genus *Hypothyris* Hübner (Nymphalidae), with descriptions of three new subspecies and early stages of *H. daphisi*. J Lepid Soci 34:152
8. Pareja M (2018) Alkaloids, plants and butterflies: a farewell to José Roberto Trigo (1956–2017). Neotrop Entomol 47:4
9. Dicke M, Sabelis MW (1988) Infochemical terminology: based on cost-benefit analysis rather than origin of compounds? Funct Ecol 2:131
10. Althaus JB, Jerz G, Winterhalter P, Kaiser M, Brun R, Schmidt TJ (2014) Antiprotozoal activity of *Buxus sempervirens* and activity-guided isolation of *O*-tigloylcyclovirobuxeine-B as the main constituent active against *Plasmodium falciparum*. Molecules 19:6184
11. Brown Jr KS, Kupchan SM (1962) A convenient separation of alkaloid mixtures by partition chromatography, using an indicator in the stationary phase. J Chromatogr 9:71
12. Brown Jr KS, Kupchan SM (1962) The structure of cyclobuxine. J Am Chem Soc 84:4590

13. Brown Jr KS, Kupchan SM (1962) The configuration of cyclobuxine and its interrelation with cycloeucalenol. J Am Chem Soc 84:4592
14. Brown Jr KS, Budzikiewicz H, Djerassi C (1963) Alkaloid studies XLII. The structures of dichotamine, 1-acetyl-aspidoalbidine and 1-acetyl-17-hydroxyaspidoalbidine: three new alkaloids from *Vallesia dichotoma* Ruiz et Pav. Tetrahedron Lett 4:1731
15. Brown Jr KS, Djerassi C (1964) Alkaloid studies. XLVI.1 The alkaloids of *Aspidosperma obscurinervium* Azembuja. A new class of heptacyclic indole alkaloids. J Am Chem Soc 86:2451
16. Brown Jr KS, Kupchan SM (1964) *Buxus* alkaloids. IV.1 The configuration of cyclobuxine and its interrelation with cycloeucalenol. J Am Chem Soc 86:4424
17. Gilbert B, Duarte AP, Nakagawa Y, Joule JA, Flores SE, Aguayo Brissolese J, Campello J, Carrazzoni EP, Owellen RJ, Blossey EC, Brown Jr KS, Djerassi C (1965) Alkaloid studies. L. The alkaloids of twelve *Aspidosperma* species. Tetrahedron 21:1141
18. Brown Jr KS, Sanchez LWE, Figueiredo AdA, Filho JMF (1966) Unusual mass spectral fragmentation of 21-oxoaspidoalbidine-type alkaloids. J Am Chem Soc 88:4984
19. Garcia RMF, Brown Jr KS (1976) Alkaloids of three *Aspidosperma* species. Phytochemistry 15:1093
20. Aniszewski T (2007) Biological significance of alkaloids. In: Aniszewski T (ed) Alkaloids–secrets of life. Elsevier Science, Amsterdam, p 141
21. Aniszewski T (2007) Biological significance of alkaloids. In: Aniszewski T (ed) Alkaloids–secrets of life. Elsevier Science, Amsterdam, p 61
22. Kurek J (2019) Alkaloids—their importance in nature and for human life. IntechOpen, London
23. Kukula-Koch WA, Widelski J (2017) Alkaloids. In: Delgoda R (ed) Pharmacognosy. Academic Press, Boston, MA, p 163
24. Waller GR, Nowacki EK (1978) The role of alkaloids in plants. In: Waller GR, Nowacki EK (eds) Alkaloid biology and metabolism in plants. Springer, Boston, MA, p 143
25. O'Connor SE (2010) Alkaloids. In: Liu H-W, Mander L (eds) Comprehensive natural products II, vol 1. Elsevier, Oxford, UK, p 977
26. Aniszewski T (2007) The ecological role of alkaloids. In: Aniszewski T (ed) Alkaloids—secrets of life. Elsevier Science, Amsterdam, p 205
27. Brown Jr KS, Trigo JR (1995) The ecological activity of alkaloids. In: Cordell GA (ed) The alkaloids: chemistry and pharmacology, vol 47. Academic Press, San Diego, p 227
28. Robins DJ (1982) The pyrrolizidine alkaloids. Progr Chem Org Nat Prod 26:327
29. Hartmann T, Witte L (1995) Chemistry, biology and chemoecology of the pyrrolizidine alkaloids. In: Pelletier SW (ed) Alkaloids: chemical and biological perspectives, vol 9. John Wiley & Sons, New York, p 155
30. Culvenor CCJ (1978) Pyrrolizidine alkaloids: occurrence and systematic importance in angiosperms. Bot Notiser 131:473
31. Ratmanova NK, Andreev IA, Leontiev AV, Momotova D, Novoselov AM, Ivanova OA, Trushkov IV (2020) Strategic approaches to the synthesis of pyrrolizidine and indolizidine alkaloids. Tetrahedron 76:131031
32. Schulz S, Beccaloni G, Brown Jr KS, Boppré M, Freitas AVL, Ockenfels P, Trigo JR (2004) Semiochemicals derived from pyrrolizidine alkaloids in male ithomiine butterflies (Lepidoptera: Nymphalidae: Ithomiinae). Biochem Syst Ecol 32:699
33. Cardoso MZ (1997) Testing chemical defence based on pyrrolizidine alkaloids. Anim Behav 54:985
34. Brown Jr KS (1984) Chemical ecology of dehydropyrrolizidine alkaloids in adult Ithomiinae Lepidoptera Nymphalidae. Rev Brasil Biol 44:435
35. Brown Jr KS (1984) Adult-obtained pyrrolizidine alkaloids defend ithomiine butterflies against a spider predator. Nature 309:707
36. Brown Jr KS (1987) Chemistry at the Solanaceae/Ithomiinae interface. Ann Missouri Bot Gard 74:359
37. Trigo JR, Witte L, Brown Jr KS, Hartmann T, Barata LES (1993) Pyrrolizidine alkaloids in the arctiid moth *Hyalurga syma.* J Chem Ecol 19:669

38. Trigo JR, Brown Jr KS, Witte L, Hartmann T, Ernst L, Barata LES (1996) Pyrrolizidine alkaloids: different acquisition and use patterns in Apocynaceae and Solanaceae feeding ithomiine butterflies (Lepidoptera: Nymphalidae). Biol J Linn Soc 58:99
39. Silva KL, Trigo JR (2002) Structure-activity relationships of pyrrolizidine, alkaloids in insect chemical defense against the orb-weaving spider *Nephila clavipes*. J Chem Ecol 28:657
40. Ferro VG, Guimarães Jr PR, Trigo JR (2006) Why do larvae of *Utetheisa ornatrix* penetrate and feed in pods of *Crotalaria* species? Larval performance vs. chemical and physical constraints. Entomol Exp Appl 121:23
41. Robinson MH, Mirick H (1971) The predatory behavior of the golden-web spider *Nephila clavipes* (Araneae: Araneidae). Psyche 78:057182
42. Vasconcellos-Neto J, Lewinsohn TM (1984) Discrimination and release of unpalatable butterflies by *Nephila clavipes*, a neotropical orb-weaving spider. Ecol Entomol 9:337
43. Freitas AVL, Trigo JR, Brown Jr KS, Witte L, Hartmann T, Barata LES (1996) Tropane and pyrrolizidine alkaloids in the ithomiines *Placidula euryanassa* and *Miraleria cymothoe* (Lepidoptera: Nymphalidae). Chemoecology 7:61
44. Trigo JR, Brown Jr KS (1990) Variation of pyrrolizidine alkaloids in Ithomiinae: a comparative study between species feeding on Apocynaceae and Solanaceae. Chemoecology 1:22
45. Trigo JR, Motta PC (1990) Evolutionary implications of pyrrolizidine alkaloid assimilation by danaine and ithomiine larvae (Lepidoptera: Nymphalidae). Experientia 46:332
46. Trigo JR, Barata LES, Brown Jr KS (1994) Stereochemical inversion of pyrrolizidine alkaloids by *Mechanitis polymnia* (Lepidoptera: Nymphalidae: Ithomiinae): specificity and evolutionary significance. J Chem Ecol 20:2883
47. Trigo J, Brown Jr KS, Henriques SA, Barata LES (1996) Qualitative patterns of pyrrolizidine alkaloids in Ithomiinae butterflies. Biochem Syst Ecol 24:181
48. Orr AG, Trigo JR, Witte L, Hartmann T (1996) Sequestration of pyrrolizidine alkaloids by larvae of *Tellervo zoilus* (Lepidoptera: Ithomiinae) and their role in the chemical protection of adults against the spider *Nephila maculata* (Araneidae). Chemoecology 7:68
49. Brückmann M, Trigo JR, Foglio MA, Hartmann T (2000) Storage and metabolism of radioactively labeled pyrrolizidine alkaloids by butterflies and larvae of *Mechanitis polymnia* (Lepidoptera: Nymphalidae, Ithomiinae). Chemoecology 10:25
50. Eisner T (1982) For love of Nature: exploration and discovery at biological field stations. Bioscience 32:321
51. Martins CHZ, Cunha BP, Solferini VN, Trigo JR (2015) Feeding on host plants with different concentrations and structures of pyrrolizidine alkaloids impacts the chemical-defense effectiveness of a specialist herbivore. PLoS One 10:e0141480
52. Cogni R, Futuyma DJ (2009) Local adaptation in a plant herbivore interaction depends on the spatial scale. Biol J Linn Soc 97:494
53. Cogni R, Trigo JR, Futuyma DJ (2011) Varying herbivore population structure correlates with lack of local adaptation in a geographic variable plant-herbivore interaction. PLos One 6:e29220
54. Verçosa D, Cogni R, Alves MN, Trigo JR (2019) The geographical and seasonal mosaic in a plant-herbivore interaction: patterns of defences and herbivory by a specialist and a non-specialist. Sci Rep 9:15206
55. Hoina A, Martins CHZ, Trigo JR, Cogni R (2013) Preference for high concentrations of plant pyrrolizidine alkaloids in the specialist arctiid moth *Utetheisa ornatrix* depends on previous experience. Arthropod-Plant Interact 7:169
56. Cogni R, Trigo JR, Futuyma DJ (2012) A free lunch? No cost for acquiring defensive plant pyrrolizidine alkaloids in a specialist arctiid moth (*Utetheisa ornatrix*). Mol Ecol 21:6152
57. Guimarães JRPR, Raimundo RLG, Bottcher C, Silva RR, Trigo JR (2006) Extrafloral nectaries as a deterrent mechanism against seed predators in the chemically protected weed *Crotalaria pallida* (Leguminosae). Aust Ecol 31:776
58. Magalhães AE, Martins CHZ, Verçosa D, Massuda KF, Trigo JR (2017) Ants visiting extrafloral nectaries and pyrrolizidine alkaloids may shape how a specialist herbivore feeds on its host plants. Arthropod-Plant Interact 11:629

59. Cogni R, Trigo JR (2016) Pyrrolizidine alkaloids negatively affect a generalist herbivore feeding on the chemically protected legume *Crotalaria pallida*. Neotrop Entomol 45:252
60. Cogni R (2010) Resistance to plant invasion? A native specialist herbivore shows preference for and higher fitness on an introduced host. Biotropica 42:188
61. Trigo JR, Martins CHZ, Cunha BP, Solferini VN (2018) Native or nonnative host plants: what is better for a specialist moth? Biol Invasions 20:849
62. Martins CHZ, Trigo JR (2016) Pyrrolizidine alkaloids in the Pericopine moth *Scearctia figulina* (Erebidae: Arctiinae): metabolism and chemical defense. J Brazil Chem Soc 27:1437
63. Giordan M, Custodio R, Trigo JR (1996) Pyrrolizidine alkaloids necine bases: ab initio, semiempirical, and molecular mechanics approaches to molecular properties. J Comput Chem 17:156
64. Klitzke CF, Trigo JR (2000) New records of pyrrolizidine alkaloid-feeding insects. Hemiptera and Coleoptera on *Senecio brasiliensis*. Biochem Syst Ecol 28:313
65. Trigo JR (2011) Effects of pyrrolizidine alkaloids through different trophic levels. Phytochem Rev 10:83
66. Han J, Xian Z, Zhang Y, Liu J, Liang A (2019) Systematic overview of aristolochic acids: nephrotoxicity, carcinogenicity, and underlying mechanisms. Front Pharmacol 10:648
67. Trigo JR (2000) The chemistry of antipredator defense by secondary compounds in Neotropical Lepidoptera: facts, perspectives and caveats. J Braz Chem Soc 11:551
68. Michl J, Ingrouille MJ, Simmonds MS, Heinrich M (2014) Naturally occurring aristolochic acid analogues and their toxicities. Nat Prod Rep 31:676
69. Comer F, Tiwari HP, Spenser ID (1969) Biosynthesis of aristolochic acid. Can J Chem 47:481
70. Attaluri S, Iden CR, Bonala RR, Johnson F (2014) Total synthesis of the aristolochic acids, their major metabolites, and related compounds. Chem Res Toxicol 27:1236
71. Jordan SA, Perwaiz S (2014) Aristolochic acids. In: Wexler P (ed) Encyclopedia of toxicology (3rd edn). Academic Press, Oxford, UK, p 298
72. Mix DB, Guinaudeau H, Shamma M (1982) The aristolochic acids and aristolactams. J Nat Prod 45:657
73. Chen Z-L, Zhu D-Y (1987) Aristolochia alkaloids. In: Brossi A (ed) The alkaloids: chemistry and pharmacology, vol 31. Academic Press, San Diego, p 29
74. Scriber JM (1995) Overview of swallowtail butterflies: taxonomic and distributional latitude. In: Scriber JM, Tsubaki Y, Lederhouse RC (eds) Swallowtail butterflies: their ecology and evolutionary biology. Scientific Publishers, Gainesville, FL, p 27
75. Tyler H, Brown Jr KS, Wilson K (1994) Swallowtail butterflies of the Americas—a study in biological dynamics, ecological diversity, biosystematics, and conservation. Scientific Publishers Inc., Gainesville, FL
76. Brower LP (1984) Chemical defence in butterflies. In: Vane-Wright RI, Ackery PR (eds) The biology of butterflies. Academic Press, New York, p 109
77. Brower LP, Brower JVZ (1964) Birds, butterflies, and plant poisons: a study in ecological chemistry. Zoologica 49:137
78. Chai P (1986) Field observations and feeding experiments on the responses of rufous-tailed jacamars (*Galbula rufficaouda*) to fee-flying butterflies in tropical rainforest. Biol J Linn Soc 29:161
79. Brown Jr KS, Damman AJ, Feeny P (1981) Troidine swallowtails (Lepidoptera: Papilionidae) in southeastern Brazil: natural history and foodplant relationships. J Res Lepidoptera 19:199
80. Klitzke CF (1992) Ecologia química e coevolução na interface Troidini (Papilionidae)/*Aristolochia* (Aristolochiaceae). Universidade Estadual de Campinas, Campinas, Biology
81. Morais ABB, Brown Jr KS (1991) Larval foodplant and other effects on Troidine guild composition (Papilionidae) in southeastern Brazil. J Res Lepidoptera 30:19
82. Klitzke CF, Brown Jr KS (2000) The occurrence of aristolochic acids in neotropical troidine swallowtails (Lepidoptera: Papilionidae). Chemoecology 10:99
83. Morais ABB (1997) Interações tróficas no sistema *Aristolochia arcuata* (Aristolochiaceae), *Battus polydamas* (Lepidoptera: Papilionidae:Troidini), e alguns de seus inimigos naturais. Universidade Estadual de Campinas, Campinas, SP, Zoology

84. Morais ABB, Brown Jr KS, Stanton MA, Massuda KF, Trigo JR (2013) Are aristolochic acids responsible for the chemical defense of aposematic larvae of *Battus polydamas* (L.) (Lepidoptera: Papilionidae)? Neotrop Entomol 42:558
85. Brown Jr KS, Trigo JR, Francini RB, Morais ABB, Motta PC (1991) Aposematic insects on toxic host plants: coevolution, colonization, and chemical emancipation. In: Price PW, Lewinsohn TM, Fernandes GW, Benson WW (eds) Plant-animal interactions — evolutionary ecology in tropical and temperate regions. John Wiley & Sons Inc., New York, p 375
86. Silva-Brandão KL, Freitas AVL, Brower AVZ, Solferini VN (2005) Phylogenetic relationships of the New World Troidini swallowtails (Lepidoptera: Papilionidae) based on COI, COII, and EF-1α genes. Mol Phylogen Evol 36:468
87. Silva-Brandão KL, Solferini VN (2007) Use of host plants by Troidini butterflies (Papilionidae, Papilioninae): constraints on host shift. Biol J Linn Soc 90:247
88. Zagrobelny M, Bak S, Møller BL (2008) Cyanogenesis in plants and arthropods. Phytochemistry 69:1457
89. Gleadow RM, Møller BL (2014) Cyanogenic glycosides: synthesis, physiology, and phenotypic plasticity. Ann Rev Plant Biol 65:155
90. Castro ECP, Zagrobelny M, Cardoso MZ, Bak S (2018) The arms race between heliconiine butterflies and *Passiflora* plants—new insights on an ancient subject. Biol Rev Cambridge Philos Soc 93:555
91. Brückner A, Raspotnig G, Wehner K, Meusinger R, Norton RA, Heethoff M (2017) Storage and release of hydrogen cyanide in a chelicerate (*Oribatula tibialis*). Proc Nat Acad Sci USA 114:3469
92. Zagrobelny M, Castro ÉCP, Møller BL, Bak S (2018) Cyanogenesis in arthropods: from chemical warfare to nuptial gifts. Insects 9:51
93. Castro ECP, Zagrobelny M, Zurano JP, Cardoso MZ, Feyereisen R, Bak S (2019) Sequestration and biosynthesis of cyanogenic glucosides in passion vine butterflies and consequences for the diversification of their host plants. Ecol Evol 9:5079
94. Brown Jr KS, Francini RB (1990) Evolutionary strategies of chemical defense in aposematic butterflies: cyanogenesis in Asteraceae-feeding American Acraeinae. Chemoecology 1:52
95. van Someren VGL (1974) List of foodplants of some East African Rhopalocera, with notes on the early stages of some Lycaenidae. J Lepid Soc 28:315
96. Nahrstedt A, Davis RH (1981) The occurrence of the cyanoglucosides, linamarin and lotaustralin, in *Acraea* and *Heliconius* butterflies. Comp Biochem Physiol B-Biochem Mol Biol 68:575
97. Zagrobelny M, Bak S, Ekstrøm CT, Olsen CE, Møller BL (2007) The cyanogenic glucoside composition of *Zygaena filipendulae* (Lepidoptera: Zygaenidae) as effected by feeding on wild-type and transgenic lotus populations with variable cyanogenic glucoside profiles. Insect Biochem Mol Biol 37:10
98. Raubenheimer D (1989) Cyanoglycoside gynocardin from *Acraea horta* (L.) (Lepidoptera: Acraeinae). J Chem Ecol 15:2177
99. Cardoso MZ (2020) The effect of cyanogenic glucosides and their breakdown products on predation by domestic chicks. Chemoecology 30:131
100. Brown Jr KS (1979) Ecologia geográfica e evolução nas florestas neotropicais. Universidade Estadual de Campinas, Campinas, Zoology

Karina L. Silva-Brandão was born in São José do Rio Preto, São Paulo, Brazil, in 1974. She obtained a degree in Biological Sciences from Universidade Estadual Paulista (IBILCE-UNESP), Brazil, in 1996 and a M.Sc. degree in Ecology from Universidade Estadual de Campinas (UNICAMP) in 2000, under J. R. Trigo's supervision. During that time, she studied the response of *Trichonephila clavipes* spiders to different types of pyrrolizidine alkaloids and became dedicated to the field of chemical ecology. For her Ph.D. thesis in ecology (2001–2005), also at the UNICAMP and with a period at Oregon State University, in Corvallis, OR, USA, she worked on the evolution of host plant use in Troidini butterflies. Since then, after a maternity leave, she has been investigating the molecular diversity of butterflies and moths of economic interest at different taxonomic levels. Only more recently did she go back to plant secondary compounds in a collaborative research with J.R. Trigo focused on gene differential expression responses.

André V. L. Freitas was born in São Vicente, São Paulo, Brazil, in 1971. He obtained his B.Sc. degree in Biological Sciences from the Universidade Estadual de Campinas (UNICAMP), Brazil, in 1991. His M.Sc. and Ph.D. degrees in ecology were awarded by UNICAMP in 1994 and 1999, working with Drs. Paulo S. Oliveira and Keith S. Brown Jr., respectively. He worked with Keith S. Brown from 1990 to 2005 investigating diverse aspects of butterfly systematics, ecology and conservation, and also collaborated with J. R. Trigo in some studies related to the chemical ecology of Ithomiini butterflies. Currently, he is a Full Professor at the Department of Animal Biology at UNICAMP. His present research has an emphasis on the systematics, ecology and conservation of Neotropical butterflies.

Márcio Zikán Cardoso was born in Rio de Janeiro, Brazil, in 1964. He obtained his B.Sc. degree from the Universidade Federal do Rio de Janeiro in 1985 and then his M.Sc. degree in 1991 from the Universidade Estadual de Campinas, Brazil, under the guidance of Keith S. Brown, Jr. He was awarded a Ph.D. degree in Biology in 2000 from the University of Texas at Austin, where he was supervised by Lawrence E. Gilbert. Upon returning to Brazil, he spent a year as a postdoctoral fellow with José Roberto Trigo at the Universidade Estadual de Campinas. In 2004, he became a faculty member at the Department of Ecology at the Universidade Federal do Rio Grande do Norte, Natal, Brazil, where he stayed until 2020, when he then moved to the Department of Ecology at the Universidade Federal do Rio de Janeiro, Brazil. He is interested in the evolutionary ecology of butterflies, notably on the evolution of chemical defense systems, anti-predator adaptations, and, in particular, aposematism and mimicry. He has worked on many aspects of butterfly biology, including behavioral ecology, population, community ecology, and conservation.

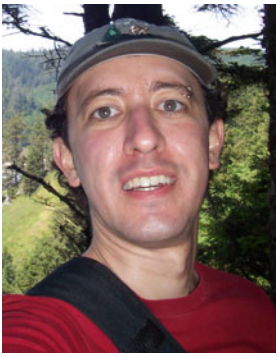

Rodrigo Cogni was born in Itatiba, São Paulo, Brazil. He obtained his B.Sc. degree in Biology in 2001 and his M.Sc. in Ecology in 2003, both at the Universidade Estadual de Campinas, Brazil. He obtained his Ph.D. degree in ecology and evolution at Stony Brook University, NY, USA in 2010. He worked as a postdoctoral associate in evolutionary genetics at this same institution from 2010 to 2012, and as a research associate in evolutionary ecology at Cambridge University, UK, from 2012 to 2014. In 2014, he returned to Brazil to join the faculty of the ecology department at the Universidade de São Paulo. He is interested in natural selection and the evolution of adaptations, and combines genomic techniques, variation in natural populations, and experimentation to study fundamental questions in this research area. In general, the main goal of his research program is to study the ecological pressures in the wild that influence the patterns of variation at the genomic level and result in the evolution of adaptations. He is interested in adaptations to abiotic factors of the environment, as well as adaptations to ecological interactions.

Ana Beatriz Barros de Morais was born in Porto Alegre, RS, Brazil, in 1958. She undertook undergraduate studies in Biology and obtained her B.Sc. degree from the Federal University of Rio Grande do Sul (UFRGS), Porto Alegre, RS, Brazil in 1980. Then, she obtained her M.Sc. degree in 1987 and a Doctor of Ecology degree in 1997, both from the Universidade Estadual de Campinas (UNICAMP), Campinas, SP, Brazil, under the guidance of Keith Spalding Brown Jr. (M.Sc.) and José Roberto Trigo. From 1992 to 2016 she was a faculty member first at the Department of Biology and later at the Department of Ecology and Evolution, CCNE, Universidade Federal de Santa Maria (UFSM), Santa Maria, RS, Brazil. Her research interests are focused on the field of insect ecology and natural history and conservation of tropical butterflies. During her scientific career, she has published 25 research articles and has supervised ten Master of Science and two doctoral theses.

A Timeline of Perezone, the First Isolated Secondary Metabolite in the New World, Covering the Period from 1852 to 2020

René Escobedo-González, Pablo Mendoza, María Inés Nicolás-Vázquez, Maricarmen Hernández-Rodríguez, Joel Martínez, and René Miranda Ruvalcaba

Contents

R. Escobedo-González
Department of Industrial Maintenance and Nanotechnology, Technological University of Juarez City, 32695 Ciudad Juarez, Chihuahua, Mexico
e-mail: renegerardo.escobedo@gmail.com

P. Mendoza · M. I. Nicolás-Vázquez · R. Miranda Ruvalcaba (✉)
Department of Chemistry, Faculty of Superior Studies Cuautitlan, National Autonomous University of Mexico, Mexico State, Campus 1, 54740 Cuautitlan Izcalli, Mexico
e-mail: mirruv@yahoo.com.mx

P. Mendoza
e-mail: pimendozas1@gmail.com

M. I. Nicolás-Vázquez
e-mail: nicovain@yahoo.com.mx

M. Hernández-Rodríguez
Cell Culture Laboratory, Medicine Higher School, National Polytechnic Institute, 11340 Mexico City, Mexico
e-mail: dra.hernandez.ipn@gmail.com

J. Martínez (✉)
Chemistry Science Faculty, Autonomous University of San Luis Potosi, San Luis Potosi 78210, Mexico
e-mail: atlanta126@gmail.com

A. D. Kinghorn, H. Falk, S. Gibbons, Y. Asakawa, J.-K. Liu, V. M. Dirsch (eds.),
Progress in the Chemistry of Organic Natural Products 116,
https://doi.org/10.1007/978-3-030-80560-9_3

1 Introduction

Perezone (**1**), pipitzahoic acid, or according to IUPAC nomenclature, (*R*)-3-hydroxy-5-methyl-2-(6-methylhept-5-en-2-yl)cyclohexa-2,5-diene-1,4-dione (Fig. 1), is recognized as the first secondary metabolite isolated in the New World by Leopoldo Río de la Loza Guillén [1] from the roots of *Perezia* (formerly *Acourtia*) specimens. Alongside this, a timeline from 1552 to 2005, in order to understand this chapter is offered in Fig. 2, and as complement the molecules have been offered throughout the chapter in different schemes.

To date, **1** has been physically and spectroscopically well characterized [2–4]: it is an orange crystalline solid. $R_f = 0.42$ (*n*-hexane/AcOEt 9:1). mp = 104 ± 1°C. UV–vis λ_{max} nm (log ε) in *n*-hexane: 203 (4.16), 261 (3.86), 400 (2.63). FT IR ν_{max}: 3305 (OH), 2976 (CH_2), 2929 (CH_3), 1648 (C = O), 1608 ($CH_{2Ar} = CH_{2Ar}$), 1389 ($CH_{2Ar} = CH_{2Ar}$) cm^{-1}. $[\alpha]_D^{20}$ –17°cm^2g^{-1} (ether). ^{1}H NMR (750 MHz, $CDCl_3$) δ/ppm: 1.20 (H-9, d, J = 7.1 Hz, 3H), 1.53 (H-15, s, 3H), 1.58 (H-10*S*, m, 1H), 1.64 (H-14, s, 3H), 1.80 (H-10(*R*), m, 1H), 1.86 (H-11(*R*), m, 1H), 1.92 (H-11(*S*), m, 1H), 2.06 (H-7, d, J = 1.6 Hz, 3H), 3.05 (H-8, m, 1H), 5.07 (H-12, ddd, J = 7.0, 5.7, 1.3 Hz, 1H), 6.48 (H-6, d, J = 1.6 Hz, 1H), 6.99 (OH, s, 1H). ^{13}C NMR (189 MHz, $CDCl_3$) δ/ppm: 14.71 (C-7), 17.63 (C-15), 18.24 (C-9), 25.70 (C-14), 26.69 (C-11), 29.33 (C-8), 34.11 (C-10), 124.48 (C-12), 124.59 (C-2),

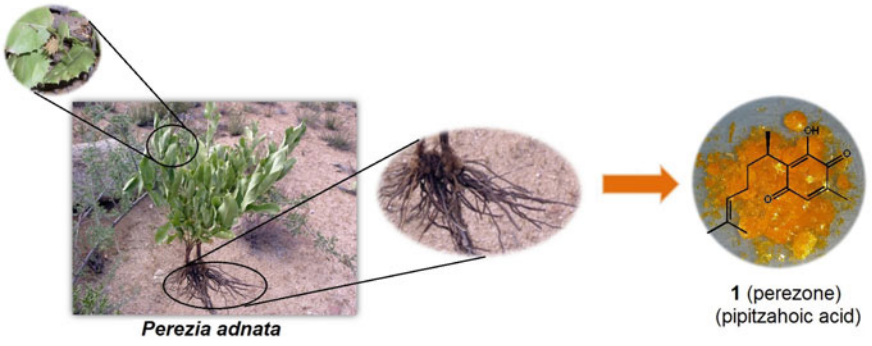

Fig. 1 Perezone (**1**) isolated from the roots of *Perezia*

131.45 (C-13), 135.88 (C-6), 140.55 (C-5), 150.98 (C-3), 184.34 (C-1), 187.39 (C-4). EI-MS (70 eV), *m/z* (% rel. abund.)[assignment]: 248(17)$M^{+\bullet}$, 233(3)$[M–CH_3]^+$, 219(2)$[M–C_2H_5]^+$, 205(6)$[M–C_2H_3O]^+$, 191(10)$[M–C_4H_9]^+$, 177(5)$[M–C_5H_{11}]^+$, 166(100)$[M–C_6H_{10}]^{+\bullet}$, 137(5)$[M–C_8H_{15}]^+$, 55(12)$[C_4H_7]^+$, 41(18)$[C_3H_5]^+$. ESI-HRMS (19 eV), exact mass for $C_{15}H_{21}O_3$, $[M + H]^+$ 249.1491 Da, corresponding to an accurate value of 249.1497 Da, error: –2.41 ppm, unsaturations: 5.

2 Timeline Covering 1552–1852–2005

For many years, the important molecule perezone (**1**) has been the subject of numerous chemical, structural, biological, and in silico studies, which are summarized in Fig. 2 in the form of a timeline stretching from 1552 to 2005, and are discussed in the following section. The structures mentioned in Fig. 2 and throughout this contribution are listed in the formula drawings that follow.

2.1 Comments on the Timeline

In the following paragraphs, 83 points of the timeline in Fig. 2 are explained and discussed in detail.

(1) In the sixteenth century, specifically in 1552, Martin de la Cruz, a Mexican physician, wrote a document entitled "Amate Cehuatl Xihuitl Pitli", a most important illustrated compilation on medicinal Mexican (Mexica) plants, from the Tenochtitlan Valley, which now corresponds to modern-day Mexico City. This work was translated from the Nahuatl to Latin by Juan Badiano as "Libellus de Medicinalibus Indorum Herbis" and significantly this compilation mentions the medicinal effects of the roots of plants of *Perezia* specimens (pipitzahua-Nahuatl) [5].

(2) It is important to highlight that in 1852, Dr. Leopoldo Río de la Loza Guillén disclosed the isolation, medicinal properties, and elemental composition of pipitzahoic acid (perezone (**1**)), which was the first pure natural product chemical isolated in the New World (specifically the American Continent) [1, 6].

(3) Several attempts to achieve the structural formula and some chemical and physical analyses were performed between 1885 and 1886, giving the empirical formula of $C_{15}H_{20}O_3$ and indicating its phenolic and quinone character [7–10].

(4) In 1899, **1** was ascribed with alkalimetric properties since it becomes rose colored with traces of alkali [11].

(5) By 1913, several perezone derivatives were prepared (α- and β-pipitzols (**2**, **3**), α- and β-acetylpipitzols (**4a**, **4b**), α- and β-benzoylpipitzols (**5a**, **5b**), hydroxyperezone (**6**), perezinone (**7**), and their empirical formulas were established [12].

(6) The first structure for **1** was proposed in 1935 [13].

(7) In 1942, a mixture of *dl*-dihydroperezone (**8**) was produced from **1**, confirming the previously proposed structure of the title compound [14].

(8) In 1954, the configuration (*R*) at C–8 for compound **1** was reported [15].

(9–14) During the year 1965, several important contributions on the scientific knowledge of **1** occurred: its correct structure was confirmed unequivocally [16–19]; the structures of its rearrangement derivatives, **2** and **3**, were elucidated [20]; compounds **1** and **6** were isolated from *Perezia alamani* [21]; and also the total synthesis of **1** was achieved [22].

(15) Perezone (**1**) and both **2** and **3** were isolated from *Perezia cuernavacana* (1966) and by thermal rearrangement of **1**, pipitzols **2–5** and several new compounds (**7** and **9–41**) were produced [23].

(16) Interesting optical properties like the circular dichroism and optical rotatory dispersion for **1** and some of its derivatives were determined in 1967 [24].

(17) During the year of 1968, several molecules related to **1** were reported (e.g., **6–7**, **42–51**) [25].

(18) Different mixture ratios of griseofulvin and **1** were prepared and proved to be active against several infections [26].

(19) ^{13}C NMR experiments were performed to correctly assign all carbon resonances of **1** as well as for some derivatives [27].

(20) Perezone and several analogs (**2**, **3**, **6**, hydroxyperezone monoisovalerate (**52**), and α-, β-, and γ-perezols (**53–55**)) were isolated from *Perezia heblecada* in 1972 [28].

(21–22) In 1974, a contribution describing several synthesis transformations of hydroxyperezone (**6**) was published [29]; in the same year, pyrazoline-*O*-methylperezone (**56**) was transformed to produce derivatives **57–60** [30].

(23–24) The isolation of **1** and various analogs (**61–64**) was reported from *Perezia runcinata* [31] and *Perezia multiflora* [32]; it is also important to note the proposal of a concerted reaction mechanism for the conversion of **1** to **2**, and **3** [33].

(25–27) A set of novel perezone derivatives was isolated in 1979 from *Acourtia thurberi* [34] (perezone angelate (**65**), 2-hydroxy-dihydroperezon-2-*O*-angelate (**66**), 2-hydroxy-dihydroperezon-5-*O*-angelate (**67**), 2-acetyl-dihydroacetateperezon-2-*O*-angelate (**68**), and 2-acetyl-dihydroacetateperezon-5-*O*-angelate (**69**)). In a ^{13}C NMR study, the positions of the methyl groups in the isopropylidene moiety were determined by means of a convenient correlation with cholesterol [35]. In the same year, the production of a spirodecenedione (**70**) and an oxatetracyclotridecenone (**71**) by employing UV irradiation of **56** was also reported [36].

(28–29) In 1980, the laxative activities of **1** and hydroxyperezone monoangelate (**72**) were studied and the effect was attributed to **72** [37]. Additionally, the methylation of hydroxyperezone (**6**) produced *O*-methylmethoxyperezone (**73**) and its UV irradiation resulted in derivatives **74–77** [38].

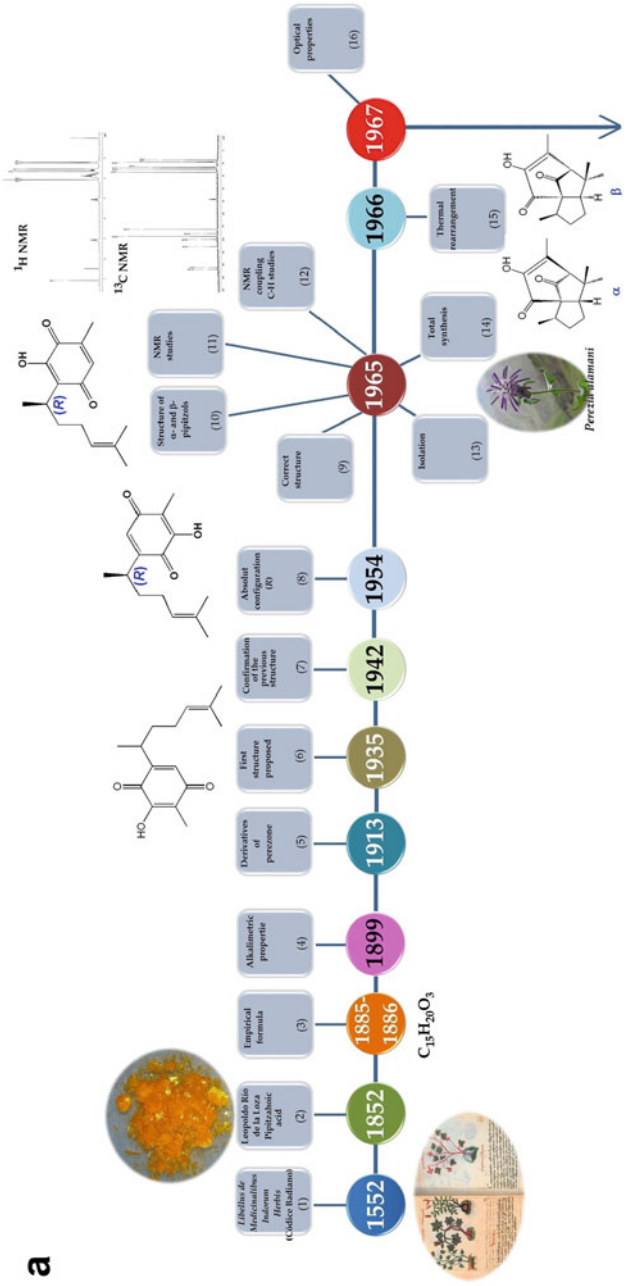

Fig. 2 Timeline of perezone, (**1**) (1552–2005)

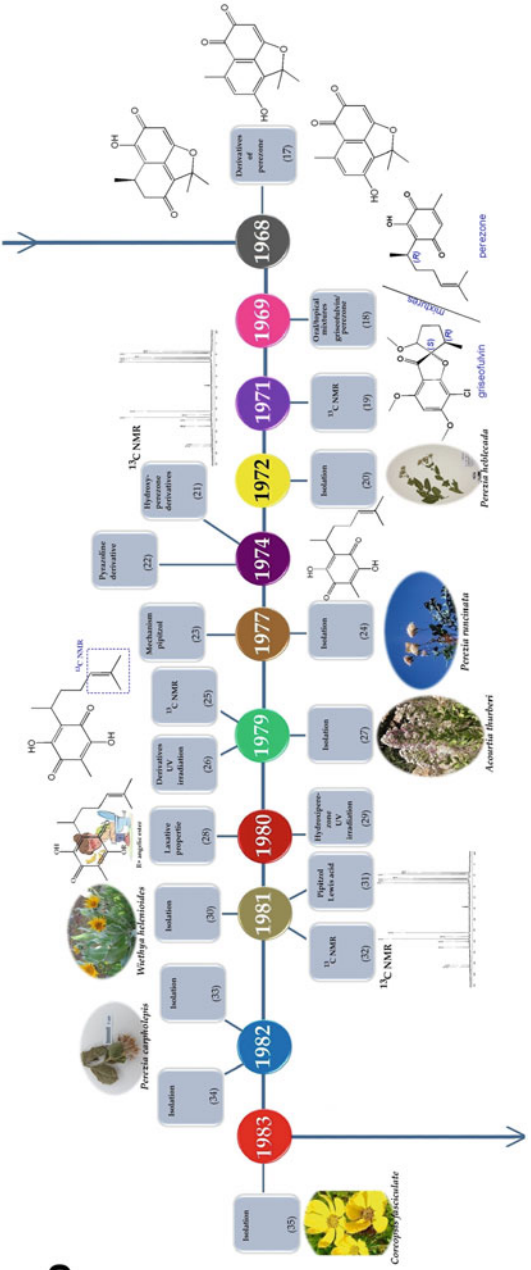

Fig. 2 (continued)

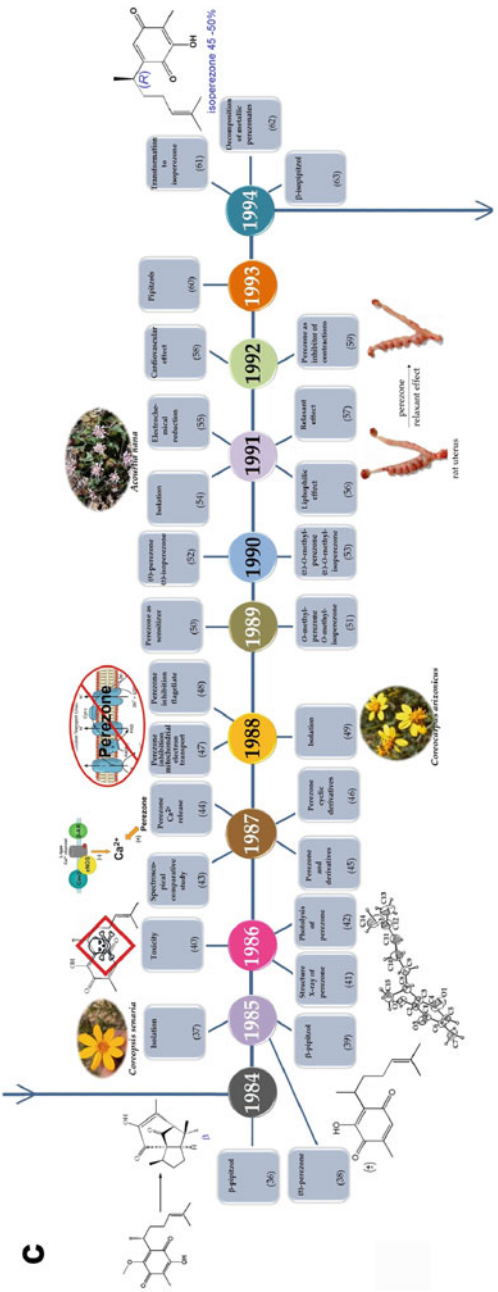

Fig. 2 (continued)

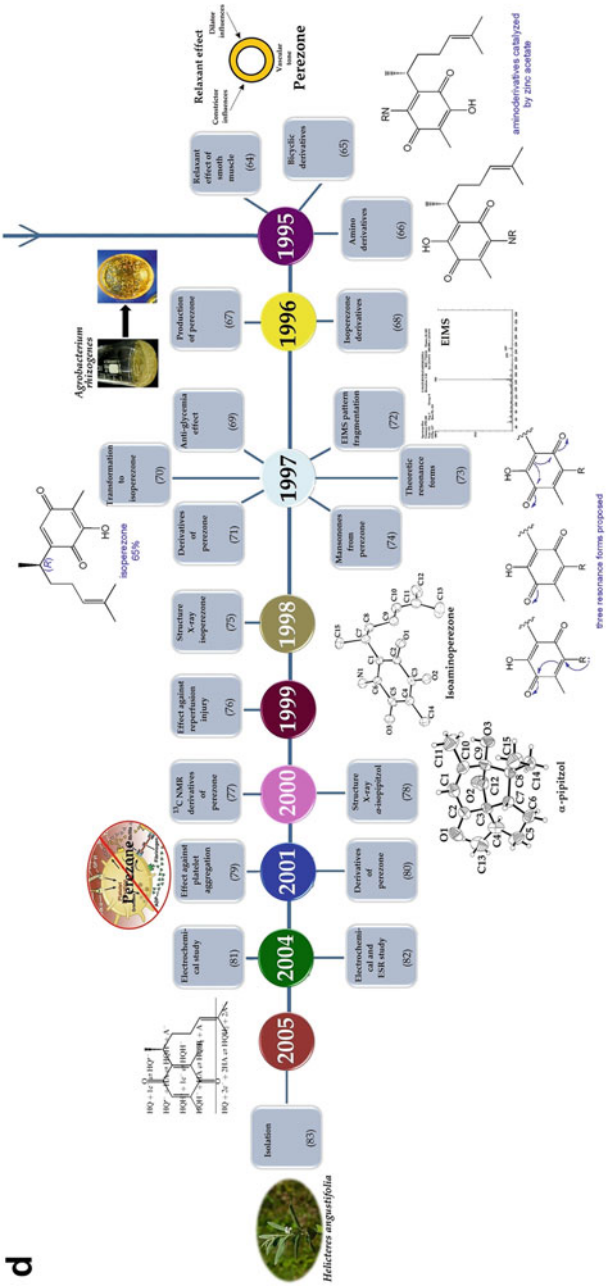

Fig. 2 (continued)

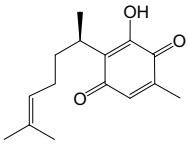

1 (perezone)

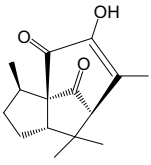

2 (α-pipitzol)

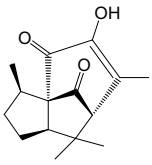

3 (β-pipitzol)

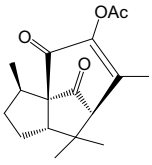

4a (α-acetylpipitzol)

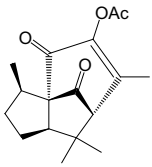

4b (β-acetylpipitzol)

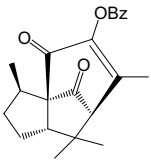

5a (α-benzoylpipitzol)

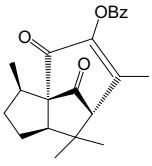

5b (β-benzoylpipitzol)

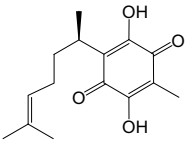

6 (hydroxyperezone)

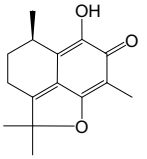

7 (perezinone)

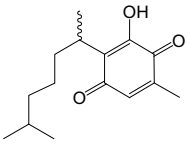

8 (*dl*-dihydroperezone)

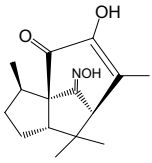

9

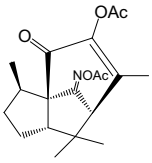

10

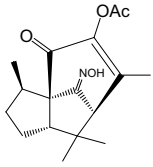

11

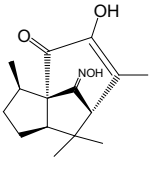

12

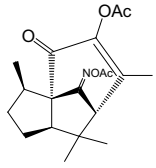

13

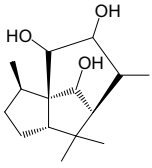

14

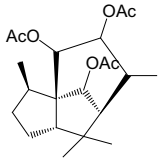

15

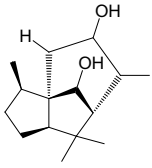

16

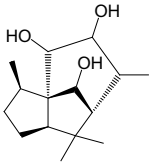

17

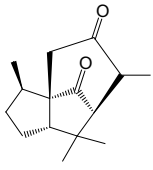

18

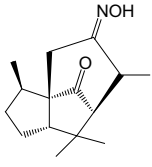

19

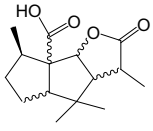

20

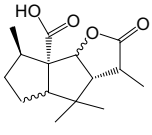

21

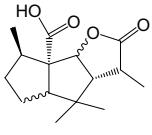

22

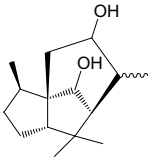

23

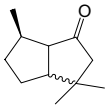

24

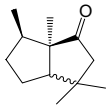

25

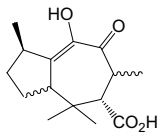

26

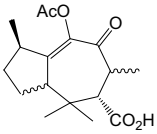

27

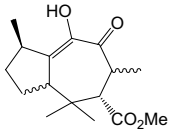

28

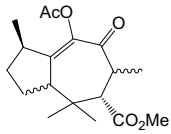

29

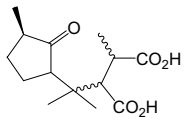

30

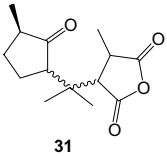

31

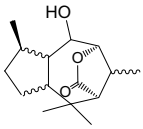

32

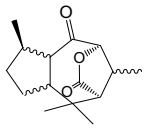

33

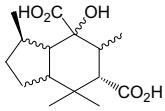

34

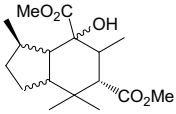

35

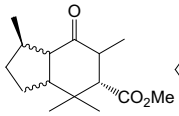

36

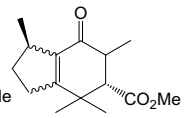

37

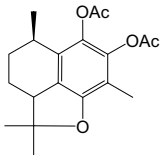

38

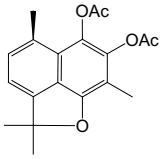

39

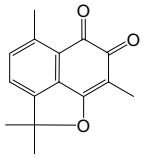

40

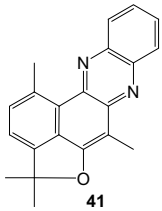

41

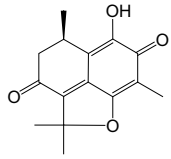

42

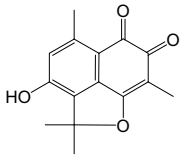

43

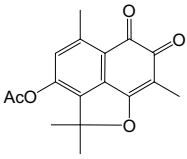

44

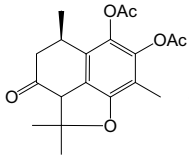

45

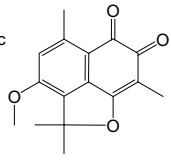

46

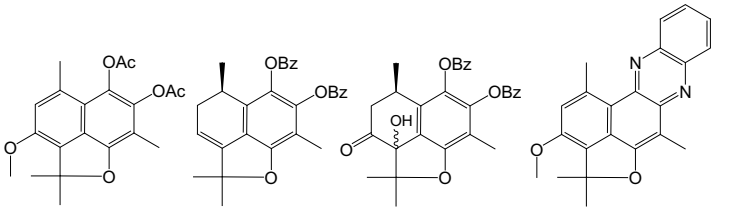

47 **48** **49** **50**

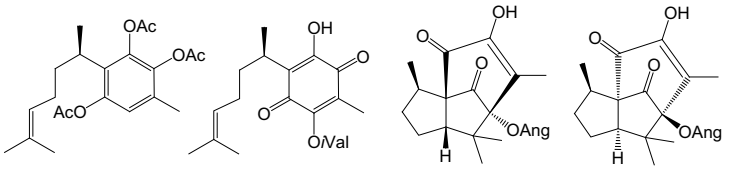

51 **52** (hydroxyperezone-monoisovalerate) **53** (α-perezol) **54** (β-perezol)

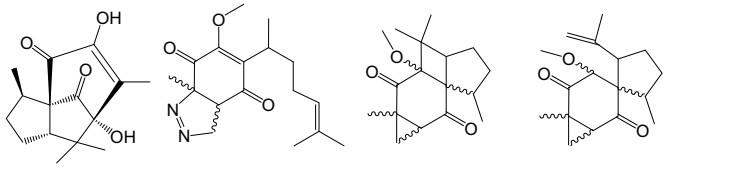

55 (γ-perezol) **56** (pyrazoline-*O*-methylperezone) **57** **58**

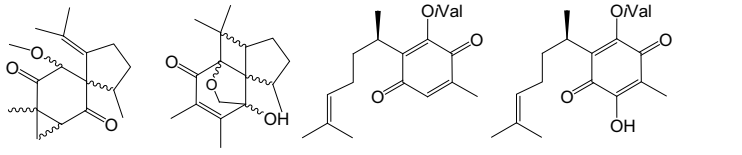

59 **60** **61** **62**

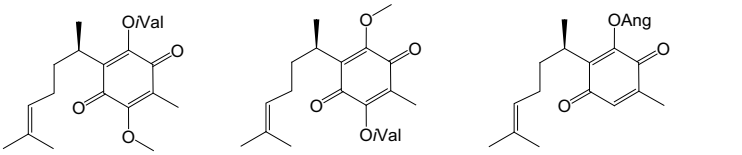

63 **64** **65** (perezone angelate)

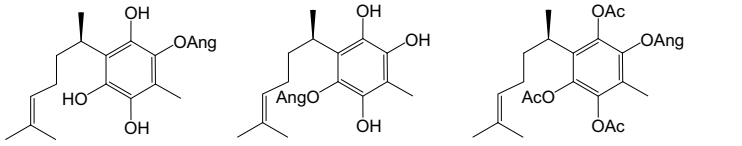

66 (2-hydroxy-dihydro-perezon-2-*O*-angelate) **67** (2-hydroxy-dihydro-perezon-5-*O*-angelate) **68** (2-acetyl-dihydroacetate-perezon-2-*O*-angelate)

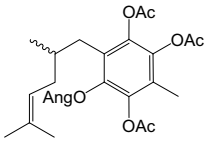

69 (2-acetyl-dihydroacetate-perezon-5-*O*-angelate)

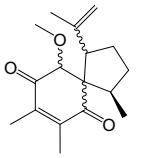

70 (spirodecedione)

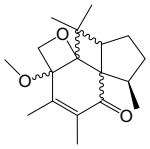

71 (oxatetracyclotri-decenone)

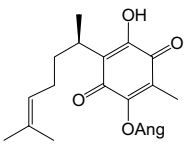

72 (hydroxyperezone-monoangelate)

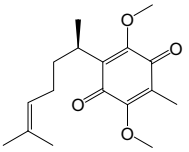

73 (*O*-methylmethoxy-perezone)

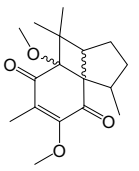

74

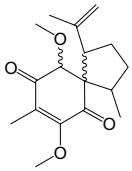

75

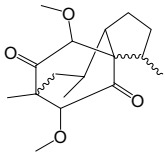

76

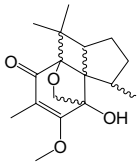

77

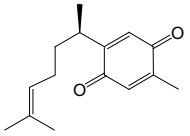

78 (6-desoxyperezone)

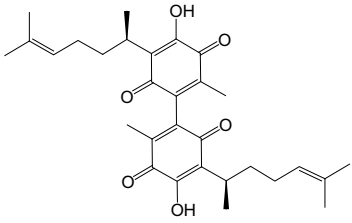

79 (diperezone)

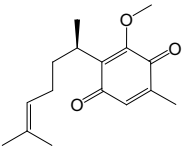

80 (methoxyperezone)

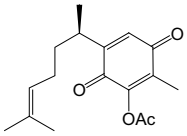

81 (6-acetylperezone)

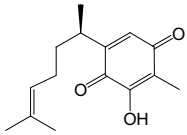

82 (isoperezone)

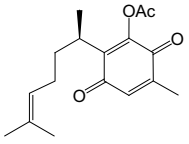

83 (2-*O*-acetylperezone)

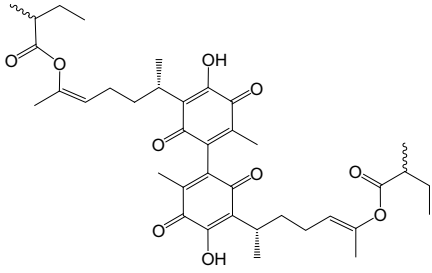

84 (6,6'-bis[2-(1,5-dimethyl-4-hexenyl)-6-(2-methylbutyroxy)]-3-hydroxy-5-methyl-*p*-benzoquinone)

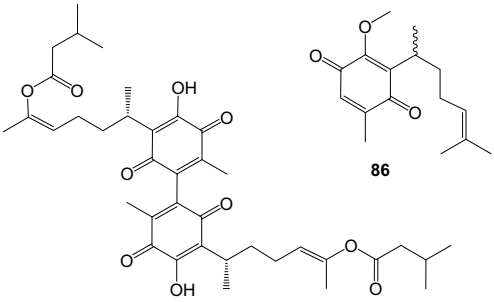

85 (6,6'-bis[2-(1,5-dimethyl-4-hexenyl-6-isovaleroxy)-3-hydroxy-5-methyl-*p*-benzoquinone])

86

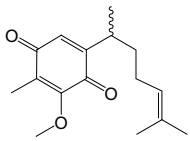

87 ((±)-*O*-methylisoperezone)

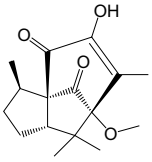

88 (7-methoxy-α-pipitzol)

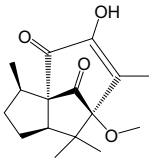

89 (7-methoxy-β-pipitzol)

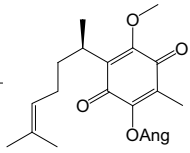

90 (*O*-methyl-6-angeloxyperezone)

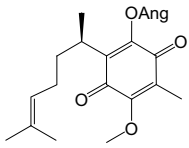

91 (*O*-angeloyl-6-methoxyperezone)

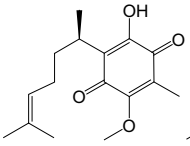

92 (6-methoxyperezone)

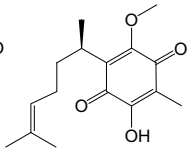

93 (*O*-methyl-6-hydroxyperezone)

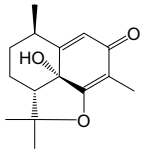

94 (dihydroisoperezinone)

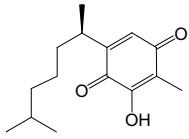

95 (dihydroisoperezone)

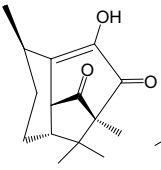

96 (β-isopipitzol)

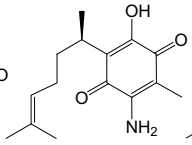

97

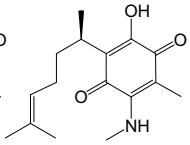

98

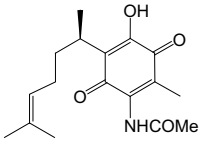

99

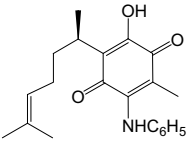

100

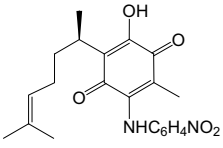

101

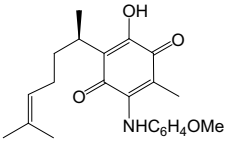

102

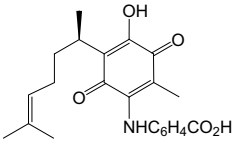

103

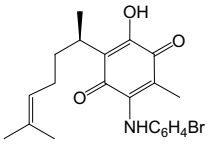

104

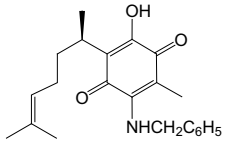

105

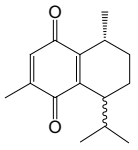

106

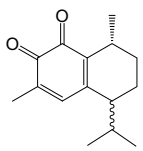

107

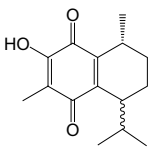

108

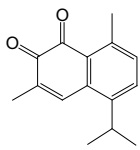

109

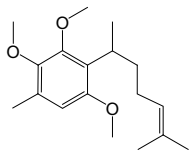

110 (perezone trimethyl ether)

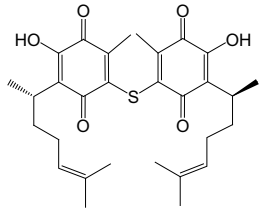

111 (6,6'-thio-bis-perezone)

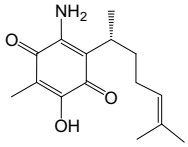

112 (aminoisoperezone)

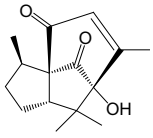

113 (α-isopipitzol)

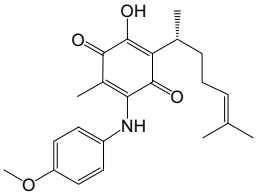

114

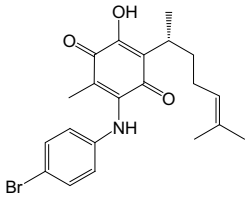

115

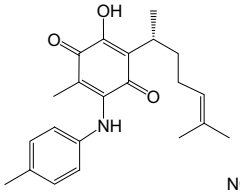

116

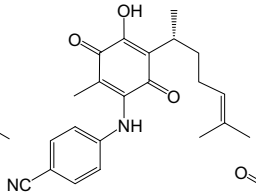

117

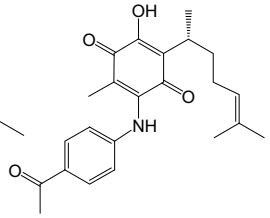

118

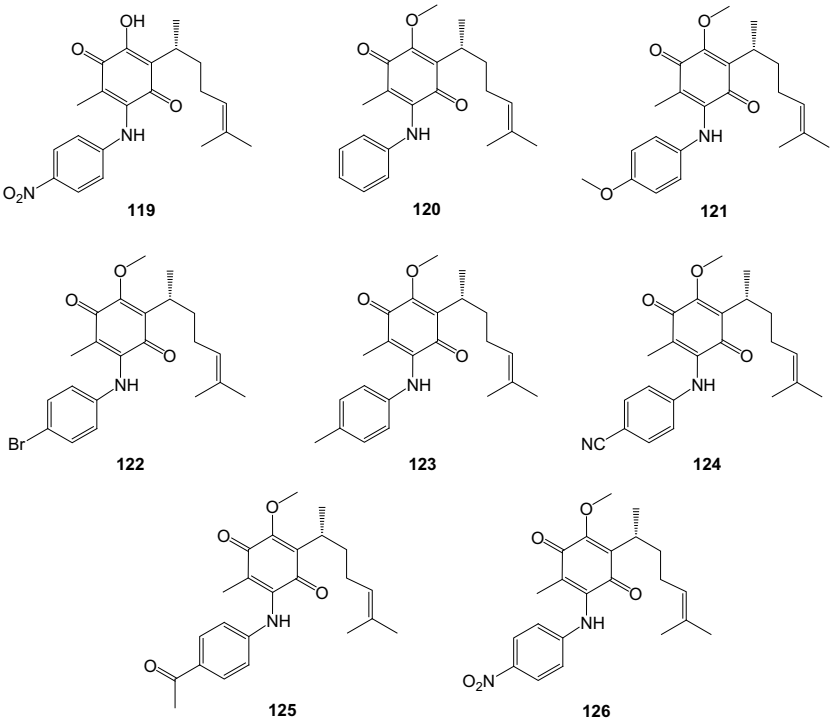

(30–32) The transformation of perezone (**1**) to the corresponding derivatives α-pipitzol (**2**) and β-pipitzol (**3**) employing BF_3 as a Lewis acid catalyst was reported in 1981 [39]; also, a contribution on the unequivocal assignments for all the ring ^{13}C NMR signals in several perezone derivatives was published [40] and from a non-polar extract of *Wyethia helenioides*, 6-desoxyperezone (**78**) was isolated [41].

(33–35) From 1982 to 1983, several reports related to the isolation of perezone (**1**) and various analogs (**2**, **3**, **61**, diperezone (**79**), methoxyperezone (**80**), and 6-acetylperezone (**81**)), from *Perezia carpholepis* [42], *Perezia alamani* var. *oolepis* [43], *Coreopsis fasciculata*, and *Coreopsis mitica* were published [44].

(36–39) During the period 1984–1985, the following results were documented: **3** was obtained from methoxyperezone (**80**) [45], the production of **80** was described in Ref. [46], the total synthesis of (±)-perezone was published [47], and the isolation of **1** and several analogs (6-acetylperezone (**81**), isoperezone (**82**), and 2-*O*-acetylperezone (**83**)) from *Coreopsis senaria* were reported [48].

(40–42) In 1986, the X-ray crystallographic determination of the structure of perezone (**1**) was published [49]. Photolysis products of **1** were characterized by NMR spectroscopy [50] and its toxicity was studied [51].

(43–46) Worthy of note is the year 1987, due to a large number of contributions related to perezone (**1**) being published: a comparative study between ^{13}C CPMAS NMR and ^{13}C NMR was undertaken, and, in addition, the X-ray structures of **6** and **1** were compared [52]. Furthermore, **1**, **82**, and **6** were produced by convenient

chemical transformations using the sesquiterpene parvifoline as a substrate [53]. Several interesting cyclic derivatives of **1** were obtained [54], and **1** was tested for its ability to cause Ca^{2+} release, demonstrating that it is dependent on the reduction of this compound, and a dose–response relationship was observed [55].

(47–49) During 1988, **1** and various analogs (**2**, **79**, 6,6′-bis[2-(1,5-dimethyl-4-hexenyl)-6-(2-methylbutyroxy)]-3-hydroxy-5-methyl-*p*-benzoquinone (**84**), and 6,6'-bis[2-(1,5-dimethyl-4-hexenyl-6-isovaleroxy)-3-hydroxy-5-methyl-*p*-benzoquinone]) (**85**) were isolated from *Coreocarpus arizonicus* [56]. Due to the favorable oxidation–reduction characteristics of **1**, it inhibits mitochondrial electron transport [57], and it was noted that both perezone (**1**) and D,L-dihydroperezone (**8**) inhibited flagellate growth of *Trypanosoma mega* [58].

(50–51) Several studies related to perezone (**1**) and various derivatives were performed in 1989. Among them, an important review of **1** was published by Joseph-Nathan and Santillan [59] summarizing chemical contributions. In the same year, it was also reported that **1** is a strong cross-reaction sensitizer in guinea pigs, when compared to hydroperezone (**6**) and abietic acid [60]. In addition, two rearrangements of cyclobutenones were described, which yielded (±)-*O*-methylperezone (**80**) and (±)-*O*-methylisoperezone (**86**) [61].

(52–63) Between 1990 and 1994, a large number of contributions to knowledge on perezone (**1**) were reported. These included the ring expansions of *tert*-butoxycyclobutenedione and of 4-alkynyl, 4-alkenyl, or 4-arylcyclobutenones, to yield racemic perezone ((±)-**1**) and racemic isoperezone ((±)-**82**) [62]. In addition, by means of the ring enlargement of various 4-alkenyl-4-hydroxycyclobutenones followed by oxidation, the formation of methoxyperezone (**80**) and (±)-*O*-methylisoperezone (**87**) was achieved [63]. Compounds **1** and analogs **2** and **3** were also isolated from *Acourtia nana* [64]. Moreover, the electrochemical reduction of **1** in the presence of benzoic acid was performed [65]. Additionally, the effects of the lipophilic nature of **1** on the release of H_2O_2 and O_2^- from whole cells were reported [66], and its muscle relaxant effects on the rat uterus were also observed [67]. The cardiovascular effects of **1** were determined in urethane–anesthetized rats [68] and it was also demonstrated that this compound can inhibit aortal ring contractions induced by histamine, norepinephrine, or KCl [69]. Several studies on the production of pipitzol derivatives were accomplished using cycloadditions of methoxyperezone (**80**): 7-methoxy-α-pipitzol (**88**), 7-methoxy-β-pipitzol (**89**), **73**, a mixture of *O*-methyl-6-angeloyloxyperezone (**90**) with *O*-angeloyl-6-methoxyperezone (**91**), 6-methoxyperezone (**92**), and *O*-methyl-6-hydroxyperezone (**93**) [70]. The interesting transformation of **1** into isoperezone (**82**) by means of a 1,2-carbonyl transposition using tetrahydropyrimidinethiol as the catalyst was also developed in this period together with the production of dihydroisoperezinone (**94**) and dihydroisoperezone (**95**) [71]. The decomposition of metallic perezonates in hydro-alkalinic solutions was reported [72], and finally by using **82** with an intramolecular cycloaddition catalyzed by $ZnBr_2$, β-isopipitzol (**96**), **7**, and **94** were produced [73].

(64–66) In 1995, a set of in vitro assays was developed showing that perezone (**1**) relaxes the basal tonus of the smooth muscle. Therefore, the effects of **1** on rat intestinal smooth muscle revealed the dose–dependent dual effect of **1** induced by

ACh, K^+, and Ba^{2+} [74]. The formation of several amino derivatives of perezone (**1**) and isoperezone (**82**) catalyzed by zinc acetate was described [75]. Two unusual bicyclo[2.2.2]octenediones were obtained by the reaction of **1** with thiourea [76].

(67–68) During 1996, the production of **1** was enhanced employing hairy roots of *Perezia cuernavacana* induced by inoculation of intermodal segments of the sterile plant with the *Agrobacterium rhizogenes* strain AR12 [77]. Moreover, several cycloaddition products were produced by UV light irradiation of 6-acetylperezone (**81**) [78].

(69–74) A fragmentation pattern from electronic ionization (EI) and collision–induced dissociation (CID) experiments of **1** and several analogs (**82**, **2**, **3**, **7**, **94**, and **96**) was established in 1997 [4]. In the same year, it was demonstrated that a root decoction of *A. thurberi* reduced glycemia in mice and hyperglycemia in rabbits. It should be noted that the water decoction contained **1**, **2**, and **3** as the principal components [79]. An interesting study in 1997, by means of theoretical calculations, established the existence of three different resonance forms of the diradical configuration of the triplet state of 12 derivatives (**6**, **92**, **97**–**105**) of perezone (**1**) [80]. The production of mansonones **106**–**109** by cyclization-oxidation of **1** and hydroxyperezone (**6**) was established [81], and the formation of perezone trimethylether (**110**) by reductive methylation was reported [82]. Finally, by addition of a small quantity of water, the isomerization of perezone (**1**) to isoperezone (**82**) through 3,4,5,6-tetrahydro-2-pyrimidinethiol was improved, yielding 65%, together with other derivatives such as 6,6´-thio-*bis*-perezone (**111**) and **112**, which were identified as by-products [83].

(75) In 1998, the structures of isoperezone (**82**) together with its analogous aminoisoperezone (**112**) as well as amino derivative **97** were determined by single-crystal X-ray diffraction analysis [86].

(76) In 1999, an in vivo study performed on a rat heart model showed that perezone (**1**) reduces the incidence of reperfusion-induced arrhythmias [85].

(77–78) A complete study by ^{13}C NMR spectroscopy was completed for several perezone derivatives [86] and the structure of α-isopipitzol (**113**) was established using an X-ray diffraction study [87].

(79–80) In 2001, it was established that **1** inhibits ADP-, epinephrine-, and collagen-induced platelet aggregation. In contrast, isoperezone (**82**), **97**, and **112** provided negative results [88]. In addition, in the same year, 13 C-6 *p*-substituted anilinebenzoquinones **114**–**126** of **1** were studied using spectroscopic, electrochemical, and theoretical techniques [89].

(81–82) During 2004, two electrochemical studies were reported: in the first instance, **1** and several analogs (**80**, **100**, **94**–**97**, **120**–**124**) were studied and established the influence of internal proton donors and external proton sources in the first electron transfer [90]. The self-protonation of perezone (**1**) in the first electron-transfer process was derived by cyclic voltammetry and double potential step chronoamperometry [91].

(83) In 2005, perezone (**1**) was isolated from *Helicteres angustifolia*, of the plant family Malvaceae [92].

3 Advances in the Period 2006–2020

To date, almost 170 years have passed since the first documentation relating to the isolation of perezone (pipitzahoic acid) (**1**). Nevertheless, studies of this interesting molecule have continued, directed not only toward solving challenging chemical problems but also in the in silico, spectroscopic, and pharmacological areas.

It is worth noting that in 1989, P. Joseph-Nathan and R. L. Santillan recognized the value of assembling information on the chemistry of **1** and its derivatives and published a review [59], as alluded to in Sect. (50), of the time line. This review covered the chemistry of naturally occurring sesquiterpene quinones isolated from the genus *Perezia* (*Acourtia*) as well as other compounds found in this genus.

Considering the importance of **1** and the research interest in this molecule by the present authors, it is hoped that this chapter will make a valuable contribution by collating relevant scientific documentation. Consequently, all available information has been compiled on perezone covering the 15-year period 2006–2020, in chronological order. Specifically, noteworthy developments on the chemical synthesis, spectroscopic, pharmacological, and in silico aspects of perezone research are covered.

3.1 Advances in Electrochemical Aspects

3.1.1 Electrochemical and ESR Studies

In 2007, C. Frontana and I. Gonzalez reported two related investigations considering both electrochemical-cyclic voltammetry (CV) and a spectroelectrochemical-electron spin resonance (ESR) study in an aprotic medium, focusing not only on perezone (**1**), but also on three known quinones, 2-hydroxy-1,4-naphthoquinone, horminone, and 7α-*O*-methyl-conacytone, which were compared [93, 94]. The electrochemical study revealed a self-protonation mechanism, occurring at the first CV signal and showing a dependence on the structures of the target molecules. The corresponding CV signals depicted in Fig. 3 involved two reduction signals (peaks Ic and IIc). Unfortunately, the first electro-generated radical anion readily disproportionated and therefore there was no possibility to analyze its structural properties by employing coupled electrochemical-ESR experiments. It is pertinent to note that, during self-protonation, a significant quantity of deprotonated quinone, corresponding to radical dianions, was generated. In this regard, the ESR study for the second reduction process displayed well-resolved ESR spectra, and the spectrum obtained relating to the radical dianions of perezone (**1**) is shown in Fig. 4. For the electrochemical procedures, a three-electrode cell was used to carry out the CV test, the working electrode was a platinum microelectrode, Et_4NBF_4 was the electrolyte support, and acetonitrile served as the solvent.

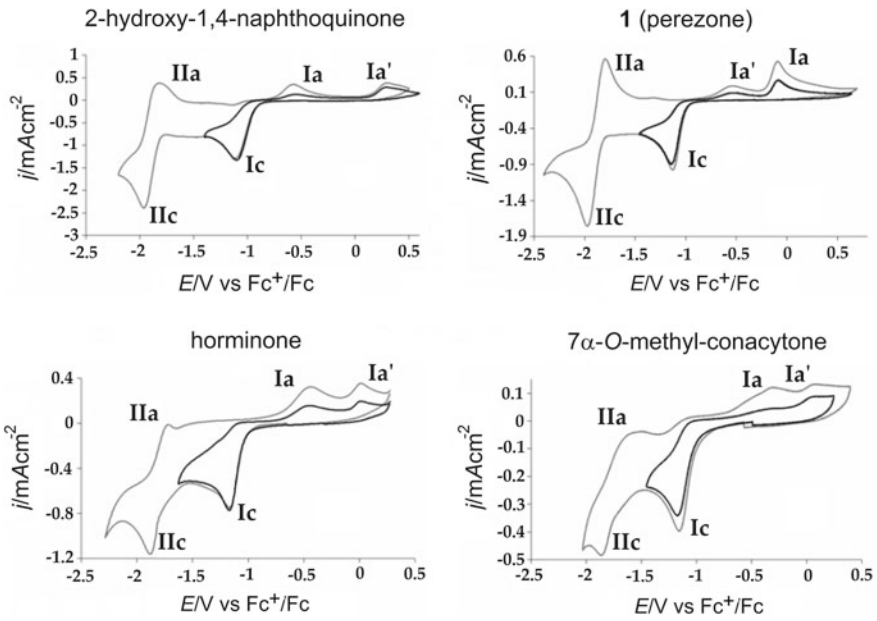

Fig. 3 Typical cyclic voltammograms of the studied α-hydroxyquinones. Adapted from Refs. [93, 94]

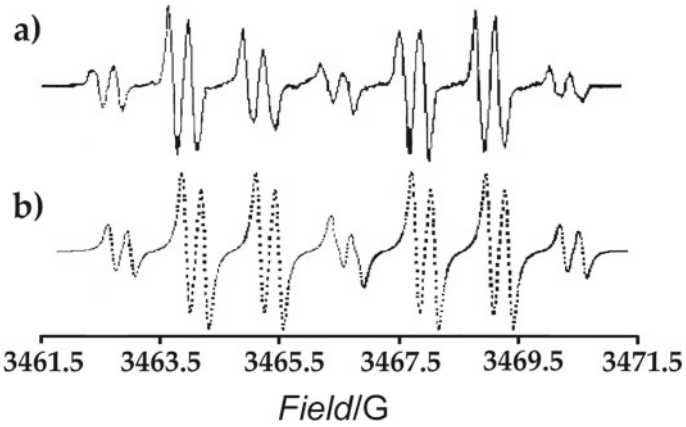

Fig. 4 ESR **a)** experimental and **b)** isotropic simulation spectra of the radical dianions of perezone (**1**). Adapted from Refs. [93, 94]

3.1.2 Effects of the Substituents on the Reactivity of Anilinoperezones: Analysis of the Influence of the C-12–C-13 Double Bond

Bautista–Martínez et al. carried out interesting electroreduction studies of perezone (**1**), dihydroperezone (**8**), and two sets of five corresponding aniline derivatives, and deduced that the double bond in the side chain can interact with the quinone ring [95]. The goal of this work was to study the electroreduction of **1** and a set of five aniline derivatives (**114**–**117**, **120**), in addition to their corresponding dihydro derivatives (**127**–**131**), as summarized in Fig. 5 by cyclic voltammetry (CV) and spectroelectrochemical-electron spin resonance (ESR) in situ. The CV experiments (Fig. 6) were performed with acetonitrile as solvent and tetraethylammonium tetrafluoroborate as the electrolyte support; polished glassy carbon was the working electrode, a platinum wire served as counterelectrode, and the reference electrode was aqueous AgCl/Ag. The ESR measurements were performed at a scan rate of 10 $mV \cdot s^{-1}$ while holding the potential scan at a position at which a stable radical signal was recorded. According to the results obtained, the authors observed weak π-π interactions of the olefin-quinone type for the reduction of the quinonic moiety. From this information, the difference between the cathodic (E_{pcI}) and anodic (E_{paI}) peak potentials (Table 1) of the corresponding dihydro derivatives could indicate an increase in acidity related to the hydroxy group at C-3, promoted by the absence of the double bond and the production of the hydroquinone. The corresponding values of the perezone aniline derivatives implied that their electroreduction testing would stop at the presence of a hydroquinone monoanion and this was in agreement with the ESR results. Moreover, with respect to the spectroelectrochemical ESR experiments, the studied molecules confirmed the presence of dianions. The ESR spectra of the electro-generated radical dianions of perezone (**1**), dihydroperezone (**8**), and the simulated isotropic structures are also depicted.

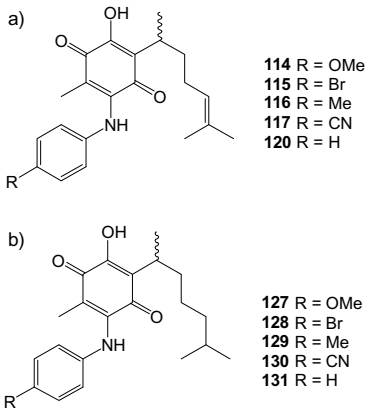

Fig. 5 a) Anilinoperezones (**114–117, 120**) and b) their hydrogenated derivatives **127–131**. Adapted from Ref. [95]

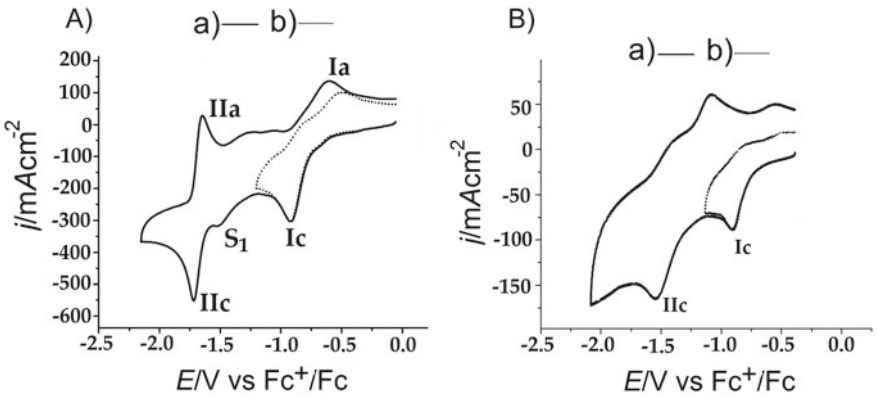

Fig. 6 A) CV of perezone (**1**): potential scan rate 0.1 versus –1. a) $E\lambda = -2.15$ V and b) $E\lambda = -1.21$ V. B) CV of dihydroperezone (**8**): potential scan rate 0.1 versus –1. a) $E\lambda = -2.1$ V, and b) $E\lambda = -1.135$ V. Adapted from Ref. [95]

Table 1 Voltamperometric parameters for APZs **114**–**117**, **120** and APZHs **127**–**131**. Data from Ref. [95]

Substituent	E_{pcI} APZ V versus Fc^+/Fc	E_{pcI} APZH V versus Fc^+/Fc	E_{pcI}-E_{paI} APZ V	E_{pcI}-E_{paI} APZH V
MeO	−1,096	−1,046	494	624
Me	−1,062	−1,040	437	565
H	−1,015	−1,035	478	695
CN	−1,011	−0,966	317	449
Br	−0,925	−0,931	449	542

3.1.3 Perezone as a Corrosion Inhibitor for AISI 1018 Steel Immersed in Sodium Chloride Solution Saturated with CO_2

Perezone (**1**) has been evaluated as a corrosion inhibitor of 1018 steel, in the presence of a corrosive 3% NaCl solution saturated with CO_2, employing the electrochemical impedance mode under both static and turbulent flow conditions. Various ethanolic solutions of this inhibitor were evaluated (5, 10, 20, and 50 ppm) [96]. The results indicated that **1** offers a good corrosion protection at a concentration of 10 ppm with 87% efficiency under static conditions, while in hydrodynamic conditions at rotation rates of 100 and 500 rpm, 96 and 95% efficiency at a concentration of 5 ppm was reached, respectively. A complementary thermodynamic analysis using a Langmuir adsorption model showed that perezone was physically adsorbed to the steel surface. In regard to electrochemical impedance measurements, these were accomplished in a three-electrode electrochemical cell. The working electrode was AISI 1018 steel and used as the rotating cylinder electrode, which allowed the simulation of turbulent flow, at relatively low rotation rates (0, 100, and 500 rpm), while the reference

electrode was saturated Ag/AgCl, and graphite was the counterelectrode. In a Nyquist diagram (corrosion inhibition) of steel versus perezone (**1**), which recorded data under static conditions, the plot extended up to Z_{re} ~370 Ωcm^2. In comparison with dynamic conditions (100 rpm) and a concentration of 5 ppm of **1**, the extreme extension occurred at Z_{re} ~1000 Ωcm^2. It should be noted that the variance obtained is due to mechanical agitation, where the solution is more homogeneous, permitting the inhibitor to adsorb to the steel surface. Nevertheless, if the rotation speed was increased, the maximum extension decreased (Z_{re} ~200 Ωcm^2, at 50 ppm). Similar changes were observed when the cylinder was rotated at 500 rpm. Finally, the authors commented that generally under hydrodynamic conditions, the adsorption of the inhibitor increases with its concentration, improving corrosion resistance.

3.2 Green Approaches

3.2.1 Eco-Contributions to the Chemistry of Perezone: A Comparative Study Using Different Modes of Activation and Solvent-Free Conditions

The synthesis of two sets of both R^3-(*R*)-perezone and R^3-(*R*)-isoperezone sulfur derivatives **132–135** and **136–139** was reported. The study was carried out through activating the reactions by means of microwave and infrared irradiations in comparison to the typical mode mantle heating, using pure MeOH as the solvent and comparing the reaction with solvent-free conditions (Scheme 1a). The authors

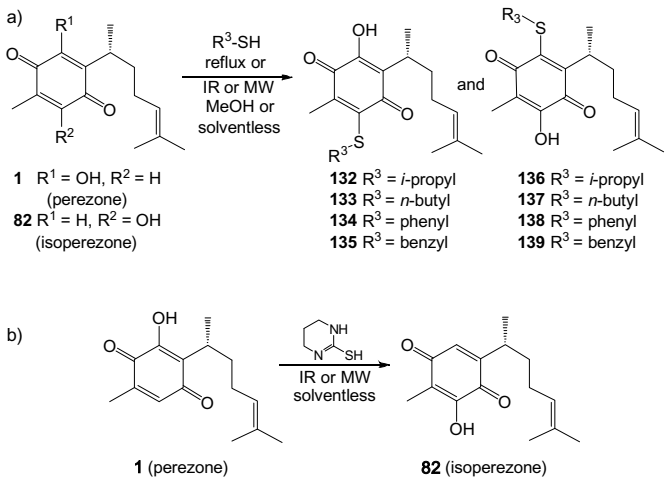

Scheme 1 a) Production of R^3-(*R*)-perezone and R^3-(*R*)-isoperezone sulfur derivatives **132–135** and **136–139**, b) transformation of perezone (**1**) to isoperezone (**82**)

utilized a reaction pathway involving a thiol in a Michael addition, followed by an in situ oxidation, and they reported moderate yields. Moreover, a novel green production of isoperezone (**82**) was achieved, using perezone (**1**) as substrate in the presence of 3,4,5,6-tetrahydropirimidinethiol, employing, by comparison, infrared or microwave irradiation under solventless conditions (Scheme 1b) [97].

3.2.2 Green Production of Indolylquinones, Derivatives of Perezone, and Related Molecules, as Possible Antineoplastic Compounds

In this area, the authors reported the formation of indolyl derivatives **142**–**145** from the quinones perezone (**1**), isoperezone (**82**), menadione (**140**), and plumbagin (**141**) (Scheme 2). The structure elucidation of the target molecules was performed by standard spectroscopic procedures. Also, comparison of the experimental and computed ^{1}H and ^{13}C NMR data with previous data acquisition, was in good agreement (Fig. 7). Calculations were carried out using the density functional theory at the (DFT)/B3LYP/6–311++G(d,p) level. Cytotoxic activity for the human cancer cell line MDA-MB-231 was evaluated and IC_{50} values of 40.6 and ca. 25 $\mu g/cm^3$ for **1** and the isoperezone indolyl derivatives, respectively. It is important to mention that the molecules were synthesized using a green approach, involving near-infrared irradiation (NIR), microwave (MW), and ball milling (BM) using Tonsil Actifil FF (TAFF) as a catalyst and solventless conditions, in comparison to the use of mantle

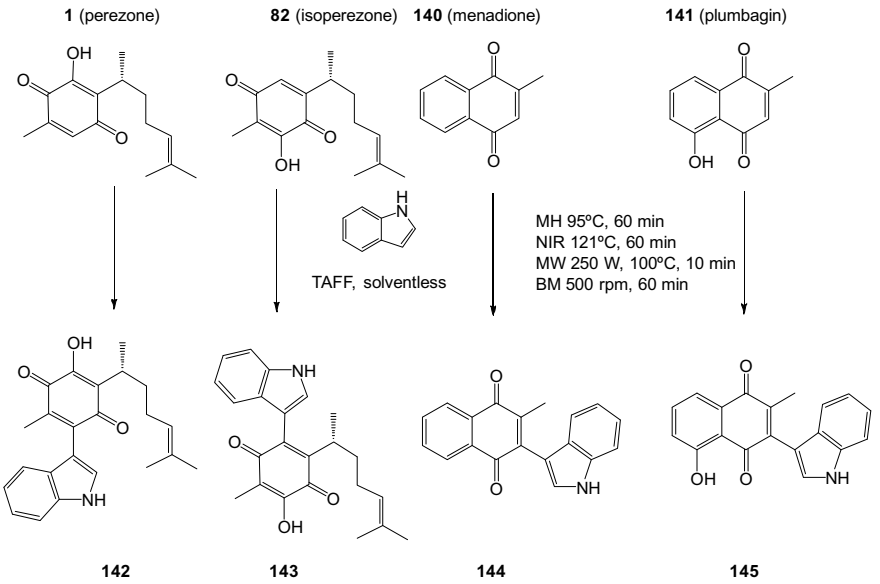

Scheme 2 Synthesis of indolylquinones **142**–**145** comparing MH, NIR, MW, and BM. Adapted from Ref. [98]

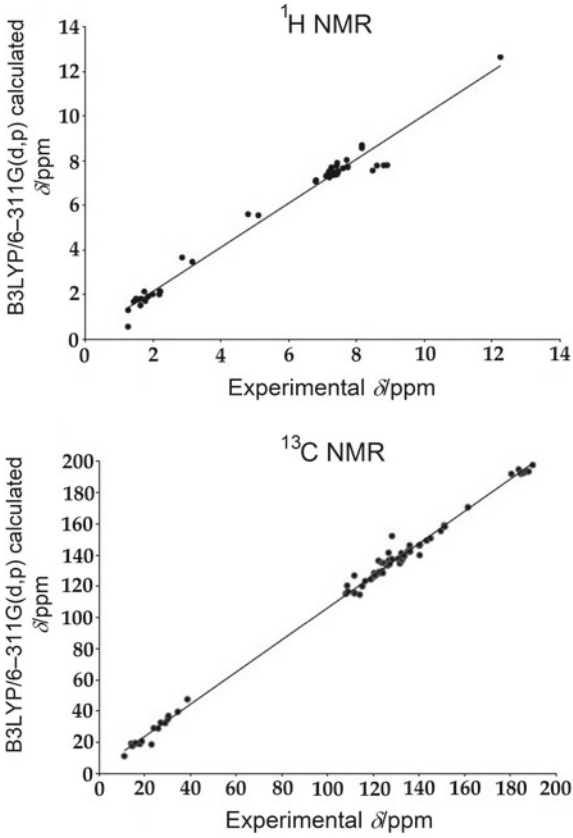

Fig. 7 Linear regression between experimental and calculated at the B3LYP/6–311++G(d,p) level of indolylquinones **147**–**150**: ^{1}H NMR and ^{13}C NMR. Adapted from Ref. [98]

heating (MH) (Scheme 2). Finally, the authors established the transformation of **1** into **82** in comparative yields to previously reported conditions, and also BM was used for first time [98].

3.2.3 A Green Approach to the Extraction of Perezone from the Roots of *Acourtia platyphylla* (A. Gray) Reveal & R.M. King: a Comparison of Four Activating Modes and Supercritical Carbon Dioxide

An innovative green method to extract perezone (**1**) from the roots of *Acourtia platyphylla* (A. Gray) Reveal & R. M. King was studied by Miranda Rubalcava et al., employing five different activating methods: NIR, MW, ultrasound (US), supercritical carbon dioxide ($scCO_2$), and mantle heating (MH) (Fig. 8). The corresponding yields under NIR, MW, US, and $scCO_2$ conditions resulted in improved results in comparison to typical MH to extract **1**, with the best processes being ultrasound and

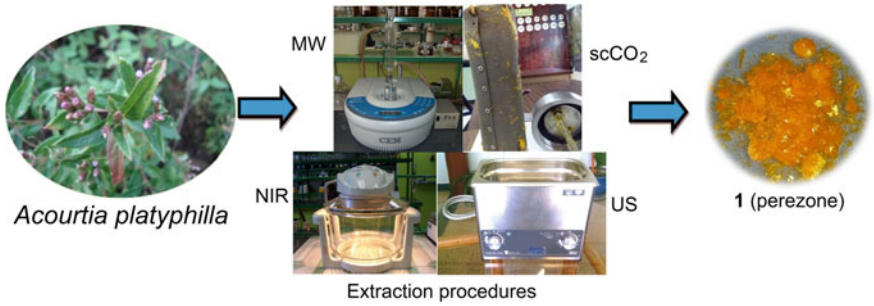

Fig. 8 Extraction of perezone (**1**) comparing NIR, MW, US, and $scCO_2$. Adapted from Ref. [99]

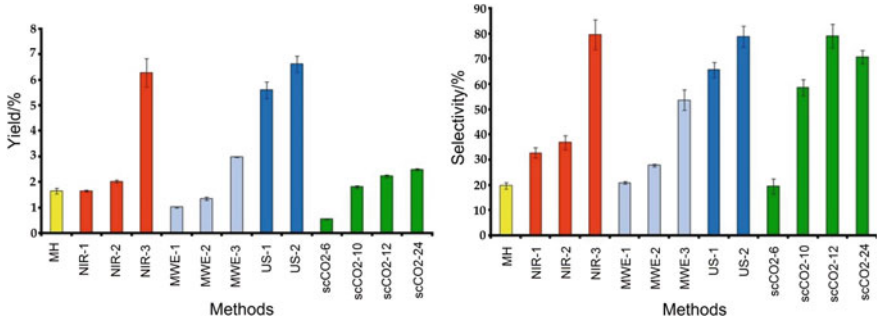

Fig. 9 Yield and selectivity obtained by the different processes for the extraction of perezone (**1**). Adapted from Ref. [99]

near-infrared irradiation (Fig. 9). It is important to highlight that in this study, the best solubility for the extraction of **1** was provided by $scCO_2$ [99].

3.3 Advances in Chemical Synthesis

3.3.1 Synthesis and Cytotoxic and Antioxidant Evaluations of Amino Derivatives of Perezone

Altogether, eight amino derivatives (**146–153**) of perezone (**1**) were synthesized by nucleophilic addition of several bioactive amines such as melatonin, tryptophan, valine, and leucine (Scheme 3). The compounds obtained were evaluated against four human tumor cell lines, namely, PC3, K562, HCT15, and SKLU1, and also for antioxidant activity. Perezone (**1**) and isoperezone (**82**) were evaluated for comparison purposes, and showed higher cytotoxic potentials against the four cell lines, but all molecules were less cytotoxic than the Adriamycin positive control drug. Derivative **146** exhibited an IC_{50} value of $7.5 \pm 0.3\ \mu M$, and was more active than perezone

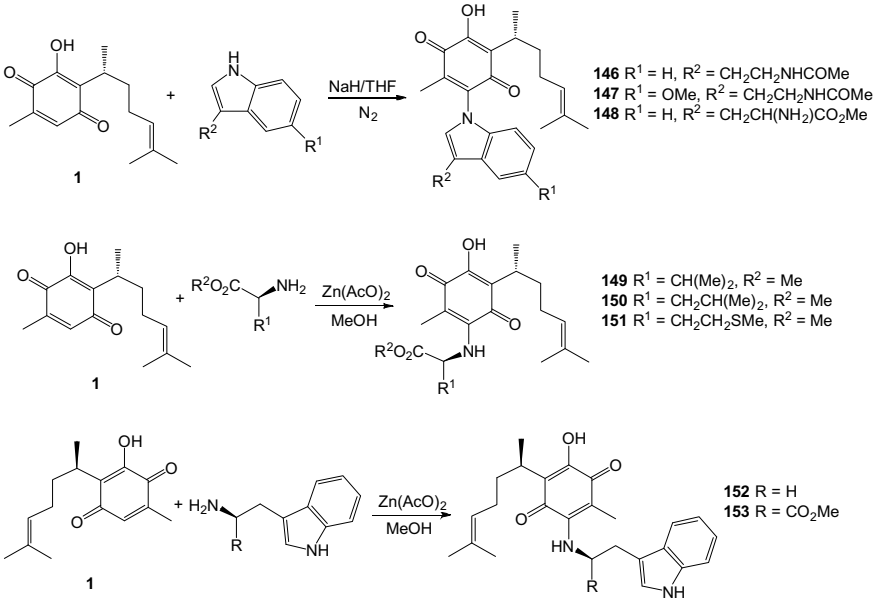

Scheme 3 Synthesis of amino derivatives **146–153** of perezone (**1**). Adapted from Ref. [100]

against HCT15 cells, while derivative **153** was selectively active against K562 cells with an IC_{50} value of $4.5 \pm 0.4\ \mu M$. Additionally, the synthesized compounds exhibited discernible cytotoxicity predominantly against the K562 leukemia cell line. For their antioxidant activity, using a thiobarbituric acid reactive substance (TBARS) assay, the most pronounced effect was observed for **148**, and it is pertinent to note that isoperezone (**82**) showed a two-fold greater antioxidant activity than its isomer [100].

3.3.2 [5+2] Cycloaddition Reactions in Organic and Natural Products Synthesis

In a review, Ylijoki and Stryker covered the [5 + 2] cycloaddition reaction using mantle heating of perezone (**1**), thereby promoting the formation of α- and β-pipitzols ((**2**) and (**3**)) (Scheme 4). One should note, however, that previous mechanistic proposals were incorrect, due to an inappropriate characterization of **1**. As demonstrated, the mechanism proceeds by a [5 + 2] cycloaddition of the pendant olefin with the pentadienyl cation as intermediate (**I**). Consequently, several intermolecular variants have been established for **1** in addition to some other quinones [101].

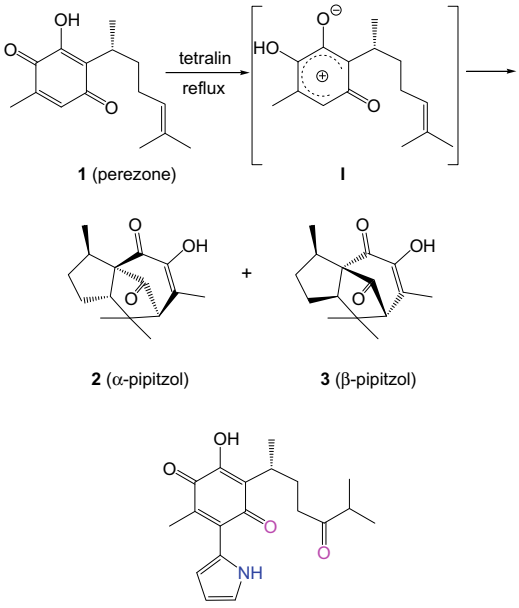

Scheme 4 [5+2] Cycloaddition of perezone (**1**) and the pyrrolyl derivative **154**. Adapted from Ref. [101]

3.3.3 A Novel Semisynthetic Anion Receptor: Synthesis and Ion Recognition of (1*H*-Pyrrol-2-yl)-4-oxo-perezone

A synthesis of (1*H*-pyrrol-2-yl)-4-oxo-perezone, or according to IUPAC nomenclature, (*R*)-2-hydroxy-6-methyl-3-(6-methyl-5-oxoheptan-2-yl)-5-(1*H*-pyrrol-2-yl)cyclohexa-2,5-diene-1,4-dione (**154**) (Scheme 4), in 44% yield starting from perezone (**1**), has been described [102]. This product is considered as a novel semisynthetic anion-guest molecule, since it clearly has an anion-recognizing region (pyrrole-hydrogen bond donor—colored blue in the formula) and a cation-recognizing region (engaged in Lewis acid interactions with the carbonyl side-chain moiety—colored magenta in the formula). It is important to note that according to the authors, **154** showed interesting complexation properties in the presence of different inorganic salts, tetrabutylammonium fluoride, chloride, bromide, and iodide, as evaluated using ^{1}H NMR titration techniques in deuterated dichloromethane. Furthermore, the cation-recognizing properties were evaluated by their corresponding colorimetric behavior with different salts, as for example, a change in color from purple to green with $Bi(NO_3)_3$, and from gray to green with $KMnO_4$, among others [102].

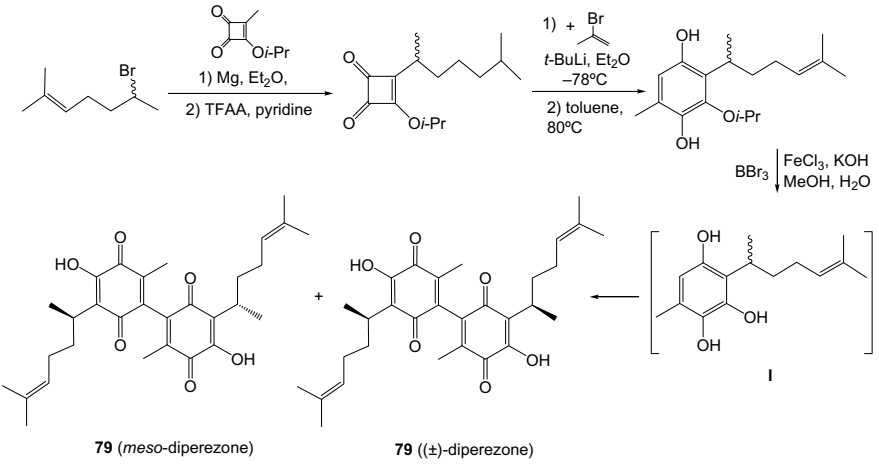

Scheme 5 Synthesis of *meso*- and (±)-diperezone (**79**). Adapted from Ref. [103]

3.3.4 A Concise Synthesis Approach to *meso*- and (±)-Diperezone

An interesting and simple synthesis of *meso*- and (±)-diperezone (**79**) was described by Gao and Hu, employing a biomimetic oxidative phenolic coupling of 1,2,4-trihydroxyarenes, applying a ring expansion of a cyclobutenone (Scheme 5). The authors reported that the key intermediate **I** is unstable and consequently they furthered the oxidative dimerization by employing $K_3[Fe(CN)_6]$/KOH. However, the products were obtained in low yields. Noteworthy is that the best result was observed using $FeCl_3$/KOH, and both diastereomers could be obtained [103]. In the same manner, the biquinoid natural product parvistamin A could be also synthesized.

3.3.5 Iron-Catalyzed Intramolecular Perezone-Type [5+2] Cycloaddition: Access to Tricyclo[6.3.1.01,6] Dodecane

In this investigation, iron chloride was employed to catalyze a perezone-type [5 + 2] cycloaddition to produce molecules structurally related to a tricyclo[6.3.1.$0^{1,6}$]-dodecane (Scheme 6). The reactions proceeded with satisfactory yields (46–93%), diastereoselectivities (6:1 to > 20:1), and extensive substrate scope. In general, the products obtained were cycloadducts with two new C–C bonds and three to four stereogenic centers. It is worth noting that two different conditions were conveniently established: catalytic $FeCl_3$/$PhCO_3t$Bu (0.5 equiv/1.0 equiv) and stoichiometric $FeCl_3$ (2 equiv). From the mechanistic point of view, the authors proposed that the reaction may proceed via iron-mediated initiation of a carbocationic center, promoting a subsequent [5 + 2] cyclization (Scheme 6) [104]. Detailed experimental procedures, spectroscopic data, ^{1}H and ^{13}C NMR spectra, and X-ray crystallographic data of the new molecules were made available.

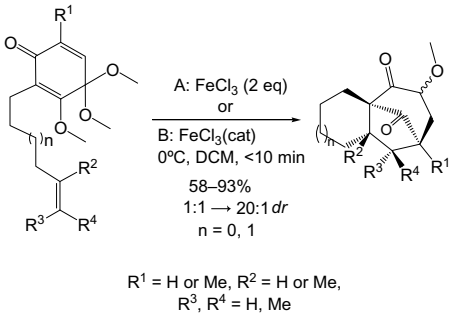

Scheme 6 Intramolecular perezone-type [5 + 2] cycloaddition. Adapted from Ref. [104]

3.3.6 Total Synthesis of (–)-Perezoperezone Through an Intermolecular [5+2] Homodimerization of Hydroxy *p*-Quinone

In this investigation, the authors presented the first copper-catalyzed ((0.1 mmol), CuI (0.005 mmol), Et_3N (0.1 mmol), THF (0.5 cm^3), 40°C, 1 h) intermolecular [5 + 2] homodimerization of a hydroxy-*p*-quinone, a procedure referred to as a perezone-type [5 + 2] cycloaddition. According to the authors, this catalytic alternative provides bicyclo[3.2.1]octadienone moieties in good yields (43–87%) and excellent diastereoselectivities (although no data were published). It is important to highlight that the use of this synthetic methodology allowed for a concise nine-step total synthesis of (–)-perezoperezone (**155**), as displayed in Scheme 7 [105]. The structures of several dimerized products were confirmed by X-ray crystallography. Generally, this intermolecular homodimerization is considered to be practical and operationally simple. Using this procedure, 36 bicyclo[3.2.1]octadienones conveniently were produced.

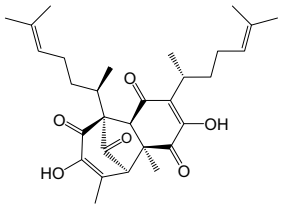

155 ((–)-perezoperezone)

Scheme 7 Formula of perezoperezone (**155**)

3.4 Advances Related to in Silico Studies

3.4.1 Remote Position Substituents as Modulators of Conformational and Reactive Properties of Quinones: Relevance of the π/π Intramolecular Interaction

Perezone (**1**) may be presented as an excellent model to study π–π interactions between a donating olefin that is rich in electrons and a quinone group of a captive nature, because the distance between these groups is very short, thereby allowing this interaction. In fact, it is commonly accepted that the first unit of isoprene is responsible for the high affinity between ubiquinone and the reduction site. Accordingly, the reduction of the olefin is clean, yielding a pure product. In addition, its molecular size allows high-level calculations that include the dispersion terms that are fundamental for the correct description of π–π intramolecular interactions. The potential energy surface is simplified when numerous stationary states that generate long and flexible chains are eliminated.

The results obtained using this model can be extrapolated easily to analogous systems such as ubiquinone Q*n*. The electrochemical study of both perezone (**1**) and dihydroperezone (**8**) was performed to evaluate their electron-transfer properties [106]. A computational study of the different conformers generated by the rotation of the carbon–carbon bond in the side chain was performed. In addition, since dispersion forces may have a relevant role in this process, the MP2 method was selected using in addition a split valence double-ξ basis set with polarization in heavy and light atoms: 6–31G(d,p). The size of this sesquiterpene molecule makes it impossible to include diffuse functions in the basis set used during the optimization procedure. There have been reports of calculations of the Hartree–Fock and DFT hybrid type of folded ubiquinones to explain their low diffusion coefficients and flexibility. This study showed the importance of weak interactions of the olefin-quinone type in the reduction process of quinones. These interactions can protect the molecules in biological media or at least modulate their electrochemical potential by modifying their conformation. Therefore, these molecules can be activated by only high specific metabolic conditions due to the capability of certain enzymes to recognize diverse conformers. Cyclic voltammetry experiments and coupled electrochemical–electron spin resonance studies showed changes in the reactivity between perezone (**1**) and dihydroperezone (**8**). These results are compatible with the presence of a low-energy π–π interaction between the C-12–C-13 double bond and the quinone ring. Theoretical calculations at the MP2/6-31G(d,p) and MP2/6–31++G(d,p)//MP2/6-31G(d,p) levels of several conformers (**1a**–**1f**) of perezone (**1**) (Fig. 10) established that a weak π–π interaction not only controls the molecular conformation, but also its diffusion coefficient and electrochemical properties. The calculations carried out confirmed that several conformers coexist in solution, with at least one gauche arrangement in the side chain, which might explain the high diffusion coefficient of coenzyme Q10 [106].

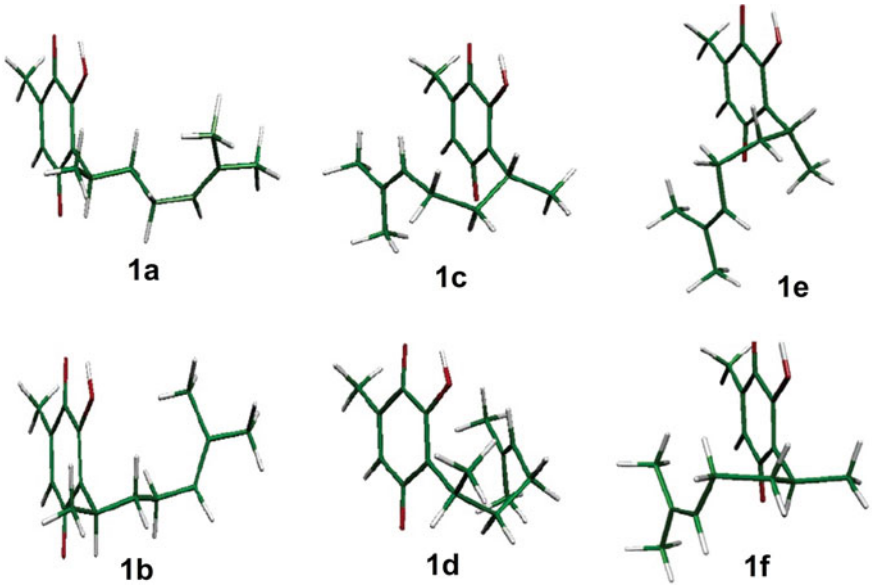

Fig. 10 Fully optimized conformers of perezone (**1**). Adapted from Ref. [106]

3.4.2 Conformational Analysis of Perezone and Dihydroperezone Using Vibrational Circular Dichroism

In this investigation, the authors reported the vibrational circular dichroism spectra of perezone (**1**) and dihydroperezone (**8**), comparing experimental data with theoretical curves obtained from density functional theory (DFT) at the B3LYP/DGDZVP level of theory, providing an excellent equilibrium between spectral accuracy and in silico time (Fig. 11). At the experimental level, as determined from $CDCl_3$ solutions, it is convenient to highlight that the corresponding spectra were remarkably similar indicating similar conformations of the target molecules.

The results were as follows: there is a strong hydrogen bond between the hydroxy group with the C-1 carbonyl group in **1**, as demonstrated by ^{1}H NMR spectroscopy. Consequently, the conformational flexibility of the molecule originates from the four rotatable C-2-C-8-C-10-C-11-C-12 bonds, resulting in 81 conformers ($3^4 = 81$) when alternate conformational arrangements around single bonded carbon atoms are considered. It is also important to note that the corresponding (*R*)-C-8 configuration was confirmed by comparison of the experimental VCD spectrum of each compound with theoretical calculations considering their conformational mobility. An extended side-chain conformation, over a folded chain conformation, seems to be preferred for perezone (**1**). In this respect, the conformational analysis of the (*R*)-C-8 enantiomer showed 19 low-energy conformers in a 10 kJ/mol energy range, while for (*R*)-C-8, with the saturated side alkyl chain, 34 conformers were considered in the first 8.4 kJ/mol. There is no vibrational circular dichroism evidence for

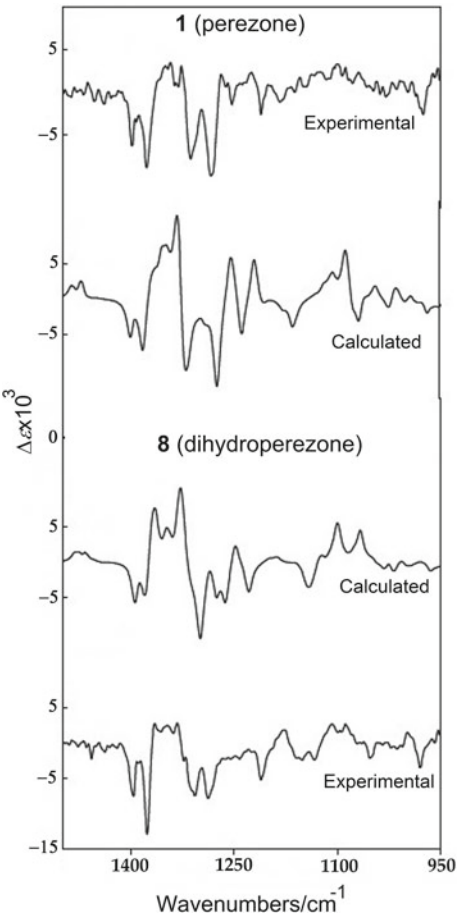

Fig. 11 Comparison of the experimental VCD spectra and calculated DFT//B3LYP/DGZVP spectra of perezone (**1**) and dihydroperezone (**8**). Adapted from Ref. [107]

preferred conformers of perezone, showing that weak π–π interactions between the alkyl chain double bond and the quinone ring control the molecular conformation. The conclusion reached, after an exhaustive conformational analysis of perezone required for a vibrational circular dichroism study, suggested preferred extended side-chain conformations [107].

3.4.3 NMR-Based Conformational Analysis of Perezone and Analogs

For this topic, Joseph-Nathan et al. emphasized that the assessment of ^{1}H NMR coupling constants is a diagnostic tool to obtain appropriate conformational information for interesting molecules. This objective was reached by applying NMR simulation software inclusive of iterative minimization of variance between modeled and experimental spin–spin data. With consideration to the previous discussion,

Table 2 ^{1}H NMR and spin–spin analysis of pro-(*R*) and pro-(*S*) signals corresponding to the hydrogen atoms at C-10 and C-11 of perezone (**1**). Data from Ref. [3]

Atom	δ/ppm	spin–spin	Hz
H-10(*R*)	1.805	$J_{10R,10S}$	−13.21
H-10(*S*)	1.581	$J_{10R,11R}$	5.97
H-11(*R*)	1.864	$J_{10R,11S}$	9.37
H-11(*S*)	1.921	$J_{10S,11S}$	6.23

the authors described a complete and detailed assignment of both chemical shifts and coupling constant values (Table 2) for three sesquiterpenes, perezone (**1**), methoxyperezone (**80**), and 6-hydroxyperezone (**6**), highlighting the pro-(*R*) and pro-(*S*) signals corresponding to the hydrogen atoms at C-10 and C-11 for **1**, by total line shape fitting computations using the PERCH iterative spectra analysis software. In general, the RMS deviation (experimental versus simulated spectra) was $\leq$ 0.06%, and it should be noted that in using in silico analysis, the pro-(*R*) and pro-(*S*) signals corresponding to the hydrogen atoms at C-10 and C-11 were obtained in a convenient manner. In general, robust resemblance to the corresponding experimental spectra was reported. The entire vicinal, allylic, and homoallylic coupling constant values corresponding to the side chain in each target molecule were extremely similar, thereby revealing that the conformation of these three molecules in solution is indeed almost identical. Finally, it must be stated that findings of double pulsed field gradient spin echo NOESY 1D experiments on **1** did not offer support for folded conformers [3].

3.4.4 The Folded Conformations of Perezone Revisited. Long-Range NOE Interactions in Small Molecules: Interpretable Small Signals or Useless Large Artifacts?

The presence of a double bond in a remote position in quinones has a remarkable influence on their structural and reactivity properties. In addition, the presence of folded structures has been used commonly as an argument to describe the relevant properties of similar quinones. The existence of conformers depends on the level of theory and for this area of investigation, the molecular geometries of perezone were determined at the M06–2X/6–31++G(d,p) level of theory (Fig. 12), and the closest interatomic distances varied with the relative orientation of the side chain. The presence of folded conformers in the conformational equilibrium was also revealed conclusively from the observed nuclear Overhauser effect (NOE). Consequently, the absence of the OH group should decrease the polarization of the carbonyl group in the quinone ring and its ability to accept charge from the olefin in the folded conformers. The least stable arrangement incorporates exclusively double bond quinone interactions. NOEs have been observed between hydrogen atoms located at distances longer than 6 Å for several small molecules with a common quinone-like framework. The results confirm the existence of folded conformers for **1** in contrast with previous reports using NMR data and vibrational circular dichroism. Due to the fact that signals of

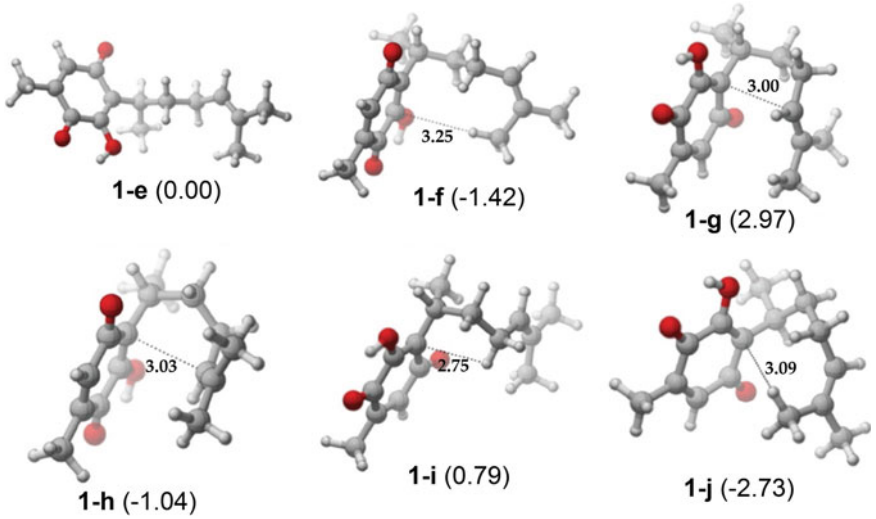

Fig. 12 Some theoretical optimized structures of perezone (**1**) with relative stabilities. Adapted from Ref. [108]

interest are very small (in the order of 1% of a normal NOE), they may be considered as artifacts originating in the decoupling modulation. Nevertheless, they represent properties that make them interesting and give them some credence as interpretable signals [108].

3.4.5 Computational Characterization of Perezone, Isoperezone, and Their Sulfur Derivatives with Anti-Inflammatory Activity

The present authors in a recent report [109] described a theoretical study to confirm the spectroscopic characterization of eight sulfur derivatives (**132–139**) of perezone (**1**) and isoperezone (**82**) (Scheme 1), and they employed the DFT/B3LYP/6–311++G(d,p) method. Hence, corresponding conformational studies for the respective sulfur-containing functionalities were performed to obtain minimum energy arrangements. The results conveniently were in agreement, and the vibrational frequency analyses; the magnitude of ^{1}H NMR; and ^{13}C NMR spectra for perezone (**1**), isoperezone (**82**), and their respective sulfur derivatives, obtained both at the theoretical and experimental levels, correlated adequately. Furthermore, the prediction of anti-inflammatory activity was extended and supported later by in vivo anti-inflammatory evaluation experiments. Docking calculations of the test compounds with COX-2 revealed that (*R*)-benzylperezone (**135**) had the highest affinity for this enzyme. Consequently, **135** was evaluated in vivo employing a contact irritant ear edema mouse model, and showed anti-inflammatory activity comparable in potency to naproxen [109].

3.4.6 Is the VCD Spectrum a Fingerprint of the Conformational Population? The Conformation of Perezone in the Spotlight

In their investigation [110], Cuevas et al. recognized the fitness of different theoretical methods based on DFT, to describe both the conformational population of perezone, and to create its theoretical vibrational circular dichroism (VCD) spectrum, and an appropriate contrast with experimental data was observed (Fig. 13). M06–2X, B3LYP, ωB97XD, and B97D functionals with 6-311++G(2d,2p) and DGDZVP basis sets were employed to establish the stationary points of minimum energy of the potential energy surface of perezone (**1**) (Fig. 14). It is noteworthy that the levels of theory employed produced a meaningfully diverse conformational population, fluctuating from 75% participation of folded conformers to <5%, without the generation of a uniform conformational order. The correct absolute configuration (*R*)-C-8 of **1** was predicted for each event [110].

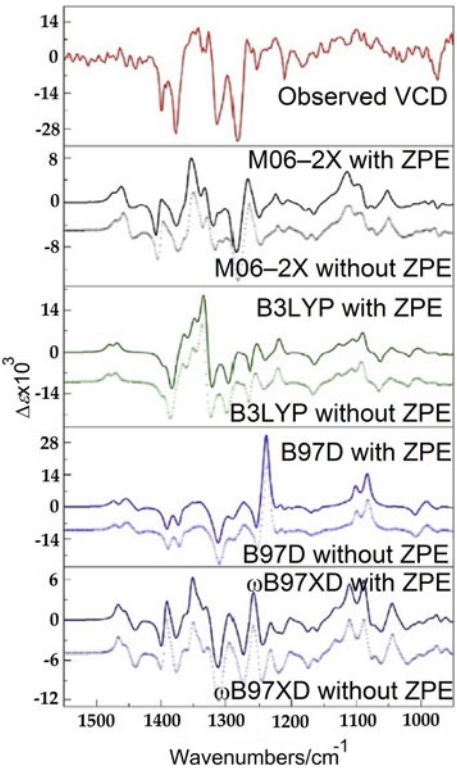

Fig. 13 Comparison of the experimental VCD spectra of perezone (**1**) with those obtained with M06–2X, B3LYP, B97D, and ωB97XD functionals. Adapted from Ref. [110]

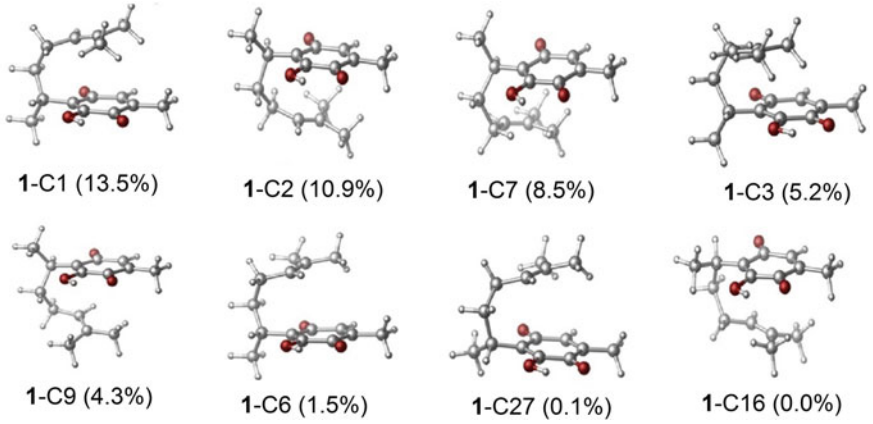

Fig. 14 Conformational populations of perezone (**1**) at M06–2X/6–31++G(2d,2p). Adapted from Ref. [110]

3.5 Advances in Investigating Biological Activities

3.5.1 Antifeedant and Phytotoxic Activities of the Sesquiterpene *p*-Benzoquinone Perezone and Some of Its Derivatives

In this work, the researchers demonstrated the antifeedant effects of perezone (**1**), isoperezone (**82**), dihydroperezone (**8**), dihydroisoperezone (**95**), and anilidoperezone (**100**) against the herbivorous insects *Spodoptera littoralis*, *Leptinotarsa decemlineata*, and *Myzus persicae*, with the most active molecules being **82** and **100**. The results showed that all compounds were active against adult *L. decemlineata* and *M. persicae*, and **82** and **100** were determined as the most potent molecules against *L. decemlineata.* For *M. persicae*, compound **82** was the most active, displaying a comparable level of activity to the positive control, polygodial. For *S. littoralis*, all of the evaluated sesquiterpenoid products had low activities in comparison to the positive control ryanodine. A phytotoxic evaluation was carried out with the seeds of *Latuca sativa* var. Carrascoy, but the sesquiterpenes tested did not affect seed germination [111].

3.5.2 Screening a Panel of Drugs with Diverse Mechanisms of Action Yields Potential Therapeutic Agents Against Neuroblastoma

The first report on the potential antineoplastic activity of **1** was published in Ref. [112] by means of an in vitro screening panel with several test compounds against neuroblastoma (NB). The authors pointed out the importance of this area of research, as NB cells metastasize at an early stage to several extra-cranial organs, and the survival of patients with NB is low. To discover novel compounds as potential chemotherapeutic

agents to treat NB, screening with a set of 96 drugs against two NB cell lines, SK-N-AS and SH-SY5Y, was carried out. The studied compounds included 8 antimetabolites, 12 DNA-intercalating agents, 12 topoisomerase inhibitors, 5 mitotic inhibitors, 44 agents affecting various additional biological pathways, and 15 compounds with unknown mechanisms of action. The obtained results revealed that 30 compounds, among them **1**, were active against the two NB cell lines at $\leq 10\ \mu M$ concentrations (Fig. 15). After 72 h of incubation of SK-N-AS and SH-SY5Y cells with 10 μM of **1**, cell viability was reduced by > 90%. Consequently, **1** was considered as a moderately active compound against the neuroblastoma cell lines utilized, although it did not significantly stimulate caspases-3 and -7 and so its mechanism of action was not determined in this investigation [112].

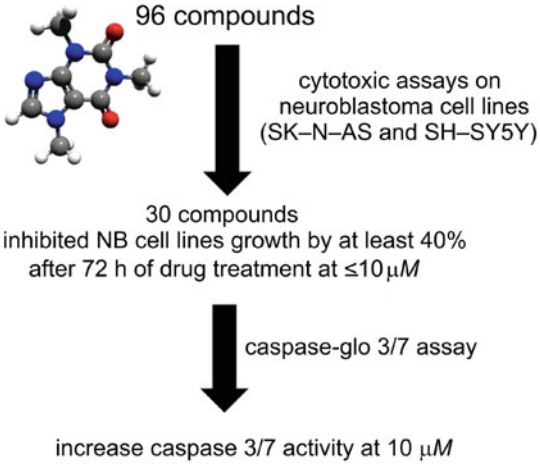

<2 fold	2–20 fold		>20 fold
helenalin	tetrandine	curcubitacin I	bortezomib analog
amonafide	EAD	17–AAG	daunorubicin
1 (perezone)	echinomycin	5-azacytidine	doxorubicin
arsenic trioxide	thioguanine	topotecan	bortezomib
CDDO-Me	alsterpaulone	maytansine	
PD 0332991	teniposide	paclitaxel	
didemnin B	vincristine	dactinomycin	
	valrubicin	mitoxantrone	
	etoposide	camptothecin	
		colchicine	

Fig. 15 Screening of a panel of drugs to search for compounds with antineuroblastoma activity

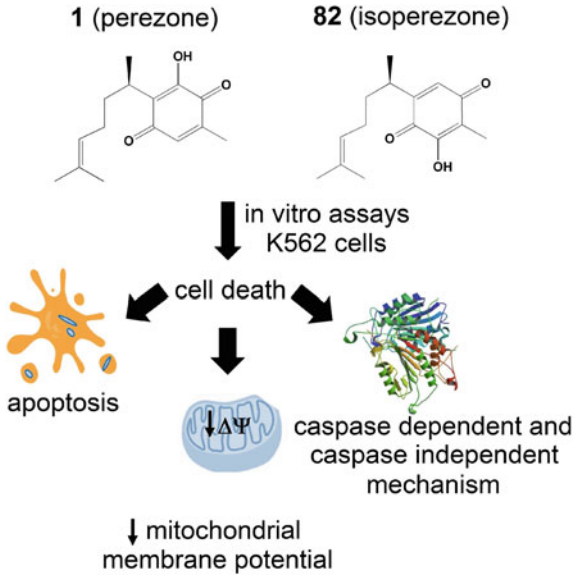

Fig. 16 Effects of perezone (**1**) and isoperezone (**82**) on K562 cells

3.5.3 Perezone and Its Isomer Isoperezone Induce Caspase-Dependent and Caspase-Independent Cell Death

The cytotoxic effect of perezone (**1**) and isoperezone (**82**) against a human erythroleukemic cell line (K562) was investigated and the potency of **1** was deemed higher than that of **82**. Apoptosis constituted the main mode of cell death as demonstrated by phosphatidylserine translocation using flow cytometry. Compounds **1** and **82** produced a reduction in mitochondrial membrane potential, showing a good correlation with the cytotoxic activities observed. In contrast, the researchers concluded that cell death was elicited for both compounds by caspase-dependent and caspase-independent mechanisms (Fig. 16) [113].

3.5.4 Perezone, from the Soft Coral *Pseudopterogorgia rigida*, Induces Oxidative Stress in Human Leukemia Cells

Owing to earlier reports concerning the cytotoxic activity of perezone (**1**) against cancer cell lines, the authors of this study considered it of interest to evaluate the cytotoxic activity of four bisabolanes in addition to **1** and triacetylperezone (**51**), with all of them isolated from a methanol-dichloromethane extract of the Caribbean gorgonian coral *Pseudopterogorgia rigida.* Six cancer cell lines were used, namely, promyelocytic leukemia (HL-60), colorectal adenocarcinoma (HCT-8), human glioblastoma (SF295), breast cancer (MDA-MB-435, MDA-MB-231), and murine melanoma (B16), and, as normal cells, murine macrophages (J774) and murine fibroblasts (L929). Only **1** exhibited a positive result with an $IC_{50} < 40\ \mu M$,

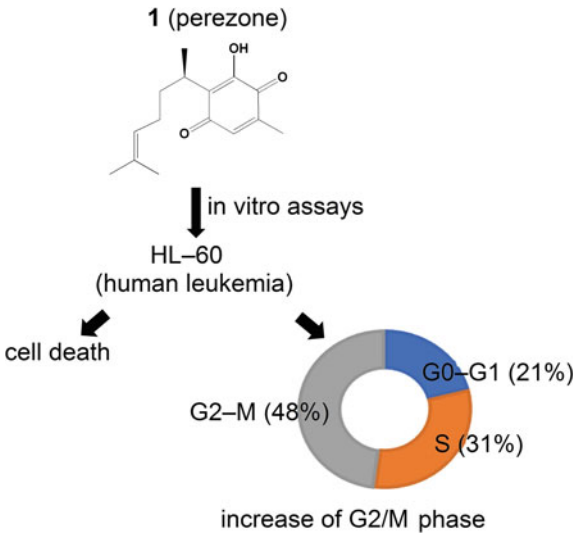

Fig. 17 Effects of perezone (**1**) against the HL-60 cell line

being the most active against the HL-60 cell line (Fig. 17). In contrast, the IC_{50} values against the normal cell lines J774 and L929 were 16.3 and 11.5 μM, respectively, showing a lack of selectivity. Alterations in the cell cycle of HL-60 cells treated with **1** after 24 h displayed an increase of the G2/M phase, accompanied by a decrease in the S phase. The authors concluded that the cytotoxic effect was related to the generation of reactive oxygen species (ROS), due to its reversibility when cells were exposed to *N*-acetylcysteine before treatment with perezone (**1**) [114].

3.5.5 Sesquiterpenes with Inhibitory Activity Against CDC25 Phosphatases from the Soft Coral *Pseudopterogorgia rigida*

The CDC25 enzymes, which belong to a family of phosphatases, are known as important regulators of the cell cycle. In addition to an increase in the expression of these enzymes in cancer cells, they are also a marker of cancer "aggressiveness." Roussis et al. screened 21 sesquiterpenes isolated from an organic extract of the Caribbean gorgonian *Pseudopterogorgia rigida* in order to find novel CDC25 inhibitors. Among the evaluated compounds, perezone (**1**) exhibited appreciable inhibition against the CDC25A, CDC25B, and CDC25C phosphatases with IC_{50} values of less than 5 μM in each case (Fig. 18) [115]. According to these findings, the authors concluded that the mechanism of action of **1**, which can explain its cytotoxic activity, is via CDC25 inhibition.

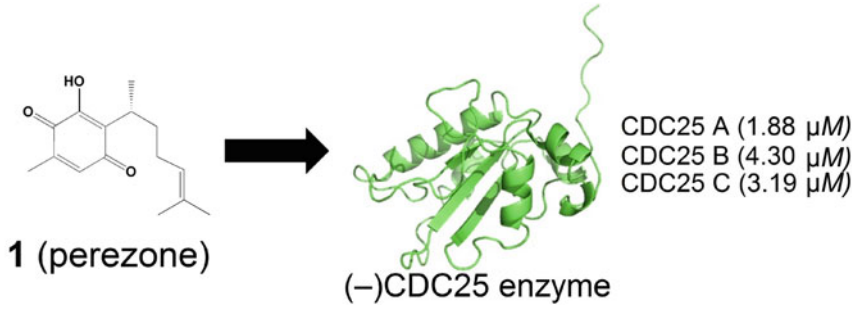

Fig. 18 Perezone (**1**) inhibits CDC25 phosphatases

3.5.6 In Silico Study of the Pharmacologic Properties and Cytotoxicity Pathways in Cancer Cells of Various Indolylquinone Analogs of Perezone

Recently, the cytotoxic effects on a human breast cancer cell line of a set of four indolylquinones **142**–**145** were reported (see Scheme 2). Additionally, quantum-chemical calculations were used extensively to study the structure activity of the biochemistry of these molecules and the authors performed calculations with descriptors that could be correlated with corresponding biological activity of the studied compounds. The determinations were accomplished using density functional theory at the (DFT/B3LYP/6–311G(d,p)) level; the computed properties were HOMO−LUMO gap energies, natural population analyses, and molecular electrostatic potential maps. With regard to the last mentioned criterion, this indicates which atoms could participate in intermolecular hydrogen bonds with receptor amino acid residues (Fig. 19). Moreover, since docking studies provide models of the possible interactions of protein residues with ligands, this allows the proposal of a biological target for a compound and can, for example, explain its pro-apoptotic activity. Thus, it was proposed that PARP-1 is the target protein proposed for indolylisoperezone (**143**) and BAK for indolylperezone (**142**). It was also recognized that the most potently cytotoxic compound was indolylisoperezone (**143**), and this was conducted by considering the smallest energy gap of the corresponding HOMO–LUMO orbitals, and consequently its high reactivity values. In addition, this approach can inform and predict toxicity risks, for example, that indolylperezone (**142**) and indolylisoperezone (**143**) could have a high risk of skin irritancy. With respect to other physicochemical properties, for example, cLog P, log S, molecular weight, and toxicity risks, these qualities have also been used to evaluate compounds as possible drugs. However, both indolylperezone (**142**) and indolylisoperezone (**143**) had the "poorest" values in these properties with respect to what would make a "good" drug molecule. The "poorer drug score" predicted for **142** and **143** is likely to be due to the high probability of skin-irritant effects in these molecules. Absorption and excretion models postulated that the exhibited human intestinal absorptions for indolylperezone (**142**)

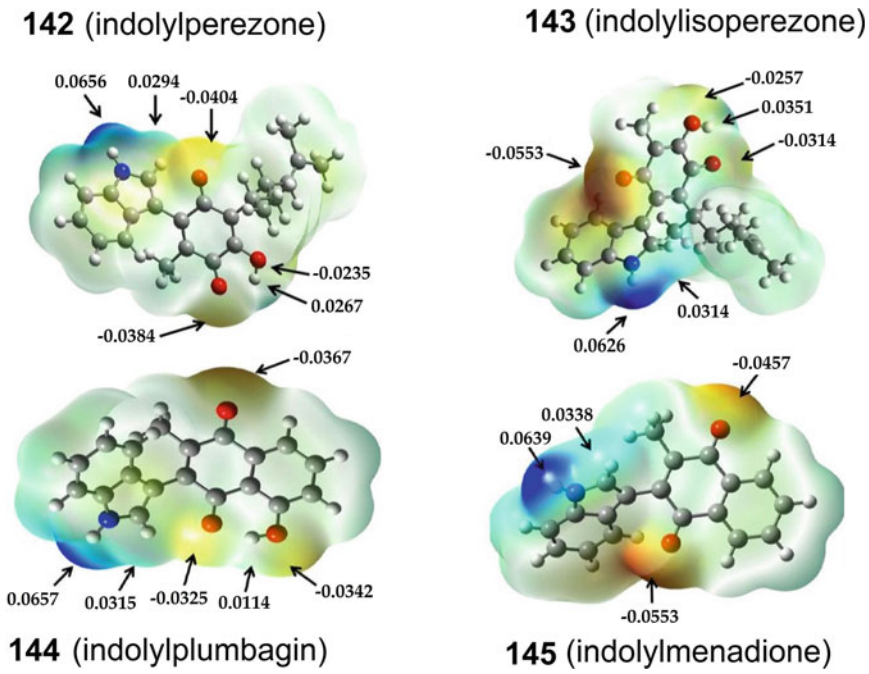

Fig. 19 Molecular electrostatic potential surface of indolylquinones **142**–**145**. Adapted from Ref. [116]

and indolylisoperezone (**143**) have a high probability of actual occurrence. For penetrating the blood–brain barrier, indolylperezone (**142**) and indolylisoperezone (**143**) had medium absorption probability values. As mentioned above, inspection of molecular docking data suggested an interaction of indolylisoperezone (**143**) to the PARP-1 and BID proteins as displaying the highest affinity (Fig. 20a, b). Possible degradation pathways of the studied compounds during human phase I and II metabolism were also predicted [116].

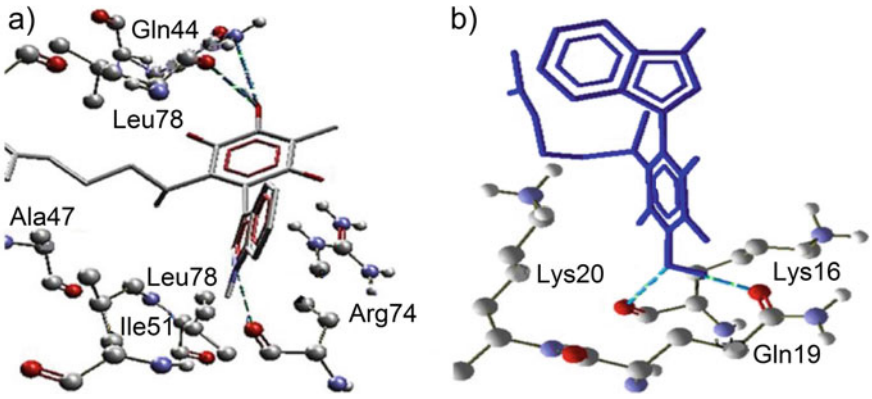

Fig. 20 a) Interaction of indolylisoperezone with PARP-1 and b) the indolylisoperezone–BIM complex. Adapted from Ref. [116]

3.5.7 Antidiabetic and Antihyperalgesic Effects of a Decoction and Purified Compounds from *Acourtia thurberi*

A study where perezone (**1**) is present involved the preclinical efficacy of the aqueous extracts of the roots of *Acourtia thurberi* by means of oral administration in mice and studying hypoglycemic, antihyperglycemic, and antihyperalgesic activities. The following results were obtained experimentally: no toxic effects, with an estimated LD_{50} >500 mg/kg and a decrease of blood glucose levels was produced in normoglycemic and nicotinamide-streptozotocin-treated mice. Ultraperformance Liquid Chromatography (UPLC) analysis of an *Acourtia thurberi* extract identified, in addition to perezone (**1**), α-pipitzol (**2**), β-pipitzol (**3**), and 8β-D-glucopyranosyloxy-4-methoxy-5-methyl-coumarin. However, although active, the corresponding evaluation disclosed minimal hypoglycemic and antihyperglycemic effects for the extract. Finally, the local administration of an *A. thurberi* aqueous extract, with the identified compounds mentioned above, showed significant inhibition on the licking time during the formalin test in healthy and hyperglycemic mice. Consequently, this extract exhibits some antinociceptive and antihyperalgesic potential [117].

3.5.8 Vasodilatory Activity of Compounds Isolated from Plants Used in Mexican Traditional Medicine

In order to develop novel vasodilators, Camacho-Corona et al. isolated a series of phytochemicals (**156**–**172**), namely, triterpenes, diterpenes, sesquiterpenes, lignans, and flavonoids (Table 3), from ten plants employed in Mexican traditional medicine; the phytochemicals obtained were evaluated to determine their vasorelaxant activity using a rat aorta model. According to the results obtained, however **1** showed poor vasorelaxant activity with an IC_{50} value of 524.5 μM [118].

Table 3 Values of half maximal effective concentration (EC_{50}) and maximum effect (E_{max}) of **1** and **3** and various test compounds. Data from Ref. [118]

Compound	$EC_{50}/\mu M$)	$E_{max}/\%$
Perezone (**1**)	524.5 ± 32.5	99.5 ± 2.2
Pipitzol (**3**)	249.4 ± 10.2	59.8 ± 2.4
3-α-Hydroxymasticadienoic acid (**156**)	206.1 ± 11.6	98.2 ± 3.1
3-α-Hydroxyturicalla-7,22-dien-26-oic acid (**157**)	331.3 ± 42.1	99.5 ± 6.1
Corosolic acid (**158**)	108.9 ± 6.7	96.4 ± 4.2
5-Hydroxy-3,7,4′-trimethoxyflavone (**159**)	377.1 ± 37.1	80.5 ± 3.7
(3*R*,4*R*,6*S*)-*p*-Menth-1-ene-3,6-diol (**160**)	1622.8 ± 73.8	99.5 ± 8.3
6-*O*-Acetylaustroinulin (**161**)	413.5 ± 22.4	47.1 ± 2.8
6,7-Diacetylaustroinulin (**162**)	261.0 ± 9.1	99.5 ± 3.8
Galphin A (**163**)	592.3 ± 21.7	99.5 ± 9.1
Galphin B (**164**)	1030.7 ± 39.4	99.5 ± 23.2
Galphimidin (**165**)	145.9 ± 9.2	99.5 ± 5.3
3β-(*E*)-*p*-Coumaryl-oxy-16β-hydroxy-20(29)-lupene (**166**)	63.2 ± 5.8	27.5 ± 1.9
β-Sitosteryl-β-D-glucopyranoside (**167**)	314.7 ± 19.7	71.2 ± 5.3
meso-Dihydroguaiaretic acid (**168**)	49.9 ± 11.2	99.8 ± 2.7
5,4′-Dihydroxy-3,7,8-trimethoxyflavone (**169**)	587.8 ± 33.4	80.5 ± 5.6
5,8,4′-Trihydroxy-3,7-dimethyflavone (**170**)	122.3 ± 7.6	99.5 ± 5.4
3′-Demethoxy-6-*O*-demethyl-isoguaiacin (**171**)	604.5 ± 60.1	91.7 ± 7.3
Pinostrobin (**172**)	234.9 ± 9.9	99.5 ± 4.8

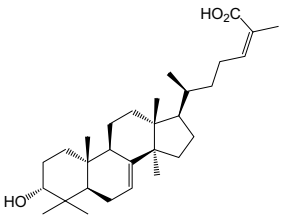

156 (3α-hydroxymasticadienoic acid)

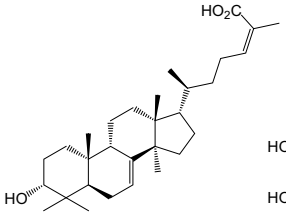

157 (3α-hydroxyturicalla-7,22-dien-26-oic acid)

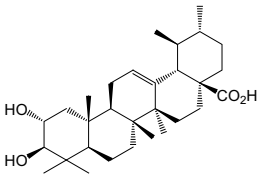

158 (corosolic acid)

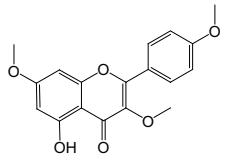

159 (5-hydroxy-3,7,4'-trimethoxyflavone)

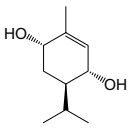

160 (3*R*,4*R*,6*S*)-*p*-menth-1-ene-3,6-diol)

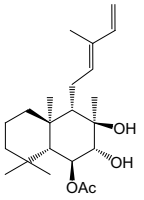

161 (6-*O*-acetylaustroinulin)

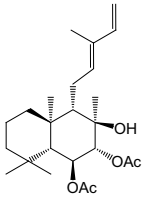

162 (6,7-diacetylaustroinulin)

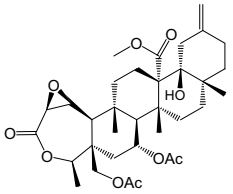

163 (galphin A)

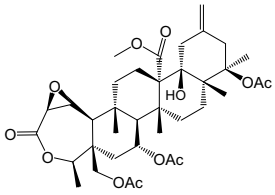

164 (galphin B)

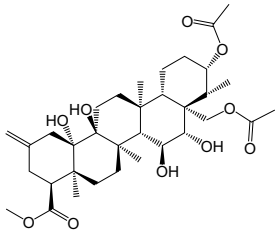

165 (galphimidin)

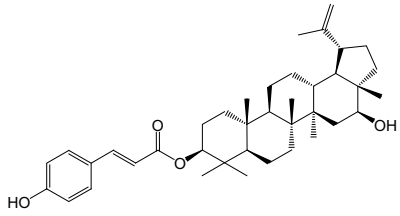

166 (3β-(*E*)-*p*-coumaryl-oxy-16β-hydroxy-20(29)-lupene)

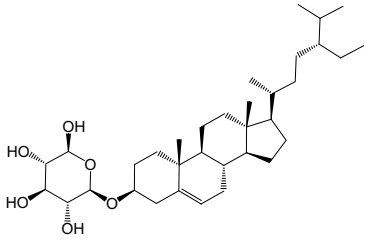

167 (β-sitosteryl-β-D-glucopyranoside)

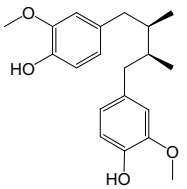

168 (*meso*-dihydroguaiaretic acid)

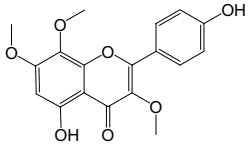

169 (5,4'-dihydroxy-3,7,8-trimethoxyflavone)

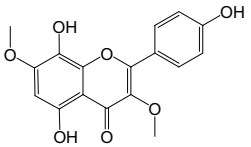

170 (5,8,4'-trihydroxy-3,7-dimethyflavone)

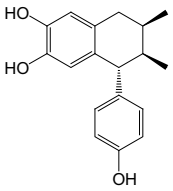

171 (3'-demethoxy-6-*O*-demethyl-isoguaiacin)

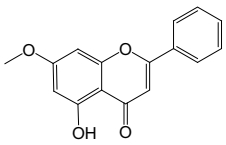

172 (pinostrobin)

3.5.9 In Vitro and Computational Studies Showing that Perezone Inhibits PARP-1 and Induces Changes in the Redox State of K562 Cells

In order to determine the mechanism of action of perezone (**1**) and to explain its cytotoxicity to cancer cells, both computational and in vitro assays were performed. Accordingly, K562 cells treated with perezone (**1**) exhibited decreased viability and a more oxidized status. An increase of the G0/G1 phase of the cell cycle and apoptosis was observed (Fig. 21). Docking studies of **1** with conformers obtained by molecular dynamics simulations of seven proteins involved in the regulation of apoptosis were performed. Since **1** showed the lowest ΔG value to poly[ADP-ribose]polymerase 1 (PARP-1) in computational studies, an in vitro enzyme inhibition assay was conducted, corroborating the PARP-1 inhibition activity of **1** (Fig. 22). The polymerase PARP-1 represents a nuclear enzyme involved in the regulation of many cellular processes, with, among these, cell cycle progression and cell death regulation. Additionally, PARP-1 overexpression in cancer cells has been related to cancer cell survival and the development of resistance against DNA-damaging drugs. In this regard, PARP-1 inhibitors represent targeted strategies to treat cancer, thus highlighting the possible importance of perezone (**1**) and related compounds [119].

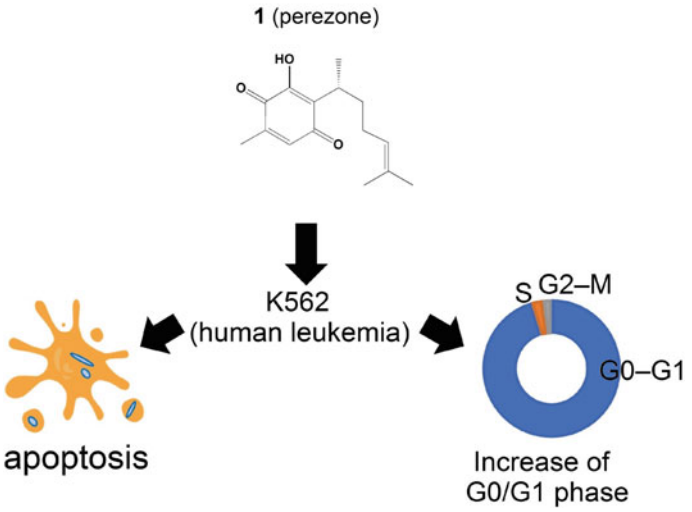

Fig. 21 Perezone (**1**) induces apoptosis and changes the cell cycle of K562 cells

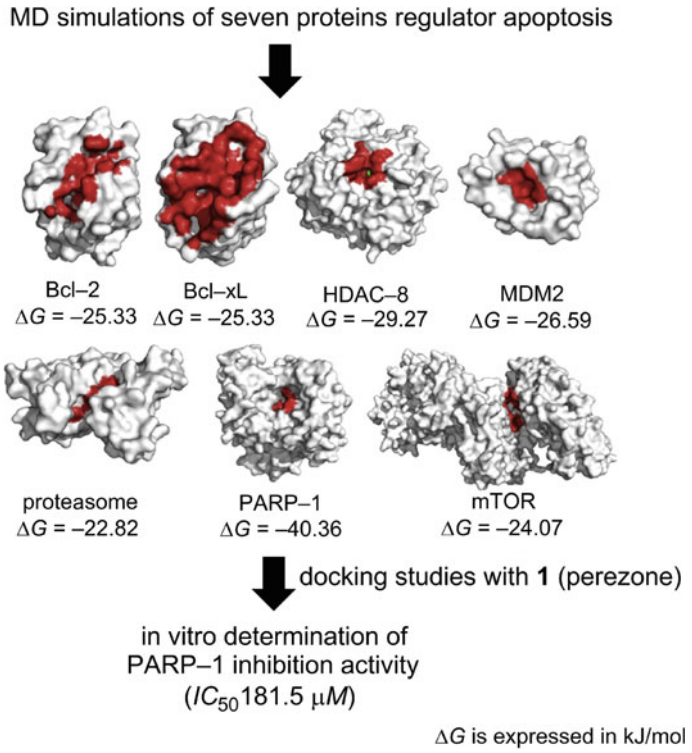

Fig. 22 Perezone (**1**) is a PARP-1 inhibitor, as evidenced by computational and in vitro studies

3.5.10 In Vitro and Computational Studies of Natural Products Related to Perezone as Potential Antineoplastic Agents

Two phytochemicals related to perezone (**1**) were evaluated by Nicolás-Vázquez and by Miranda Rubalcava et al., as potential antineoplastic agents, namely, hydroxyperezone (**6**) (OHPer) and its monoangelate (**72**) (OHPer-MAng) and computational and in vitro studies were conducted. These compounds were characterized structurally employing thermal analysis, IR spectrometry, and X-ray diffraction techniques. Both compounds were evaluated in vitro against six cancer cell lines (K562, MCF-7, MDA-MB-231, HeLa, U373, A549) and against non-malignant cells to determinate their cytotoxic potencies the type of induced cell death, the ability to avoid cell migration, and for any changes at the redox status of the cell. The inhibition of PARP-1 and the corresponding theoretical analysis of the potential binding mode of **1** were also explored by docking studies. Cell proliferation assessment showed that OHPer-MAng-induced apoptosis in a triple-negative breast cancer (TNBC) cell line (MDA-MB-231: IC_{50} 3.53 μM), and that it was less cytotoxic to Vero cells, human lymphocytes, and rat endothelial cells (Fig. 23). The treatment of MDA-MB-231 cells with OHPer-MAng showed inhibition of migration by these cancer cells.

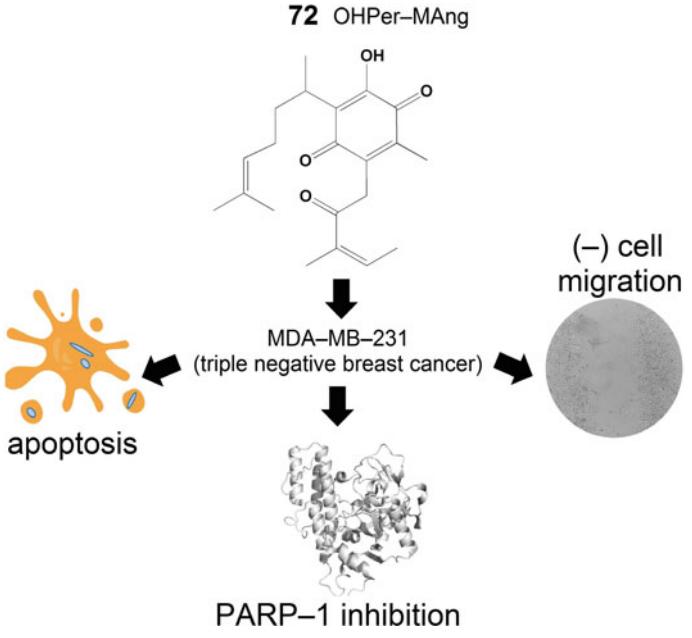

Fig. 23 The monoangelate of perezone (**72**) showed cytotoxicity and inhibits cell migration in MDA–MB–231 cells

The induction of an oxidative stress state, like other quinones and PARP-1 inhibition, is consistent with the pro-apoptotic activity of OHPer-MAng. Docking studies showed that OHPer-MAng can establish strong non-bonding interactions with the lateral chains of Tyr235, Hys201, Tyr246, Ser203, Asn207, and Gly233 located at the catalytic site of PARP-1, likewise supporting the antiproliferative activity of OHPer-MAng against the TNBC cell line used [2].

3.6 Miscellaneous Advances

3.6.1 Time-Dependent Perezone Production in Different Culture Systems of *Acourtia cordata*

In 2012, a study to propagate and to conserve the germplasm of perezone (**1**) was described. The authors developed in vitro and ex vitro culture systems of *Acourtia cordata* (Fig. 24), in a time-dependent study. They found that in in vitro conditions, the average perezone amount recovered was 5.21 mg g^{-1} dry weight. However, when the plants were cultured in ex vitro conditions, perezone (**1**) concentration levels in the plant roots increased logarithmically, realizing an average perezone (**1**) content of 2.4 mg g^{-1} dry weight at the 12th week, to 43.6 mgg^{-1} dry weight at the 31st week. Furthermore, the amount at the 31st week was similar to that obtained in wild roots [120].

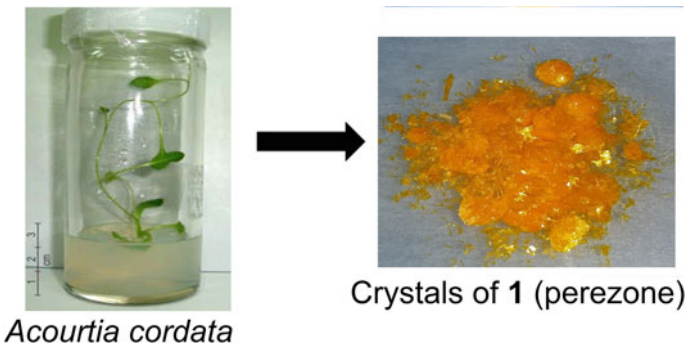

Fig. 24 In vitro production of perezone (**1**). Adapted from Ref. [120]

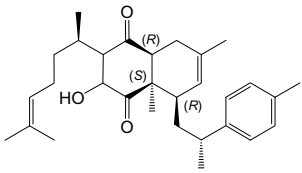

173 (curcuperezone)

Fig. 25 The new bisabolane curcuperezone (**173**) isolated from *Pseudopterogorgia rigida*. Adapted from Ref. [121]

3.6.2 Perezoperezone and Curcuperezone: Bisabolane Dimers from the Soft Coral *Pseudopterogorgia rigida*

In this study, the authors reported the isolation of three terpenoids, which constitute a rare class of bisabolane sesquiterpenoids, along with perezoperezone (**155**) (Scheme 7), curcuperezone (**173**) (Fig. 25), and diperezone (**79**) as minor constituents of a dichloromethane/methanol extract of the Caribbean soft coral *Pseudopterogorgia rigida*. The structures of these compounds were established by means of NMR and MS experiments. On the basis of the interpretation of their spectroscopic data, **173** and **79** were established as non-symmetrical dimeric structures [121].

3.6.3 Characterization and Comparison of Perezone with Some Analogs: An Experimental and Theoretical Study

In another investigation, theoretical studies to optimize the geometry of perezone (**1**) were carried out (Fig. 26a) and the results obtained were compared with values from experimental single-crystal X-ray diffraction data. It was found that the experimental values of atomic distances, angles, and dihedral angles were in good agreement with the theoretical values. Moreover, the corresponding IR spectra (theoretical, experimental) were also in good agreement. Docking studies of **1** showed it had a considerable number of non-bonding interactions with caspase-3, specifically with the largest interaction energies being with residues Cys285, Hys237, and Ala284. In a complementary study using horminone, thymoquinone, and isoperezone (**82**) as ligands and a protein related to apoptosis (caspase-3) as receptor, steric hindrance and the presence of corresponding functional groups are important for the biological activity of these natural products (Fig. 26b). Finally, docking score energy values were in good agreement with the experimental cytotoxicity results obtained from experiments in which perezone (**1**) and analogs were studied against different types of cancer cell lines [122].

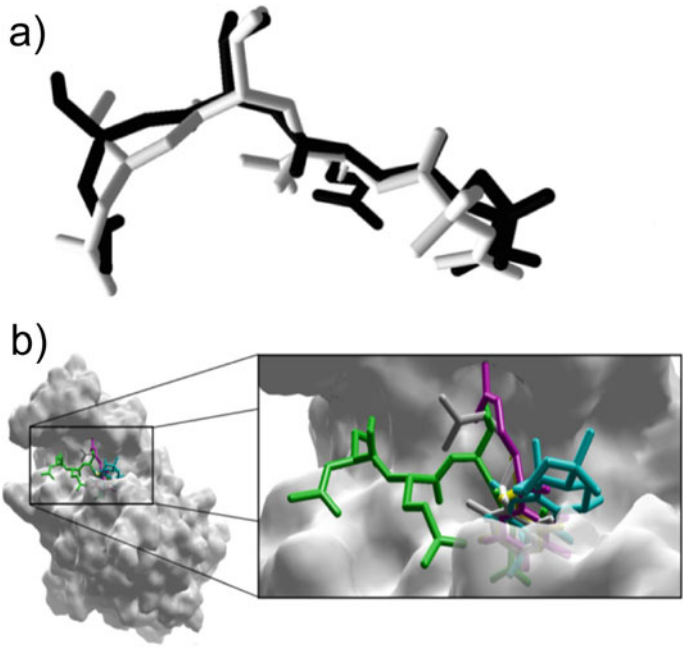

Fig. 26 a) Conformation of perezone (**1**) ligand (black), and the conformation of the best fit of **1** with minimum energy (white), b) Docking view of the active site caspase-3 (perezone (**1**): green, isoperezone (**82**): gray, thymoquinone: blue, and horminone: purple). Adapted from Ref. [122]

4 Recent Results from the Laboratory of the Present Authors

4.1 Advances in Biological Activity Investigations

4.1.1 The Search of Chemically Related Compounds to Perezone as Possible Anti-Neoplastic Agents

Due to the moderate cytotoxicity potency of **1**, coupled with its inhibition of by PARP-1, evaluation of natural products chemically related to perezone (**1**) is considered of interest. If selected molecules from this search also show PARP-1 inhibition activity, then they have potential utility in treating cancer types with high PARP-1 expression. Hernandez Rodriguez et al. performed computational and in vitro studies of seven compounds chemically related to perezone (**1**) (Fig. 27) to search for an additional analog with antiglioblastoma multiforme activity. The PARP-1 protein is highly expressed in glioblastoma multiforme (GBM) cells. Docking studies with PARP-1 were undertaken to select molecules with the best affinities. In addition, absorption, distribution, metabolism, excretion, and toxicity (ADMET) calculations were also

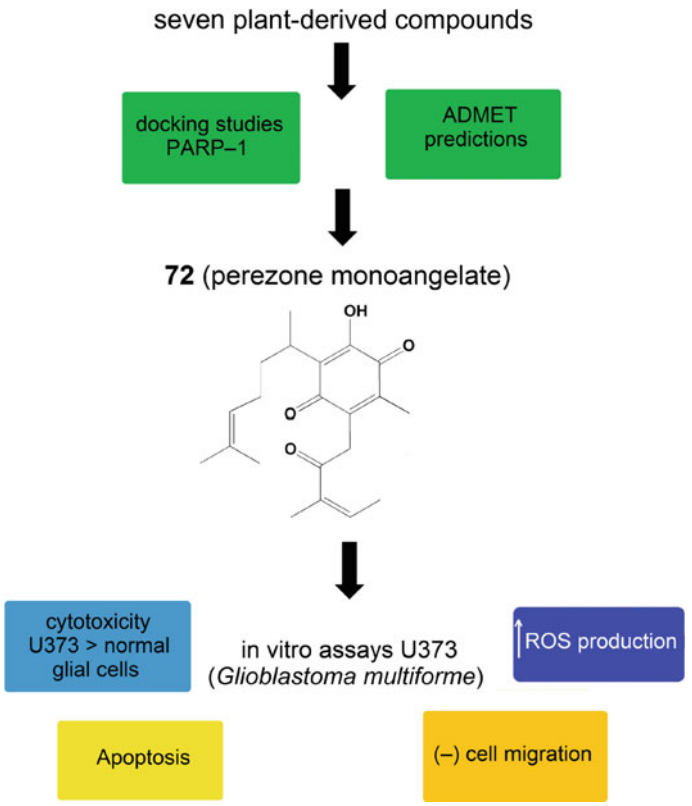

Fig. 27 Chemically related compounds to perezone (**1**) as an anti-GBM agent

performed. According to the computational studies conducted, perezone angelate (**72**) was selected, as it showed the highest affinity for PARP-1 and a high probability of being able to permeate cell membranes and the blood–brain barrier. In an in vitro study of **72** in U373 glioblastoma cells, this showed its ability to induce apoptosis in this cell line (IC_{50} 6.44 μM) and it inhibited cell migration, being less cytotoxic to glial cells (IC_{50} 173.66 μM). This supports its potential anti-GBM activity [123].

4.1.2 Wound-Healing Activity Study of Perezone

Several other pharmacological properties have been attributed to **1**, among them wound healing. After an extensive literature search, it appears that this effect has not been fully evaluated. Based on this premise, the research group of the present authors carried out some studies of the scarring activity of perezone at the cellular level. The first assay performed was for the fibroblast viability by perezone (**1**) using a multiple test method (MTT) assay. The results showed that concentrations lower

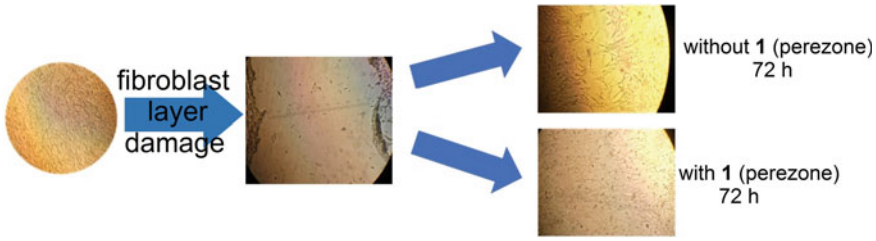

Fig. 28 In vitro wound-healing activity of perezone (**1**)

than 6 μ*M* of perezone increased fibroblast populations. In addition, this effect was also observed in an in vitro study of a scratch wound-healing assay (Fig. 28). The wound closure process was observed for 72 h, showing an increase in the repair velocity in the presence of perezone [124].

4.2 Advances Related to in Silico Studies

4.2.1 Computational Studies to Explore the Binding Mode of Perezone to PARP-1

To understand the PARP-1-perezone (**1**) interaction at the molecular level, docking studies and molecular dynamics (MD) simulations were performed by Nicolás-Vázquez et al. (Fig. 29). Quantum chemistry studies were carried out to compare perezone (**1**) in the gas phase and after docking studies. The results revealed that the presence of a large and deep cavity in the catalytic site of PARP-1 allowed non-bonding interactions to perezone (**1**). Molecular dynamic simulations over 50 ns showed that the PARP-1-perezone complex was stable, and interactions were postulated with three hydrogen bonds with Tyr235, Ala219, and Arg217. In addition, three

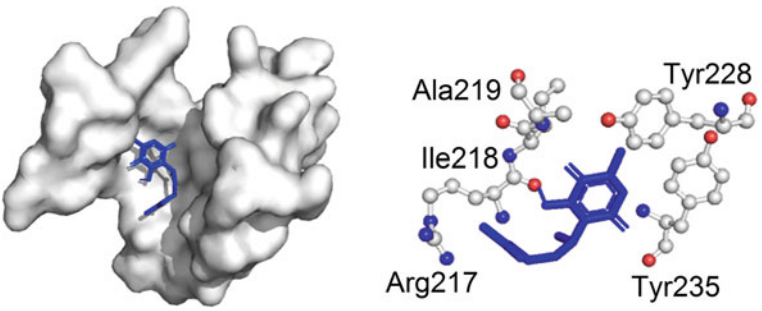

Fig. 29 Non–bonding interactions that drive the recognition of perezone (**1**) by PARP-1 as evidenced by docking studies and molecular dynamics simulations

hydrophobic interactions with Ile218, Ile231, and Tyr228 were maintained during the entire simulation. Quantum chemistry results showed that after docking studies, perezone gained charge (40%). The calculated HOMO–LUMO gap (ΔE_{gap}) value of perezone indicated that this molecule exhibits internal stability. In conclusion, the results obtained by Nicolás-Vázquez et al. give greater credence for **1** acting as a PARP-1 inhibitor [125].

4.2.2 Can (*S*)-Stereoisomers of Perezone and its Derivatives Show Similar Activity to its (*R*)-Stereoisomers? A Computational Characterization and Docking Study

Work has been performed in order to investigate the potential significance of the (*S*)-stereoisomer (a hypothetical molecule, **174**) of the naturally occurring (*R*)-perezone (**1**). Accordingly, the molecular properties of **174** at a theoretical level, and of (*S*)-isoperezone (**175**), together with the (*S*)-configured derivatives **176**–**183**, corresponding to the (*R*)-configured sulfur derivatives **132**–**139** of Scheme 1 and displayed in Fig. 30, were compared with the equivalent experimental and (*R*)-stereoisomer results, employing DFT at B3LYP/6–311++G(d,p) level. These DFT methods allowed the accurate determination of several molecular properties, such as geometrical, electronic, and spectroscopic parameters. Additionally, chemical reactivity descriptors were employed to analyze the reactivity of the hypothetical molecular systems. Thus, in the present investigation, the global reactivity profiles such

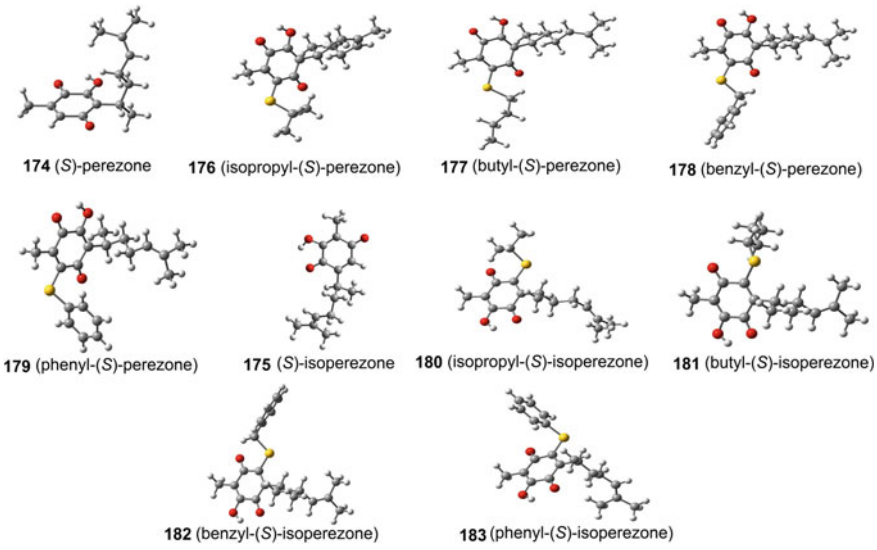

Fig. 30 The theoretical optimized (*S*)-structures of perezone (**174**), (*S*)-isoperezone (**175**) and their sulfur derivatives **176**–**183**

as electron affinity, electronegativity, chemical hardness, and electrophilicity index were calculated in order to gain insights into the activity of perezone (**1**) and its derivatives. Furthermore, docking studies allowed a determination of the possible binding mode of the (*S*)-stereoisomeric compounds on cyclooxygenase-2 (COX-2). Finally, a PASS prediction for biological activity was also employed. The results revealed that the maximum values of gap energy of each group (R)/(*S*) perezone and isoperezone derivatives were obtained for isopropyl-(*S*)-perezone (**176**), (*R*)-benzylperezone (**135**), isopropyl-(*S*)-isoperezone (**180**), and (*R*)-benzyl-isoperezone (**139**). (*S*)-Configured sulfur derivatives displayed higher ΔG values when interacting with COX-2 in comparison with (*R*)-sulfur derivatives due to steric hindrance, and consequently they are less active. With regard to the prediction of biological activity, it was proposed that the compounds could show both antineoplasic and mucomembranous protective activities [126].

4.2.3 Theoretical and Experimental Studies of Perezone Solubility in Supercritical Carbon Dioxide

In a previous investigation, the present authors reported a perezone extraction procedure using supercritical carbon dioxide. For this, the perezone solubility process in supercritical carbon dioxide ($scCO_2$) was determined at different temperatures, 40, 50, and 60°C, and different pressures, 8,063,000, 9,303,000, 10,650,000, and 14,820,000 Pa and the experimentally recognized solubility data were correlated with the Chrastil and Modified Chrastil equations to obtain thermodynamic parameters (Fig. 31). Moreover, a theoretical study was undertaken to describe the solubility process (Fig. 32). The experimental data for the solubility of perezone in $scCO_2$ did not correlate satisfactorily with the Chrastil equation ($r^2 = 0.7695$), but, however,

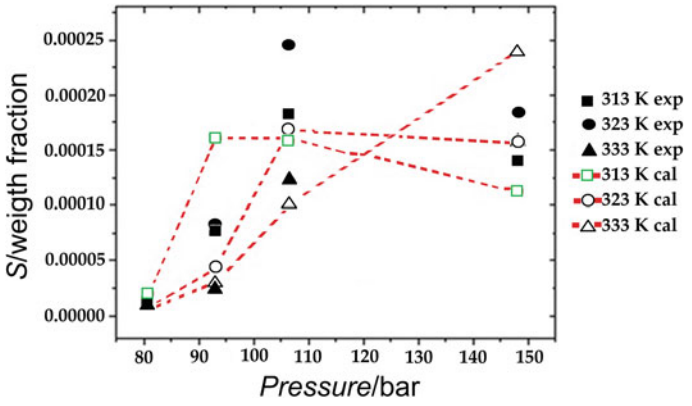

Fig. 31 Solubility of perezone (**1**) (mathematical modeling)

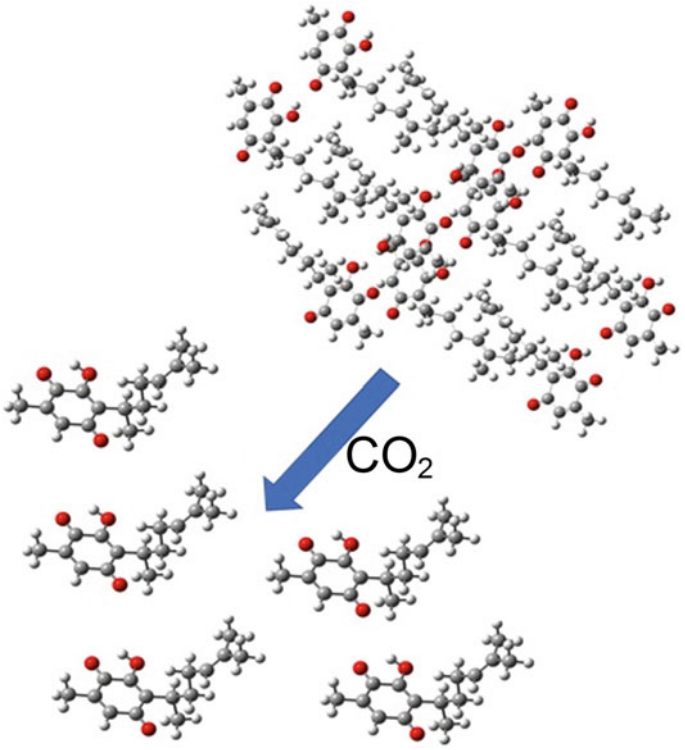

Fig. 32 Theoretical optimization of the solubility of perezone (**1**) in supercritical carbon dioxide

the modified Chrastil equation offered a better fit with a correlation of $r^2 = 0.9055$. Based on the statistical parameters of the absolute average of the relative deviations and the quadratic correlation, the modified Chrastil equation better reproduces the experimental results for the solubility of perezone in $scCO_2$ than the Chrastil equation [127].

4.3 Green Approaches

4.3.1 A Green Approach to the Oxidation of the Perezone C-12–C-13 Double Bond: A Theoretical Study and Cytotoxic Evaluation of the Corresponding Products

The oxidation of the C-12–C-13 double bond of perezone (**1**) and isoperezone (**82**) was carried out using green chemistry strategies (Scheme 8). First, the corresponding epoxides **184** and **185** were obtained employing a biocatalyzed reaction obtaining yields greater than 75%. Subsequently, the epoxides were subjected to stirring in

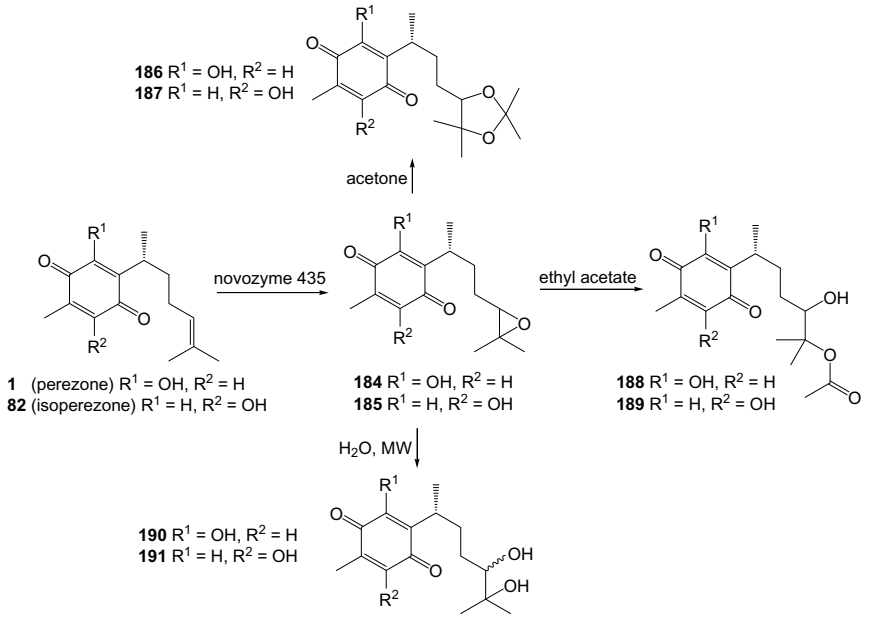

Scheme 8 Schematic representation of the C-12–C-13 double bond oxidation

the presence of mixtures of water and acetone and water and ethyl acetate. Through the processes, the ketals **186** and **187** and the corresponding monoacetylated diols **188** and **189** of **1** were obtained in moderate yields (30–40%). Finally, the epoxides were suspended in water and subjected to microwave irradiation, obtaining the corresponding diols **190** and **191** each in a yield of 80%. Spectroscopic characterization confirmed the proposed structures. Additionally, the eight new molecules were evaluated as cytotoxic agents against human breast cancer cells using an MTT procedure, and by monitoring the cytotoxic action for 72 h. The results showed that the derivatives of perezone were more active than those of isoperezone, with derivatives **184** and **187** being the most active compounds ($IC_{50} = 2.50$ and 2.74 $\mu g/cm^3$, respectively) (Fig. 33). Also, the experimental data were compared with theoretical results at the quantum level (Fig. 34a), allowing determination of the geometric parameters of the molecules, and these were in agreement with reported data of similar molecules. With respect to a molecular docking study with the human apopain protein (Fig. 34b), it was detected that molecules with the highest cytotoxic effects had the highest protein binding energy namely, −419.1 kJ/mol for perezone epoxide (**184**) and −405.9 kJ/mol for isoperezone acetonide (**187**) [128].

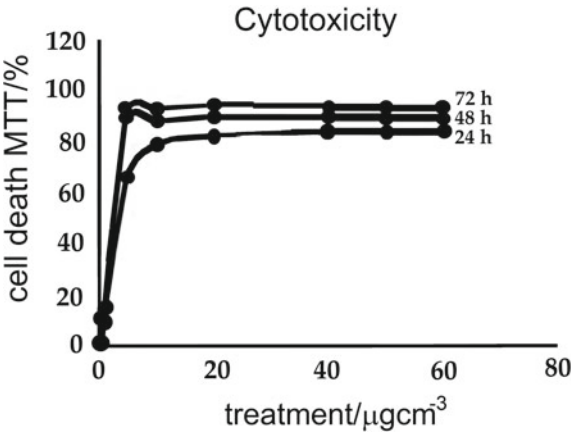

Fig. 33 Representative results of the cytotoxic effect of **184** at different times

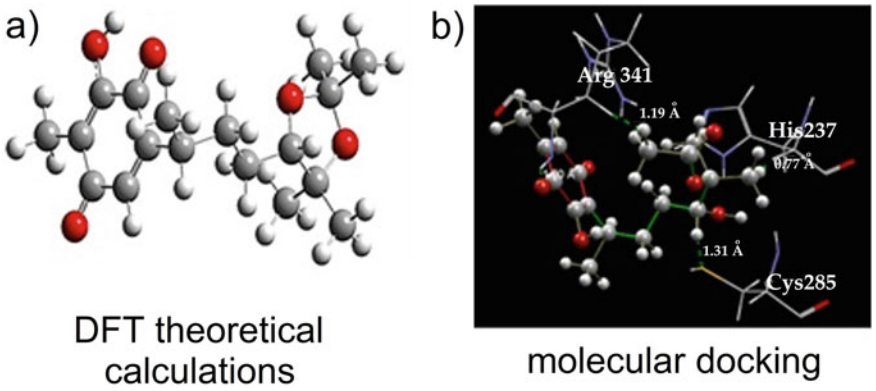

Fig. 34 a) DFT-level molecular optimization and b) molecular docking with the apopain protein

4.4 Synthesis of Perezone Derivatives

A series of 18 novel ligands **192–209** have been synthesized from perezone (**1**) and isoperezone (**82**). These molecules provided a series of metal complexes (**210**–**227**), which are analogous to *cis*-platin (Scheme 9). Presently, the current authors are carrying out studies against various cell lines, specifically on testicular, ovarian, and breast cancer, targeting the fact that these are cell lines resistant to *cis*-platin and analogous therapeutic agents [129].

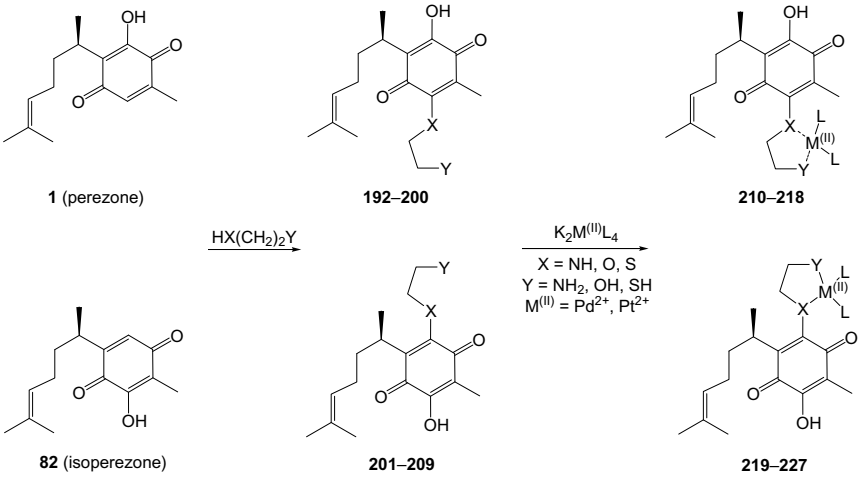

Scheme 9 Synthesis of analogs of *cis*-platin from perezone (**1**)

5 Conclusions

An overview comprising both a historical introduction (1552–1852–2005) and significant and appropriate information from more recent research (2006–2020) of the sesquiterpene quinone, commonly known as perezone (**1**), is described in this chapter. This molecule is recognized as the first secondary metabolite isolated in a crystalline form in the New World (American continents, 1852). In addition, important advances have been provided by work conducted from several points of view, namely, chemical synthesis (including amino derivatives of perezone), the green production of derivatives of **1**, the formation of anion receptors from **1**, and the production of (–)-perezoperezone, among others. Spectroscopic studies including ^{1}H NMR and two-dimensional NMR data to establish accurate chemical shifts and coupling constants of perezone (**1**) and some analogs have been surveyed. Furthermore, high-resolution mass spectra by electrospray ionization have been reported. Pharmacological and biological studies, focusing on antifeedant, antidiabetic, vasodilatory, and cytotoxic activities, are summarized. Reports from the authors' own research group, involving the activity of **1** and its analogs on the PARP-1 protein, have been mentioned. Moreover in silico research, summarized since such first work was conducted in 1997 (which established three different resonance forms for perezone employing theoretical calculations), to very recent work (2020, on π–π interactions, the computational characterization of **1** and analogs, to the conformational analysis by VCD or NMR), has been presented. Finally, the synthesis is described of interesting metal complexes of perezone derivatives that are due to be evaluated for cancer cell cytotoxic activity.

Acknowledgments The authors are grateful to PAPIIT-UNAM IN212421, in addition to the Dirección General de Cómputo y de Tecnologías de Información y Comunicación (DGTIC-UNAM) for the use of the supercomputer MIZTLI-LANCAD-UNAM-DGTIC-400. Thanks are due to Moisés Hernández Duarte for technical assistance. Pablo Mendoza acknowledges CONACyT for a Ph.D. scholarship (CVU 685907/628682).

References

1. Río de la Loza L (1852) Discurso pronunciado por el Catedrático de Química Médica de la Escuela de Medicina, en el acto público del ramo, el día 23 de Noviembre de 1852. Escritos de Leopoldo Río de la Loza, Escalante, México 1911:94
2. Hernández-Rodríguez M, Mendoza Sánchez P, Macías Perez ME, Rosales Cruz E, Mera Jiménez E, Aceves-Hernández JM, Nicolás-Vázquez MI, Miranda Ruvalcaba R (2020) In vitro and computational studies of natural products related to perezone as anti-neoplastic agents. Biochimie 171–172:158
3. Zepeda LG, Burgeño-Tapia E, Pérez-Hernández N, Cuevas G, Joseph-Nathan P (2013) NMR-based conformational analysis of perezone and analogues. Magn Reson Chem 51:245
4. Cortés E, Ortiz B, Sánchez-Obregón R, Walls F, Yuste F (1997) The mass spectral fragmentation of perezone and related compounds. Rapid Commun Mass Spectrom 11:904
5. García Guerrero CD, Blanco Dávila F (2004) La cirugía plástica y el Códice de la Cruz-Badiano. Med Univ 6:51
6. Joseph-Nathan P (2007) Homenaje al doctor Don Leopoldo Río de la Loza en el bicentenario de su natalicio. Bol Soc Quím Méx 1:173
7. Mylius F (1885) Über die Pipitzahoinsäure. Ber 18:480
8. Mylius F (1885) Pipitzahoic acid or perezone. Ber 18:936
9. Anschütz R, Leather W (1885) Über einige Derivate der Pipitzahoinsäure. Ber 18:715
10. Anschütz R (1885) Über die Pipitzahoinsäure. Ber 18:709
11. Duyk M (1899) Perezone, a new indicator for alkalimetry. Ann Chem Anal Chem Appl Rev Chem anal Reunions 4:372
12. Percy Remfry FG (1913) Perezone. J Chem Soc Trans 103:1076
13. Kögl F, Boer AG (1935) The constitution of perezone. Rec Trav Chim 54:779
14. Yamaguchi K (1942) Hydroxyquinones. VII. Synthesis of *dl*-dihydroperezone.Yakugaku Zasshi 62:491
15. Arigoni D, Jeger O (1954) Über Sesquiterpene und Azulene. 111. Mitt. Über die absolute Konfiguration des Zingiberens. Helv Chim Acta 37:881
16. Walls F, Salmon M, Padilla J, Joseph-Nathan P, Romo J (1965) Structure of perezone. Bol Inst Quim UNAM 17:3
17. Archer DA, Thomson RH (1965) Structure of perezone. Chem Commun:345
18. Wagner ER, Moss RD, Brooker RM (1965) A correction of the structure of perezone. Tetrahedron Lett:4233
19. Bates RB, Paknikar SK, Thalacker VP (1965) A 1,3-addition by a hydroquinone: the structure of perezone. Chem Ind:1793
20. Walls F, Padilla J, Joseph-Nathan P, Giral F, Romo J (1965) The structures of α- and β-pipitzols. Tetrahedron Lett 21:1577
21. Garcia T, Dominguez E, Romo J (1965) Isolation of hydroxyperezone from *Perezia alamani*. Bol Inst Quim UNAM 17:16
22. Cortes E, Salmon M, Walls F (1965) Total synthesis of perezone and α- and β-pipitzols. Bol Inst Quim UNAM 17:19
23. Walls F, Padilla J, Joseph-Nathan P, Giral F, Escobar M, Romo J (1966) Studies in perezone derivatives: structures of the pipitzols and perezinone. Tetrahedron 22:2387

24. Padilla J, Romo J, Walls F, Crabbe P (1967) Optical properties of derivatives of the perezone series and of pipitzols. Rev Soc Quím Méx 11:7
25. Joseph-Nathan P, Reyes J, González MP (1968) Contribution to the chemistry of perezone. Tetrahedron 24:4007
26. Chandler AD Jr, Florestano HJ (The Dow Chemical Company) (1969) Griseofulvin-perezone composition. US Pat No 3,471,615A
27. Joseph-Nathan P, Gonzalez MP, Johnson LRF, Shoolery JN (1971) Natural abundance carbon-13 NMR studies of perezone and derivatives. Org Magn Reson 3:23
28. Joseph-Nathan P, González MP, Rodríguez VM (1972) Terpenoids of *Perezia heblecada.* Phytochemistry 11:1803
29. Joseph-Nathan P, González MP, García GE (1974) Further studies on hydroxyperezone derivatives. Tetrahedron 30:3461
30. Salazar I, Enríquez R, Díaz E, Walls F (1974) The photochemical rearrangement of 5-(1′,5′-dimethylhex-4′-enyl)-6-methoxy-7a-methyl-3*H*-indazole-4,7(3a*H*,7a*H*)-dione, the pyrazoline derivative of *O*-methylperezone. Aust J Chem 27:163
31. Joseph-Nathan P, García GE, Mendoza V (1977) Quinones from *Perezia runcinata.* Phytochemistry 16:1086
32. Bohlmann F, Zdero C (1977) Über Inhaltsstoffe der Tribus Mutisieae. Phytochemistry 16:239
33. Joseph-Nathan P, Mendoza V, García E (1977) The reaction mechanism of the perezone-pipitzol transformation. Tetrahedron 33:1573
34. Bohlmann F, Zdero C, King RM, Robinson H (1979) Neueperezon-derivate aus *Acourtia thurberi.* Phytochemistry 18:1894
35. Joseph-Nathan P, Mejía G, Abramo-Bruno D (1979) ^{13}C NMR assignment of the side-chain methyls of C_{27} steroids. J Am Chem Soc 101:1289
36. Barrios H, Salazar I, Enriquez R, Diaz E, Walls F (1979) Isolation and structure determination of two new products formed by the irradiation of pyrazolino-*O*-methylperezone. Rev Latinoam Quim 10:69
37. Enríquez R, Ortega J, Lozoya X (1980) Active components in *Perezia* roots. J Ethnopharmacol 2:389
38. Barrera E, Barrios H, Walls F (1980) Intramolecular photocycloaddition of *O*-methylmethoxyperezone. Rev Soc Quím Méx 24:161
39. Sánchez IH, Yañez R, Enríquez R, Joseph-Nathan P (1981) A reaction mechanism change in the Lewis acid catalyzed perezone-pipitzol transformation. J Org Chem 46:2818
40. Joseph-Nathan P, Abramo-Bruno D, Ortega DA (1981) Carbon-13 NMR studies of benzoquinones. Org Magn Reson 15:311
41. Bohlmann F, Zdero C, Robinson H, King RM (1981) A diterpene, a sesquiterpene quinone and flavones from *Wyethia helenioides.* Phytochemistry 20:2245
42. Joseph-Nathan P, Hernández JD, Román LU, García E, Mendoza V (1982) Sesquiterpenes from *Perezia carpholepis.* Phytochemistry 21:669
43. Joseph-Nathan P, Hernández JD, Román LU, García E, Mendoza V, Mendoza S (1982) Coumarin and terpenoids from *Perezia alamani* var. *oolepis.* Phytochemistry 21:1129
44. Bohlmann F, Ahmed M, Grenz M, King RM, Robinson H (1983) Bisabolene derivatives and other constituents from *Coreopsis* species. Phytochemistry 22:2858
45. Sánchez IH, Basurto F (1984) The stereocontrol of the perezone to pipitzol transformation. J Nat Prod 47:382
46. Sánchez IH, Larraza MI (1985) Formal total synthesis of β-pipitzol. Tetrahedron 41:2355
47. Sánchez IH, Mendoza S, Calderón M, Larraza MI, Flores HJ (1985) Total synthesis of (±)-perezone. J Org Chem 50:5077
48. Bohlmann F, Banerjee S, Jakupovic J, King RM, Robinson H (1985) Bisabolene derivatives and acetylenic compounds from Peruvian *Coreopsis* species. Phytochemistry 24:1295
49. Soriano-García M, Toscano RA, Flores-Valverde E, Montoya-Vega F, López-Celis I (1986) Structure of 2-(1,5-dimethyl-4-hexenyl)-3-hydroxy-5-methyl-1,4-benzoquinone (perezone), a sesquiterpene. Acta Cryst C 42:327

50. Barrios H, Salazar I, Díaz E, Walls F, Joseph-Nathan P (1986) Carbon-13 NMR studies on perezone transformation products. Rev Latinoam Quím 16:163
51. Jimenez-Cardoso JM, Alcantara G, Campos E, Carabez A, Wusterhaus A (1986) Light and electron microscopy of hepatocytes of rats treated with perezone. Preliminary report. Arch Invest Med 17:313
52. Joseph-Nathan P, Martínez E, Rojas M, Santillan RL (1987) The solid-state versus the solution structure of 6-hydroxyperezone. J Nat Prod 50:860
53. García GE, Mendoza V, Guzmán BA (1987) Perezone and related sesquiterpenes from parvifoline. J Nat Prod 50:1055
54. Joseph-Nathan P, Garibay ME, Santillan RL (1987) BF_3-catalyzed cycloadditions of naturally occurring sesquiterpene *p*-benzoquinones. J Org Chem 52:759
55. Cuéllar A, Cárabez A, Chávez E (1987) Ca^{2+} releasing effect of perezone on adrenal cortex mitochondria. Life Sci 41:2047
56. Jolad SD, Timmermann BN, Hoffmann JJ, Bates RB, Camou FA, Cole JR (1988) Sesquiterpenoids from *Coreocarpus arizonicus*. Phytochemistry 27:3545
57. Carabez TA, Sandoval ZF (1988) The action of the sesquiterpene benzoquinone, perezone, on electron transport in biological membranes. Arch Biochem Biophys 260:293
58. De Pahn EM, Molina Portela MP, Stoppani AOM (1988) Effects of quinones and nitrofurans on *Trypanosoma mega* and *Crithidia fasciculata.* Rev Argent Microbiol 20:107
59. Joseph-Nathan P, Santillan RL (1989) The chemistry of perezone and its consequences. In Atta-ur-Rahman (ed) Studies in natural products chemistry, vol 5 (Part B). Elsevier, Amsterdam, p 763, and references therein
60. Hausen BM, Soriano-Garcia M, Flores-Valverde E (1989) The sensitizing capacity of hydroxyperezone. Contact Derm 21:120
61. Perri ST, Dyke HJ, Moore HW (1989) Rearrangement of cyclobutenones to 2,5- and 2,6-dialkylated 1,4-benzoquinones. Synthesis of *O*-methylperezone and *O*-methylisoperezone. J Org Chem 54:2032
62. Ehnsen A, Karabelas K, Heerding JM, Moore HW (1990) Synthesis of hydroxyquinones and related compounds: semisquaric acids, (±)-terreic acid, (±)-perezone, and (±)-isoperezone. J Org Chem 55:1177
63. Perri ST, Moore HW (1990) Rearrangements of cyclobutenones. Synthesis of benzoquinones from 4-alkenyl-4-hydroxycyclobutenones. J Am Chem Soc 112:1897
64. Zdero C, Bohlmann F, Sanchez H, Dominguez XA (1991) Isocedrene derivatives and other constituents from *Acourtia nana.* Phytochemistry 30:2695
65. González FJ, Aceves JM, Miranda R, González I (1991) The electrochemical reduction of perezone in the presence of benzoic acid in acetonitrile. J Electroanal Chem 310:293
66. Molina Portela MP, De Pahn EM, Galeffi C, Stoppani AOM (1991) Effect of lipophilic *ortho*-naphthoquinones on the growth and peroxide production by *Leptomonas seymouri* and *Crithidia fasciculata.* Rev Argent Microbiol 23:1
67. Perusquia M, Ibanez R, Alcantara G (1991) Relaxant effect of perezone on contraction of isolated rat uterus. Med Sci Res 19:857
68. Vidrio H, Alcantara G (1992) Cardiovascular effects of perezone in the anesthesized rat. Rev Fac Med UNAM 35:104
69. Garcia X, Cano L, Herrera L, Magana NR, Alcantara G, Gijon E (1992) Perezone relaxing vascular action. Proc West Pharmacol Soc 35:93
70. Joseph-Nathan P, Burgeño-Tapia E, Santillan RL (1993) Further $BF_3{\cdot}Et_2O$-catalyzed cycloadditions of sesquiterpenic *p*-benzoquinones. J Nat Prod 56:1758
71. Rodríguez-Hernández A, Barrios H, Collera O, Enríquez RG, Ortiz B, Sánchez-Obregón R, Walls F, Yuste F, Reynolds WF, Yu M (1994) Isomerization of perezone into isoperezone and preparation of dihydroisoperezinone. Nat Prod Lett 4:133
72. Barcelo Quintal ID, Solis Correa HE, Flores Valverde E (1994) Kinetic stability of perezonates of cobalt, nickel, and zinc in hydro-alcohol solutions. Rev Soc Quím Méx 38:110
73. Yuste F, Barrios H, Díaz E, Ortiz B, Sánchez-Obregón R, Walls F (1994) The structure of β-isopipitzol. Tetrahedron Lett 35:9329

74. Garcia X, Alcantara-Sarabia G, Cartas-Heredia L, Gijon E (1995) Actions of perezone on rat smooth muscle. Gen Pharmacol 26:1741
75. Enríquez RG, Ortiz B, Alducin E, Walls F, Gnecco D, Yu M, Reynolds WF (1995) The reaction of perezone and isoperezone with hydroxylamine: a surprisingly facile method for introducing an NH_2 group into the quinone functionality. Nat Prod Lett 6:103
76. Reynolds WF, Yu M, Ortiz B, Rodríguez A, Yuste F, Walls F, Enríquez RG, Gnecco D (1995) Detailed characterization by two-dimensional NMR of two unusual bicyclo[2.2.2]octanedione derivatives produced by the reaction of perezone with thiourea. Magn Reson Chem 33:3
77. Arellano J, Vázquez F, Villegas T, Hernández G (1996) Establishment of transformed roots culture of *Perezia cuernavacana* producing the sesquiterpene quinone perezone. Plant Cell Rep 15:455
78. Yuste F, Barrios H, Díaz E, Enríquez RG, González-Gutiérrez L, Ortiz B, Sánchez-Obregón R, Walls F (1996) The ultraviolet irradiation of isoperezone acetate. 2D NMR structure elucidation. Nat Prod Lett 8:181
79. Alarcon-Aguilar FJ, Roman-Ramos R, Jimenez-Estrada M, Reyes-Chilpa R, Gonzales-Paredes B, Flores-Saenz JL (1997) Effects of three Mexican medicinal plants (Asteraceae) on blood glucose levels in healthy mice and rabbits. J Ethnopharmacol 55:171
80. Rubio M, Ramírez GG, García Jiménez F, Salcedo R, Belmont MA (1997) About perezone derivatives, a theoretical approach. J Mol Struct THEOCHEM 397:239
81. Garcia E, Mendoza V, Guzman JA (1997) Formation of mansonones from naturally occurring *para*-benzoquinones. Nat Prod Lett 11:67
82. Frontana BA, Cárdenas J, Rodríguez-Hahn L, Baeza A (1997) Preparative electrochemical reductive methylation of *ortho*-hydroxy-*para*-benzoquinones. Tetrahedron 53:469
83. Burgeño-Tapia E, Joseph-Nathan P (1997) Detailed studies on perezone rearrangements. Monatsh Chem 128:651
84. Enríquez RG, Fernández-G JM, Gnecco D, Pénicaud A, Reynolds WF (1998) The crystal and molecular structure of isoperezone, aminoperezone, and isoaminoperezone: a comparative study of their crystal packing. J Chem Crystallogr 28:529
85. Téllez FJ, Carvajal K, Cruz D, Cárabez A, Chávez E (1999) Effect of perezone on arrhythmias and markers of cell injury during reperfusion in the anesthetized rat. Life Sci 65:1615
86. Burgeño-Tapia E, Joseph-Nathan P (2000) ^{13}C NMR substituent chemical shifts in hydroxyl-*p*-benzoquinones. Magn Reson Chem 38:390
87. Huipe-Nava E, Mendoza GV, García GE, Gúzman JA, Salvador JL, Soriano-García M (2000) Structure of α-isopipitzol (4,8,8,10-tetramethyl-9-hydroxy-2,12-dioxotricyclo[5,3,1,$0^{3,7}$]undec-1-en). Anal Sci 16:1239
88. de la Peña A, Izaguirre R, Baños G, Viveros M, Enríquez RG, Fernández-G JM (2001) Effect of perezone, aminoperezone and their corresponding isomers isoperezone and isoaminoperezone upon in vitro platelet aggregation. Phytomedicine 8:465
89. Aguilar-Martínez M, Bautista-Martínez JA, Macías Ruvalcaba N, González I, Tovar E, Marín del Alizal T, Collera O, Cuevas G (2001) Molecular structure of substituted phenylamine α-OMe- and α-OH-*p*-benzoquinone derivatives. Synthesis and correlation of spectroscopic, electrochemical, and theoretical parameters. J Org Chem 66:8349
90. Bautista-Martínez JA, GonzálezI A-M (2004) Correlation of voltammetric behavior of α-hydroxy- and α-methoxy-quinones with the range of acidity level in acetonitrile. J Electroanal Chem 573:289
91. Frontana C, Frontana-Uribe BA, González I. Electrochemical and ESR study on the transformation processes of α-hydroxyquinones. J Electroanal Chem 573:307
92. Guo XD, Huang ZS, Bao YD, An LK, Ma L, Gu LQ (2005) Two new sesquiterpenoids from *Helicteres angustifolia.* Chin Chem Lett 16:49
93. Frontana C, González I (2007) Structural factors affecting the reactivity of natural α-hydroxyquinones. An electrochemical and ESR study. ECS Trans 3:13
94. Frontana C, González I (2007) Effects of the molecular structure on the electrochemical properties of naturally occurring α-hydroxyquinones. An electrochemical and ESR study. J Electroanal Chem 603:155

95. Bautista-Martínez JA, Frontana C, Solano-Peralta A, Reyes-Hernández CI, Cuevas G, González I, Aguilar-Martinez M (2007) Influence of the substituent on the reactivity of anilinoperezones. Analysis of the influence of the C-12–C-13 double bond. ECS Trans 3:45
96. Espinoza-Vázquez A, Rodríguez-Gómez FJ, Mata R, Madariaga-Mazón A, Ángeles-Beltrán D (2017) Perezone as corrosion inhibitor for AISI 1018 steel immersed in NaCl saturated with CO_2. J Solid State Electrochem 21:1687
97. Martínez J, Velasco-Bejarano B, Delgado F, Pozas R, Torres Domínguez HM, Trujillo Ferrara JG, Arroyo GA, Miranda R (2008) Eco-contribution to the chemistry of perezone, a comparative study, using different modes of activation and solventless conditions. Nat Prod Commun 3:1465
98. Escobedo-González RG, Pérez Martínez H, Nicolás-Vázquez MI, Martínez J, Gómez G, Nava Serrano J, Carranza Téllez V, Vargas-Requena CL, Miranda Ruvalcaba R (2016) Green production of indolylquinones, derivatives of perezone, and related molecules, promising antineoplastic compounds. J Chem 2016:ID3870539
99. Escobedo-González R, Vázquez-Cabañas A, Martínez-González A, Mendoza-Sánchez P, Saavedra-Leos Z, Cruz-Olivares J, Nava Serrano J, Martínez J, Miranda Ruvalcaba R (2019) Green approach extraction of perezone from the roots of *Acourtia platyphilla* (A. Gray): a comparison of four activating modes and supercritical carbon dioxide. Molecules 24:3035
100. Concepción Lozada M, Soria-Arteche O, Ramírez Apan MT, Nieto-Camacho A, Enríquez RG, Izquierdo T, Jiménez-Corona A (2012) Synthesis, cytotoxic and antioxidant evaluations of amino derivatives from perezone. Bioorg Med Chem 20:5077
101. Ylijoki KEO, Stryker JM (2013) [5+2] cycloaddition reactions in organic and natural product synthesis. Chem Rev 113:2244
102. Chacón-García L, Valle-Sánchez M, Contreras-Celedon CA (2013) A novel semisynthetic anion receptor: synthesis and ion recognition of (1*H*-pyrrol-2-yl)-4-oxo-perezone. Lett Org Chem 10:632
103. Gao S, Hu X (2017) A concise synthetic approach to parvistemin A and (±)-diperezone. Org Chem Front 4:1493
104. Liu Y, Wang X, Chen S, Fu S, Liu B (2018) Iron-catalyzed intramolecular perezone-type [5+2] cycloaddition: access to tricyclo[6.3.1.$0^{1,6}$]dodecane. Org Lett 20:2934
105. Long Y, Ding Y, Wu H, Qu C, Liang H, Zhang M, Zhao X, Long X, Wang S, Puno P-T, Deng J (2019) Total synthesis of (–)-perezoperezone through an intermolecular [5+2] homodimerization of hydroxyl *p*-quinone. Angew Chem Int Ed 58:17552
106. Roura-Pérez G, Quiróz B, Aguilar-Martínez M, Frontana C, Solano A, González I, Bautista-Martínez JA, Jiménez-Barbero J, Cuevas G (2007) Remote position substituents as modulators of conformational and reactive properties of quinones. Relevance of the π/π intramolecular interaction. J Org Chem 72:1883
107. Burgeño-Tapia E, Cerda-García-Rojas CM, Joseph-Nathan P (2012) Conformational analysis of perezone and dihydroperezone using vibratonial circular dichroism. Phytochemistry 74:190
108. Reyes-López E, Quiroz-García B, Carpio-Martínez P, Jiménez-Barbero J, Cortés-Guzmán F, Esturau-Escofet N, Cuevas G (2017) The folded conformation of perezone revisited. Long range nOe interaction in small molecules: interpretable small signals or useless large artifacts? J Mex Chem Soc 61:177
109. Martínez J, Hernández Rodríguez M, Escobedo-González R, Nicolás-Vázquez MI, Saavedra-Leos Z, Miranda Ruvalcaba R (2019) Computational characterization of perezone, isoperezone, and their sulfur-derivatives: anti-inflammatory activity. ChemSelect 4:13333
110. Rojo-Portillo T, Reyes-López E, Hernández-Huerta E, Quiroz-García B, Joseph-Nathan P, Sánchez-Castellanos M, Cuétara-Guadarrama F, Cuevas G (2020) Is the VCD spectrum a fingerprint of the conformational population? The conformation of perezone in the spotlight. J Mol Struct 1202:127273
111. Burgeño-Tapia E, Castillo L, González-Coloma A, Joseph-Nathan P (2008) Antifeedant and phytotoxic activity of the sesquiterpene *p*-benzoquinone perezone and some of its derivatives. J Chem Ecol 34:766

112. Gheeya JS, Chen Q-R, Benjamin CD, Cheuk AT, Tsang P, Chung J-Y, Metaferia BB, Badgett TC, Johansson P, Wei JS, Hewitt SM, Khan J (2009) Screening a panel of drugs with diverse mechanisms of action yields potential therapeutic agents against neuroblastoma. Cancer Biol Ther 8:2386
113. Sánchez-Torres LE, Torres-Martínez JA, Godínez-Victoria M, Omar J-M, Velasco-Bejarano B (2010) Perezone and its isomer isoperezone induce caspase-dependent and caspase-independent cell death. Phytomedicine 17:614
114. Abreu PA, Wilke DV, Araujo AJ, Marinho-Filho JDB, Ferreira EG, Ribeiro CMR, Pinheiro LS, Amorim JW, Valverde AL, Epifanio RA, Costa-Lotufo LV, Jimenez PC (2015) Perezone, from the gorgonian *Pseudopterogorgia rigida*, induces oxidative stress in human leukemia cells. Rev Bras Farmacogn 25:634
115. Georgantea P, Ioannou E, Evain-Bana E, Bagrel D, Martinet N, Vagias C, Roussis V (2016) Sesquiterpenes with inhibitory activity against CDC25 phosphatases from the soft coral *Pseudopterogorgia rigida*. Tetrahedron 72:3262
116. Escobedo-González RG, Vargas-Requena CL, Moyers-Montoya E, Aceves-Hernández JM, Nicolás-Vázquez MI, Miranda Ruvalcaba R (2017) In silico study of the pharmacologic properties and cytotoxicity pathways in cancer cells of various indolylquinone analogues of perezone. Molecules 22:1060
117. Martínez AL, Madariaga-Mazón A, Rivero-Cruz I, Bye R, Mata R (2017) Antidiabetic and antihyperalgesic effects of a decoction and compounds from *Acourtia thurberi*. Planta Med 83:534
118. Luna-Vázquez FJ, Ibarra-Alvarado C, Camacho-Corona MR, Rojas-Molina A, Rojas-Molina I, García A, Bah M (2018) Vasodilator activity of compounds isolated from plants used in Mexican traditional medicine. Molecules 23:1474
119. Hernández-Rodríguez M, Mendoza Sánchez PI, Macias Perez ME, Rosalez Cruz E, Mera Jiménez E, Nicolás-Vázquez MI, Miranda Ruvalcaba R (2019) In vitro and computational studies showed that perezone inhibits PARP-1 and induces changes in the redox state of K562 cells. Arch Biochem Biophys 671:225
120. Gómez-Serrano G, Cristiani-Urbina E, Villegas-Garrido TL (2012) Time-dependent perezone production in different culture systems of *Acourtia cordata*. Cent Eur J Biol 7:507
121. Georgantea P, Ioannou E, Vagias C, Roussis V (2013) Perezoperezone and curcuperezone: bisabolane dimers from the soft coral *Pseudopterogorgia rigida*. Tetrahedron Lett 54:6920
122. Escobedo-González RG, Bahena L, Arias Tellez JL, Hinojosa Torres J, Miranda Ruvalcaba R, Aceves-Hernández JM (2015) Characterization and comparison of perezone with some analogues. Experimental and theoretical study. J Mol Struct 1097:98
123. Hernández-Rodríguez M, Mendoza Sánchez PI, Macias Perez ME, Rosales Cruz E, Mera Jiménez E, Żołek T, Maciejewska D, Nicolás-Vázquez MI, Miranda Ruvalcaba R (2021) Search of perezone chemically related compounds as possible anti-neoplastic agents. Med Chem Res, submitted
124. Escobedo González RG, Martínez J, Vargas Requena C, Hernández-Rodríguez M, Nicolás-Vázquez MI, Moyers Montoya ED, Miranda Ruvalcaba R (2021) Wound healing perezone acitivy study. Bioorg Med Chem, submitted
125. Hernández-Rodríguez M, Nicolás-Vázquez MI, Macías Pérez ME, Mera Jiménez E, Miranda Ruvalcaba R (2020) Computational studies to explore the binding mode of perezone to PARP-1. Int J Quantum Chem, submitted
126. Martínez J, Hernández-Rodríguez M, Saavedra-Leos Z, Miranda Ruvalcaba R, Escobedo-González R, Nicolás-Vázquez MI (2020) Can (*S*)-stereoisomers of perezone and its derivatives show similar activity to its (*R*)-stereoisomers? A computational characterization and docking study. ChemSelect, submitted
127. Escobedo González RG, Cruz-Olivares J, Nicolás-Vázquez MI, Miranda Ruvalcaba R (2020) Theoretical and experimental study of perezone solubility in supercritical dioxide. J Chem Eng Data, submitted

128. Escobedo González RG, Martínez J, Aceves-Hernández JM, Vargas Requena C, Hernández-Rodríguez M, Nicolás-Vázquez MI, Miranda Ruvalcaba R (2020) Green approach to perezone C-12–C-13 oxidizing synthesis, theoretical study and cytotoxic evaluation of the corresponding products. Bioorg Med Chem, submitted
129. Mendoza Sánchez P (2021) Nuevas contribuciones a la química de la perezona (New contributions to the chemistry of perezone). Ph.D. Thesis, Faculty of Superior Studies Cuautitlan-UNAM, Cuautitlan Izcalli-State of Mexico, in progress

René Escobedo-González obtained a B.Sc. degree in Chemistry in 2007, followed by an M.Sc. degree in Material Science in 2012 from the Autonomous University of Juarez City (UACJ), and then a Ph.D. degree in Chemistry in 2019 at the National Autonomous University of Mexico (UNAM), performed under the guidance Professor René Miranda Ruvalcaba. He was appointed as a professor at Monterrey's Technological Institute (ITESM) and the Autonomous University of Juarez City (UACJ). Currently, Dr. Escobedo holds a researcher position at the Technological University of Juárez City. His main research lines are in green organic chemistry and natural products, in silico studies on biologically interesting molecules, and the design of nanobiomaterials. He is the co-author of 11 publications in international scientific journals and a member of the National Research Mexican system (CONACYT—level 1).

Pablo Mendoza obtained a B.Sc. degree in Chemistry in 2017, followed by an M.Sc. degree (with honors) in Chemical Science in 2019, and is currently in his second year of a Ph.D. degree program in Chemical Science at the National Autonomous University of Mexico (UNAM), under the supervision of Professor René Miranda Ruvalcaba. Presently, Mr. Mendoza holds a teaching position at the Faculty of Higher Studies Cuautitlán (FES Cuautitlán), a multidisciplinary and decentralized entity of UNAM, delivering organic chemistry courses in heterocyclic chemistry and spectroscopy. The main goal of his research is in achieving the synthesis of perezone hybrid platinum-like metal complexes as potential alternatives to cis-platin derivatives in several cancer therapies. Much of his research is within the scope of green chemistry, the core philosophy of his work.

María Inés Nicolás-Vázquez obtained a B.Sc. degree in Pharmaceutical Chemistry and Biology in 1992, followed by an M.Sc. in Physical Chemistry in 1998, and a Ph.D. degree in Sciences in 2005 at the Universidad Nacional Autónoma de México (UNAM). She has been an academic since 2006 at the Department of Chemistry Sciences FESC-UNAM, and has published about 35 peer-reviewed papers. These have included a series of studies on theoretical and computational chemistry, in particular the quantum theory of molecular electronic structure. The aim is to comprehend electronic structure calculations, spectroscopic procedures, reaction mechanisms, and intermolecular interactions to understand the behavior of molecules with intersting chemical and biological properties. Further interests include the design and computational studies of known drugs and their derivatives, as well as those molecules obtained as natural products or by chemical synthesis, thereby addressing their interaction with biological targets. For this last area, docking methods are used to predict preferred orientations to form stable complexes with their targets. This may in turn be used to predict the strength of association or binding affinity between each target and ligand.

Maricarmen Hernández-Rodríguez obtained her Ph.D. degree in Medical Sciences at the Superior School of Medicine in 2017, supervised by Professor Martha Cecilia Rosales Hernández. She obtained a Postdoctoral Research Fellowship at the Faculty of Higher Studies Cuautitlán (Professor René Miranda Ruvalcaba, from 2017 to 2019). She was appointed as Research Professor (from 2019–present), at the Superior School of Medicine of the National Polytechnic Institute, Mexico. She has focused her research on the design of novel compounds with biological activities, and has published 19 peer-reviewed papers and two book chapters. Her research group routinely determines the cytotoxic activities of test compounds in cell cultures. The aim is to develop novel treatments to treat cancer and Alzheimer's disease.

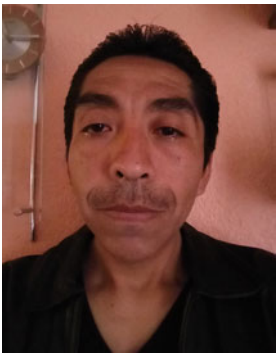

Joel Martínez obtained a B.Sc. degree in Industrial Chemistry in 2003, followed by an M.Sc. degree in Sciences in 2006, and a Ph.D. degree in Sciences in 2013 focusing on green chemistry at the Autonomous National University of Mexico (Mexico), with Professor René Miranda Ruvalcaba as his advisor. Dr. Martínez undertook postdoctoral work in the group of Professor Pedro A. Alonso Dávila at the Autonomous University of San Luis Potosi, from 2015 to 2017 (Mexico). Currently, he holds a research position at the Chemistry Sciences Faculty at the Autonomous University of San Luis Potosi. His main research focus is on the synthetic modification of natural products employing green chemistry protocols, and extraction of several secondary metabolites using alternative energy sources such as near infrared irradiation, microwave irradiation, and ultrasound. Additionally, his group has carried out theoretical

studies on molecules obtained in order to better understand their geometrical and molecular properties. He has published 17 peer-reviewed papers, and has been a co-author of a book on green chemistry, and written four book chapters. Also, Dr. Martínez has supervised ten B.Sc. theses and one M.Sc. thesis.

René Miranda Ruvalcaba obtained a B.Sc. degree in Chemistry, followed by an M.Sc. degree in Organic Chemistry, and a Ph.D. degree in Chemical Sciences, with all three being obtained from The National Autonomous University of Mexico (UNAM) under the guidance of Professor Manuel de Jesus Salmon Salazar. He has been an academic for almost 47 years and has been the recipient of numerous awards. Examples are: "The National Award for Teaching Chemistry (Mexican Chemical Society, 2021)", "The Annual Award for Teaching Natural Sciences (UNAM, 2017)", the highest level academic recognition over almost 30 years (UNAM), and a higher research award (level III) of the National Research Mexican System (CONACYT). His main academic focus is on teaching heterocyclic chemistry/green chemistry—investigating green chemistry and using substrates and interesting secondary metabolites, and in silico studies of natural products. He has authored or coauthored more than 155 articles, reviews, and books.

Biologically Active Constituents from Plants of the Genus *Xanthium*

Nguyen Thi Thuy Linh, Ninh The Son, Nguyen Thi Thu Ha, Nguyen Thanh Tra, Le Thi Tu Anh, Sibao Chen, and Nguyen Van Tuyen

Contents

N. T. T. Linh · N. T. Son (✉) · N. T. T. Ha · N. T. Tra · L. T. Tu Anh
Department of Applied Biochemistry, Institute of Chemistry, Vietnam Academy of Science and Technology, 18 Hoang Quoc Viet, Caugiay, Hanoi, Vietnam
e-mail: yamantson@mail.com

N. T. T. Linh
e-mail: thuylinh1992.bk@gmail.com

N. T. T. Ha
e-mail: thuha.vast@gmail.com

N. T. Tra
e-mail: nguyenthanhtravast@gmail.com

L. T. Tu Anh
e-mail: ln.tuanh@gmail.com

S. Chen
Department of Applied Biochemistry and Chemical Technology, The Hong Kong Polytechnic University, Hung Hom, Hong Kong, China
e-mail: sibao.chen@polyu.edu.hk

N. Van Tuyen
Department of Medicinal Chemistry, Institute of Chemistry, Vietnam Academy of Science and Technology, 18 Hoang Quoc Viet, Caugiay, Hanoi, Vietnam
e-mail: ngvtuyen@hotmail.com

A. D. Kinghorn, H. Falk, S. Gibbons, Y. Asakawa, J.-K. Liu, V. M. Dirsch (eds.),
Progress in the Chemistry of Organic Natural Products 116,
https://doi.org/10.1007/978-3-030-80560-9_4

1 Introduction

Xanthium species (cockleburs) are a genus of flowering plants of the family Asteraceae. This genus, consisting of 25 species, is now distributed in many parts of the world but it originated from South America [1]. With a long history of traditional ethnomedical use, *Xanthium* species have been recognized as being of significant value to manage various diseases. As a typical example, *Xanthium strumarium*, also known as "Cang Er Zi" in traditional Chinese medicine, has been used for treating nasal problems and congestion [2]. Also, all parts of *X. strumarium* have been recommended traditionally to treat leukoderma, poisonous bites of insects, epilepsy, ear infections, rheumatism, tuberculosis, and urinary and gastric disorders [2, 3]. In Bolivia, a root decoction of *X. spinosum* (spiny cocklebur) is taken to treat arteriosclerosis and hypertension, while certain communities in North America have used a leaf decoction of this species for snakebites and lung problems [4]. The genus *Xanthium* biosynthesizes bioactive molecules such as terpenoids, phenols, sulfur and nitrogen-containing compounds, sterols, flavonoids, quinones, coumarins, fatty acids, and miscellaneous substances [5–10]. In particular, terpenoids have been regarded as the major constituents and display many bioactivities. For example, purified sesquiterpenoid derivatives from *X. strumarium* significantly inhibited the proliferation of AGS cells by TRAIL-resistance overcoming activity [11], while monoterpene glucosides from this plant have anti-inflammatory activity [12]. Crude extracts, fractions as well as secondary metabolites obtained from the genus *Xanthium* have exhibited a myriad of biomedical-related properties, inclusive of cytotoxic, antioxidative, anti-inflammatory, antibacterial, antifungal, antidiabetic, and antiangiogenic activities [11, 13–16].

During the past seven decades, experimental studies on *Xanthium* species have increased greatly. In parallel with this, previous review articles have afforded only specific descriptions of *X. strumarium* [2, 3], but a comprehensive overview for the whole genus *Xanthium* is missing. The current contribution aims to fill this gap, by providing in-depth information on the phytochemical and biological aspects of this genus.

2 Phytochemical Investigations

In recognition of the contribution of natural products to drug discovery programs, searching for biologically active secondary metabolites from herbal plants has received great attention over the last two centuries by laboratory scientists. In parallel with this, the procedures for the isolation, purification, and structural determination of these isolated compounds have improved as a result of significant advances in chromatographic techniques, such as thin-layer chromatography (TLC), column chromatography (CC), gas chromatography (GC), and high-performance liquid chromatography (HPLC), as well as spectroscopic approaches for structural elucidation, such as nuclear magnetic resonance (NMR), and mass spectrometry (MS), e.g., Refs. [17–24].

With respect to the genus *Xanthium*, phytochemical investigations have focused on various plant parts of 15 species, including *X. brasilicum*, *X. canadense*, *X. catharticum*, *X. cavanillesii*, *X. chinense*, *X. indicum*, *X. italicum*, *X. macrocarpum*, *X. mongolicum*, *X. orientale*, *X. pennsylmnicum*, *X. pungens*, *X. sibiricum*, *X. spinosum*, and *X. strumarium* (Fig. 1).

To the maximum extent possible, this contribution attempts to summarize all of the isolated metabolites from *Xanthium* species, primarily based upon the outcome of modern chromatographic and spectroscopic methods. Based on their similar structural classes and with each in alphabetical order (Table 1), 300 isolated metabolites have been compiled, consisting of terpenoids (**1**–**147**) (Figs. 2 and 3), simple phenols (**148**–**183**) (Fig. 4), sulfur- and nitrogen-containing compounds (**184**–**212**) (Fig. 5), lignans (**213**–**250**) (Fig. 6), sterols (**251**–**266**) (Fig. 7), flavonoids (**267**–**273**), quinones (**274** and **275**), coumarins (**276**–**277**), fatty acids (**278**–**288**), and other miscellaneous compound types (**298**–**292**) (Fig. 8), along with isolated compounds from endophytic fungi associated with *Xanthium* species (**293**–**300**) (Fig. 9). In addition, 30 compounds have been identified from the volatile oils of *Xanthium* species (Fig. 10).

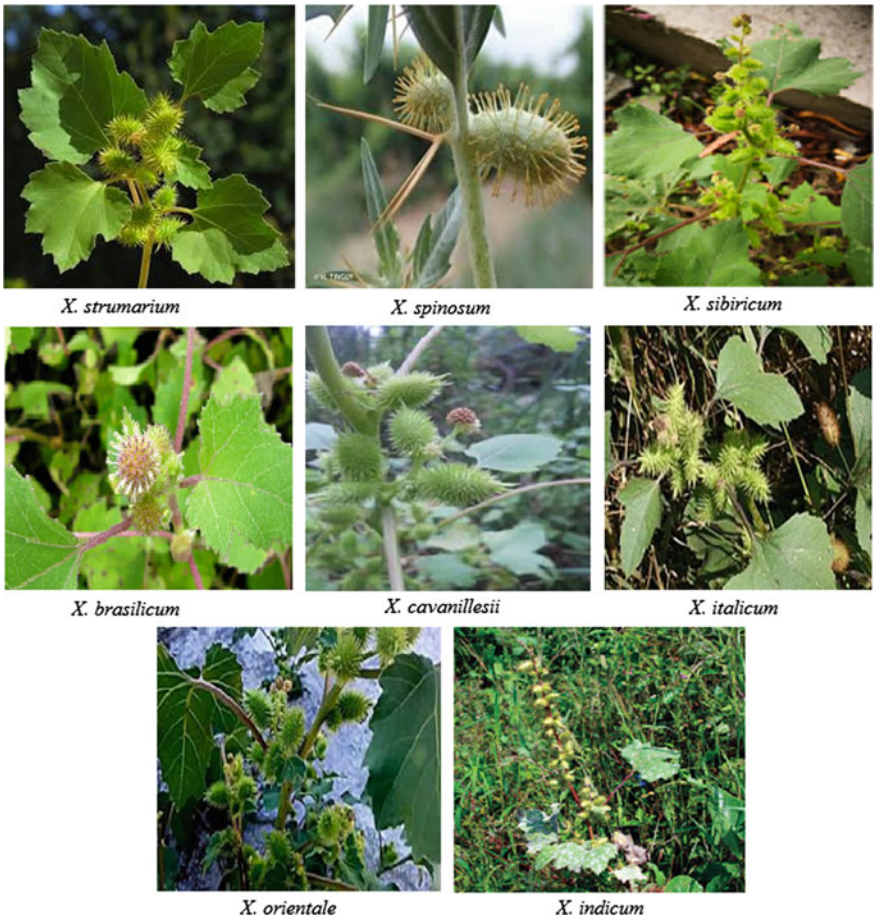

Fig. 1 The main *Xanthium* species subjected to phytochemical and biological studies

2.1 Terpenoids

2.1.1 Sesquiterpenoids

Xanthanolides

Sesquiterpenoids are the main class of isolated compounds obtained from plants in the genus *Xanthium.* Such compounds have been found to be based on various skeletons, but xanthanolides are predominant. A group of 78 xanthanolides (**1**–**78**) is included in Table 1 [4, 8, 9, 11, 15, 16, 25–63].

As shown in Fig. 2, an important feature of xanthanolide structures arises from their stereochemistry. Methylation normally occurs at C-10 ((*S*)-configuration),

Table 1 Chemical constituents from the genus *Xanthium*

No.	Compound	Species	Ref.
Terpenoids			
Sesquiterpenoids			
Xanthanolides			
1	2-Acetoxy-4,5-epoxyxanthanolide-1,4-endoperoxide	*X. pungens* aerial parts	[25]
2	Anhydrodehydroivalbin	*X. spinosum* aerial parts	[26]
3	Bis-norxanthanolide	*X. cavanillesii* aerial parts	[27]
4	Cyclospinosolide	*X. spinosum* aerial parts	[26]
5	Deacetylxanthanol	*X. orientale* whole plant, *X. strumarium* leaves and aerial parts	[11, 26, 28]
6	Deacetylxanthiuminol	*X. spinosum* aerial parts	[29]
7	2-Deacetyl-11β,13-dihydroxyxanthinin	*X. sibiricum* roots	[30]
8	2-Desoxy-6-*epi*-parthemollin	*X. sibiricum* roots	[30]
9	1β,4β,4α,5α-Diepoxyxanthat-11(13)-en-12-oic acid	*X. strumarium* aerial parts	[31]
10	4-*O*-Dihydroinusoniolide	*X. strumarium* aerial parts	[26]
11	11α,13-Dihydro-4*H*-xanthalongin	*X. sibiricum* roots	[30]
12	11α,13-Dihydroxanthatin	*X. strumarium* aerial parts	[31, 32]
13	11α,13-Dihydro-8-*epi*-xanthatin	*X. catharticum* aerial parts, *X. sibiricum* aerial parts	[9, 33]
14	11α,13-Dihydroxanthinin	*X. strumarium* leaves	[11]
15	11β,13-Dihydroxanthinosin	*X. strumarium* seeds	[34]
16	11αH,13-Dihydroxanthumin	*X. cavanillesii* aerial parts	[27]

(continued)

Table 1 (continued)

No.	Compound	Species	Ref.
17	11α,13-Dihydroxanthuminol	*X. strumarium* leaves	[11]
18	11β,13-Dihydroxanthatin	*X. sibiricum* roots	[30]
19	4,15-Dinor-1,11(13)-xanthadiene-3,5β:12,8β-diolide	*X. brasilicum* aerial parts	[35]
20	2-*epi*-Xanthumin	*X. indicum* aerial parts, *X. pungens* aerial parts	[25, 36]
21	4-*epi*-Isoxanthanol	*X. cavanillesii* flowers, *X. macrocarpum* leaves and fruits, *X. spinosum* leaves, *X. strumarium* aerial parts	[15, 26, 31, 37–39]
22	4-*epi*-Xanthanol	*X. cavanillesii* flowers, *X. macrocarpum* leaves and fruits, *X. spinosum* leaves, *X. strumarium* aerial parts	[15, 26, 31, 37–39]
23	4-*epi*-Xanthinine	*X. cavanillesii* flowers	[37]
24	8-*epi*-Xanthatin	*X. brasilicum* aerial parts, *X. canadense* leaves, *X. indicum* aerial parts, *X. pungens* fruits and aerial parts, *X. strumarium* aerial parts	[25, 35, 36, 40, 41]
25	8-*epi*-Xanthatin-1α,5α-epoxide	*X. sibiricum* aerial parts	[9]
26	8-*epi*-Xanthatin-1β,5β-epoxide	*X. brasilicum* aerial parts, *X. cavanillesii* aerial parts, *X. indicum* aerial parts, *X. pungens* aerial parts, *X. sibiricum* aerial parts	[9, 25, 27, 35, 36, 42]
27	1α,5α-Epoxy-1,5-dihydroxanthatin (1α,5α-Epoxyxanthatin)	*X. orientale* whole plants, *X. spinosum* leaves, aerial parts, and whole plants, *X. strumarium* aerial parts	[26, 28, 29, 31, 39, 43]

(continued)

Table 1 (continued)

No.	Compound	Species	Ref.
28	1α,5β-Epoxy-1,5-dihydroxanthatin (1β,5β-Epoxyxanthatin)	*X. spinosum* aerial parts and whole plants, *X. strumarium* aerial parts	[26, 29, 31, 43]
29	1α,5α-Epoxy-1,5,11α,13-tetrahydro-8-*epi*-xanthatin	*X. catharticum* aerial parts	[33]
30	1α,5β-Epoxy-1,5,11α,13-tetrahydro-8-*epi*-xanthatin	*X. catharticum* aerial parts, *X. cavanillesii* aerial parts	[27, 33]
31	4β,5α-Epoxy-10αH-xanthan-1(2),11(13)-dien-7β,8β-olide	*X. cavanillesii* aerial parts	[44]
32	4β,5β-Epoxyxanthatin-1α,4α-endoperoxide	*X. mongolicum* whole plant, *X. strumarium* aerial parts	[31, 45]
33	1β-Hydroxy-5α-chloro-8-*epi*-xanthatin	*X. sibiricum* aerial parts	[9]
34	2-Hydroxytomentosin	*X. cavanillesii* aerial parts, *X. indicum* aerial parts, *X. pungens* aerial parts, *X. strumarium* aerial parts	[25, 27, 36, 41, 46]
35	2-Hydroxytomentosin-1β,5β-epoxide	*X. strumarium* aerial parts	[41]
36	2-Hydroxyxanthinosin	*X. macrocarpum* leaves and fruits, *X. sibiricum* aerial parts	[15, 47]
37	4-Hydroxyxanthinosin	*X. macrocarpum* fruits	[15]
38	Inusoniolide	*X. sibiricum* aerial parts	[47]
39	Isoxanthanol	*X. spinosum* aerial parts, *X. strumarium* leaves and aerial parts	[26, 41, 48]
40	Mongolide D	*X. mongolium* aerial parts	[49]
41	Mongolide E	*X. mongolium* aerial parts	[49]
42	Norxanthantolide A	*X. sibiricum* roots	[30]

(continued)

Table 1 (continued)

No.	Compound	Species	Ref.
43	Norxanthantolide B	*X. sibiricum* roots	[30]
44	Norxanthantolide C	*X. sibiricum* roots	[30]
45	Norxanthantolide D	*X. sibiricum* roots	[30]
46	Norxanthantolide E	*X. sibiricum* roots	[30]
47	Norxanthantolide F	*X. sibiricum* roots	[30]
48	2-*O*-*β*-D-Glucopyranosyl-11*α*, 13-dihydro-8-*epi*-deacetylxanthiuminol	*X. spinosum* aerial parts	[50]
49	4-*O*-*β*-D-Glucopyranosyl-11*α*, 13-dihydro-8-*epi*-deacetylxanthiuminol	*X. spinosum* aerial parts	[50]
50	2-Oxo-4-*O*-acetyl-desacetylxanthanol	*X. spinosum* whole plants	[43]
51	4-Oxo-bedfordia acid	*X. cavanillesii* roots and aerial parts, *X. indicum* aerial parts, *X. macrocarpum* leaves and fruits, *X. mongolicum* whole plants, *X. strumarium* whole plants and aerial parts	[15, 16, 26, 31, 36, 37, 45, 46]
52	Pungiolide A	*X. brasilicum* aerial parts, *X. pungens* fruits and aerial parts, *X. sibiricum* aerial parts	[9, 25, 32, 35]
53	Pungiolide B	*X. brasilicum* aerial parts, *X. pungens* aerial parts	[25, 35]
54	Pungiolide C	*X. pungens* fruits	[32]
55	Pungiolide D	*X. sibiricum* aerial parts	[9]
56	Pungiolide E	*X. sibiricum* aerial parts	[9]
57	Pungiolide F	*X. chinense* fruits	[8]

(continued)

Table 1 (continued)

No.	Compound	Species	Ref.
58	Pungiolide G	*X. chinense* fruits	[8]
59	Pungiolide H	*X. chinense* fruits	[8]
60	Pungiolide I	*X. chinense* fruits	[8]
61	Pungiolide J	*X. chinense* fruits	[8]
62	Pungiolide K	*X. chinense* fruits	[8]
63	Pungiolide L	*X. chinense* fruits	[8]
64	Pungiolide M	*X. chinense* fruits	[8]
65	Pungiolide N	*X. chinense* fruits	[8]
66	Pungiolide O	*X. chinense* fruits	[51]
67	Tomentosin	*X. indicum* aerial parts, *X. pungens* aerial parts, *X. sibiricum* aerial parts, *X. strumarium* aerial parts	[25, 36, 41, 42]
68	Xanthanol	*X. spinosum* aerial parts, *X. strumarium* leaves	[26, 48]
69	Xanthanol acetate	*X. cavanillesii* aerial parts	[46]
70	Xanthatin	*X. cavanillesii* aerial parts, *X. macrocarpum* leaves and fruits, *X. mongolium* aerial parts and whole plants, *X. orientale* aerial parts and whole plants, *X. sibiricum* roots and aerial parts, *X. spinosum* epigeal parts, leaves, aerial parts, and whole plants, *X. strumarium* burs, leaves, fruits, aerial parts, and whole plants	[15, 16, 26, 28–32, 38, 39, 43, 45–47, 49, 52–59]

(continued)

Table 1 (continued)

No.	Compound	Species	Ref.
71	Xanthinin	*X. macrocarpum* fruits, *X. occidentale* aerial parts, *X. orientale* aerial parts, *X. pennsylvanicum* leaves	[15, 60–62]
72	Xanthinosin	*X. macrocarpum* leaves and fruits, *X. mongolium* aerial parts and whole plants, *X. orientale* aerial parts and whole plants, *X. sibiricum* roots and aerial parts, *X. strumarium* burs, leafs, seeds, fruits, aerial parts, and whole plants	[11, 15, 16, 26, 28, 30, 31, 34, 45, 47, 49, 53–55]
73	Xanthipungolide	*X. brasilicum* aerial parts, *X. pungens* aerial parts	[25, 35]
74	Xanthnon	*X. sibiricum* aerial parts	[47]
75	Xantholide A	*X. canadense* roots	[63]
76	Xantholide B	*X. canadense* roots	[63]
77	Xanthumin	*X. canadense* leaves, *X. cavanillesii* aerial parts, *X. indicum* aerial parts, *X. occidentale* aerial parts, *X. pungens* aerial parts, *X. strumarium* aerial parts	[25, 27, 36, 40, 41, 62]
78	Ziniolide	*X. catharticum* roots, *X. spinosum* roots	[4, 33]
Eudesmanolides			
79	12-Carboxyeudesma-3,11(13)-diene	*X. pungens* aerial parts	[25]
80	(2*R*,4α*R*,5*R*,8α*S*)-Decahydro-5-hydroxy-4α-methyl-α,8-bis(methylene)-2-naphthaleneacetic acid	*X. pungens* aerial parts	[25]
81	Hydroxylindestenolide	*X. sibiricum* roots	[30]

(continued)

Table 1 (continued)

No.	Compound	Species	Ref.
82	Isoalantolactone	*X. canadense* roots, *X. indicum* aerial parts	[36, 64]
83	Judaicin	*X. pungens* aerial parts	[25]
84	3-Oxocostusic acid	*X. pungens* aerial parts	[25]
85	β-Selinene	*X. indicum* aerial parts, *X. mongolicum* whole plants	[36, 45]
86	Seucoeudesmanolide	*X. indicum* aerial parts	[36]
87	8αH-Seucoeudesmanolide	*X. indicum* aerial parts	[36]
88	Sibirolide A	*X. sibiricum* roots	[30]
89	Sibirolide B	*X. sibiricum* roots	[30]
Eremophilanolides			
90	Eremophil-1(10),11(13)-dien-12,8β-olide	*X. canadense* roots, *X. sibiricum* aerial parts	[42, 64]
91	(11*R*)-Eremophil-1(10)-en-12,8β-olide	*X. canadense* roots, *X. sibiricum* aerial parts	[42, 64]
92	Sibiriolide A	*X. sibiricum* aerial parts	[65]
93	Sibiriolide B	*X. sibiricum* aerial parts	[65]
94	Sibiriolide C	*X. sibiricum* aerial parts	[42]
95	Sibiriolide D	*X. sibiricum* aerial parts	[42]
96	Xanthanodiene	*X. cavanillesii* roots, *X. indicum* aerial parts	[36, 37]
Megastigmanes			
97	Dehydrovomifoliol	*X. mongolicum* whole plants, *X. spinosum* leaves	[39]

(continued)

Table 1 (continued)

No.	Compound	Species	Ref.
98	(2*E*,4*E*,1′*S*,2′*R*,4′*S*,6′*R*)-Dihydrophaseic acid	*X. sibiricum* fruits	[66]
99	Dihydrophaseic acid sodium salt 4′-*O*-*β*-D-glucopyranoside	*X. sibiricum* fruits	[67]
100	(3*S*,5*R*,6*S*,7*E*)-5,6-Epoxy-3-hydroxy-7-megastigmene-9-one	*X. strumarium* fruits	[54]
101	Grasshopper ketone	*X. chinense* fruits	[51]
102	(6*R*,9*S*)-3-Oxo-*α*-ionol *β*-D-glucopyranoside	*X. chinense* fruits	[51]
103	Phaseic acid	*X. sibiricum* roots	[30]
104	(6*S*,9*R*)-Vomifoliol	*X. mongolicum* whole plants	[45]
Guaianolides and germacranolides			
105	4*β*-Hydroxypseudoguaia-11(13)-en-12-oic acid	*X. pungens* aerial parts	[25]
106	Isoguaiene	*X. indicum* aerial parts	[36]
107	Germacrene D	*X. indicum* aerial parts	[36]
108	Linderanlide C	*X. sibiricum* roots	[30]
Others			
109	5-Azuleneacetic acid	*X. sibiricum* aerial parts	[47]
110	Lasidiol *p*-methoxybenzoate	*X. catharticum* roots, *X. mongolicum* whole plants, *X. orientale* whole plants	[28, 33, 45]
Monoterpenoids			
111	Geranyl 6-*O*-*β*-D-apiofuranosyl-*β*-D-glucopyranoside	*X. chinense* fruits	[6]

(continued)

Table 1 (continued)

No.	Compound	Species	Ref.
112	(6*E*)-3-Hydroxymethyl-7-methylocta-1,6-dien-3-ol 8-*O*-*β*-D-glucopyranoside	*X. sibiricum* fruits	[68]
113	(6*Z*)-3-Hydroxymethyl-7-methylocta-1,6-dien-3-ol 8-*O*-*β*-D-glucopyranoside	*X. sibiricum* fruits	[68]
114	Loliolide	*X. spinosum* leaves, *X. strumarium* fruits	[39, 54]
115	(*E*)-2-Methyl-6-methyleneocta-2,7-dien-1-ol *β*-D-apiofuranosyl-(1 → 6)-*β*-D-glucopyranoside	*X. chinense* fruits	[6]
116	(*Z*)-2-Methyl-6-methyleneocta-2,7-dien-1-ol *β*-D-apiofuranosyl-(1 → 6)-*β*-D-glucopyranoside	*X. chinense* fruits	[6]
117	(+)-(5*Z*)-6-Methyl-2-ethenyl-5-hepten-1,2,7-triol	*X. sibiricum* fruits	[66]
118	(−)-(5*Z*)-6-Methyl-2-ethenyl-5-hepten-1,2,7-triol	*X. sibiricum* fruits	[66]
119	Myrtenol 6-*O*-*β*-D-apiofuranosyl-*β*-D-glucopyranoside	*X. chinense* fruits	[6]
120	Neryl 6-*O*-*β*-D-apiofuranosyl-*β*-D-glucopyranoside	*X. chinense* fruits	[6]
121	3*β*-Norpinan-2-one 3-*O*-*β*-D-apiofuranosyl-(1 → 6)-*β*-D-glucopyranoside	*X. sibiricum* fruits	[68]
122	Xanmonoter A	*X. strumarium* fruits	[12]
123	Xanmonoter B	*X. strumarium* fruits	[12]
Diterpenoids			
124	Atractyloside	*X. chinense* fruits, *X. strumarium* fruits	[6, 69]
125	Carboxytractyloside	*X. sibiricum* fruits, *X. strumarium* fruits and burs	[69–71]
126	4′-Desulfated-atractyloside	*X. chinense* fruits, *X. spinosum* aerial parts	[6, 50]

(continued)

Table 1 (continued)

No.	Compound	Species	Ref.
127	4′-Desulfated-carboxytractyloside	*X. spinosum* aerial parts	[50]
128	3′,4′-Desulfated atractyloside (3′,4′-Didesulfated atractyloside)	*X. chinense* fruits, *X. sibiricum* fruits, *X. spinosum* aerial parts	[6, 50, 71]
129	3′,4′-Didesulfated carboxytractyloside	*X. chinense* fruits, *X. pungens* burs, *X. spinosum* aerial parts	[6, 50, 72]
130	3′,4′-Didesulfated carboxytractyloside analog	*X. pungens* burs	[72]
131	Fructusnoid A	*X. strumarium* fruits	[73]
132	Fructusnoid B	*X. strumarium* fruits	[73]
133	Fructusnoid C	*X. strumarium* fruits	[73]
134	Fructusnoid D	*X. chinense* fruits	[6]
135	Fructusnoid E	*X. chinense* fruits	[6]
136	2*β*-*O*-*β*-D-Glucopyranosyl-15*α*-hydroxy-kaur-16-en-18,19-dicarboxylic acid	*X. spinosum* aerial parts	[50]
137	Phytol	*X. indicum* aerial parts	[36]
Triterpenoids			
138	*α*-Amyrin	*X. strumarium* leaves	[13]
139	Betulin	*X. orientale* whole plants, *X. sibiricum* roots	[5, 28]
140	Betulinic acid	*X. orientale* whole plants, *X. sibiricum* roots	[5, 28]
141	Erythrodiol	*X. sibiricum* roots	[5]
142	Lupeol	*X. orientale* whole plants, *X. strumarium* aerial parts	[28, 74]

(continued)

Table 1 (continued)

No.	Compound	Species	Ref.
143	Lupeol palmitate	*X. sibiricum* stems	[75]
144	Oleanolic acid	*X. orientale* whole plants	[28]
145	Squalene	*X. strumarium* leaves	[57]
146	Taraxerol	*X. canadense* roots	[64]
147	Taraxerol monoacetate	*X. canadense* roots	[64]
Simple phenols			
148	2,4-Bis(4-hydroxybenzyl)phenol	*X. strumarium* seeds	[34]
149	Caffeic acid	*X. sibiricum* fruits, *X. strumarium* fruits and seeds	[13, 34, 67, 76–78]
150	Caffeic acid choline ester	*X. sibiricum* fruits	[67]
151	Caffeic acid ethyl ester	*X. sibiricum* roots	[30]
152	4-*O*-Caffeoylquinic acid methyl ester (cryptochlorogenic acid methyl ester)	*X. chinense* fruits, *X. sibiricum* fruits	[51, 67]
153	5-*O*-Caffeoylquinic acid	*X. strumarium* fruits	[76]
154	5-*O*-Caffeoylquinic acid methyl ester (Neochlorogenic acid methyl ester)	*X. sibiricum* fruits, *X. strumarium* fruits	[7, 78, 79]
155	Chlorogenic acid	*X. sibiricum* fruits, *X. strumarium* fruits	[67, 76, 79, 80]
156	Chlorogenic acid methyl ester (methyl chlorogenate)	*X. chinense* fruits, *X. sibiricum* fruits	[51, 71]
157	Coniferaldehyde (3-Methoxy-4-*trans*-hydroxycinnamaldehyde)	*X. sibiricum* fruits, *X. strumarium* seeds	[34, 54, 78]
158	1,3-Di-*O*-caffeoylquinic acid (Cynarin)	*X. occidentale* leaves, *X. strumarium* fruits	[7, 79, 81]
159	1,4-Di-*O*-caffeoylquinic acid	*X. strumarium* fruits	[76]

(continued)

Table 1 (continued)

No.	Compound	Species	Ref.
160	1,5-Di-*O*-caffeoylquinic acid	*X. strumarium* fruits	[7, 76, 77, 79]
161	3,4-Di-*O*-caffeoylquinic acid	*X. cavanillesii* fruits	[82]
162	3,5-Di-*O*-caffeoylquinic acid	*X. cavanillesii* fruits, *X. strumarium* fruits	[7, 79, 82, 83]
163	4,5-Di-*O*-caffeoylquinic acid	*X. strumarium* fruits	[76]
164	2,4′-Dihydroxyphenyl methane	*X. strumarium* seeds	[34]
165	4,4′-Dihydroxydiphenyl methane	*X. strumarium* seeds	[34]
166	2,3-Dihydroxy-1-(4-hydroxy-3-methoxyphenyl)-propan-1-one	*X. sibiricum* fruits	[68]
167	3,4-Dihydroxybenzoic acid ethyl ester	*X. sibiricum* roots	[30]
168	3,4-Dihydroxybenzaldehyde	*X. strumarium* fruits	[84]
169	Ferulic acid	*X. sibiricum* fruits, *X. strumarium* fruits	[67, 76, 78, 80]
170	3-Hydroxy-1-(4-hydroxy phenyl) propan-1-one	*X. strumarium* fruits	[7]
171	7-(4-Hydroxy-3-methoxyphenyl) -1-phenylhept-4-en-3-one	*X. sibiricum* roots	[5]
172	*p*-Hydroxybenzaldehyde	*X. strumarium* seeds and fruits	[34, 54]
173	Icariside F2	*X. chinense* fruits	[51]
174	1,3,5-Tri-*O*-caffeoylquinic acid	*X. cavanillesii* fruits, *X. strumarium* fruits	[7, 76, 77, 79, 82, 83]
175	Methyl caffeate	*X. strumarium* seeds	[34]
176	Methyl *p*-benzoate	*X. mongolicum* whole plants	[45]
177	Methyl-3,5-di-*O*-caffeoylquinate	*X. strumarium* fruits	[7, 79]
178	Methyl-4,5-di-*O*-caffeoylquinate	*X. strumarium* fruits	[76]

(continued)

Table 1 (continued)

No.	Compound	Species	Ref.
179	3-Methyl-4,4′-dihydroxydiphenyl methane	*X. strumarium* seeds	[34]
180	Potassium 3-*O*-caffeoyl quinate	*X. strumarium* fruits	[76]
181	Protocatechuic acid	*X. strumarium* fruits	[7, 79]
182	Vanillin	*X. strumarium* seeds	[34]
183	Vanillic acid	*X. strumarium* seeds	[34]
Sulfur-containing compounds			
Thiazinediones			
184	2-Hydroxy-xanthiazone	*X. strumarium* seeds, *X. sibiricum* fruits	[10, 85]
185	2-Hydroxy-7-hydroxymethyl-8,8-dimethyl-4,8-dihydrobenzo[1,4]thiazine-3,5-dione -11-*O*-*β*-D-glucopyranoside	*X. strumarium* fruits	[80]
186	7-Hydroxymethyl-8,8-dimethyl-4,8-dihydrobenzo[1,4]-thiazine-3,5-dione (Xanthiazone)	*X. sibiricum* fruits, *X. strumarium* fruits and seeds	[10, 34, 76, 80, 85–87]
187	7-Hydroxymethyl-8,8-dimethyl-4,8-dihydrobenzo[1,4]thiazine-3,5-dione-11-*O*-*β*-D-glucopyranoside (Xanthiazone *O*-*β*-D-glucopyranoside or Thiazine-3,5-dione-11-*O*-glucopyranoside)	*X. strumarium* fruits	[7, 34, 80]
188	7-Hydroxymethyl-8,8-dimethyl-4,8-dihydrobenzo[1,4]thiazine-3,5-dione-(2-*O*-caffeoyl)-*β*-D-glucopyranoside	*X. strumarium* fruits	[88, 89]

(continued)

Table 1 (continued)

No.	Compound	Species	Ref.
189	7-Hydroxymethyl-8,8-dimethyl-4,8-dihydrobenzo[1,4]-thiazine-3,5-dione-11-*O*-[β-D-apiofuranosyl-(1 → 6)-*O*- D-glucopyranoside] or 7-[(β-D-apiofuranosyl-(1 → 6)-β-D-glucopyranosyl)oxymethy]-8,8-dimethyl-4,8-dihydrobenzo [1,4]thiazine-3,5-dione	*X. chinense* fruits, *X. sibiricum* fruits	[51, 68, 87]
190	Xanthialdehyde	*X. sibiricum* fruits, *X. strumarium* seeds	[10, 34]
191	Xanthiazinone	*X. sibiricum* fruits	[86]
192	(+)-Xanthiazinone A	*X. sibiricum* fruits	[10]
193	(–)-Xanthiazinone A	*X. sibiricum* fruits	[10]
194	(+)-Xanthiazinone B	*X. sibiricum* fruits	[10]
195	(–)-Xanthiazinone B	*X. sibiricum* fruits	[10]
196	(+)-Xanthiazinone C	*X. sibiricum* fruits	[10]
197	(–)-Xanthiazinone C	*X. sibiricum* fruits	[10]
198	Xanthiazinone D	*X. sibiricum* fruits	[10]
199	Xanthiside	*X. pungens* fruits, *X. sibiricum* fruits	[10, 67, 70, 86, 87, 90]
Xanthienopyrans and a thiophene			
200	Dihydro-xanthienopyran	*X. sibiricum* fruits	[10]
201	(+)-Xanthienopyran	*X. pungens* fruits, *X. sibiricum* fruits,	[10, 66, 86, 91]
202	(–)-Xanthienopyran	*X. sibiricum* fruits, *X. strumarium* seeds and fruits	[10, 34, 54, 66]

(continued)

Table 1 (continued)

No.	Compound	Species	Ref.
203	Sibiricumthionol	*X. sibiricum* fruits	[10, 66]
Nitrogen-containing compounds			
Amides			
204	Cytidine	*X. strumarium* fruits	[7]
205	*N*-(1′-D-Deoxyxyltolyl)-6,7-dimethyl-1,4-dihydro-2,3-quinoxalinedione	*X. sibiricum* fruits	[67]
206	5-Methyluracil	*X. sibiricum* roots	[92]
207	5-Hydroxypyrrolidin-2-one	*X. sibiricum* fruits	[86]
208	Succinimide	*X. strumarium* seeds	[34]
209	Uracil	*X. sibiricum* roots	[92]
Amines			
210	Adenosine	*X. sibiricum* fruits	[68]
211	Indole-3-carboxaldehyde	*X. strumarium* seeds	[34]
212	Indole-3-carboxylic acid	*X. strumarium* seeds	[34]
Lignans			
213	Balanophonin	*X. strumarium* fruits	[54]
214	Balanophonin A	*X. sibiricum* fruits	[93]
215	(1*S*,2*R*)-1,2-Bis(4-hydroxy-3-methoxyphenyl)-1,3-propanediol	*X. sibiricum* fruits, *X. strumarium* seeds	[85, 93]
216	Chushizisin E	*X. sibiricum* fruits	[93]
217	Cleomiscosin A	*X. sibiricum* roots	[92]
218	Cleomiscosin C	*X. sibiricum* roots	[92]

(continued)

Table 1 (continued)

No.	Compound	Species	Ref.
219	(–)-(7*R*,8*S*)-Dehydrodiconiferyl alcohol	*X. sibiricum* roots and fruits	[30, 93]
220	(+)-7′-Dehydrosismbrifolin	*X. sibiricum* roots	[30]
221	(–)-7′-Dehydrosismbrifolin	*X. sibiricum* roots	[30]
222	(+)-(7*S*,8*R*)-Dihydrodehydroconiferyl alcohol (*rel*-(2*α*,3*β*)-7-*O*-methylcedrusin)	*X. strumarium* seeds	[34, 85]
223	(7*R*,8*S*)-Dihydrodehydrodiconiferyl alcohol 4-*O*-*β*-D-glucopyranoside	*X. sibiricum* fruits	[93]
224	Diospyrosin	*X. sibiricum* fruits	[93]
225	(–)-9,9′-*O*-Di-(*E*)-feruloyl-*seco*-isolariciresinol	*X. sibiricum* roots	[92]
226	*erythro*-Guaiacylglycerol-*β*-coniferyl aldehyde ether	*X. strumarium* seeds	[85]
227	*erythro*-Guaiacylglycerol-8-*O*-4′-(coniferyl alcohol) ether	*X. strumarium* seeds	[85]
228	Fructusol	*X. strumarium* seeds	[85]
229	(–)-1-*O*-*β*-D-Glucopyranosyl-2-{2-methoxy-4-[1-(*E*)-propen-3-ol] phenoxy}-propane-3-ol	*X. sibiricum* fruits	[93]
230	(–)-(2*R*)-1-*O*-*β*-D-glucopyranosyl-2-{2-methoxy-4-[(*E*)-formylviny1]phenoxy} propane-3-ol	*X. sibiricum* fruits	[93]

(continued)

Table 1 (continued)

No.	Compound	Species	Ref.
231	1-(4-Hydroxy-3-methoxy)-phenyl-2-[4-(1,2,3-trihydroxypropyl)-2-methoxy]-phenoxy-1,3-propandiol	*X. sibiricum* fruits	[93]
232	2-(4-Hydroxy-3-methoxyphenyl)-3-(2-hydroxy-5-methoxyphenyl)-3-oxo-1-propanol	*X. sibiricum* fruits	[93]
233	Jatrocin B	*X. sibiricum* roots	[92]
234	Leptolepisol D	*X. sibiricum* fruits	[93]
235	4-Oxopinoresinol	*X. sibiricum* roots	[5]
236	(−)-Pinoresinol	*X. mongolicum* whole plants, *X. sibiricum* fruits, *X. strumarium* seeds and fruits	[34, 45, 54, 93]
237	(+)-Sibiricumin A	*X. sibiricum* fruits	[94]
238	(–)-Sibiricumin A	*X. sibiricum* fruits	[94]
239	(–)-Simulanol	*X. sibiricum* fruits	[93]
240	Syringaresinol	*X. sibiricum* roots	[92]
241	*threo*-Dihydroxy-dehydrodiconiferyl alcohol	*X. sibiricum* fruits	[93]
242	*threo*-Guaiacylglycerol-8′-vanillic acid ether	*X. sibiricum* roots	[30]
243	*threo*-Guaiacylglycerol-β-coniferyl aldehyde ether (8)	*X. strumarium* seeds	[85]
244	*threo*-Guaiacylglycerol-8-*O*-4′-(coniferyl alcohol) ether	*X. strumarium* seeds	[85]
245	*threo*-1-Phenyl-(4′-hydroxy-3′-methoxy)-2-phenyl-(4″-hydroxy-3″-methoxy)-1,3-propanediol	*X. strumarium* seeds	[85]

(continued)

Table 1 (continued)

No.	Compound	Species	Ref.
246	Xanthiumnolic A	*X. strumarium* fruits	[95]
247	Xanthiumnolic B	*X. strumarium* fruits	[95]
248	Xanthiumnolic C	*X. strumarium* fruits	[95]
249	Xanthiumnolic D	*X. strumarium* fruits	[95]
250	Xanthiumnolic E	*X. strumarium* fruits	[95]
Sterols			
251	14-Methyl-12,13-dehydro-sitosterol-heptadeconate	*X. strumarium* leaves	[13]
252	Daucosterol	*X. mongolicum* whole plants, *X. sibiricum* roots and fruits, *X. strumarium* leaves, seeds, and fruits	[5, 34, 45, 54, 58, 71, 78, 92]
253	5α,8α-Epidioxy-(22*E*)-ergosta-6,22-dien-3β-ol (Ergosterol peroxide)	*X. sibiricum* roots and stems	[45, 92]
254	6β-Hydroxystigmast-4-en-3-one	*X. sibiricum* roots	[5]
255	6β-Hydroxystigmast-4,22-dien-3-one	*X. sibiricum* roots	[5]
256	7α-Hydroxy-β-sitosterol (stigmast-5-ene-3β,7α-diol)	*X. strumarium* fruits	[54]
257	7-Ketositosterol	*X. sibiricum* roots	[5]
258	3-Oxo-$\Delta^{(4,5)}$-sitostenone	*X. sibiricum* roots	[5]
259	6′-Palmitoxyl-β-daucosterin	*X. strumarium* fruits	[54]
260	β-Sitostenone	*X. sibiricum* roots	[92]

(continued)

Table 1 (continued)

No.	Compound	Species	Ref.
261	β-Sitosterol	*X. mongolicum* whole plants, *X. orientale* aerial parts, *X. sibiricum* roots and fruits, *X. strumarium* seeds, fruits, and aerial parts	[5, 34, 45, 54, 60, 74, 78, 92]
262	Spinasterol	*X. orientale* whole plants	[28]
263	β-Stigmasterol	*X. sibiricum* roots and stems, *X. strumarium* leaves, seeds and aerial parts	[5, 34, 58, 34, 74, 75]
264	β-Stigmasteryl-β-D-glucoside	*X. sibiricum* stems, *X. strumarium* seeds	[34, 75]
265	Stigmast-4-ene-3β,6α-diol	*X. strumarium* fruits	[54]
266	Stigmast-4-en-6-ol-3-one	*X. sibiricum* roots	[92]
Flavonoids, quinones, coumarins, fatty acids, and miscellaneous compounds			
Flavonoids			
Isoflavones			
267	Formononetin	*X. strumarium* fruits	[80]
268	Luteone	*X. mongolicum* whole plants	[45]
269	Ononin (4′-Methyoxylisoflavone-7-*O*-β-D-glucopyranoside)	*X. sibiricum* fruits, *X. strumarium* fruits	[71, 80]
Flavones			
270	Jaceidin	*X. macrocarpum* fruits	[15]
271	Patuletin-3-glucuronide	*X. strumarium* fruits	[7]
272	Quercetin	*X. mongolicum* whole plants, *X. strumarium* fruits	[45, 54]
273	Quercetin-3-*O*-glucuronide	*X. strumarium* fruits	[7]
Quinones			

(continued)

Table 1 (continued)

No.	Compound	Species	Ref.
274	Emodin	*X. orientale* whole plants	[28]
275	5-Hydroxy-3,6-dimethoxy-7-methyl-1,4-naphthalenedione	*X. sibiricum* roots	[5]
Coumarins			
276	Scopoletin	*X. orientale* whole plants, *X. sibiricum* roots	[5, 28, 92]
277	Scopolin	*X. mongolicum* whole plants, *X. sibiricum* stems	[45, 75]
Fatty acids and related compounds			
278	Fumaric acid ethyl ester	*X. sibiricum* fruits	[71]
279	Hexadecanoic acid	*X. strumarium* leaves	[13]
280	Heptacosanoic acid	*X. sibiricum* stems	[75]
281	3(*Z*)-Hexenyl-β-D-glycoside	*X. mongolicum* whole plants	[45]
282	Methyl hexadecanoate	*X. orientale* whole plants	[28]
283	Nonadecanoic acid	*X. sibiricum* roots	[92]
284	Oleic acid	*X. orientale* whole plants	[28]
285	Pentatriacontan-1-ol	*X. strumarium* aerial parts	[74]
286	Succinic acid	*X. sibiricum* fruits	[78]
287	Triacontanol	*X. orientale* whole plants	[28, 60]
288	Tridec-1-ene-3,5,7,9,11-pentayne	*X. canadense* roots	[96]
Miscellaneous compounds			
289	3-Cycloheptene-1-acetic acid	*X. sibiricum* aerial parts	[47]

(continued)

Table 1 (continued)

No.	Compound	Species	Ref.
290	(2*S*,3*R*)-2,3 -Dihydroxy-2-methylbutyrolactone	*X. strumarium* seeds	[34]
291	5-(Hydroxymethyl)furfural	*X. strumarium* seeds	[34]
292	Raffinose	*X. strumarium* fruits	[7, 79]
Compounds from endophytic fungi associated with Xanthium species			
293	Alternuisol	*X. italicum* leaves	[1]
294	Alternariol	*X. italicum* leaves	[1]
295	Brefeldin A	*X. occidentale* leaves	[97]
296	α,β-Dehydrocurvularin	*X. occidentale* leaves	[97]
297	Euajavanicol A	*X. sibiricum* roots	[98]
298	Eupenicinicol A	*X. sibiricum* roots	[98]
299	Eupenicinicol C	*X. sibiricum* roots	[98]
300	Eupenicinicol D	*X. sibiricum* roots	[98]

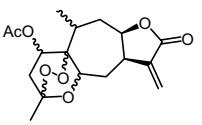

1

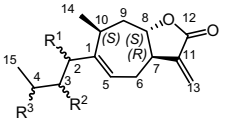

2 R^1 = O, R^2, R^3 = $\Delta^{3,4}$
5 R^1 = R^3 = α-OH, R^2 = H
6 R^1 = R^3 = OH, R^2 = H
10 R^1 = R^2 = H, R^3 = OH
21 R^1 = α-OH, R^2 = H, R^3 = β-OAc
22 R^1 = α-OAc, R^2 = H, R^3 = β-OH
23 R^1 = β-OAc, R^2 = H, R^3 = O
36 R^1 = OH, R^2 = H, R^3 = OI
37 R^1 = R^2 = H, R^3 = OH
38 R^1 = R^2 = H, R^3 = O
39 R^1 = OH, R^2 = H, R^3 = OAc
50 R^1 = O, R^2 = H, R^3 = OAc
70 R^1 = R^2 = $\Delta^{2,3}$, R^3 = O
72 R^1 = R^2 = H, R^3 = O
73 R^1 = α-OAc, R^2 = H, R^3 = α-OH
74 R^1 = H, R^2 = R^3 = OH

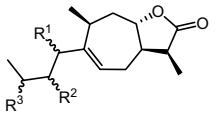

11 R^1 + R^2 = $\Delta^{2,3}$, R^3 = OH
12 R^1 + R^2 = $\Delta^{2,3}$, R^3 = O
14 R^1 = R^2 = H, R^3 = O
17 R^1 = R^2 = H, R^3 = OH

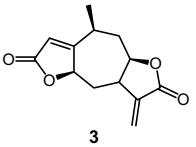

3

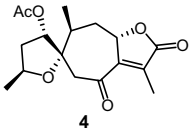

4

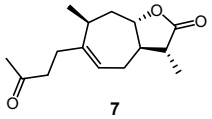

7

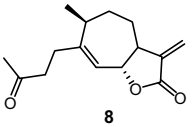

8

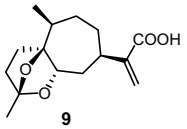

9

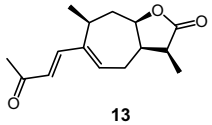

13

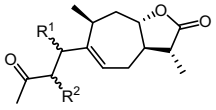

15 R^1 = R^2 = H
18 R^1 + R^2 = $\Delta^{2,3}$

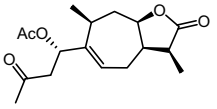

16

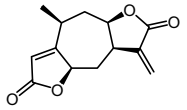

19

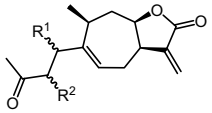

20 R^1 = β-OAc, R^2 = H
24 R^1 + R^2 = $\Delta^{2,3}$
34 R^1 = α-OH, R^2 = H
71 R^1 = R^2 = H
77 R^1 = α-OAc, R^2 = H

Fig. 2 Sesquiterpenoids from the genus *Xanthium*

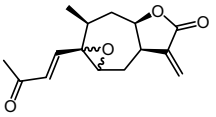

25 1α,5α-epoxide
26 1β,5β-epoxide

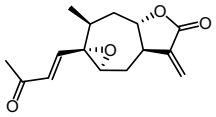

27 1α,5α-epoxide
28 1β,5β-epoxide

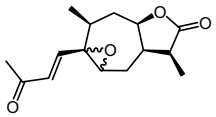

29 1α,5α-epoxide
30 1β,5β-epoxide

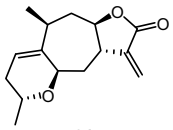

31

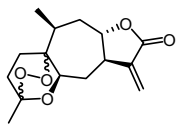

32

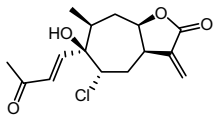

33

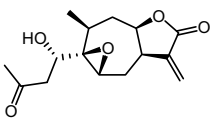

35

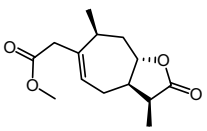

42

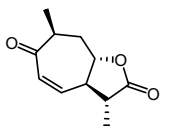

43

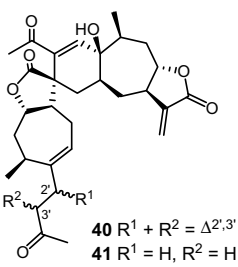

40 $R^1 + R^2 = \Delta^{2',3'}$
41 R^1 = H, R^2 = H

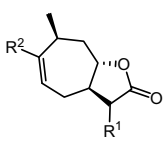

44 $R^1 = \beta$-CH_3, R^2 = COOH
45 $R^1 = \alpha$-CH_3, R^2 = COOH
46 $R^1 = \alpha$-CH_3, R^2 = CHO

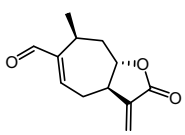

47

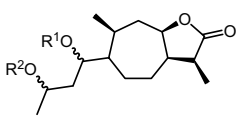

48 $R^1 = \beta$-Glc, R^2 = H
49 R^1 = H, $R^2 = \beta$-Glc

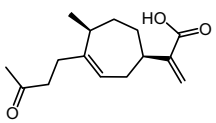

51

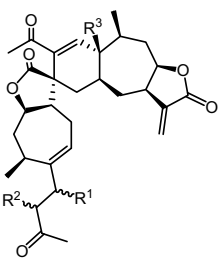

52 $R^1 + R^2 = \Delta^{2',3'}$, R^3 = OH
54 $R^1 + R^2 = \Delta^{2',3'}$, R^3 = H
56 $R^1 = R^2 = R^3$ = H
61 $R^1 = R^2$ = H, R^3 = OAc
62 $R^1 = R^2 = R^3$ = H

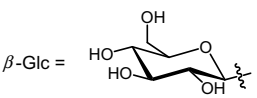

Fig. 2 (continued)

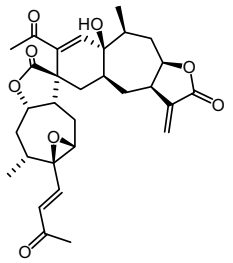

53

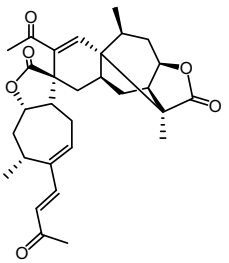

55

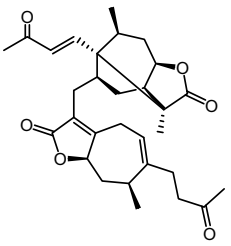

57

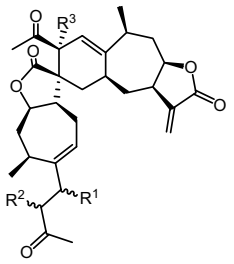

58 $R^1 = R^2 = R^3 = H$
59 $R^1 + R^2 = \Delta^{2',3'}$, $R^3 = OH$
60 $R^1 = R^2 = H$, $R^3 = OH$

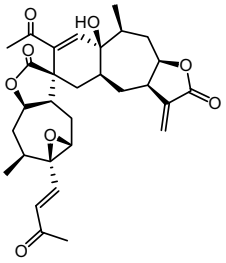

63

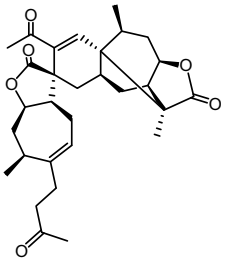

64

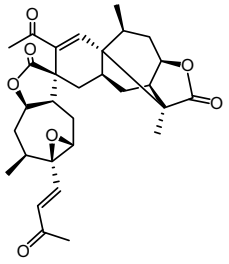

65

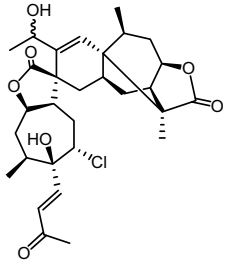

66

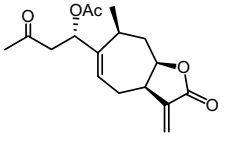

67

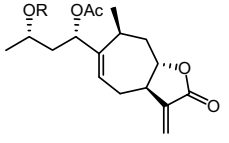

68 R = H
69 R = Ac

Fig. 2 (continued)

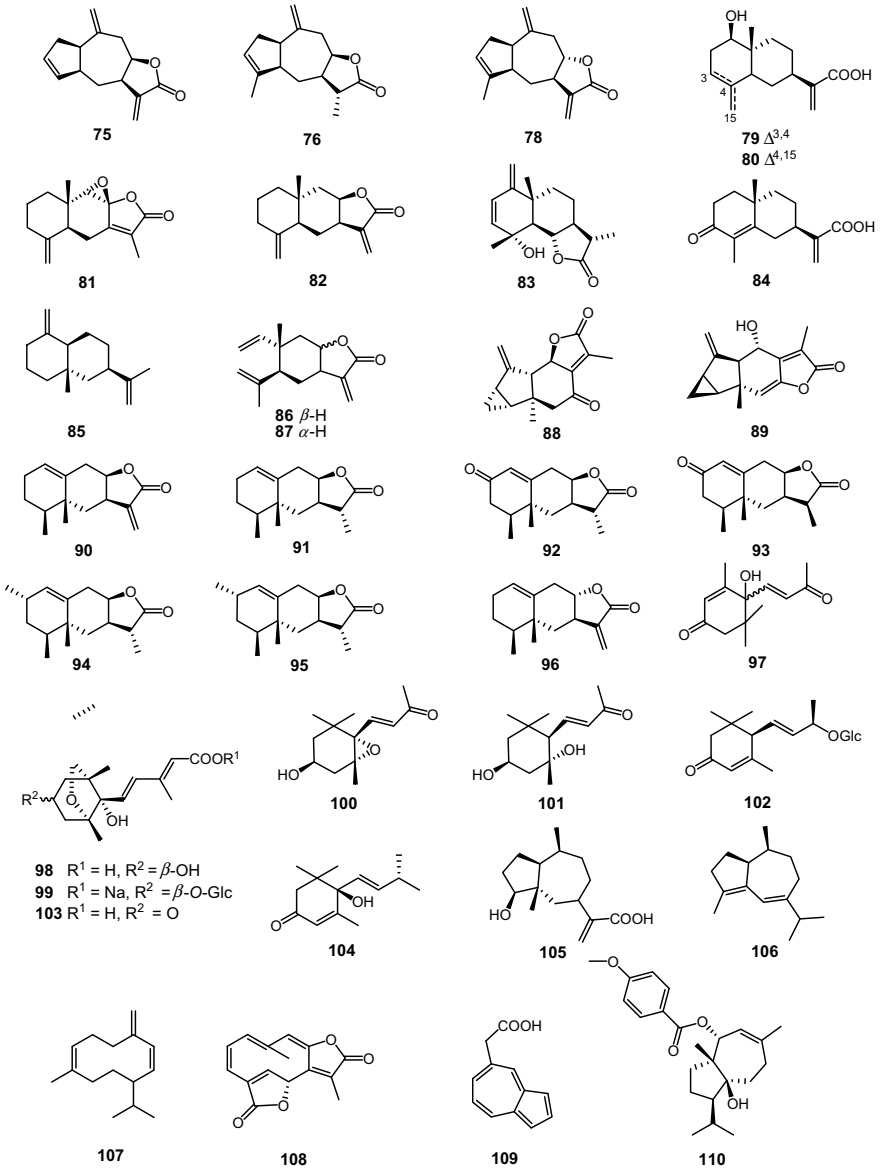

Fig. 2 (continued)

whereas (*S*)- or (*R*)-configurations can be found at C-7 and C-8. *Xanthium* xanthanolides are also substituted with an aliphatic side chain at C-1, a double bond (or oxirane ring) at C-1 and C-5, and an *exo*-methylene (or methyl group) at C-11. Numerous compounds, such as 4-*epi*-isoxanthanol (**21**), 4-*epi*-xanthanol (**22**), 8-*epi*-xanthatin (**24**), 8-*epi*-xanthatin-1β,5β-epoxide (**26**), 1α,5α-epoxyxanthatin (**27**), 2-hydroxytomentosin (**34**), 4-oxo-bedfordia acid (**51**), tomentosin (**67**), xanthatin (**70**), xanthinin (**71**), xanthinosin (**72**), and xanthumin (**77**), have been isolated frequently and occur abundantly. As a representative example, xanthumin (**77**) is a major secondary metabolite from *Xanthium* species, and it has been reported to be present in *X. cavanillesii* aerial parts, *X. macrocarpum* leaves and fruits, *X. mongolium* aerial parts and whole plants, *X. orientale* aerial parts and whole plants, *X. sibiricum* roots and aerial parts, *X. spinosum* epigeal parts, leaves, aerial parts, and whole plants, *X. strumarium* burs, leaves, fruits, aerial parts, and whole plants [15, 16, 26, 28–32, 38, 39, 43, 45–47, 49, 52–59]. It should be noted that while Ref. [49] refers to "*Xanthium mogolium* Kitag", according to several plant taxonomic databases its correct species name is "*mongolium*".

Using silica gel CC, TLC, and HPLC for compound purification, the novel xanthanolide, 2-acetoxy-4,5-epoxyxanthanolide-1,4-endoperoxide (**1**), was isolated from an Et_2O-MeOH-CH_2Cl_2 (1:1:1) extract of *X. pungens* aerial parts [25]. Besides several known secondary metabolites, the 90% MeOH extract of *X. spinosum* aerial parts was found to contain two new xanthanolides, anhydrodehydroivalbin (**2**) and cyclospinosolide (**4**), while a new analog, 4-*O*-dihydroinusoniolide (**10**), was isolated from the 90% MeOH extract of *X. strumarium* aerial parts [26]. A combined silica gel CC and HPLC procedure led to the isolation of two new xanthanolides, bis-norxanthanolide (**3**) and 11αH,13-dihydroxanthumin (**16**) from a $CHCl_3$ extract of *X. cavanillesii* aerial parts [27]. Deacetylxanthanol (**5**) was documented to occur in *X. orientale* whole plants and *X. strumarium* leaves and aerial parts [11, 26, 28], while three new naturally occurring xanthanolides, deacetylxanthiuminol (**6**), 1α,5α-epoxy-1,5-dihydroxanthatin (**27**), and 1α,5β-epoxy-1,5-dihydroxanthatin (**28**), were detected in *X. spinosum* aerial parts for the first time [29].

Xanthium sibiricum is an annual herb that has been listed in traditional Chinese medicine for the treatment of various diseases, such as leukoderma, scrofula, headache, and cancer [30]. A phytochemical investigation of the 95% EtOH extract of its roots has resulted in the isolation and NMR structure determination of four known xanthanolide derivatives, namely, 2-deacetyl-11β,13-dihydroxyxanthinin (**7**), 2-desoxy-6-*epi*-parthemollin (**8**), 11α,13-dihydro-4*H*-xanthalongin (**14**), and 11β,13-dihydroxanthatin (**18**), and in particular, the six new analogs norxanthantolides A–F (**42**–**47**) [30]. Repeated chromatographic purification over silica gel columns of a petroleum ether-Et_2O-MeOH (1:1:1) extract of *X. strumarium* aerial parts yielded three new xanthanolides, 1β,4β,4α,5α-diepoxyxanthat-11(13)-en-12-oic acid (**9**), 11α,13-dihydroxanthatin (**12**), and 4β,5β-epoxyxanthatin-1α,4α-endoperoxide (**32**) [31]. Likewise, in searching for potential anticancer agents from *X. strumarium* species, two new xanthanolides, 11α,13-dihydroxanthinin (**14**), and 11α,13-dihydroxanthuminol (**17**) were obtained from a MeOH extract of its leaves

[11]. The MeOH extract of the aerial parts of the medicinal plant *X. cathartium* has been subjected to chromatographic separation. Besides several known compounds, three new xanthanolides, 11α,13-dihydro-8-*epi*-xanthatin (**13**), 1α,5α-epoxy-1,5,11α,13-tetrahydro-8-*epi*-xanthatin (**29**), and 1α,5β-epoxy-1,5,11α,13-tetrahydro-8-*epi*-xanthatin (**30**), were characterized [33]. A phytochemical study of the petroleum ether-Et_2O (1:1) extract of *X. indicum* aerial parts led to the isolation of 13 xanthanolides, two of which, 2-*epi*-xanthumin (**20**) and 8-*epi*-xanthatin-1β,5β-epoxide (**26**), were isolated from Nature for the first time [36]. 8-*epi*-Xanthatin-1α,5α-epoxide (**25**) and 1β-hydroxy-5α-chloro-8-*epi*-xanthatin (**33**) are two hitherto unreported metabolites that were isolated from a crude MeOH extract of *X. sibiricum* aerial parts [9]. The chemical shifts of the unique 5-CHCl group of **33** were found at δ_H 4.05 (X-part of ABX system, $J_{app.} = 7.5$ Hz) and δ_C 65.4 ppm ($CDCl_3$) [9]. 2-Hydroxy-tomentosin (**34**) could be identified in several *Xanthium* species, but its 1β,5β-epoxide **35** proved to be undocumented in the prior literature and was purified from a petroleum ether-Et_2O (2:1) extract of *X. strumarium* aerial parts [41]. 2-Hydroxyxanthinosin (**36**) and 4-hydroxyxanthinosin (**37**), two metabolites of xanthinosin (**72**), are characteristic of *X. macrocarpum* aerial parts [15]. Both isoxanthanol (**39**) and xanthanol (**68**) were separated from *X. spinosum* and *X. strumarium* [26, 41, 48], but to date, xanthanol acetate (**69**) has been found only in *X. cavanillesii* aerial parts [46]. Based on NMR and MS structure elucidation procedures, three compounds isolated from *X. spinosum* species, 2-*O*-β-D-glucopyranosyl-11α,13-dihydro-8-*epi*-deacetylxanthiuminol (**48**), 4-*O*-β-D-glucopyranosyl-11α,13-dihydro-8-*epi*-deacetylxanthiuminol (**49**), and 2-oxo-4-*O*-acetyl-desacetylxanthanol (**50**), were determined as three new xanthanolides [43, 50]. In efforts to find bioactive compounds from the genus *Xanthium*, xanthipungolide (**73**) was obtained as a newly isolated compound from *X. pungens* aerial parts, and it was then also detected in the aerial parts of *X. brasilicum* [25, 35]. The novel xanthanolide, xanthnon (**74**) is present in *X. sibiricum* aerial parts, whereas the two novel analogs, xantholides A (**75**) and B (**76**), were determined as constituents of *X. canadense* roots [47, 63].

Of particular interest, phytochemical work on *Xanthium* species demonstrated the occurrence of members of an unusual class of dimeric xanthanolides. Thus, by a combination of NMR analysis and ECD measurements, the chemical structures of mongolides D (**40**) and E (**41**) were elucidated as two uncommon dimeric xanthanolides, isolated from *X. mongolium* dried aerial parts [49]. These two compounds only differed at C-2′ and C-3′ (Fig. 2). Similarly, new analogs **52**–**66** were isolated, in which pungiolides A–C (**52**–**54**), pungiolides D (**55**) and E (**56**), and pungiolides F–O (**57**–**66**) have been obtained and characterized from *X. pungens*, *X. sibiricum*, and *X. chinense*, respectively, for the first time [8, 9, 25, 51].

Eudesmanolides

Phytochemical investigations of *Xanthium* species have shown eudesmanolides as a second prominent group of *Xanthium* sesquiterpenoids. A listing of 11 of these secondary metabolites (**79**–**89**) is provided in Table 1 [25, 30, 36, 45,

64]. Besides representatives of the xanthanolides, *X. pungens* also accumulates high concentration levels of eudesmanolides, and 12-carboxyeudesma-3,11(13)-diene (**79**), (2*R*,4α*R*,5*R*,8α*S*)-decahydro-5-hydroxy-4α-methyl-8α-bis(methylene)-2-naphthaleneacetic acid (**80**), judaicin (**83**), and 3-oxocostusic acid (**84**) have been found only in this species [25]. Isoalantolactone (**82**) and β-selinene (**85**) occur in several *Xanthium* species, but two well-known compounds, seucoeudesmanolide (**86**) and 8α-seucoeudesmanolide (**87**), were isolated only from *X. indicum* aerial parts thus far [36, 45, 64]. Phytochemical work on a 95% EtOH extract of the fruits of *X. sibiricum* coupled with NMR spectroscopic interpretation established sibirolides A (**88**) and B (**89**) as two new naturally occurring 3/5/6/5 tetracyclic eudesmane sesquiterpene lactones [30].

Eremophilanolides

Eremophilanolides are the third most common class of sesquiterpenes isolated from the genus *Xanthium.* Herein is compiled a list of seven *Xanthium* eremophilanolides **90**–**96** (Table 1 and Fig. 2) [37, 42, 64, 65]. Significantly, most of them were characterized as new isolates not described before in the literature, except for compound **96**. Eremophil-1 (**10**), 11(13)-dien-12,8β-olide (**90**), and (11*R*)-eremophil-1(10)-en-12,8β-olide (**91**) were isolated from *X. canadense* roots initially, and found later in *X. sibiricum* aerial parts [42, 64]. Four isomers, which were named sibiriolides A–D (**92**–**95**), were newly isolated compounds from a 95% EtOH extract of *X. sibiricum* aerial parts [42, 65].

Megastigmanes

A further subclass of sesquiterpenoids isolated from the genus *Xanthium* to be mentioned are the megastigmane derivatives (**97**–**104**) [39, 45, 51, 54, 66, 67]. These compounds, present in both the free form and as glycosides, have been found in five *Xanthium* species, namely, *X. chinense*, *X. mongolicum*, *X. sibiricum*, *X. spinosum*, and *X. strumarium* (Table 1 and Fig. 2). Thus, dehydrovomifoliol (**97**) was detected in *X. mongolicum* whole plants and *X. spinosum* leaves, and dihydrophaseic acid sodium salt 4′-*O*-β-D-glucopyranoside (**99**), (3*S*,5*R*,6*S*,7*E*)-5,6-epoxy-3-hydroxy-7-megastigmene-9-one (**100**), grasshopper ketone (**101**), (6*R*,9*S*)-3-*oxo*-α-ionol β-D-glucopyranoside (**102**), phaseic acid (**103**), and (6*S*,9*R*)-vomifoliol (**104**) have been obtained from plants of the genus *Xanthium.* In particular, compound **98** as obtained from *X. sibiricum* fruits, proved to be a new derivative of compound **103**, and its absolute configuration was assigned unambiguously as (2*E*,4*E*,1′*S*,2′*R*,4′*S*,6′*R*) by means of X-ray diffraction analysis [66].

Guaianolides, Germacranolides, and Other Sesquiterpenoids

Xanthium sesquiterpenoids have representatives of the guaianolides (**105**–**106**), germacranolides (**107** and **108**), and of other sesquiterpenoid classes (**109** and **110**) [25, 28, 30, 33, 36, 45, 47]. This is the first time that isoguaiene (**106**), germacrene D (**107**), linderanlide C (**108**), and 5-azulene acetic acid (**109**) have been detected within the genus *Xanthium.* Besides sesquiterpene lactone-type xanthanolides, an Et_2O-MeOH-CH_2Cl_2 (1:1:1) extract of the *X. pungens* aerial parts also contained a new guaianolide, 4β-hydroxypseudoguaia-11(13)-en-12-oic acid (**105**) [25]. Likewise, the daucane sesquiterpene lasidiol *p*-methoxybenzoate (**110**) was isolated initially from *X. catharticum* roots and subsequently found in the whole plants of *X. mongolicum* and *X. orientale* [28, 33, 45].

2.1.2 Monoterpenoids

The genus *Xanthium* is also a source of monoterpenoids. A list of 13 compounds of this type (**111**–**123**) is given in Table 1, with their structures shown in Fig. 3 [6, 12, 39, 54, 66, 68]. Of the monoterpenoids of *Xanthium* species, geranyl derivatives represent the main type, with or without glycosylation at the terminal carbons. Members of this class occur in the aerial parts of *X. chinense*, *X. sibiricum*, *X. spinosum*, and *X. strumarium.* Applying a sequential separation protocol with macroporous resin D101, polyamide (30–60 mesh), and reversed-phase ODS HPLC and HPLC for isolation, two new monoterpenoid glycosides, (*E*)-2-methyl-6-methyleneocta-2,7-dien-1-ol β-D-apiofuranosyl-(1 → 6)-β-D-glucopyranoside (**115**) and (*Z*)-2-methyl-6-methyleneocta-2,7-dien-1-ol β-D-apiofuranosyl-(1 → 6)-β-D-glucopyranoside (**116**), in addition to three known compounds, geranyl 6-*O*-β-D-apiofuranosyl-β-D-glucopyranoside (**111**), myrtenol 6-*O*-β-D-apiofuranosyl-β-D-glucopyranoside (**119**), and neryl 6-*O*-β-D-apiofuranosyl-β-D-glucopyranoside (**120**), were isolated from the 95% EtOH extract of *X. chinense* fruits [6]. A phytochemical study of a 70% EtOH extract of *X. sibiricum* fruits led to the isolation and spectroscopic determination of a pair of new diastereomers, (6*E*)-3-hydroxymethyl-7-methylocta-1,6-dien-3-ol 8-*O*-β-D-glucopyranoside (**112**) and (6*Z*)-3-hydroxymethyl-7-methylocta-1,6-dien-3-ol-8-*O*-β-D-glucopyranoside (**113**), along with a new analog, 3β-norpinan-2-one 3-*O*-β-D-apiofuranosyl-(1 → 6)-β-D-glucopyranoside (**121**) [68]. A further study of *X. sibiricum* fruits identified a pair of enantiomeric monoterpenoids, namely, (+)- and (–)-(5*Z*)-6-methyl-2-ethenyl-5-hepten-1,2,7-triol (**117**) and (**118**) [66]. The well-known monoterpenoid loliolide (**114**) is one of the chemical constituents of *X. spinosum* leaves and *X. strumarium* fruits [39, 54], and two new geranyl derivatives, xanmonoters A (**122**) and B (**123**) were reported in *X. strumarium* fruits [12].

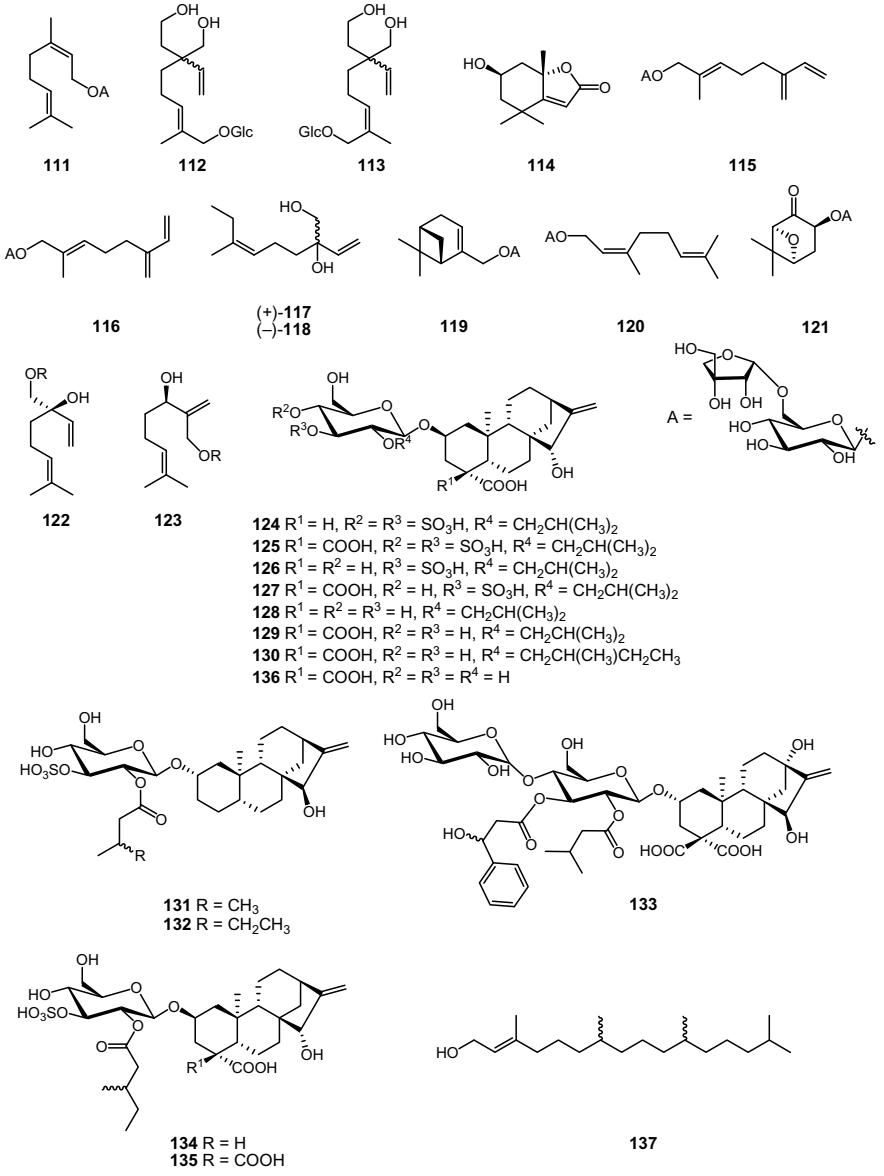

Fig. 3 Monoterpenoids, diterpenoids, and triterpenoids from the genus *Xanthium*

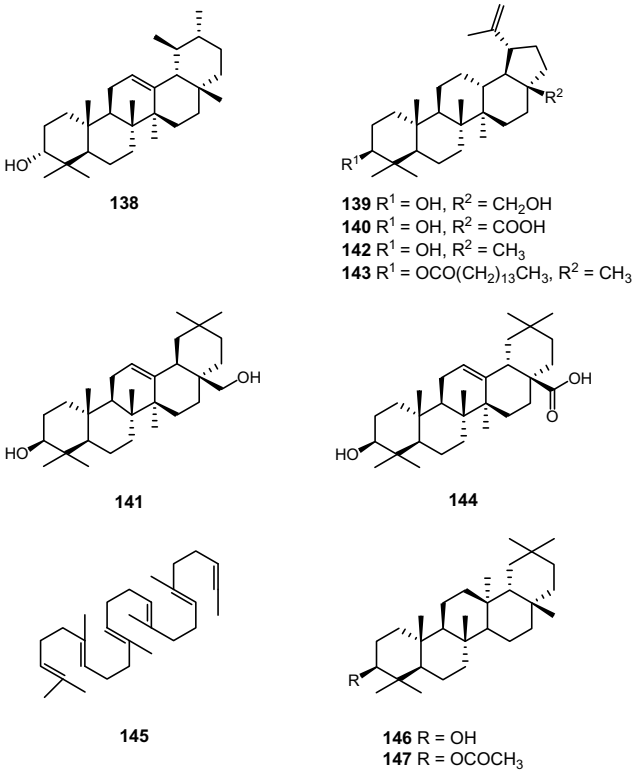

Fig. 3 (continued)

2.1.3 Diterpenoids

Diterpenoids are a further class of terpenoids to have been isolated from *Xanthium* species. From the literature, in Table 1 the chemical structures of 14 compounds (**124**–**137**) are compiled [6, 36, 50, 69–72]. All of these compounds were isolated from the aerial parts of *Xanthium* species. Except for phytol (**137**), the remaining compounds **124**–**136** are formed by glycosylation at C-2 of an *ent*-kaurane diterpene nucleus (Fig. 3). On occasion, esterification at C-2, as well as sulfation at C-3 and C-4 of the glycosyl moieties occurs. Thus, atractyloside (**124**) and carboxytractyloside (**125**) are the main diterpenoid constituents in several *Xanthium* species, but their 4′-desulfated derivatives **126** and **127** are two new secondary metabolites that were characterized from the aerial parts of *X. spinosum* [6, 50, 69–71]. 3′,4′-Desulfated atractyloside (**128**) is a known compound, but 3′,4′-didesulfated carboxytractyloside (**129**) and its 3′,4′-didesulfated carboxytractyloside derivative (**130**), which were first isolated from the burs of *X. pungens*, constitute two further new natural products [71]. The 70% aqueous EtOH extract of *X. strumarium* fruits was found to contain three new rearranged *ent*-kauranoid glycosides, fructusnoids A–C (**131**–**133**). Fructusnoids D

(**134**) and E (**135**), isolated from the 95% EtOH extract of *X. chinense* fruits [6], show the same structural pattern as compounds **131** and **132**. 2β-*O*-β-D-Glucopyranosyl-15α-hydroxy-kaur-16-en-18,19-dicarboxylic acid (**136**) is similar to isolates **124**–**130**, which were isolated from the MeOH residue of *X. spinosum* aerial parts [50].

2.1.4 Triterpenoids

Triterpenoids are a class of compounds displaying a wide range of structural types. Members of this class, comprising the isolated compounds **138**–**147**, have been found in several species of the genus *Xanthium*, such as *X. canadense*, *X. orientale*, *X. sibiricum*, and *X. strumarium* (Table 1 and Fig. 3) [5, 13, 28, 58, 64, 74, 75]. α-Amyrin (**138**) and squalene (**145**) have been observed in the leaves of *X. strumarium* [13, 58], whereas betulin (**139**) and betulinic acid (**140**) were detected in both *X. orientale* whole plants and *X. sibiricum* roots [5, 28]. Lupeol (**142**) and oleanolic acid (**144**) are triterpenes found in *X. orientale* whole plants, while the roots and the leaves of *X. sibiricum* also contain erythrodiol (**141**) and lupeol palmitate (**143**), respectively [5, 28, 75]. Taraxerol (**146**) and its monoacetate (**147**) are distributed widely among various plant genera, but in *Xanthium*, they were only found in *X. canadense* roots [64].

2.2 Simple Phenols

Accumulating evidence has shown that monophenolic compounds with simple structural patterns are a significant characteristic of *Xanthium* plants. A detailed list of 66 isolated compounds (**148**–**183**) is shown in Table 1 and their formulas are represented in Fig. 4 [5, 7, 13, 30, 34, 45, 51, 54, 67, 71, 76–84]. Secondary metabolites with substitutions of caffeoyl units at sugar carbons, such as in compounds **152**–**163**, are the main representatives of this class. For example, Lee et al. have isolated ten simple phenols, including 2,4-bis(4-hydroxybenzyl)phenol (**148**), caffeic acid (**149**), coniferaldehyde (**157**), 2,4′-dihydroxyphenyl methane (**164**), 4,4′-dihydroxydiphenyl methane (**165**), *p*-hydroxybenzaldehyde (**172**), methyl caffeate (**175**), 3-methyl-4,4′-dihydroxydiphenyl methane (**179**), vanillin (**182**), and vanillic acid (**183**), from a MeOH extract of *X. strumarium* seeds [34]. Further chromatographic separations on *X. strumarium* roots also led to the identification of various additional known simple phenolic compounds, such as 5-*O*-caffeoylquinic acid (**153**), 5-*O*-caffeoylquinic acid methyl ester (**154**), 1,4-di-*O*-caffeoylquinic acid (**159**), 1,5-di-*O*-caffeoylquinic acid (**160**), 3-hydroxy-1-(4-hydroxy phenyl)-propan-1-one (**170**), methyl-3,5-di-*O*-caffeoylquinate (**177**), potassium 3-*O*-caffeoyl quinate (**180**), and protocatechuic acid (**181**) [7, 76, 77, 79]. Such phenolic compounds further occur in *X. cavanillesii*, *X. chinense*, *X. mongolicum*, *X. occidentale*, and *X. sibiricum*. For instance, caffeic acid choline ester (**150**) and 2,3-dihydroxy-1-(4-hydroxy-3-methoxyphenyl)-propan-1-one (**166**) were found to be present in *X. sibiricum* fruits

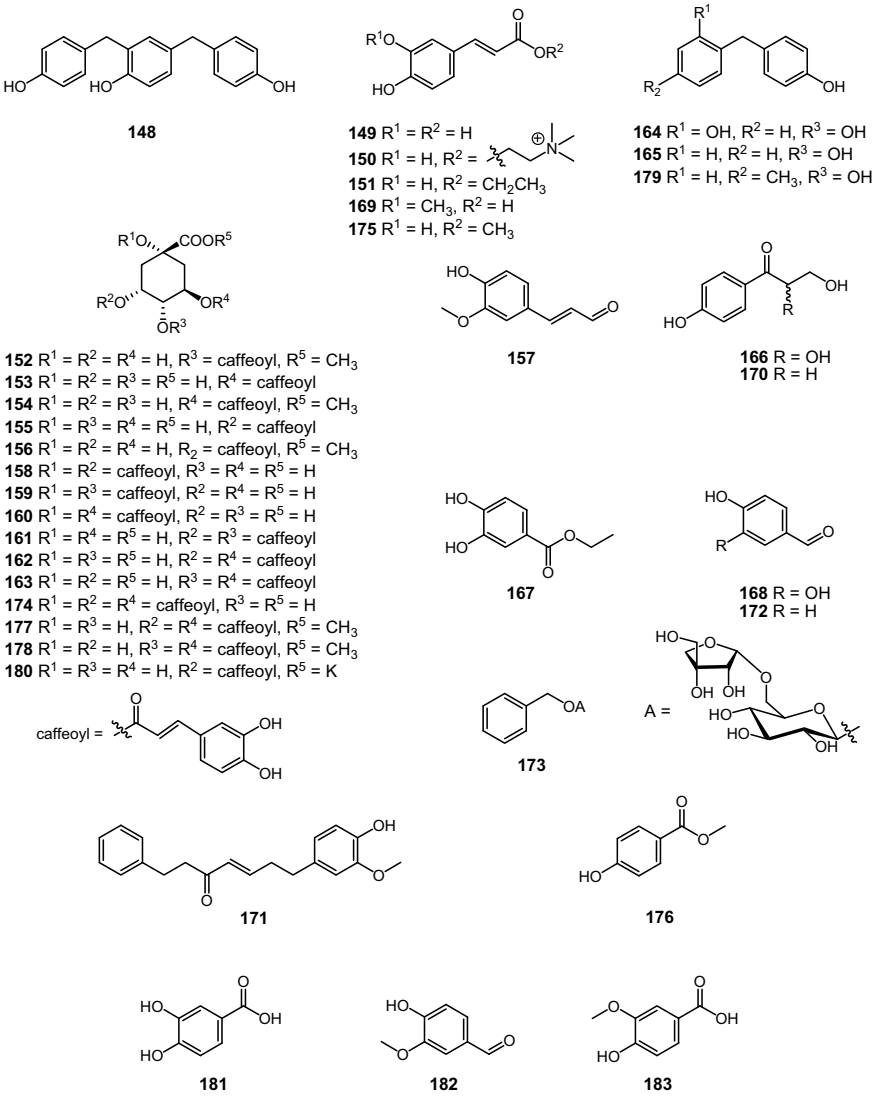

Fig. 4 Simple phenols from the genus *Xanthium*

[66, 67], while the roots of this species contained caffeic acid ethyl ester (**151**), 3,4-dihydroxybenzoic acid ethyl ester (**167**), and 7-(4-hydroxy-3-methoxyphenyl)-1-phenylhept-4-en-3-one (**171**) [5, 30]. Besides their presence in *X. sibiricum* fruits, 4-*O*-caffeoyl quinic acid methyl ester (**152**) and chlorogenic acid methyl ester (**156**) have been isolated from *X. chinense* fruits [51, 67, 71]. Phytochemical analysis of an ethanol extract of *X. cavanillesii* fruits yielded 5-di-*O*-caffeoylquinic acid (**162**), 4,5-di-*O*-caffeoylquinic acid (**163**), and 1,3,5-tri-*O*-caffeoylquinic acid (**174**) [82].

In the genus *Xanthium*, the compound methyl *p*-benzoate (**176**) has only been found in *X. mongolicum* whole plants [45].

2.3 Sulfur-Containing Compounds

The plants of genus *Xanthium* have so far been found to possess sulfur-containing compounds with the main types being xanthiazones (**184–199**) [7, 10, 34, 51, 68, 77, 80, 85–90], xanthienopyrans (**200–202**) [10, 34, 54, 66, 86, 91], and a thiophene (**203**) [10, 66]. All of these metabolites (Fig. 5) have been first isolated for the first time from members of the genus *Xanthium*, except for compound **200** (Fig. 2). As shown in Table 1, sulfur-containing compounds occur occasionally in *X. chinense* and *X. pungens* but are more frequently observed in *X. sibiricum* and *X. strumarium.* Generally, *Xanthium* xanthiazones display substitutions of the hydroxy group at C-2 and the saccharide or pyrrolidinone moieties at C-7 (Fig. 2). Glucopyranosyl and apiofuranosyl-(1 → 6)-*O*-D-glucopyranosyl groups can be seen as characteristic of glycone units of *Xanthium* xanthiazones. The fruits of *X. sibiricum* species contain the four new xanthiazones 2-hydroxy-xanthiazone (**184**), 7-hydroxymethyl-8,8-dimethyl-4,8-dihydrobenzo[1,4]-thiazine-3,5-dione-11-*O*-[*β*-D-apiofuranosyl-(1 → 6)-*O*-D-glucopyranoside] (**189**), xanthiazinone (**191**), and xanthiazinone D (**198**), as well as three new racemic natural products, (±)-xanthiazinone A (**192** + **193**), (±)-xanthiazinone B (**194** + **195**), and (±)-xanthiazinone C (**196 197**) [10, 68, 85–87]. These racemic mixtures were separated into their enantiomers by means of enantioselective HPLC, with the structures proved by X-ray crystallography. However, according to a recent publication, the chemical structure of xanthiazinone (**191**) had to be revised as (±)-xanthiazinone A (**192** + **193**) [10]. Four other new derivatives, 2-hydroxy-7-hydroxymethyl-8,8-dimethyl-4,8-dihydrobenzo[1,4]thiazine-3,5-dione-11-*O*-*β*-D-glucopyranoside (**185**), 7-hydroxymethyl-8,8-dimethyl-4,8-dihydrobenzo[1,4]-thiazine-3,5-dione (**186**), 7-hydroxymethyl-8,8-dimethyl-4,8-dihydrobenzo[1,4]thiazine-3,5-dione-11-*O*-*β*-D-glucopyranoside (**187**), and 7-hydroxymethyl-8,8-dimethyl-4,8-dihydrobenzo[1,4]thiazine-3,5-dione-(2-*O*-caffeoyl)-*β*-D-glucopyranoside (**188**) have been identified as constituents of *X. strumarium* fruits [77, 80, 89].

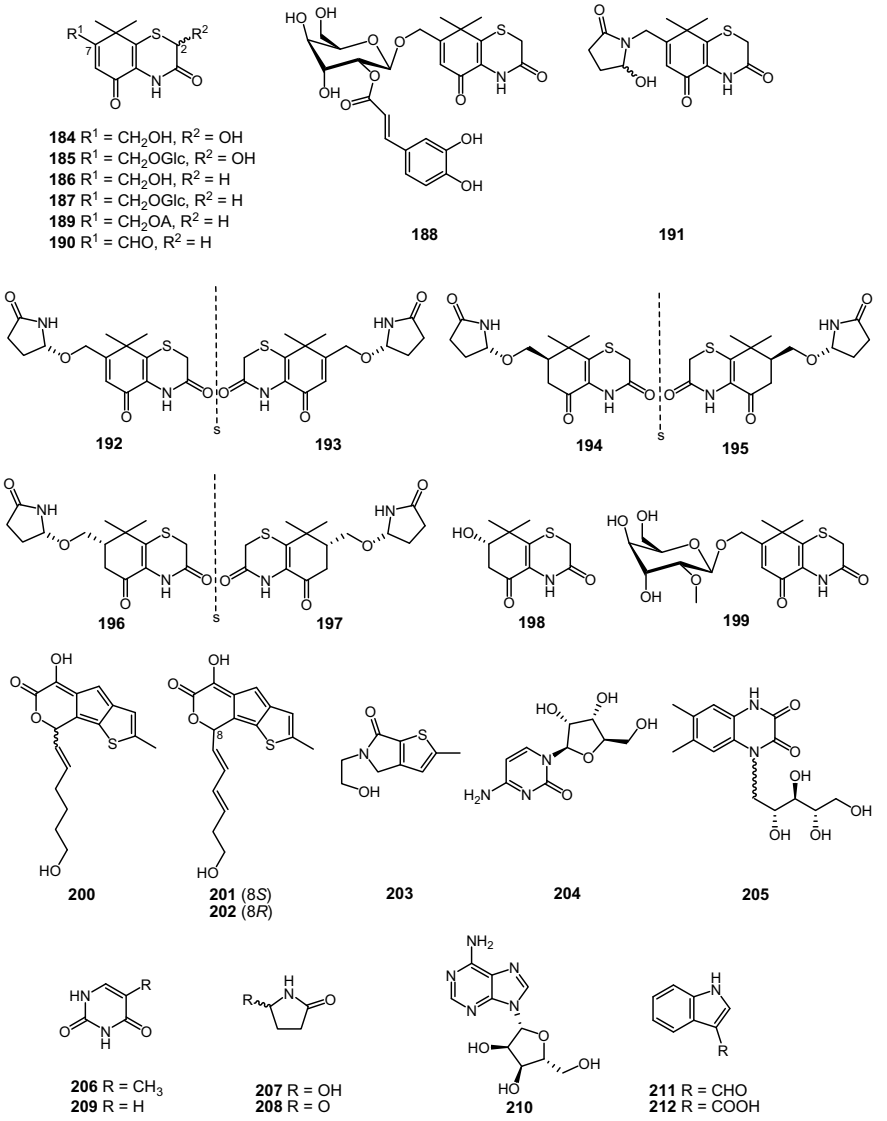

Fig. 5 Sulfur- and nitrogen-containing compounds from the genus *Xanthium*

In 2008, Lee et al. isolated the two new metabolites xanthialdehyde (**190**) and (–)-xanthienopyran (**202**) from *X. strumarium* seeds [34], while two new other compounds, xanthiside (**199**) and (+)-xanthienopyran (**201**), were detected in *X. pungens* fruits [91]. Being structurally related to thiophene, the new metabolite sibiricumthionol (**203**) was isolated from *X. sibiricum* fruits [10, 66].

2.4 Nitrogen-Containing Compounds

Nitrogen-containing compounds have been detected in the two plants *Xanthium strumarium* and *X. sibiricum.* As shown in Table 1 and Fig. 5, compounds **204**–**209** and **210**–**212** are from the classes of cyclic amides and nitrogen heterocyclic structural classes, respectively [7, 34, 67, 68, 92]. Utilizing RP-18 column chromatography for the final purification step, the nucleoside cytidine (**204**) was isolated from the EtOAc fraction of *X. strumarium* [7]. Bioassay-guided separation of the MeOH extract of *X. strumarium* seeds afforded 28 compounds, including succinimide (**208**) and the two nitrogen-containing heterocyclic compounds indole-3-carboxaldehyde (**211**) and indole-3-carboxylic acid (**212**) [34]. From *X. sibiricum* fruits, two nitrogen heterocyclic compounds *N*-(1′-D-deoxyxylitolyl)-6,7-dimethyl-1,4-dihydro-2,3-quinoxalinedione (**205**) and 5-hydroxypyrrolidin-2-one (**207**), and the nucleoside adenosine (**210**) were isolated [66, 86], whereas two other pyrimidine derivatives 5-methyluracil (**206**) and uracil (**209**) were found in the roots of this species [92].

2.5 Lignans

The genus *Xanthium* may be considered an abundant source of numerous lignan skeletons. Altogether, 38 secondary metabolites of this class (**213**–**250**) are included in Table 1 [5, 30, 34, 45, 54, 85, 93–95]. Lignans are found in two species, in particular, *X. strumarium* and *X. sibiricum*, and are differentiated by their main structural types, such as a benzofuran (**213**), a phenylpropanoid (**215**), a coumarino-lignoid in **217**, and a furofuran in **236** (Fig. 6). Based on comparison with the literature, 14 known lignans were isolated and identified from a 70% EtOH extract of *X. sibiricum* fruits, including balanophonin A (**214**), (1*S*,2*R*)-1,2-*bis*(4-hydroxy-3-methoxyphenyl)-1,3-propanediol (**215**), chushizisin E (**216**), (–)-(7*R*,8*S*)-dehydrodiconiferyl alcohol (**219**), (7*R*,8*S*)-dihydrodehydrodiconiferyl alcohol 4-*O*-*β*-D-glucopyranoside (**223**), diospyrosin (**224**), (–)-1-*O*-*β*-D-glucopyranosyl-2-{2-methoxy-4-[1-(*E*)-propen-3-ol]phenoxyl}-propane-3-ol (**229**), (−)-(2*R*)-1-*O*-*β*-D-glucopyranosyl-2-{2-methoxy-4-[(*E*)-formylviny1]phenoxyl-propane-3-ol (**230**),

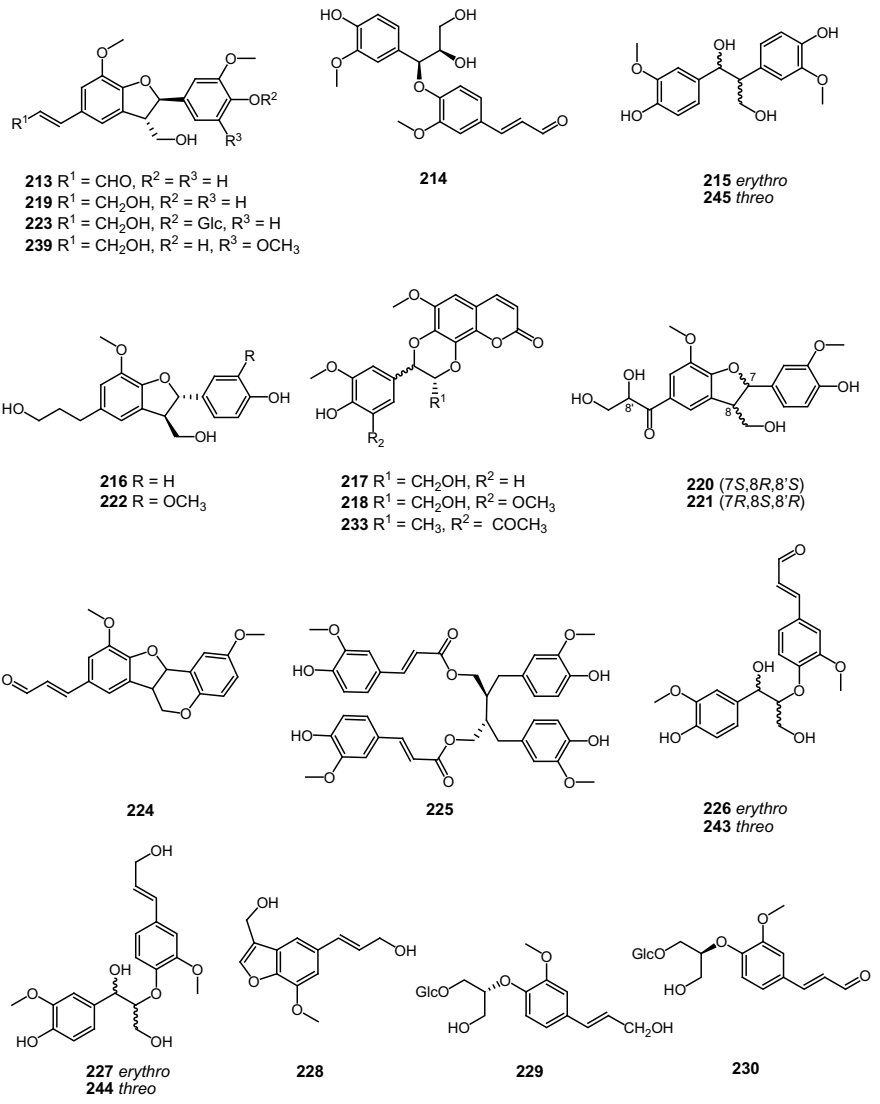

Fig. 6 Lignans from the genus *Xanthium*

1-(4-hydroxy-3-methoxy)-phenyl-2-[4-(1,2,3-trihydroxypropyl)-2-methoxy]-phenoxy-1,3-propandiol (**231**), 2-(4-hydroxy-3-methoxyphenyl)-3-(2-hydroxy-5-methoxyphenyl)-3-oxo-1-propanol (**232**), leptolepisol D (**234**), (–)-pinoresinol (**236**), (–)-simulanol (**239**), and *threo*-dihydroxy-dehydrodiconiferyl alcohol (**241**) [93]. Furthermore, a 70% EtOH extract of the roots of *X. sibiricum* contained cleomiscosins A (**217**) and C (**218**), (–)-9,9′-*O*-di-(*E*)-feruloyl-*seco*-isolariciresinol (**225**), jatrocin B (**233**), and syringaresinol (**240**) [92]. Of particular interest

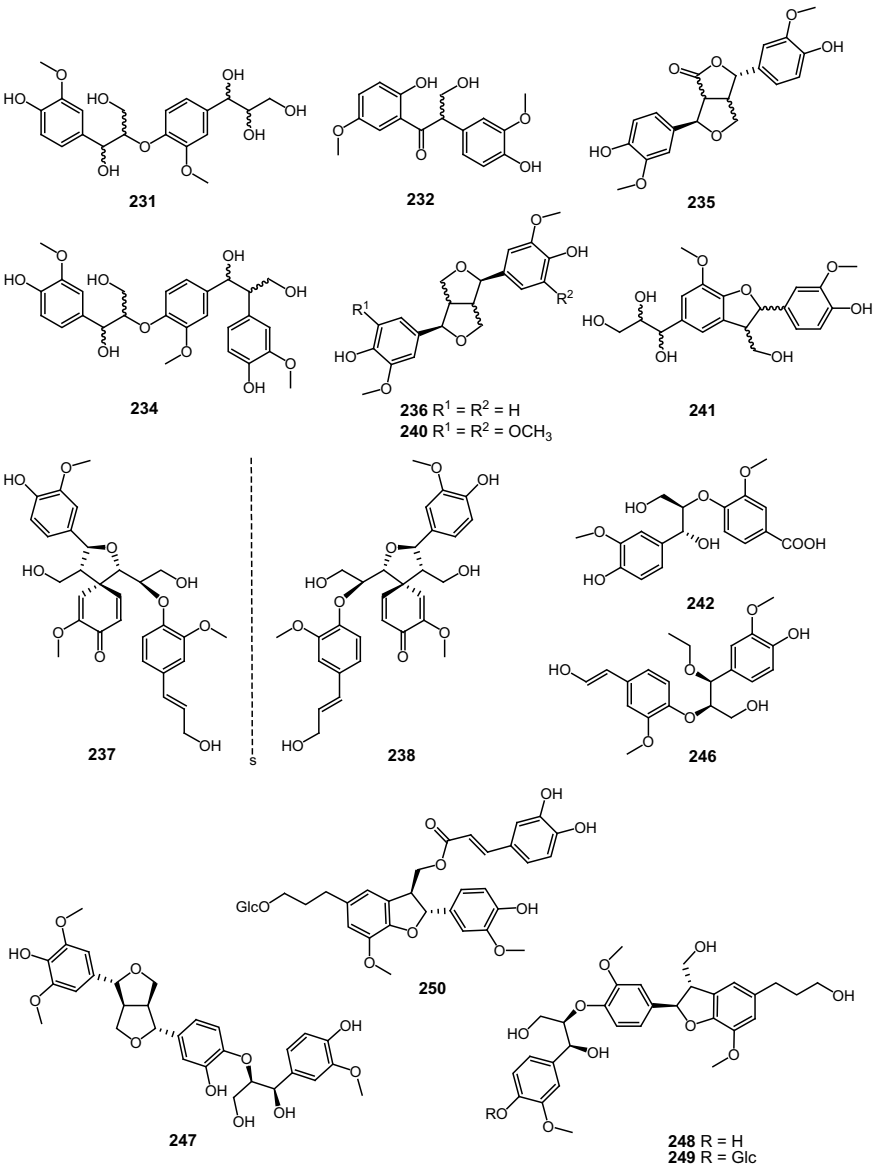

Fig. 6 (continued)

are the enantiomeric lignans of the benzofuran type. Thus, (+)- and (–)-7′-dehydrosismbrifolin (**220**) and (**221**) were isolated from a 95% EtOH extract of *X. sibiricum* fruits, whereas utilizing an enantioselective HPLC technique for the final step of the chromatographic process, a pair of rare sesquineolignans, (+)-(**237**) and (–)-sibiricumin A (**238**) were isolated from a 95% EtOH extract of *X. sibiricum* roots [30, 94]. In an ongoing phytochemical study by Chen et al., the benzofuran balanophonin (**213**) and the furofuran lignan (–)-pinoresinol (**236**) were detected in *X. strumarium* fruits [54]. The new benzofuran-type lignan, fructusol (**228**), in addition to the six known lignans (1*S*,2*R*)-1,2-*bis*(4-hydroxy-3-methoxyphenyl)-1,3-propanediol (**5**), (+)-(7*S*,8*R*)-dihydrodehydroconiferyl alcohol (*rel*-(2α,3β)-7-*O*-methylcedrusin) (**222**), *erythro*-guaiacylglycerol-β-coniferyl aldehyde ether (**226**), *erythro*-guaiacylglycerol-8-*O*-4′-(coniferyl alcohol) ether (**227**), *threo*-guaiacylglycerol-β-coniferyl aldehyde ether (**243**), *threo*-guaiacylglycerol-8-*O*-4′-(coniferyl alcohol) ether (**244**), and *threo*-1-phenyl-(4′-hydroxy-3′-methoxy)-2-phenyl-(4″-hydroxy-3″-methoxy)-1,3-propanediol (**245**), were isolated from the $CHCl_3$-MeOH (1:1) extract of *X. strumarium* seeds [85]. Using HPLC for chromatographic separations and interpretation of CD spectra to solve their stereochemistry thus led to the isolation and characterization of five new lignans, xanthiumnolics A–E (**246**–**250**) from a 70% aqueous EtOH extract of *X. strumarium* fruits [95].

2.6 Sterols

Steroids occur naturally in both plants or animals. Sterols and related compounds originating from plants when used as nutritional supplements may help to modulate cholesterol absorption in humans [99]. *Xanthium* species, especially the two taxa *X. strumarium* and *X. sibiricum*, are good sources of these compounds. By means of NMR analysis, 16 compounds (**251**–**266**) were assignable to the sterol group (Table 1 and Fig. 7) [5, 13, 28, 34, 45, 54, 58, 60, 71, 74, 75, 78]. Three common phytochemicals, daucosterol (**252**), β-sitosterol (**261**), and β-stigmasterol (**263**) have been isolated from *Xanthium* plants. For example, compound **261** has been found to occur in extracts of *X. mongolicum* whole plants, *X. orientale* aerial parts, *X. sibiricum* roots and fruits, and *X. strumarium* seeds, fruits, and aerial parts [5, 34, 45, 54, 60, 74, 78, 92]. In contrast to these three compounds, their derivatives 14-methyl-12,13-dehydro-sitosterol-heptadeconate (**251**), 7α-hydroxy-β-sitosterol (**256**), 6′-palmitoxyl-β-daucosterin (**259**), and stigmast-4-ene-3β,6α-diol (**265**) were obtained only from the leaves or the fruits of *X. strumarium* [13, 54]. It has been found that *X. sibiricum* is a major source of sterols. 5α,8α-*epi*-Dioxy-(22*E*)-ergosta-6,22-dien-3β-ol, also known as ergosterol peroxide (**253**), has been found to be present in both the roots and the stems of this species [45, 92]. In contrast, 6β-hydroxystigmast-4-en-3-one (**254**), 6β-hydroxystigmast-4,22-dien-3-one (**255**), 7-ketositosterol (**257**), 3-oxo-$\Delta^{(4,5)}$-sitostenone (**258**), β-sitostenone (**260**), and stigmast-4-en-6-ol-3-one (**266**) were purified only from the roots [5, 92]. The known compound β-stigmasteryl-β-D-glucoside (**264**) was initially detected in *X. sibiricum* stems, and then also observed in *X. strumarium* seeds [34, 75].

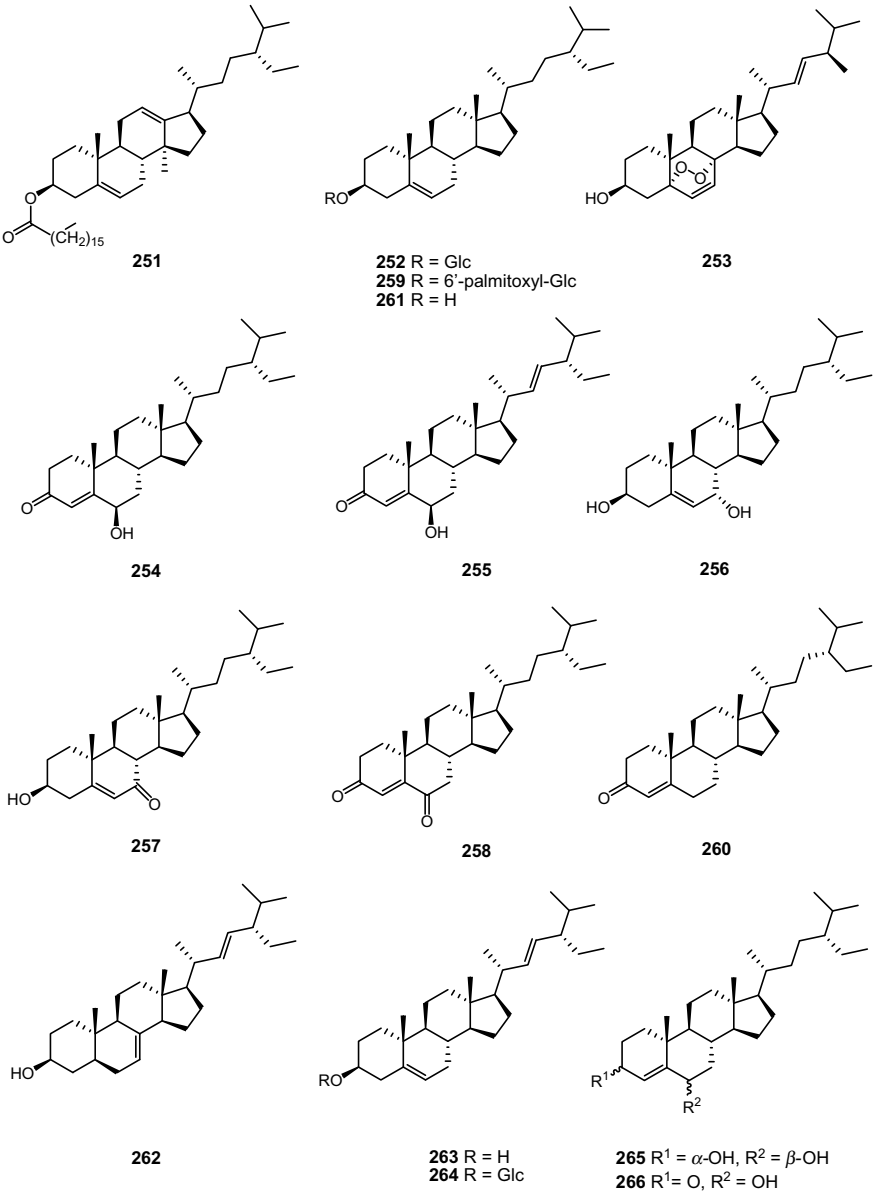

251

252 R = Glc
259 R = 6'-palmitoxyl-Glc
261 R = H

253

254

255

256

257

258

260

262

263 R = H
264 R = Glc

265 R^1 = α-OH, R^2 = β-OH
266 R^1= O, R^2 = OH

Fig. 7 Sterols from the genus *Xanthium*

2.7 *Flavonoids, Quinones, Coumarins, Fatty Acids, and Miscellaneous Compounds*

2.7.1 Flavonoids

Flavonoids are very widely distributed in the plant kingdom, e.g. Ref. [100]. Phytochemical work on *Xanthium* plants has shown the presence of isoflavones **267**–**269** and flavones **270**–**273** (Table 1 and Fig. 8) [7, 15, 45, 54, 71, 80]. Together with sulfur-containing compounds, the 75% aqueous EtOH extract of the ripe fruits of

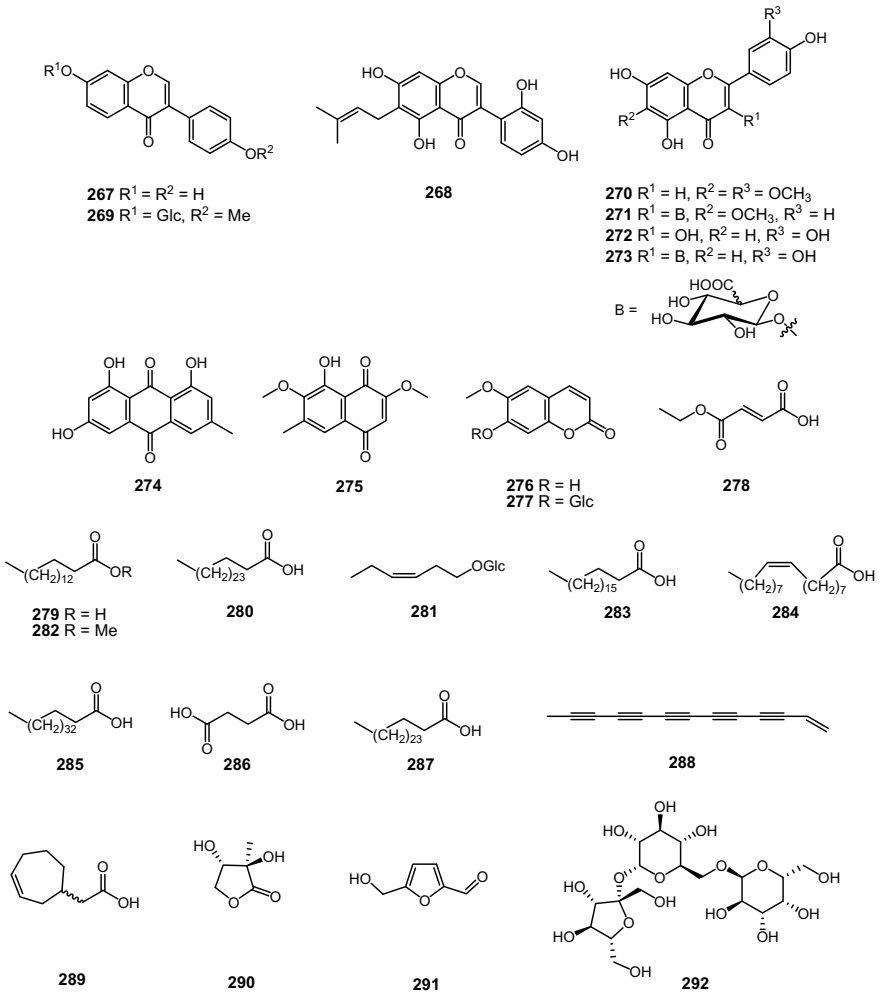

Fig. 8 Flavonoids, quinones, coumarins, fatty acids, and miscellaneous compounds from the genus *Xanthium*

X. strumarium contained the isoflavones formononetin (**267**) and ononin (**269**) [80], while luteone (**268**) was isolated from *X. mongolicum* whole plants [45]. The flavone jaceidin (**270**) was found to be present in a 0.0004% yield in *X. macrocarpum* fruits [15]. Among *Xanthium* species, *X. strumarium* has been widely investigated phytochemically. Its fruits were reported to contain the flavone quercetin (**272**) and the two flavone glycosides patuletin-3-glucuronide (**271**) and quercetin-3-*O*-glucuronide (**273**) [7, 45].

2.7.2 Quinones and Coumarins

In parallel with the main secondary metabolites mentioned above, *Xanthium* plant extracts contain also compounds of the quinone and coumarin type. In a recent publication, the anthraquinone emodin (**274**) was isolated from *X. orientale* whole plants [28]. After sequential column chromatography isolation steps, a crystalline compound from a 75% EtOH extract of *X. sibiricum* roots was identified as the new quinone 5-hydroxy-3,6-dimethoxy-7-methyl-1,4-naphthalenedione (**273**) (Fig. 8) [5]. The whole plants of *X. orientale* and the roots of *X. sibiricum* both were found to produce the coumarin scopoletin (**276**), while the whole plants of *X. mongolicum* and the stems of *X. sibiricum* afforded another coumarin, scopolin (**277**) [5, 28, 45, 75, 92].

2.7.3 Fatty Acids and Miscellaneous Compounds

Fatty acid derivatives are a further compound type present in *Xanthium* species. On the basis of chromatographic isolation work and NMR structural determinations, 11 such compounds (**278**–**288**) are included in Table 1 and illustrated in Fig. 8. Most were obtained from nonpolar fractions of the five plants *X. canadense*, *X. mongolicum*, *X. orientale*, *X. sibiricum*, and *X. strumarium* [13, 28, 45, 60, 71, 74, 75, 78, 92, 96]. *X. sibiricum* fruits contain fumaric acid ethyl ester (**278**) and succinic acid (**286**), whereas heptacosanoic acid (**280**) and nonadecanoic acid (**283**) were reported as two constituents of its stems and roots, respectively [71, 75, 78, 92]. Apart from the main bioactive compounds, the aerial parts of *X. strumarium* species contain hexadecanoic acid (**279**) and pentatriacontan-1-ol (**285**), while the whole plants of *X. orientale* afforded methyl hexadecanoate (**282**), oleic acid (**284**), and triacontanol (**287**) [13, 28, 60, 74]. (3*Z*)-Hexenyl-β-D-glycoside (**281**) was found in *X. mongolicum* whole plants [45]. A potential ovicidal metabolite with a long alkyne sidechain was isolated from *X. canadense* roots, with the structure tridec-1-ene-3,5,7,9,11-pentayne (**288**) [96].

In addition to other constituents, in turn *X. sibiricum* aerial parts were shown to contain 3-cycloheptene-1-acetic acid (**289**) [47]. *X. strumarium* seeds were found to contain two molecules, (2*S*,3*R*)-2,3-dihydroxy-2-methylbutyrolactone (**290**) and 5-(hydroxymethyl)furfural (**291**) [34], while its fruits showed the presence of the free sugar raffinose (**292**) [7, 79].

2.8 *Compounds from Endophytic Fungi Associated with* Xanthium *Species*

Endophytic fungi are typical symbiotic microorganisms present in plants and often accumulate biologically active constituents with various potential roles [21]. Recently, alternuisol (**293**) and alternariol (**294**) were shown to be two major phytotoxins of the fungus *Alternaria* sp. infecting *X. italicum* leaves (Table 1 and Fig. 9) [1]. These two compounds at a concentration of 10.0 mg/cm^3 showed 11 and 75% inhibition, respectively, of the root growth of the monocotyledonous plant *Pennisetum alopecuroides*. Two constituents from the fungus *Alternaria zinniae* that infected *X. occidentale* leaves, brefeldin A (**295**), and α,β-dehydrocurvularin (**296**), were investigated against the larvae of *Artemia salina* (brine shrimp). It was found that compound **295** (at. 10^{-5}M) caused 100% lethality of the test organism, while compound **296** was inactive at the concentration level used [97]. The endophytic fungus *Eupenicillium* sp. LG41 was isolated from *X. sibiricum* roots and its EtOAc extract afforded four compounds, namely, eujavanicol A (**297**), eupenicinicol A (**298**), and eupenicinicols C (**299**), and D (**300**) [98]. The latter two compounds were new natural products.

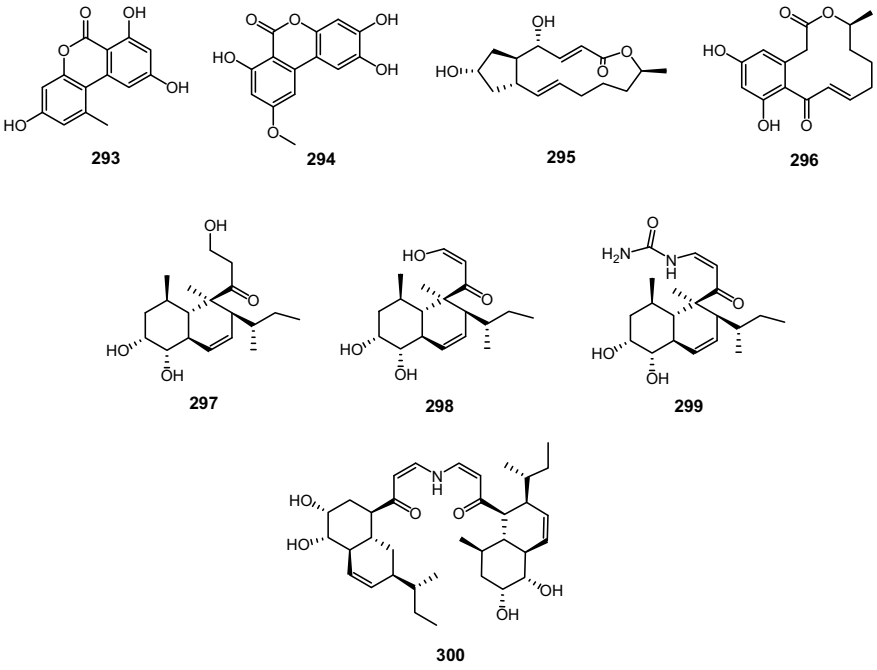

Fig. 9 Compounds from endophytic fungi associated with *Xanthium* species

2.9 *Volatile Oil Constituents of* Xanthium *Species*

Members of the genus *Xanthium* species have been shown to produce volatile oils containing a variety of organic compounds. Table 2 presents the percentages of the main components in *Xanthium* volatile oils (>5.0%) derived by GC–MS analysis. Terpenoids were found as the main compounds present in *Xanthium* essential oil

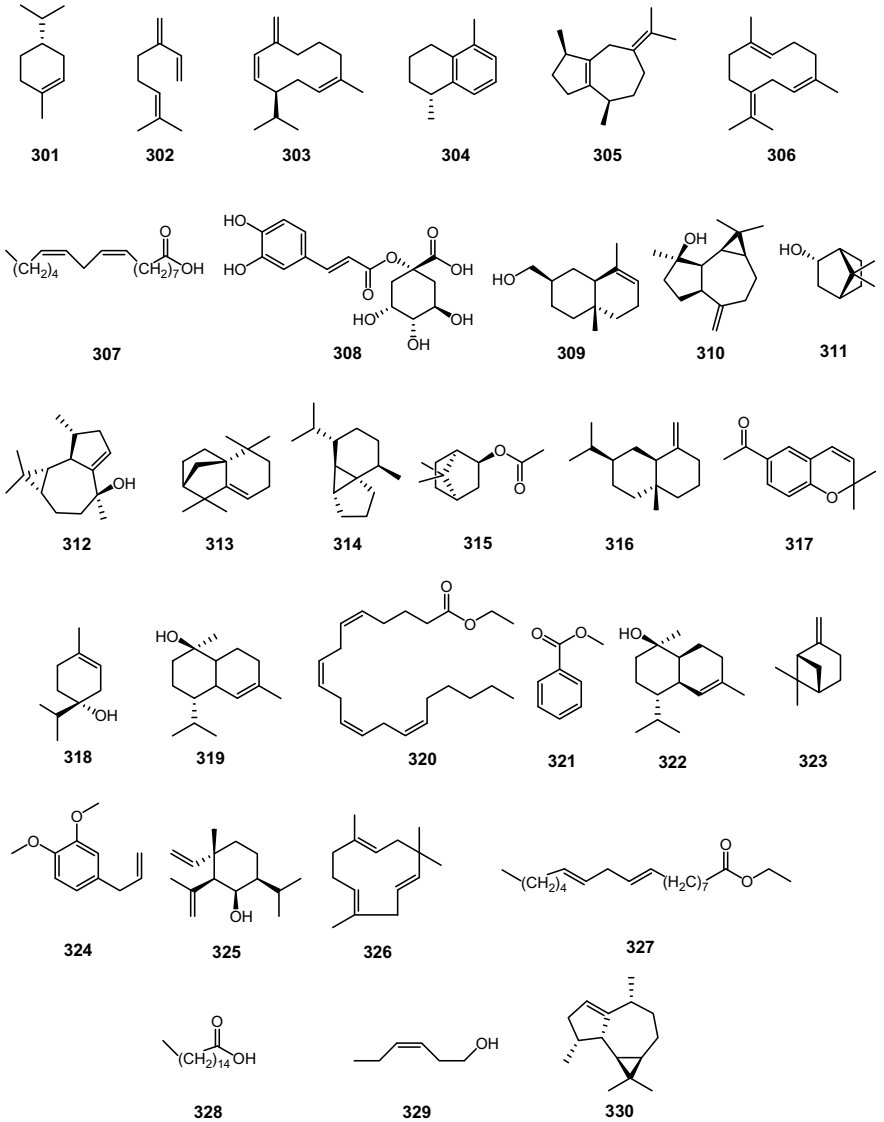

Fig. 10 Volatile *Xanthium* oil constituents

Table 2 Essential oil constituents of representative *Xanthium* species

Species	Collection	Part(s) used	Main constituents	Ref.
X. strumarium	North America	Aerial parts	Limonene (**301**) (48.23%), myrcene (**302**) (14.31%), and germacrene D (**303**) (13.92%)	[111]
	Egypt	Leaves	1,5-Dimethyltetralin (**304**) (14.17%), α-eudesmol (**309**) (10.60%), (–)-spathulenol (**310**) (7.54%), borneol (**311**) (6.59%), ledene alcohol (**312**) (6.46%), and isolongifolene (**313**) (5.06%)	[101]
	Zabol/Iran	Leaves	*cis*-β-Guaiene (**305**) (34.2%), limonene (**301**) (20.3%), and borneol (**311**) (11.6%)	[102]
	Khoramabad/Iran	Leaves	Limonene (**301**) (24.7%), borneol (**311**) (10.6%), β-cubebene (**314**) (6.3%), and bornyl acetate (**315**) (5.9%)	[112]
		Stems	Bornyl acetate (**315**) (19.5%), limonene (**301**) (15.0%), β-selinene (**316**) (10.1%), borneol (**311**) (7.9%), desmethoxy-encecalin (**317**) (6.0%), terpinene-4-ol (**318**) (5.4%), and α-cadinol (**319**) (5.3%)	
	Cuba	Stems and leaves	Arachidonic acid ethyl ester (**320**) (9.5%), and benzoic acid methyl ester (**321**) (7.1%)	[113]
X. italicum	China	Aerial parts	Limonene (**301**) (51.61%), germacrene B (**306**) (6.98%), δ-cadinol (**322**) (5.94%), and β-pinene (**323**) (5.6%)	[114]
X. italicum	Serbia	Stems	Germacrene D (**303**) (12.8%), methyleugenol (**324**) (5.4%), and β-cubebene (**314**) (5.0%)	[103]
		Fresh fruits	Germacrene B (**306**) (28.7%), shyobunol (**325**) (16.7%), and α-humulene (**326**) (8.4%)	
		Mature fruits	Germacrene B (**306**) (31.3%) and α-humulene (**326**) (11.8%)	
X. sibiricum	Shanghai/China	Fruits	Linoleic acid (**307**) (80.24%) and 9,12-octadecadienoic acid ethyl ester (**327**) (5.97%)	[105]
	Hebei/China	Fruits	Linoleic acid (**307**) (70.75%), and palmitic acid (**328**) (10.25%)	

(continued)

Table 2 (continued)

Species	Collection	Part(s) used	Main constituents	Ref.
X. mongolicum	Shandong/China	Fruits	Linoleic acid (**307**) (77.71%), and palmitic acid (**328**) (7.84%)	
X. canadense	Japan	Leaves	Germacrene D (**303**) (28.5%), and (*Z*)-3-hexen-1-ol (**329**) (5.3%)	[104]
X. cavaillesii	Argentina	Aerial parts	Limonene (**301**) (43.6%), and aromadendrene (**330**) (4.6%)	[106]

samples. In a recent report, limonene (**301**) (48.23%), myrcene (**302**) (14.31%), and germacrene D (**303**) (13.92%) (Fig. 10) were identified as the main components in the essential oils of North American *X. strumarium* aerial parts [111]. *Xanthium strumarium* species are widely distributed throughout the world. Its leaf volatile oil, from a specimen collected in Egypt, contained the main component 1,5-dimethyltetralin (**304**) (14.17%), as compared with *cis*-β-guaiene (**305**) (34.2%) and limonene (**301**) (24.7%) in samples collected from the Zabol and Khoramabad areas of Iran [101, 102]. Germacrene D (**303**) varied from 12.8% in Serbian *X. italicum* stems to 28.5% in Japanese *X. canadense* leaf volatile oil [103, 104]. It was shown that germacrene B (**306**) reached up to 28.7–31.3% in the essential oils of the fresh and mature fruits of Serbian *X. italicum* [103]. Linoleic acid (**307**) is present in over 70% of the fruit volatile oils of Chinese *X. mongolicum* and *X. sibiricum* [105]. *X. cavanillesii* essential oil was found as a major component in the monoterpene limonene (**301**) (43.6%) [106].

Phytochemical analysis utilizing HPLC is one of the fastest procedures available to identify and confirm the presence of each component in plant extracts (e.g., Refs. [18, 107]). Han et al. reported 2007 that the HPLC–DAD–MS^n analysis of an *n*-butanol fraction of *X. strumarium* fruits indicated the presence of several caffeoylquinic acid derivatives, namely, 1-*O*-caffeoylquinic acid (**308**), 3-*O*-caffeoylquinic acid (**155**), chlorogenic acid (**153**), 4-*O*-caffeoylquinic acid (cynarin) (**158**), 1,3-*O*-dicaffeoylquinic acid (**158**), 1,4-*O*-dicaffeoylquinic acid (**159**), 1,5-*O*-dicaffeoylquinic acid (**162**), 1,3,5-*O*-tricaffeoylquinic acid (**174**), and 3,4,5-*O*-tricaffeoylquinic acid [108]. Using the UF-HPLC-PDA, Wang et al. (2015) confirmed that derivatives of caffeoylquinic acid are constituents of *X. strumarium* fruits [109]. *X. strumarium* and *X. sibiricum* seem to have a close relationship since an HPLC–ESI–MS/MS investigations of the 50% MeOH extract of *X. sibiricum* fruits showed caffeoylquinic acid derivatives as the main components [110].

3 Biological Activities

3.1 Cytotoxic Activity

Sesquiterpenoids derived from *Xanthium* species have been subjected to various growth inhibition investigations using cancer cell lines. For example, the five sesquiterpenoids deacetylxanthanol (**5**), lasidiol *p*-methoxybenzoate (**110**) (16 μM), 11α,13-dihydroxanthinin (**14**), 11α,13-dihydroxanthuminol (**17**) (20 μM), and xanthinosin (**72**) (8 μM) inhibited the proliferation of AGS cells, to demonstrate TRAIL-resistance overcoming activity [11].

In a cytotoxicity assay against SNU387 cells, two monomeric xanthanolides (**25** and **33**) and two dimeric xanthanolides (**55** and **56**) had the following IC_{50} values: 1β-hydroxy-5α-chloro-8-*epi*-xanthatin (**33**) (IC_{50} 5.1 μM) > 8-*epi*-xanthatin-1α,5α-epoxide (**25**) (IC_{50} 9.6 μM) > pungiolide E (**56**) (IC_{50} 11.7 μM) > pungiolide D (**55**) (IC_{50} 14.6 μM) [9]. The monomeric isomers **25** and **33** with respective IC_{50} values of 9.5 and 20.7 μM against A-549 cells were also more active than the dimeric isomers **55** and **56** (deemed as inactive, $IC_{50} > 40$ μM) [9]. Compound **33** also significantly inhibited the growth of SK-Hep-1, HepG2, SMMC-7721, and Huh-7 cells, having IC_{50} values of 1.57, 1.63, 2.40, and 2.12 μM, respectively [115].

With the presence of an α-methylene-γ-lactone moiety in their structure, the three sesquiterpenoids 8-*epi*-xanthatin-1β,5β-epoxide (**26**), tomentosin (**67**), and eremophil-1,11(13)-dien-12,8β-olide (**90**) showed discernible cytotoxic effects against the five human cancer cell lines Huh-7, KB, Jurkat, BGC-823, and KE-97, with IC_{50} values ranging from 1.1 to 18.0 μM, as compared with those for the standard compound staurosporine (IC_{50} 0.15–0.58 μM) [42].

Xanthatin (**70**) contains an α-methylene-γ-lactone moiety, which might also be responsible for its cytotoxicity against HeLa cells (IC_{50} value of 4.92 μM), but it was noted that this compound displayed less potent cytotoxicity to noncancerous HEK 293T and BEAS-2B cells [116]. On searching for bioactive constituents from *X. strumarium* leaves, the four isolated compounds xanthatin (**70**), squalene (**145**), stigmasterol (**263**), and β-sitosterol-*O*-glucoside (**252**) inhibited HL-60 cell proliferation with IC_{50} values in the order: **145** (7.09 $\mu g/cm^3$) < **252** (24.91 $\mu g/cm^3$) < **263** (50.07 $\mu g/cm^3$) < **70** (52.50 $\mu g/cm^3$), while the standard compound diminazene aceturate gave an IC_{50} value of >128 $\mu g/cm^3$ [58]. The sesquiterpene lactone xanthantin (**70**), once again showed cytotoxicity against Hep-G2 and L1210 cells with IC_{50} values of 49.0 μM and 12.3 μM, respectively [58]. Two dimeric xanthanolides, mongolides D (**40**) and E (**41**) displayed IC_{50} values of 8.46 μM and 19.20 μM against the MDA-MB-231 breast cancer cell line, which were less potent than that for xanthinin (**71**) (IC_{50} 3.57 μM) [49].

Members of other compound classes isolated from *Xanthium* species have been evaluated for their cytotoxicity against cancer cell lines. Among 16 isolates from *X. orientale*, He et al. reported that a xanthanolide (**70**), a triterpenoid (**140**), and a quinone (**274**) displayed respective IC_{50} values of 11.3–13.2, 53.4–58.5, and 80–120 μM against the two human cancer cell lines Hep-G2 and A-549 [28]. The simple

phenol **168** caused a 50% growth inhibition of U937 cells at a high concentration of 300 μM [84].

3.2 Antioxidative Activity

The antioxidative activity of *Xanthium* extracts has been attributed to the presence of constituents such as simple phenols, sulfur-containing compounds, sterols, and other derivatives [13, 34, 81]. 1,3-Di-*O*-caffeoylquinic acid (**158**), also known as cynarin, strongly inhibited radiation-induced oxidation of chlorogenate via the prevention of free radical attack [81]. (–)-Xanthienopyran (**202**), purified from *X. strumarium*, gave an IC_{50} value of 1.72 $\mu g/cm^3$ and hence exhibited inhibition of superoxide anion generation from human neutrophils induced by formyl-L-methionyl-L-leucyl-L-phenylalanine, as compared to the reference compound, diphenyleneiodonium (IC_{50} 0.16 $\mu g/cm^3$) [34]. The triterpenoid, α-amyrin (**138**), the sterol, 14-methyl-12,13-dehydro-sitosterol-heptadeconate (**251**), and the fatty acid, hexadecanoic acid (**279**) all showed weak DPPH radical-scavenging capacity, with IC_{50} values ranging from 76.2 to 106.4 $\mu g/cm^3$, with the reference compound ascorbic acid affording a comparative IC_{50} value of 11.41 $\mu g/cm^3$ [13].

3.3 Anti-Inflammatory Activity

In an inflammation-related assay, the three xanthanolides, 4-oxo-bedfordia acid (**51**), xanthatin (**70**), and xanthinosin (**72**) were evaluated as inhibitors of nitric oxide synthesis, in the following order of potency ($IC_{50}/\mu M$): **70** (0.47) > **72** (11.12) > **51** (136.5). The activity of compounds **70** and **72** in this assay may be explained by the presence of a lactone ring conjugated with an exomethylene moiety in each case while a free carboxylic acid group occurs in the marginally active compound **51** [16]. The two novel monoterpene glucosides, xanmonoters A (**122**) and B (**123**), also showed IC_{50} values of 17.4 and 22.1 μM, respectively, in inhibiting NO production, as compared with the positive control aminoguanidine (IC_{50} 3.6 μM) [12]. The lignan xanthiumnolic E (**250**) exhibited anti-inflammatory activity in terms of lipopolysaccharide (LPS)-induced NO production with an IC_{50} value of 8.73 μM, while its analogs **246**–**249** displayed less potent IC_{50} values of 15.6–47.6 μM, in comparison to aminoguanidine (IC_{50} 1.25 μM) that was used as the positive control [95]. More recently, 14 isolated compounds from *X. sibiricum* fruits have been investigated with respect to their anti-inflammatory activity as determined by the inhibition of NO production [10]. Among them, two thiazinediones, 2-hydroxy-xanthiazone (**184**) and (+)-xanthiazinone B (**194**), had comparable IC_{50} values to the positive control dexamethasone (IC_{50} 10.5 μM). In an anti-inflammatory assay as determined by 5-LOX inhibition, ziniolide (**78**) from *X. spinosum* roots and the reference compound apigenin, showed comparative IC_{50} values of 69 and 20 μM, respectively [4].

3.4 Antibacterial and Antifungal Activities

There have been many studies reported on the evaluation of the antibacterial and antifungal activities of isolated compounds from X*anthium* species. Apart from anti-inflammatory activity, compounds **138**, **251**, and **279** were further subjected to growth inhibition tests against *Staphylococcus aureus*, *Escherichia coli*, *Pseudomonas aeruginosa*, *Candida albicans*, and *Kluyveromyces marxianus.* The results indicated that **138** exhibited the greatest effect (*MIC* 6.25–12.5 $\mu g/cm^3$), followed by **251** and **279** (*MIC* 6.25–50 $\mu g/cm^3$) in comparison to the antibacterial positive control ciprofloxacin (*MIC* 6.25 $\mu g/cm^3$) [13]. In contrast, the three compounds **184, 186**, and **228** failed to inhibit *C. albicans* (MIC_{90} > 128 $\mu g/cm^3$) [85]. Among the tested xanthanolides **21**, **22**, **36–37**, **51**, and **70–72**, the well-known compound **70**, containing an α,β-unsaturated carbonyl group in the cyclopentanone ring showed antifungal activity against *C. albicans* and *C. glabrata*, while the remaining compounds were inactive [15]. Compound **70** was also tested against *Bacillus* sp. with *MIC* values of 12.5–100 $\mu g/cm^3$, and with 25–100 $\mu g/cm^3$ against *Candida* sp., *Pichia* sp., *Saccharomycopsis* sp., and *Torulaspora* sp. [58]. The two common sterols **252** and **261** isolated from *X. sibiricum* roots seem promising antibacterial agents since they had remarkable *MIC* values of 0.35 and 0.17 $\mu g/cm^3$ against *E. coli*, and better than that of new anthraquinone **275** (*MIC* 2.78 $\mu g/cm^3$) and the positive control ciprofloxacin (*MIC* 0.69 $\mu g/cm^3$) [5]. The functional group at C-11 seems to be responsible for the differential antibacterial results of the two compounds eupenicinicols C (**299**) and D (**300**), of which **300** exhibited potent antibacterial activity against *S. aureus* with a *MIC* value of 0.1 $\mu g/cm^3$, while compound **299** was inactive [98].

3.5 Antidiabetic Effects

Herbal medicines are used worldwide in ethnomedicine as often effective alternatives in diabetes treatment modalities. In this regard, Hsu et al. evaluated the hypoglycemic activity of isolated compounds from *X. strumarium*, especially caffeic acid (**149**) [13]. This compound (at 0.5–3.0 mg/kg, intravenous injection) caused a plasma glucose decrease of 23.8 and 33.4% in streptozotocin-induced diabetic rats and NIDDM-rats (rats with insulin-resistance), respectively, as compared with values for the positive control metformin (100 mg/kg for ZTZ-rats, 18.4% decrease; 10 mg/kg for NIDDM-rats, 28.2% decrease, oral administration) [13]. In a study on aldose reductase inhibition, it was found that the number of caffeoyl groups among simple phenolic groups provided different results. Thus phenol **174**, containing three caffeoyl groups, exhibited a rat lens AR (rhAR) inhibitory IC_{50} value of 0.12 μM and a recombinant human AR (rhAR) inhibitory IC_{50} value of 0.71 μM, followed by compounds **158**, **160**, **162**, and **177** containing two caffeoyl groups (IC_{50} values of 0.19–1.90 μM for rAR and IC_{50} values of 0.67–0.134 μM for rAR). Compounds **154** and **155** have one caffeoyl

group each and had IC_{50} values of 3.11–9.24 μM for rAR and an IC_{50} value of 4.69 μM for rhAR [79].

3.6 Other Bioactivities

Pharmacological studies have also evaluated the activities of *Xanthium* secondary metabolites in various miscellaneous biological studies. Xanthatin (**70**) isolated from *X. spinosum* and the positive control paclitaxel displayed respective IC_{50} values of 0.028 and 0.002 μM in an antiangiogenic assay [59]. Compound **70** induced antitrypanosomal activity against *Trypanosoma brucei brucei* with an IC_{50} value of 2.63 $\mu g/cm^3$ in comparison to the standard drug diminazene aceturate (IC_{50} 0.088 $\mu g/cm^3$) [58]. In a brine shrimp lethality assay, the guaianolide ziniolide (**78**) from *X. catbarticum* roots, showed a toxicological LC_{50} value of 14.0 ppm [33]. Thiazinedione **188** served to ameliorate nasal symptoms and decreased IgE levels in allergic rhinitis mice [88]. The two *ent*-kaurene glycosides **124** (50–200 mg/kg) and **125** (50–150 mg/kg) did not affect the lung, heart, spleen, and the central nervous system in mice [69].

3.7 Biological Activities of Extracts

Cytotoxicity assays of *Xanthium* species have mostly focused on *X. strumarium* extracts. A methanol extract of *X. strumarium* seeds suppressed the growth of the three cancer cell lines Jurkat, HepG2, and L929 with the respective IC_{50} values of 50.18, 112.9, and 163.0 $\mu g/cm^3$, while IC_{50} values of 48.73, 68.74, and 111.0 $\mu g/cm^3$ were found for its EtOAc fraction, respectively [117]. Piloto-Ferrer et al. investigated both the cytotoxicity and in vivo antitumor evaluation of various extracts and fractions of *X. strumarium* aerial parts, which were conducted using CT26WT murine colon cancer cells [118]. A xanthatin-containing fraction (10 μM) exhibited a reported IC_{50} value of 8.3 μM, and three different extractives showed discernible growth inhibition effects in a mouse xenograft study. In another report, a 70% ethanol extract of *X. strumarium* fruits inhibited weakly the growth and proliferation of the HCC cell line, with an IC_{50} value of 100 $\mu g/cm^3$ [119]. In addition, the chloroform and methanol extracts of *X. strumarium* fruits (50 $\mu g/cm^3$) were evaluated as potential ATG4B inhibitors to suppress the growth and metastasis of colorectal cancer cells (inhibited 30% of HCT116 cell migration and up to 50% for DLD-1 cells) [120].

Collectively, the biological test results including some pharmacological evaluation data of extracts of *Xanthium* species constituents are summarized in Table 3.

When evaluated for potential anti-inflammatory activity, a 95% ethanolic extract of *X. strumarium* leaves, at concentrations of 100, 200, and 400 mg/kg, caused a

Table 3 Biological activities of isolated compounds and plant extracts from the genus *Xanthium*

Compound(s)	Conc.	Model	Effect	Ref.
Cytotoxic activity				
5 and **110**	16 μM	In vitro	Inhibited the proliferation of AGS cells in TRAIL-resistance overcoming activity	[11]
14 and **17**	20 μM	In vitro	Inhibited the proliferation of AGS cells in TRAIL-resistance overcoming activity	[11]
25		In vitro	$IC_{50} = 9.6\ \mu M$, SNU387 cells $IC_{50} = 9.5\ \mu M$, A-549 cells	[9]
26, 67, and **90**		In vitro	$IC_{50} = 1.1$–$18.0\ \mu M$, Huh-7, KB, Jurkat, BGC-823, and KE-97 cells	[42]
33		In vitro	$IC_{50} = 5.1\ \mu M$, SNU387 cells $IC_{50} = 20.7\ \mu M$, A-549 cells	[9]
33		In vitro	$IC_{50} = 1.57\ \mu M$, SK-Hep-1 cells $IC_{50} = 1.63\ \mu M$, HepG2 cells $IC_{50} = 2.40\ \mu M$, ASMMC-7721 cells $IC_{50} = 2.12\ \mu M$, Huh-7 cells	[115]
40		In vitro	$IC_{50} = 8.46\ \mu M$, MDA-MB-231 cells	[49]
41		In vitro	$IC_{50} = 19.20\ \mu M$, MDA-MB-231 cells	[49]
55		In vitro	$IC_{50} = 14.6\ \mu M$, SNU387 cells	[9]
56		In vitro	$IC_{50} = 11.7\ \mu M$, SNU387 cells	[9]
70		In vitro	$IC_{50} = 4.92\ \mu M$, HeLa cells less-toxicity/HEK 293 T and BEAS-2B cells	[116]
70		In vitro	$IC_{50} = 52.50\ \mu g/cm^3$, HL-60 cells	[58]

(continued)

Table 3 (continued)

Compound(s)	Conc.	Model	Effect	Ref.
70		In vitro	$IC_{50} = 11.3–13.2\ \mu M$, Hep-G2, and A-549 cells	[28]
70		In vitro	$IC_{50} = 49.0\ \mu M$, Hep-G2 cells $IC_{50} = 12.3\ \mu M$, L1210 cells	[59]
71		In vitro	$IC_{50} = 3.57\ \mu M$, MDA-MB-231 cells	[49]
72	$8\ \mu M$	In vitro	Inhibited the proliferation of AGS cells in TRAIL-resistance overcoming activity	[11]
140		In vitro	$IC_{50} = 53.4–58.5\ \mu M$, Hep-G2, and A-549 cells	[28]
145		In vitro	$IC_{50} = 7.09\ \mu g/cm^3$, HL-60 cells	[58]
168	$300\ \mu M$	In vitro	50% Growth inhibition, U937 cells	[84]
252		In vitro	$IC_{50} = 24.91\ \mu g/cm$, HL-60 cells	[58]
263		In vitro	$IC_{50} = 50.07\ \mu g/cm$, HL-60 cells	[58]
274		In vitro	$IC_{50} = 80–120\ \mu M$, Hep-G2, and A-549 cells	[28]
Antioxidative activity				
138 and **279**		In vitro	$IC_{50} = 76.2–106.4\ \mu g/cm^3$, DPPH radical scavenging	[13]
158		In vitro	To strongly inhibit the radiation-induced oxidation of chlorogenate	[81]
202		In vitro	$IC_{50} = 1.72\ \mu g/cm^3$, inhibition of O^{2-} generation	[34]
Anti-inflammatory activity				

(continued)

Table 3 (continued)

Compound(s)	Conc.	Model	Effect	Ref.
51		In vitro	$IC_{50} = 136.5\ \mu M$/NO synthetic inhibition	[16]
70		In vitro	$IC_{50} = 0.47\ \mu M$/NO synthetic inhibition	[16]
72		In vitro	$IC_{50} = 11.12\ \mu M$/NO synthetic inhibition	[16]
78		In vitro	$IC_{50} = 69\ \mu M$/5-LOX productive inhibition	[4]
122		In vitro	$IC_{50} = 17.4\ \mu M$/NO synthetic inhibition	[12]
123		In vitro	$IC_{50} = 22.1\ \mu M$/NO synthetic inhibition	[12]
184		In vitro	$IC_{50} = 10.5\ \mu M$/NO synthetic inhibition	[10]
194		In vitro	$IC_{50} = 10.5\ \mu M$/NO synthetic inhibition	[10]
246–249		In vitro	$IC_{50} = 15.6$–$47.6\ \mu M$, LPS-induced NO production	[95]
250		In vitro	$IC_{50} = 8.73\ \mu M$, LPS-induced NO production	[95]
Antibacterial and antifungal activities				
70		In vitro	$MIC = 12.5$–$100\ \mu g/cm^3$, *Bacillus* sp. $MIC = 25$–$10\ \mu g/cm^3$, *Candida* sp., *Pichia* sp., *Saccharomycopsis* sp., and *Torulaspora* sp.	[58]
138		In vitro	*MIC* 6.25–12.5 $\mu g/cm^3$, *S. aureus*, *E. coli*, *P. aeruginosa*, *C. albicans*, and *K. marxianus*	[13]
184, 186, and **228**		In vitro	$MIC_{90} > 128\ \mu g/cm^3$, inactive	[85]

(continued)

Table 3 (continued)

Compound(s)	Conc.	Model	Effect	Ref.
251 and **279**		In vitro	*MIC* 6.25–50 μg/cm^3, *S. aureus*, *E. coli*, *P. aeruginosa*, *C. albicans*, and *K. marxianus*	[13]
252		In vitro	*MIC* = 0.35 μg/cm^3, *E. coli*	[5]
261		In vitro	*MIC* = 0.17 μg/cm^3, *E. coli*	[5]
275		In vitro	*MIC* = 2.78 μg/cm^3, *E. coli*	[5]
299		In vitro	Inactive, *E. coli*	[98]
300		In vitro	*MIC* = 0.1 μg/cm^3, *S. aureus*	[98]
Antidiabetic activity				
149	0.5–3.0 mg/kg	In vivo	Plasma glucose decreased 23.8% in streptozotocin-induced diabetic rats Plasma glucose decreased 33.4% in rats with insulin-resistance	[13]
154–155		In vitro	IC_{50} = 3.11–9.24 μ*M*, inhibitory effect on rat lens AR (rAR) IC_{50} = 4.69 μ*M*, inhibitory effect on recombinant human AR (rhAR)	[79]
158, 160, 162, and **177**		In vitro	IC_{50} = 0.19–1.90 μ*M*, inhibitory effect on rAR IC_{50} = 0.81–1.34 μ*M*, inhibitory effect on rhAR	[79]
174		In vitro	IC_{50} = 0.12 μ*M*, inhibitory effect on rAR IC_{50} = 0.71 μ*M*, inhibitory effect on rhAR	[79]

(continued)

Table 3 (continued)

Compound(s)	Conc.	Model	Effect	Ref.
Other bioactivities				
70		In vitro	$IC_{50} = 0.028\ \mu M$, antiangiogenic activity	[59]
70		In vitro	$IC_{50} = 2.63\ \mu g/cm$, antitrypanosomal activity against *Trypanosoma brucei brucei*	[58]
78		In vitvo	$LC_{50} = 14.0$ ppm, lethality effect on brine shrimp	[33]
124	50–200 mg/kg	In vivo	Not toxic to lung, heart, spleen, and the central nervous system in rodents	[88]
125	50–150 mg/kg	In vivo	Not toxic to lung, heart, spleen, and the central nervous system in rodents	[88]
Biological activities of extracts				
Methanol extract of *X. strumarium* seeds		In vitro/cytotoxicity	$LC_{50} = 50.18\ \mu g/cm^3$, Jurkat cells $LC_{50} = 112.9\ \mu g/cm^3$, HepG2 cells $LC_{50} = 163\ \mu g/cm^3$, L929 cells	[117]
Ethyl acetate fraction of *X. strumarium* seeds		In vitro/cytotoxicity	$LC_{50} = 48.73\ \mu g/cm^3$, Jurkat cells $LC_{50} = 68.74\ \mu g/cm^3$, HepG2 cells $LC_{50} = 111.0\ \mu g/cm^3$, L929 cells	[117]
Xanthatin fraction of *X. strumarium* aerial parts	$10\ \mu M$	In vitro/cytotoxicity	$IC_{50} = 10.8\ \mu M$, CT26WT cells	[118]
	5 mg/kg	In vivo/cytotoxicity	Showed the same effect as the positive control oxaliplatin (6 mg/kg) against a CT26WT cell mouse xenograft tumor model	

(continued)

Table 3 (continued)

Compound(s)	Conc.	Model	Effect	Ref.
70% ethanol extracts *of X. strumarium* fruits	100 μg/cm^3	In vitro/cytotoxicity	IC_{50} = 100 μg/cm^3, HCC cells	[119]
Chloroform and methanol extracts of *X. strumarium* fruits	50 μg/cm^3	In vitro/cytotoxicity	Inhibited 30% of HCT116 cell migration and up to 50% for DLD-1 cells	[120]
95% ethanolic extract of *X. strumarium* leaves	100, 200 and 400 mg/kg	In vivo/anti-inflammation	Decreased the edema volume stimulated by carrageenan after 12 days of treatment	[121]
Aqueous extract of *X. strumarium* leaves	400 mg/kg		Decrease in the edema volume stimulated by carrageenan after 12 days of treatment	
Methanol extract *X. strumarium* aerial parts	300 μg/cm^3	In vitro/anti-inflammation	Inhibited NO (97%) and PGE2 (66%) productions	[124]
Methanol extract *of X. sibiricum* roots	400 μg/cm^3	In vitro/anti-inflammation	Inhibited LPS-stimulated NO production and inducible nitric oxide synthase (iNOS)	[122]
75% Ethanol extract of *X. strumarium* fruits	75 mg/kg	In vivo/antiarthritis	Reduced the spleen index, COX-2, 5-LOX levels, and the amount sof proinflammatory cytokines TNF-α, IL-1β	[123]
Chloroform extract of *X. strumarium* roots	125 μg/cm^3	In vitro/antioxidant	IC_{50} = 24.85 μg/cm^3, DPPH radical-scavenging activity IC_{50} = 9.23 μg/cm^3, hydrogen peroxide radicals scavenging activity	[125]
Ethanol extract of *X. strumarium* roots	100 μg/cm^3		IC_{50} = 29.81 μg/cm^3, DPPH radical-scavenging activity IC_{50} = 10.18 μg/cm^3, hydrogen peroxide radicals scavenging activity	

(continued)

Table 3 (continued)

Compound(s)	Conc.	Model	Effect	Ref.
Methanol extract of *X. strumarium* fruits		In vitro/antioxidant	93.68%/DPPH radical-scavenging activity	[126]
Methanol extract of *X. strumarium* fruits		In vitro/antidiabetes	$IC_{50} = 15.25\ \mu g/cm^3$, α-glucosidase inhibition	[126]
Chloroform and hexane soluble fractions of *X. strumarium* roots	5 g/kg body weight/acute toxicity study (single oral dose)	In vivo/toxicology	No toxicity to Wistar rats at the dose levels used	[127]
	1.000 mg/kg/ subacute study (28 days treatment)			
Water extract of *X. strumarium* fruits	7.5, 15.0 and 30 g/kg	In vitro MTT assay LDH assay	Showed hepatotoxic effect as manifested on liver enzyme levels	[128]
Water extract of *X. sibiricum* fruits	100 $\mu g/cm^3$	In vitro/toxicology	No toxicity to blood cell membranes	[129]
50% Ethanol extract of *X. strumarium* leaves	5, 50, 500, and 1000 $\mu g/cm^3$	In vitro/antitrypanosomal	Inhibited the growth of the *Trypanosoma evansi* parasite	[130]
	100, 300, and 1000 $\mu g/cm^3$	In vivo/antitrypanosomal	Decreased the growth of *T. evansi*	

decrease of the edema volume stimulated by carrageenan after 12 days of treatment, whereas an aqueous extract was only active in this regard at a concentration of 400 mg/kg [121]. The methanolic extract (300 μg/cm^3) of *X. strumarium* aerial also inhibited the production of inflammatory mediators NO (up to 97%) and prostaglandin E2 (66%). The target of its action was identified as PDK1. In the same manner, the methanol extract (400 μg/cm^3) of *X. sibiricum* roots induced anti-inflammatory activity by inhibiting LPS-stimulated NO production and inducible nitric oxide synthase via suppressing the nuclear factor κB (NF-κB) and STAT3 pathways [122].

A 75% ethanolic extract (75 mg/kg) *of X. strumarium* fruits was investigated in Freund's complete adjuvant-induced arthritis model in rats, and found to reduce the spleen index, COX-2 and 5-LOX levels, as well as levels of the proinflammatory cytokines TNF-α and IL-1β, but it increased IL-1β levels [123]. A methanolic extract of *X. strumarium* aerial parts (300 μg/cm^3) mediated anti-inflammatory action via PDK1 enzyme inhibition in the NF-κB signaling pathway [124].

In terms of potential antioxidative activity, the chloroform (125 μg/cm^3) and the ethanol (100 μg/cm^3) extracts of *X. strumarium* roots gave IC_{50} values of 24.85 and 29.81 μg/cm^3 in a DPPH radical-scavenging assay and were comparable in potency levels with those of the positive controls ascorbic acid (IC_{50} 27.35 μg/cm^3) and BHT (IC_{50} 26.01 μg/cm^3) [125]. These two extracts were further shown to capture hydrogen peroxide radicals with IC_{50} values of 9.23 and 10.18 μg/cm^3, respectively, with the positive control being active at 8.89 μg/cm^3 [125]. Likewise, a methanol extract of *X. strumarium* fruits trapped the DPPH radicals up to 93.68% in a FRAP antioxidative assay, and inhibited the α-glucosidase enzyme with an IC_{50} value of 15.25 μg/cm^3 in an antidiabetic assay [126].

It was found that the acute (5 g/kg body weight for single oral dose) and subacute (1.0 g/kg body weight for 28 days) administration routes of the chloroform and hexane-soluble extracts of *X. strumarium* roots displayed no toxicity symptoms in Wistar rats [127]. However, a hepatotoxic effect of an aqueous extract of *X. strumarium* fruits (7.5, 15.0, and 30.0 g/kg/day) may be due to its suppression of mitochondrial function [128]. The aqueous extract of *X. sibiricum* fruits, even at the highest dose tested of 100 μg/cm^3, did not effect the blood cell membranes [129].

A crude 50% ethanol extract of *X. strumarium* leaves exhibited in vitro antitrypanosomal activity against *Trypanosoma evansi*-infected mice, although a 1000 mg/kg dose of plant extract was toxic to the host animals [130].

4 Synthesis Aspects

As mentioned above, naturally occurring sesquiterpenoids of the xanthanolide type are the largest group of compounds isolated so far from *Xanthium*. They have been recognized as showing antitumor, anti-inflammatory, and antibacterial effects [16, 58]. Both monomeric and dimeric xanthanolides have been subjected to chemical synthesis investigations.

4.1 Synthesis of Monomeric Xanthanolides

A major component of *Xanthium* species is xanthatin (**70**) and therefore this became a focus of synthesis work. It was synthesized for the first time according to Shishido's method. As outlined in Fig. 11, the synthesis route started from bicyclic lactone **331**, and needed 19 linear steps for completion [131].

The stereochemistry at C-8 of the bicyclic lactone **331** was the main consideration. By opening the lactone ring, and the performance of a Mitsunobu reaction, hydrolysis, and lactonization, compound **331** was converted into the *trans*-fused lactone **334**. The formation of the C-2,C-3 side chain and the C-1,C-5 double bond in **337** was achieved by adopting a Lewis acid-catalyzed carbonyl ene-reaction. Through several reaction steps, the key bicyclic compound **339** was synthesized, which was further phenylselenylated and subjected to oxidization-elimination to yield the α-methylene lactone **340**. The synthesis of xanthatin (**70**) was completed by a cross methathesis (CM) reaction with an overall yield of 7.6% [131].

As outlined in Fig. 12 [132], Shindo et al. achieved a highly efficient synthesis strategy of xanthatin (**70**) from the oxazolidinone **342** in 14 steps with an 8.7% yield. The amide **343** was obtained in high diastereoselectivity by asymmetric alkylation of

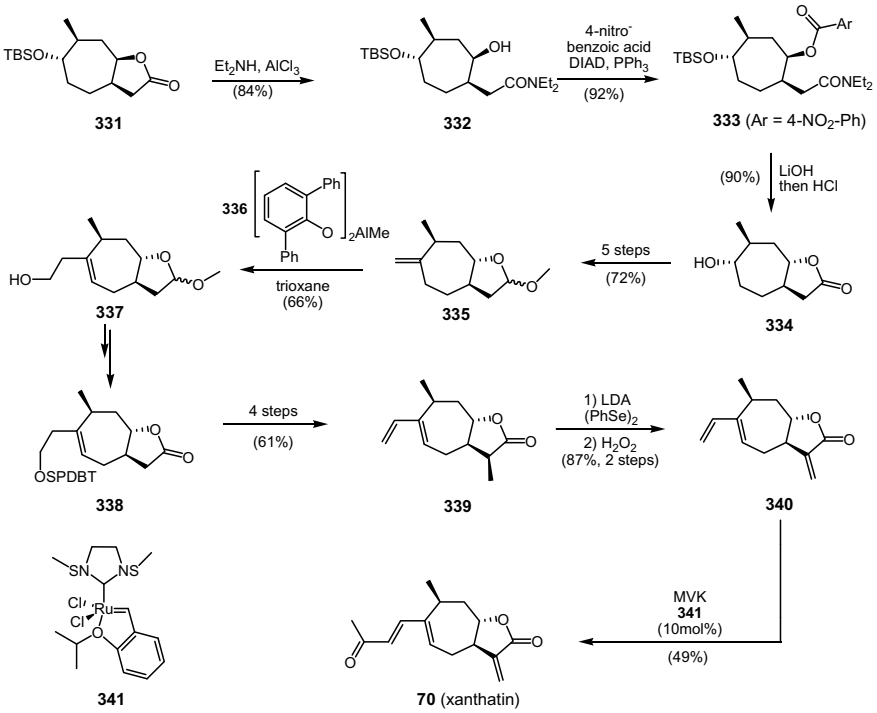

Fig. 11 Shishido's synthesis of (–)-xanthatin (**70**)

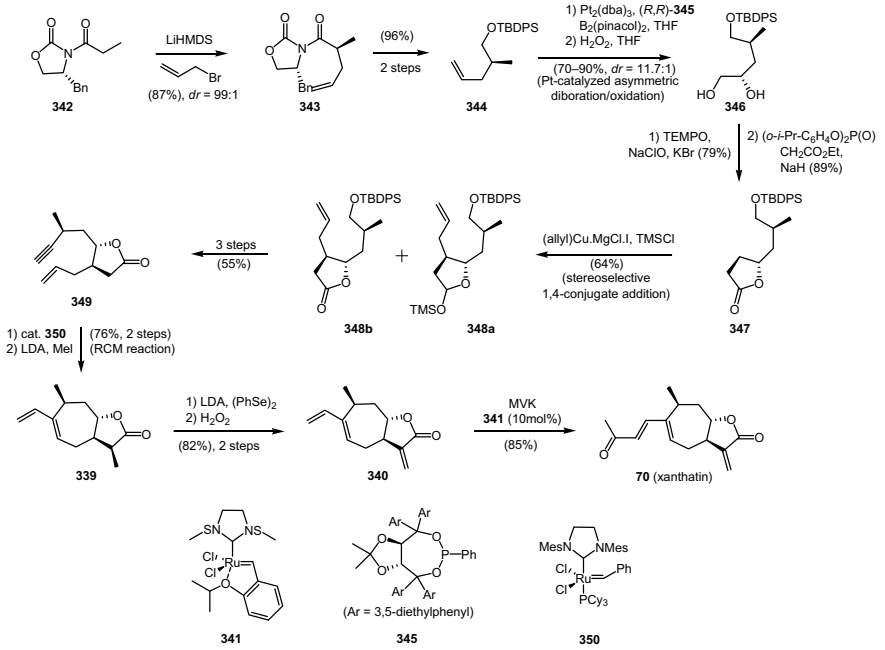

Fig. 12 Shindo's synthesis of (–)-xanthatin (**70**)

342, and was then subjected to reduction to give **344**. Diol **346**, which was obtained through an intriguing Pt-catalyzed asymmetric diboration of **344**, was selectively oxidized with TEMPO, subjected to a Wittig reaction, and lactonized to yield γ-butenolide **347**.

The use of an allylcopper reagent in the presence of trimethylsilyl chloride (TMSCl) supported the transformation of **347** into the 1,4-adduct **348b**. Subsequently, the key intermediate **349** without any epimerization at the C-10 position, was produced through stereoselective 1,4-conjugate addition followed by deprotection, oxidation, and Seyferth-Gilbert alkyne synthesis. The ring-closing metathesis of the intermediate **349** was performed using the Grubbs catalyst **350** to give the seven-membered carbocycle **339**, which then could be used to synthesize xanthatin (**70**) in three steps following Shishido's procedure.

The further monomeric xanthanolide, 8-*epi*-xanthatin (**24**), is a 5/7-*cis*-xanthanolide. Martin et al. have synthesized this compound in 14 steps with a 5.5% overall yield, as illustrated in Fig. 13 [133]. The synthesis commenced with the conversion of the commercially available ester **351** into an unstable aldehyde that was immediately subjected to the Corey-Fuchs olefination protocol in the presence of 2,6-lutidine to provide the vinyl dibromide **352** over two steps. When **352** was treated with excess *n*-butyllithium, and then triisopropylsilyl trifluoromethanesulfonate (TIPSOTf) and KCN, the reduction that followed with diisobutylaluminium hydride (DIBAL-H) resulted in aldehyde **353** (37% yield). Toward this end, the

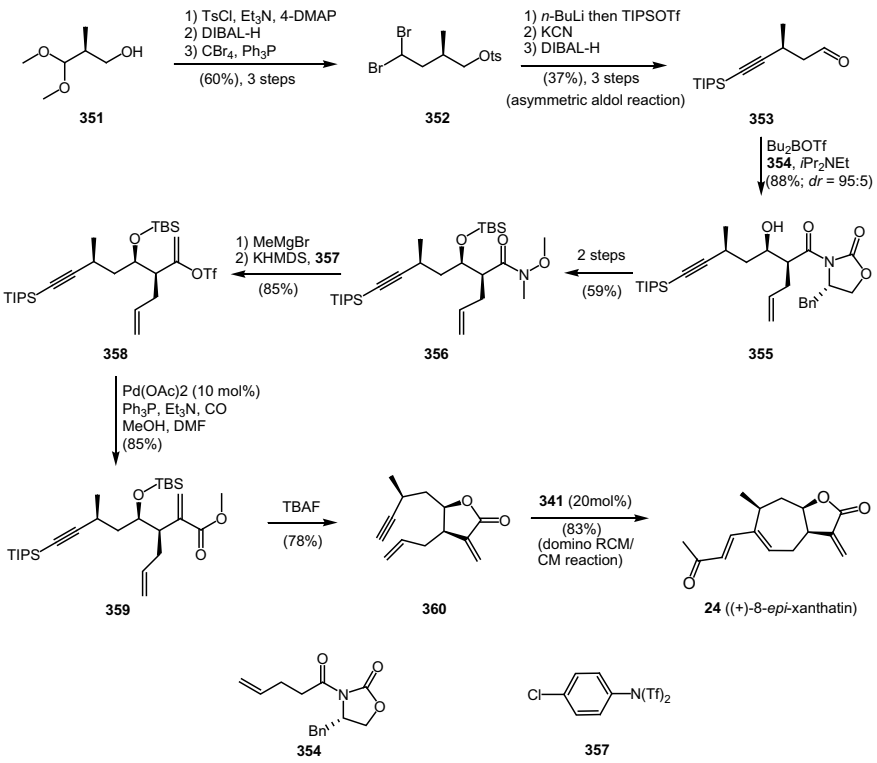

Fig. 13 Martin's synthesis of 8-*epi*-xanthatin (**24**)

boron enolate derived from oxazolidinone **354** reacted with aldehyde **353** to provide alcohol **355** in 88% yield ($dr > 95{:}5$). In order to afford the γ-butyrolactone, **355** was first elaborated into enol triflate **358** through four steps. This was followed by palladium-catalyzed carbonylation to give acrylate **359**. 8-*epi*-Xanthantin (**24**) was the result of a tandem ring-closing enyne metathesis/cross-metathesis reaction of lactone **360**.

4.2 Synthesis of Dimeric Xanthanolides

The dimeric xanthanolide, pungiolide D (**55**), has been synthesized from the monomeric 8-*epi*-xanthatin (**24**) [134]. The Diels–Alder dimerization of 8-*epi*-xanthatin (**24**) was performed in PhMe/EtOH at 110°C to afford the pentacyclic dimer prepungiolide (**362**). Then, **362** underwent C-3′ epimerization to yield **363** during the course of chromatographic purification. Upon heating at elevated temperature, **363** could be converted into pungiolide D (**55**) via an intramolecular ene cyclization. Notably, compound **55** was also obtained from monomer **24** via a one-pot synthesis

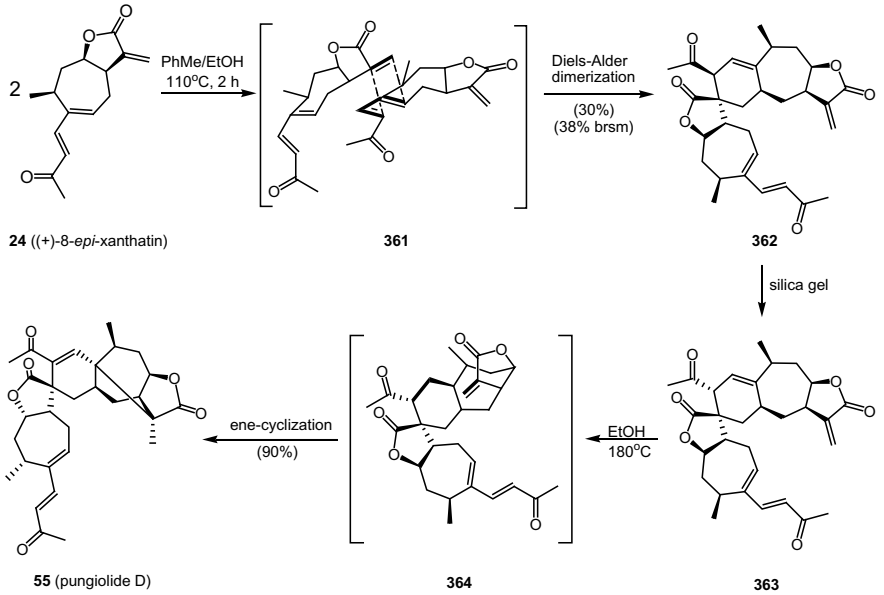

Fig. 14 Tang's synthesis of pungiolide D (**55**)

under high temperature (180°C) in EtOH with a yield of 40%. The overall process is outlined in Fig. 14.

5 Conclusions

The current chapter endeavors to provide useful information on the phytochemistry and biological testing of *Xanthium* species. To date, 15 members of this genus, including *X. brasilicum*, *X. canadense*, *X. catharticum*, *X. cavanillesii*, *X. chinense*, *X. indicum*, *X. italicum*, *X. macrocarpum*, *X. mongolicum*, *X. orientale*, *X. pennsylmnicum*, *X. pungens*, *X. sibiricum*, *X. spinosum*, and *X. strumarium* have been investigated in some detail phytochemically. Chemical constituents characterized by *Xanthium* species have included terpenoids, simple phenols, sulfur- and nitrogen-containing compounds, lignans, sterols, flavonoids, quinones, coumarins, and fatty acids. Among 300 secondary metabolites reported to date, sesquiterpenoids of the xanthanolide type are characteristic of the genus *Xanthium*. The dimeric xanthanolides, mongolides D (**39**) and E (**40**), pungiolides A–O (**52**–**60**), and thiazinediones **184**–**199** were new when first reported. Gas chromatography-mass spectrometric analysis has shown the widespread presence of terpenoids in *Xanthium* essential oils, while HPLC procedures have been useful to demonstrate the occurrence of caffeoyl phenolic derivatives with the members of this genus. *Xanthium* plant extracts and

several isolated compounds have been evaluated for their cytotoxicity and antioxidant, antibacterial, antifungal, and antidiabetes activities. Constituents from the two species *X. spinosum* and *X. strumarium* have been the main topics of such biological examinations. Despite the fact that there have been many in vitro biological and some in vivo pharmacological studies on *Xanthium* extracts and their purified constituents, the basic knowledge of the mechanisms of cellular action involved is not yet very well understood.

Acknowledgments The writing of this chapter was supported by the Vietnam Academy of Science and Technology, Vietnam-2020.

References

1. Tang J, Huang L, Liu Y, Toshmatov Z, Zhang C, Shao H (2020) Two phytotoxins isolated from the pathogenic fungus *Alternaria* sp. of the invasive weed *Xanthium italicum*. Chem Biodivers 17:e2000043
2. Fan W, Fan L, Peng C, Zhang Q, Wang L, Li L, Wang J, Zhang D, Peng W, Wu C (2019) Traditional uses, botany, phytochemistry, pharmacology, pharmacokinetics and toxicology of *Xanthium strumarium* L.: a review. Molecules 24:359
3. Kamboj A, Saluja AK (2010) Phytopharmacological review of *Xanthium strumarium* L. (Cocklebur). Int J Green Pharm 4:129
4. Bader A, Giner RM, Martini F, Schinella GR, Ríos JL, Braca A, Prieto JM (2013) Modulation of COX, LOX and NFκB activities by *Xanthium spinosum* L. root extract and ziniolide. Fitoterapia 91:284
5. Chen WH, Liu WJ, Wang Y, Song XC, Guang Y (2015) A new naphthoquinone and other antibacterial constituents from the roots of *Xanthium sibiricum*. Nat Prod Res 29:739
6. Cheng Y, Fu J, Chen L, Li LL, Qu J (2019) Diterpenoid glycosides and monoterpenoid glycosides from the fruits of *Xanthium chinense*. J Asian Nat Prod Res 21:207
7. Hwang HS, Wang Z, Ha NY, Soon SL (2016) *Xanthium strumarium* as an inhibitor of α-glucosidase, protein tyrosine phosphatase 1β, protein glycation and $ABTS^+$ for diabetic and its complication. Molecules 21:1241
8. Qu J, Deng S, Li L, Liu Y, Li Y, Ma S, Chen X, Yu S (2016) Cytotoxic dimeric xanthanolides from fruits of *Xanthium chinense*. Phytochemistry 132:115
9. Wang L, Wang J, Li F, Liu X, Chen B, Tang YX, Wang MK (2013) Cytotoxic sesquiterpene lactones from aerial parts of *Xanthium sibiricum*. Planta Med 79:661
10. Xia Z, Xu T, Zhang H, Chen Y, Xu W, Zhou G (2020) Bioactive sulfur-containing compounds from *Xanthium sibiricum*, including a revision of the structure of xanthiazinone. Phytochemistry 173:112293
11. Karmakar UK, Ishikawa N, Toume K, Arai MA, Sadhu SK, Ahmed F, Ishibashi M (2015) Sesquiterpenes with TRAIL-resistance overcoming activity from *Xanthium strumarium*. Bioorg Med Chem 23:4746
12. Jiang H, Xing X, Yan M, Guo X, Yang L, Yang L (2019) Two new monoterpene glucosides from *Xanthium strumarium* subsp. *sibiricum* with their anti-inflammatory activity. Nat Prod Res 33:3383
13. Kaur M, Kamboj A, Rathour A, Saluja AK (2015) Isolation and characterization of constituents from the leaves of *Xanthium strumarium* and their evaluation for antioxidant and antimicrobial potential. Nat Prod Chem Res 3:2
14. Hsu FL, Chen YC, Cheng JT (2000) Caffeic acid as active principle from the fruit of *Xanthium strumarium* to lower plasma glucose in diabetic rats. Planta Med 66:228

15. Lavault M, Landreau A, Larcher G, Bouchar JP, Pagniez F, Pape PL, Richomme P (2005) Antileishmanial and antifungal activities of xanthanolides isolated from *Xanthium macrocarpum*. Fitoterapia 76:363
16. Yoon JH, Lim HJ, Lee HJ, Kim HD, Jeon R, Ryu JH (2008) Inhibition of lipopolysaccharide-induced inducible nitric oxide synthase and cyclooxygenase-2 expression by xanthanolides isolated from *Xanthium strumarium*. Bioorg Med Chem Lett 18:2179
17. Son NT (2020) A mini-review of the tropical plant *Cratoxylum fomosum* ssp. *pruniflorum*: phytochemical and pharmacological aspects. Lett Org Chem 17:327
18. Son NT, Elshamy AI (2021) Flavonoids and other non-alkaloidal constituents of genus *Erythrina*: phytochemical review. Comb Chem High Throughput Screen 24:20
19. Son NT (2019) Genus *Miliusa*: a review of phytochemistry and pharmacology. Evid Based Compl Alt Med 2019:ID 8314693
20. Son NT (2019) Genus *Erythrophleum*: botanical description, traditional use, phytochemistry and pharmacology. Phytochem Rev 18:571
21. Son NT (2019) Secondary metabolites of genus *Pandanus* – an aspect of phytochemistry. Mini-Rev Org Chem 16:689
22. Son NT (2018) Notes on the genus *Paramignya*: phytochemistry and biological activity. Bull Fac Pharm Cairo Univ 56:1
23. Son NT (2017) An overview of the genus *Prismatomeris*: phytochemistry and biological activity. Bull Fac Pharm Cairo Univ 55:11
24. Son NT (2017) A review on the medicinal plant *Dalbergia odorifera* species: phytochemistry and biological activity. Evid Based Compl Alt Med 2017:ID 7142370
25. Ahmed AA, Jakupovic J, Bohlmann F, Regaila HA, Ahmed AM (1990) Sesquiterpene lactones from *Xanthium pungens*. Phytochemistry 29:2211
26. Macro JA, Sanz-Cervera JF, Corral J, Carda M, Jakupovic J (1993) Xanthanolides from *Xanthium*: absolute configuration of xanthinol, isoxanthanol and their C-4 epimers. Phytochemistry 34:1569
27. de Riscula EC, Fortuna MA, Catalan CAN, Diaz JG, Herz W (1994) Xanthanolides and a bis-norxanthanolide from *Xanthium cavanillessii*. Phytochemistry 35:1588
28. He Y, Lei D, Yang Q, Qi H, Almira K, Askar D, Jin LPL (2019) *Xanthium orientale* subsp. *italicum* (Moretti) Greuter: bioassay-guided isolation and its chemical basis of antitumor cytotoxicity. Nat Prod Res 35:2433
29. Omar AA, Elrashidy EM, Ghazy NA, Metwally AM, Ziesche J, Bohlmann F (1984) Xanthanolides from *Xanthium spinosum*. Phytochemistry 23:915
30. Shi YS, Liu YB, Ma SG, Li Y, Qu J, Li L, Yuan SP, Hou Q, Li YH, Jiang JD, Yu SS (2015) Bioactive sesquiterpenes and lignans from the fruits of *Xanthium sibiricum*. J Nat Prod 78:1526
31. Mahmoud AA (1998) Xanthanolides and xanthane epoxide derivatives from *Xanthium strumarium*. Planta Med 64:724
32. Ahmed AA, Mahmoud AA, El-Gamal AA (1999) A xanthanolide diol and a dimeric xanthanolide from *Xanthium* species. Planta Med 65:470
33. Cumanda J, Marinoni G, Bernardi MD, Vidari G, Finzi PV (1991) New sesquiterpenes from *Xanthium catharticum*. J Nat Prod 54:460
34. Lee CL, Huang PC, Hsieh PW, Hwang TL, Hou YY, Chang FR, Wu YC (2008) (–)-Xanthienopyran, a new inhibitor of superoxide anion generation by activated neutrophils, and further constituents of the seeds of *Xanthium strumarium*. Planta Med 74:1276
35. Nour AMM, Khalid SA, Kaiser M, Brun R, Abdallah WE, Schmidt TJ (2009) The antiprotozoal activity of sixteen Asteraceae species native to Sudan and bioactivity guided isolation of xanthanolides from *Xanthium brasilicum*. Planta Med 75:1363
36. Bohlmann F, Singh P, Joshi KC, Singh CL (1982) Xanthanolides from *Xanthium indicum*. Phytochemistry 21:1441
37. Olivaro C, Rostan V, Bandera D, Moyna G, Vazquez A (2016) Xanthane sesquiterpenoids from the roots and flowers of *Xanthium cavanillesii*. Nat Prod Res 30:2238
38. Pinel B, Audo G, Mallet S, Lavault M, Poype FDL, Seraphin D, Richomme P (2007) Multigrams scale purification of xanthanolides from *Xanthium macrocarpum*. J Chromatogr A 1151:14

39. Yuan Z, Zheng X, Zhao Y, Liu Y, Zhou S, Wei C, Hu Y, Shao H (2018) Phytotoxic compounds isolated from leaves of the invasive weed *Xanthium spinosum*. Molecules 23:2840
40. Kawazu K, Nakajima S, Ariwa M (1979) Xanthumin and 8-*epi*-xanthatin as insect development inhibitors from *Xanthium canadense* Mill. Experientia 35:1294
41. Malik MS, Sangwan NK, Dhindsa KS (1992) Xanthanolides from *Xanthium strumarium*. Phytochemistry 32:206
42. Bui VB, Liu ST, Zhu JJ, Xiong J, Zhao Y, Yang GX, Xia G, Hu JF (2012) Sesquiterpene lactones from aerial parts of *Xanthium sibiricum* and their cytotoxic effects on human cancer cell lines. Phytochem Lett 5:685
43. Mogib MA, Dawidar AM, Methwally MA, Elzahab MB (1991) Xanthanolides from *Xanthium spinosum*. Phytochemistry 30:3461
44. Olivaro C, Vazquez A (2009) A new bioactive xanthanolide from *Xanthium cavanillesii*. Nat Prod Res 23:388
45. Zhang SJ, Liu H, Li J, Wang J, Zhang WZ (2015) Study on chemical constituents from whole herbs of *Xanthium mongolicum*. Zhongcaoyao 46:329
46. Favier LS, Maria Alejandra OM, Wendel GH, Borkowski EJ, Giordano OS, Pelzer L, Tonn CE (2005) Anti-ulcerogenic activity of xanthanolide sesquiterpenes from *Xanthium cavanillesii* in rats. J Ethnopharmacol 100:260
47. Hu D, Yang S, Yuan C, Han G, Shen H (2012) Isolation and identification of chemical consitutents in *Xanthium sibiricum*. Zhongcaoyao 43:640
48. Winters TE, Geissman TA, Safir D (1969) Sesquiterpene lactones of *Xanthium* species. Xanthanol and isoxanthanol, and correlation of xanthinin with ivalbin. J Org Chem 34:153
49. Xu F, Xiao C, Xue L, Lei M, Hu L (2017) Two new dimeric xanthanolides isolated from *Xanthium mogolium* Kitag plant. Tetrahedron Lett 58:1312
50. Piacente S, Pizza C, de Tommasi ND, Simone FD (1996) Sesquiterpene and diterpene glycosides from *Xanthium spinosum*. Phytochemistry 41:1357
51. Fei WP, Dong DS, Jing Q, Shan YS (2018) A new dimeric xanthanolide from fruits of *Xanthium chinense*. Zhongguo Zhong Yao Za Zhi 43:532
52. Babakhodzhaev A, Kasymov SZ, Sidyakin GP (1973) Xanthatin from *Xanthium spinosum*. Chem Nat Compd 4:559
53. Bohlmann F, Zdero C, (1981) An isomer of xanthanol from *Xanthium orientale*. Phytochemistry 20:2429
54. Chen J, Wang R, Shi YP (2013) Chemical constituents from *Fructus Xanthii*. Zhongcaoyao 44:1717
55. Erosa IR, Huang Y, Hickie RA, Sutherland RG, Barl B (2007) Xanthatin and xanthinosin from the burs of *Xanthium strumarium* L. as potential anticancer agents. Can J Physiol Pharmacol 85:1160
56. Ginesta-Perla E, Garcia-Breijo FJ, Primo-Yufera E (1994) Antimicrobial activity of xanthatin from *Xanthium spinosum* L. Lett Appl Microbiol 18:206
57. Kanauchi M, Shibano T, Shindo H, Suzuki M, Kakuta T, Yoshizawa K, Koizumi T (1999) Structure of antibacterial substance in extract of Cocklebur leaves used for preparation of wheat-Koji (qu) described in the Chinese classic "Chi-min-yao-shu" and its effect on the growth of bacteria and yeasts. Food Sci Technol Res 5:323
58. Nibret E, Youns M, Krauth-Siegel RL, Wink M (2011) Biological activities of xanthatin from *Xanthium strumarium* leaves. Phytother Res 25:1883
59. Romero M, Zanuy M, Rosell E, Cascante M, Piulats J, Front-Bardia M (2015) Opimization of xanthatin extraction from *Xanthium spinosum* L. and its cytotoxic, anti-angiogenesis and antiviral properties. Eur J Med Chem 90:491
60. Dominguez XA, Perez FM, Leyter L (1971) Xanthinin and β-sitosterol from *Xanthium orientale*. Phytochemistry 10:2828
61. Geisssman TA, Deuel P, Bonde EK, Addicott FA (1954) Xanthinin: a plant growth-regulating compound from *Xanthium pennsylvanicum*. J Am Chem Soc 76:685
62. Khafagy SM, Metwally AM (1970) Isolation of a crystalline sesquiterpenic keto-lactone from *Xanthium occidentale*. Planta Med 18:318

63. Tahara T, Sakuda Y, Kodama M, Fukazawa Y, Ito S (1980) Structures of xantholides A and B, two new guaianolides from *Xanthium canadense* Mill. Tetrahedron Lett 21:1861
64. Tanaka N, Yazawa T, Aoyama K, Murakami T (1976) Chemische Untersuchungen der Inhaltsstoffe von *Xanthium canadense* MILL. Chem Pharm Bull 24:1419
65. Zhang XQ, Ye WC, Jiang RW, Yin ZQ, Zhao SX, Mak TCW, Yao XS (2006) Two new eremophilanolides from *Xanthium sibiricum*. Nat Prod Res 20:1265
66. Shi YS, Li L, Liu YB, Ma SG, Li Y, Qu J, Liu Q, Shen ZF, Chen XG, Yu SS (2015) A new thiophene and two new monoterpenoids from *Xanthium sibiricum*. J Asian Nat Prod Res 17:1039
67. Zhi C, Lun W, Bin C, Fu L, Mingkui W (2011) Chemical constituents from *Fructus Xanthii*. Chin J App Environ Biol 17:350
68. Jiang H, Yang L, Liu C, Hou H, Wang Q, Wang Z, Yang B, Kuang H (2013) Four new glycosides from the fruit of *Xanthium sibiricum* Patr. Molecules 18:12464
69. Wang Y, Han T, Xue LM, Han P, Zhang QY, Huang BK, Zhang H, Ming QL, Peng W, Qin LP (2010) Hepatotoxicity of kaurene glycosides from *Xanthium strumarium* L. fruits in mice. Pharmazie 66:445
70. Craig JC, Mole ML, Billters S, El-Feraly F (1976) Isolation and identification of the hypoglycemic agent, carboxyatractylate, from *Xanthium strumarium*. Phytochemistry 15:1178
71. Qiu Y, Wang Y, Dong W, Zheng C (2010) Chemical constituents in fruits of *Xanthium sibiricum*. Zhongguo Huaxue Zazhi 20:214
72. MacLeod JK, Moeller PDR, Franke FP (1990) Two toxic kaurene glycosides from the burrs of *Xanthium pungens*. J Nat Prod 53:451
73. Jiang H, Ma GX, Yang L, Xing XD, Yan ML, Zhang YY, Wang QH, Kuang HX, Xu XD (2016) Rearranged *ent*-kauranoid glycosides from the fruits of *Xanthium strumarium* and their antiproliferative activity. Phytochem Lett 18:192
74. Thang LQ, Hang TT (2018) Study on chemical constituents of *Xanthium strumarium* L. growing in Quang Binh province, Vietnam. Int J Green Herbal Chem 7:105
75. Zhang X, Qi J, Ye W, Zhao S (2004) Chemical constituents from *Xanthium sibiricum*. Xuebao 35:404
76. Han T, Li HL, Hu Y, Zhang QY, Huang BK, Zheng HC, Rahman K, Qin LP (2006) Phenolic acids in Fructus Xanthii and determination of contents of total phenolic acids in different species and populations of *Xanthium* in China. J Chin Integr Med 4:194
77. Ma YT, Huang MC, Hsu FL, Chang HF (1998) Thiazinedione from *Xanthium strumarium*. Phytochemistry 48:1083
78. Dai YH, Cui Z, Wang D, Li JL (2008) Chemical constituents from the fruits of *Xanthium sibiricum*. J Shenyang Univ 25:630
79. Yoon HN, Lee MY, Kim JK, Suh HW, Lim SS (2013) Aldose reductase inhibitory compounds from *Xanthium strumarium*. Arch Pharmacal Res 36:1090
80. Han T, Li H, Zhang Q, Zheng H, Qin L (2006) New thiazinediones and other components from *Xanthium strumarium*. Chem Nat Compd 42:567
81. Sato M, Hiraoka A, Watanabe M (1993) Inhibition of γ-irradiation induced oxidation of chlorogenate by 1,3-dicaffeoylquinate in *Xanthium occidentale*. Phytochemistry 33:1357
82. Taranto AG, Costa SCC, Leite AFH, De Sa MS, Soares MBP, Mussi MM, Branco A (2017) Caffeoylquinic acids from antiplasmodial active extract of *Xanthium cavanillesii* fruits and their molecular modelling studies. Nat Prod Res 31:729
83. Agata I, Goto S, Hanato T, Nishibe S, Okuda T (1993) 1,3,5-Tri-*O*-Caffeoylquinic acid from *Xanthium strumarium*. Phytochemistry 33:508
84. Lee BH, Yoon SH, Kim YS, Kim SK, Moon BJ, Bae YS (2008) Apoptotic cell death through inhibition of protein kinase CKII activity by 3,4-dihydroxybenzaldehyde purified from *Xanthium strumarium*. Nat Prod Res 22:1441
85. Yin RH, Bai X, Feng T, Dong ZJ, Li ZH, Liu JK (2016) Two new compounds from *Xanthium strumarium*. J Asian Nat Prod Res 18:354
86. Dai YH, Cui Z, Li JL, Wang D (2008) A new thiaziedione from the fruits of *Xanthium sibiricum*. J Asian Nat Prod Res 10:303

87. Zhi C, Lun W, Fu L, Wang MK (2013) A new thiazinedione glycoside from the fruit of *Xanthium sibiricum*. Chem Nat Compd 49:977
88. Peng W, Ming QL, Han Ping, Zhang QY, Jiang YP, Zheng CJ, Han T, Qing LP (2014) Anti-allergic rhinitis effect of caffeoylxanthiazonoside isolated from fruits of *Xanthium strumarium* L. in rodent animals. Phytomedicine 21:824
89. Qin L, Han T, Li H, Zhang Q, Zheng H (2006) A new thiazinedione from *Xanthium strumarium*. Fitoterapia 77:245
90. Mahmoud AA, Ahmed AA, Al-Shiry SS, Spring O (2005) A new heterocylic glucoside from the fruits of *Xanthium pungens*. Nat Prod Res 19:585
91. Mahmoud AA, Ahmed AA, Linuma M, Tanaka T, Takahashi Y, Naganawa H (1995) Xanthienopyran, A novel thienocyclopentapyran in fruits of *Xanthium pungens*. Tetrahedron Lett 36:8985
92. Kan S, Chen G, Han C, Chen Z, Song X, Ren M, Jiang H (2011) Chemical constituents from the roots of *Xanthium sibiricum*. Nat Prod Res 25:1243
93. Jiang H, Yang L, Xing XD, Yan ML, Guo XY, Su XL, Sun YP, Yang BY, Wang QH, Kuang HX (2018) Study on lignans from *Xanthii Fructus*. Zhongguo Zhong Yao Za Zhi 43:2097
94. Shi Y, Liu Y, Li Y, Li L, Qu J, Ma S, Yu S (2014) Chiral resolution and absolute configuration of a pair of rare racemic spirodienone sesquineolignans from *Xanthium sibiricum*. Org Lett 16:5406
95. Jiang H, Yang L, Ma GX, Xing XD, Yan ML, Zhang YY, Wang QH, Yang BY, Kuang HX, Xu XD (2017) New phenylpropanoid derivatives from the fruits of *Xanthium sibiricum* and their anti-inflammatory activity. Fitoterapia 117:11
96. Nakajima S, Kawazu K (1977) Tridec-1-ene-3,5,7,9,11-pentayne, an ovicidal substance from *Xanthium canadense*. Agric Biol Chem 41:1801
97. Vurro M, Evidente A, Andolfi A, Zonno MC, Giordano F, Motta A (1998) Brefeldin A and α,β-dehydrocurvularin, two phytotoxins from *Alternaria zinnia*e, a biocontrol agent of *Xanthium occidentale*. Plant Sci 138:67
98. Li G, Kusari S, Golz C, Laatsch H, Strohmann C, Spiteller M (2017) Epigenetic modulation of endophytic *Eupenicillium* sp. LG41 by a histone deacetylase inhibitor for production of decalin-containing compounds. J Nat Prod 80:983
99. Ostlund RE, Racette SB, Stenson WF (2003) Inhibition of cholesterol absorption by phytosterol-replete wheat germ compared with phytosterol-depleted wheat germ. Am J Clin Nutr 77:1385
100. Son NT, Harada K, Cuong NM, Fukuyama Y (2017) Two new carboxyethylflavanones from the heartwood of *Dalbergia tonkinensis* and their antimicrobial activities. Nat Prod Commun 11:1721
101. El-Gawad AA, Elshamy A, El-Nasser AEG, Gaara A, Assaeed A (2019) Volatiles profiling, allelopathic activity, and antioxidant potentiality of *Xanthium strumarium* leaves essential oil from Egypt: evidence from chemometrics analysis. Molecules 24:584
102. Sharifi-Rad J, Hoseini-Alfatemi SM, Sharifi-Rad M, Sharifi-Rad M, Iriti M, Sharifi-Rad M, Sharifi-Rad R, Raeisi S (2015) Phytochemical compositions and biological activities of essential oil from *Xanthium strumarium* L. Molecules 20:7034
103. Mitic VD, Ilic MD, Jovanovic O, Stankov-Jovanovic VP, Markovic MS, Stojanovic GS (2019) Essential oil composition of *Xanthium italicum* from Serbia. Nat Prod Commun 2019. https://doi.org/10.1177/1934578XI9849968
104. Sakuda Y, Tahara T (1982) The consituents of essential oil from *Xanthium canadense* Mill. J Oleo Sci 31:151
105. Han T, Zhang H, Li HL, Zhang QY, Zheng HC, Qin LP (2008) Composition of supercritical fluid extracts of some *Xanthium* species from China. Chem Nat Compd 44:655
106. Taher HA, Ubuiergo GO, Talenti ECJ (1985) Constituents of the essential oil of *Xanthium cavanillesii*. J Nat Prod 48:857
107. Son NT, Tsuyoshi Y, Yoshiyasu F (2018) Chemotaxonomic aspects of the constituents of the plant *Dalbergia tonkinensis*. Biochem Syst Ecol 78:98

108. Han T, Li HL, Zhang QY, Han P, Zheng HC, Rahman K, Qin LP (2007) Bioactivity guided fractionation for anti-inflammatory and analgesic properties and constituents of *Xanthium strumarium* L. Phytomedicine 14:825
109. Wang Z, Hwang SH, Huang B, Lim SS (2015) Identification of tyrosinase specific inhibitors from *Xanthium strumarium* fruit extract using ultrafltration-high performance liquid chromatography. J Chromatogr B 1002:319
110. Han T, Zhang QY, Zhang H, Wen J, Wang Y, Huang BK, Rahman K, Zheng HC, Qin LP (2009) Authentication and quantitative analysis on the chemical profile of *Xanthium* fruit (Cang-Er-Zi) by high performance liquid chromatography-diode-array detection tandem mass spectroscopy method. Anal Chim Acta 634:272
111. Lawson SK, Sharp LG, Powers CN, McFeeters RL, Satyal P, Setzer WN (2020) Volatile compositions and antifungal activities of native American medicinal plants: focus on the Asteraceae. Plants 9:126
112. Esmaeili A, Rustaiyan A, Akbari MT, Moazami N, Masoudi S, Amiri H (2006) Composition of the essential oils of *Xanthium strumarium* L. and *Cetaurea solstitialis* L. from Iran. J Essent Oil Res 18:427
113. Ferrer JP, Zampini IC, Cuello AS, Francisco M, Romero A, Valdivia D, Gonzalez M, Salas C, Lamar AS, Isla MI (2016) Cytotoxic compounds from aerial organs of *Xanthium strumarium.* Nat Prod Commun 11:371
114. Shao H, Zhang YM, Nam P, Huang XL, Zhang C (2013) Chemical composition and phytotoxic activity of the volatile oil of invasive *Xanthium italicum* Morretti from Xinjiang, China. J Arid Land 5:324
115. Fang XY, Zhang H, Zhao L, Tan S, Ren QC, Wang L, Shen XF (2018) A new xanthatin analogue 1β-hydroxy-5α-chloro-8-*epi*-xanthatin induces apoptosis through ROS-mediated ERK/p38 MAPK activation and JAK2/STAT3 inhibition in human hepatocellular carcinoma. Biochimie 152:43
116. Liu R, Shi D, Zhang J, Li X, Han X, Yao X, Fang J (2018) Xanthatin promotes apoptosis via inhibiting thioredoxin reductase and eliciting oxidative stress. Mol Pharmaceutics 15:3285
117. Al-Mekhlafi FA, Abutaha N, Mashaly AMA, Nasr FA, Ibrahim KE, Wadaan MA (2017) Biological activity of *Xanthium strumarium* seed extracts on different cancer cell lines and *Aedes caspius*, *Culex pipiens* (Diptera: Culicidae). Saudi J Biol Sci 24:817
118. Piloto-Ferrer J, Sanchez-Lamar A, Francisco M, González ML, Merino N, Aparicio G, Pérez C, Rodeiro I, Lopes MTP (2019) *Xanthium strumarium´*s xanthatin induces mitotic arrest and apoptosis in CT26WT colon carcinoma cells. Phytomedicine 57:236
119. Kim J, Jung KH, Ryu HW, Kim DY, Oh SR, Hong SS (2019) Apoptotic effects of *Xanthium strumarium* via PI3K/AKT/mTOR pathway in hepatocellular carcinoma. Evid-Based Complement Alternat Med 2019:ID2176701
120. Chang HW, Liu PF, Tsai WL, Hu WH, Hu YC, Yang HC, Lin WY, Weng JR, Shu CW (2019) *Xanthium strumarium* fruit extract inhibits ATG4B and diminishes the proliferation and metastatic characteristics of colorectal cancer cells. Toxins 11:313
121. Patil MVK, Kandhare AD, Bhise SD (2012) Anti-arthritic and anti-inflammatory activity of *Xanthium strumarium* L. ethanolic extract in Freund's complete adjuvant induced arthritis. Biomed Aging Pathol 2:6
122. Ju A, Cho YC, Cho S (2015) Methanol extracts of *Xanthium sibiricum* roots inhibit inflammatory responses via the inhibition of nuclear factor-κB (NF-κB) and signal transducer and activator of transcription 3 (STAT3) in murine macrophages. J Ethnopharmacol 174:74
123. Lin B, Han P, Yue W, Ma XQ, Rahman K, Zheng CJ, Qin LP, Han T (2014) Anti-arthritic activity of *Xanthium strumarium* L. extract on complete Freund's adjuvant induced arthritis in rats. J Ethnopharmacol 155:248
124. Hossen MJ, Cho JY, Kim D (2016) PDK1 in NF-κB signaling is a target of *Xanthium strumarium* methanolic extract-mediated anti-inflammatory activities. J Ethnopharmacol 190:251
125. Sridharamurthy NB, Yogananda R, Srinivas U (2011) In-vitro antioxidant and antilipidemic activities of *Xanthium strumarium* L. Curr Trends Biotechnol Pharm 5:1362

126. Ingawale AS, Sadi MB, Nguyen LT, Ngan TB (2018) Optimization of extraction conditions and assessment of antioxidant, α-glucosidase inhibitory and antimicrobial activities of *Xanthium strumarium* L. fruits. Biocatal Agric Biotechnol 14:40
127. Aranjani JM, Rao CM, Manuel A, Rao JV, Udupa N, Hebbar K (2012) Acute and subacute toxicity of chloroform and hexane extracts of root of *Xanthium strumarium*. Comp Clin Pathol 21:1223
128. Xue LM, Zhang QM, Han P, Jiang YP, Yan RD, Wang Y, Rahman K, Jia M, Han T, Qin LP (2014) Hepatotoxic constituents and toxicological mechanism of *Xanthium strumarium* L. fruits. J Ethnopharmacol 152:272
129. Yu J, Song MZ, Wang J, Li YF, Lin P, Que L, Bao Z (2013) In vitro cytotoxicity and in vivo acute and chronic toxicity of *Xanthii Fructus* and its processed product. BioMed Res Int 2013:ID 403491
130. Talakal TS, Dwivedi SK, Sharma SR (1995) In vitro and in vivo antitrypanosomal activity of *Xanthium strumarium* leaves. J Ethnopharmacol 49:141
131. Yokoe H, Yoshida M, Shishido K (2008) Total synthesis of (–)-xanthatin. Tetrahedron Lett 49:3504
132. Matsumoto K, Koyachi K, Shindo M (2013) Asymmetric total syntheses of xanthatin and 11,13-dihydroxanthatin using a stereocontrolled conjugate allylation to γ-butenolide. Tetrahedron 69:1043
133. Kummer DA, Brenneman JB, Martin SF (2005) Application of a domino intramolecular enyne metathesis/cross metathesis reaction to the total synthesis of (+)-8-*epi*-xanthatin. Org Lett 7:4621
134. Feng J, Lei X, Bao R, Li Y, Xiao C, Hu L, Tang Y (2017) Enantioselective and collective total syntheses of xanthanolides. Angew Chem 129:16541

Nguyen Thi Thuy Linh obtained her Master's degree in the field of organic chemistry at Irkutsk National Research Technical University, Russia. She was then appointed as a Ph.D. student at the Graduate University of Science and Technology in 2019. From 2018, she started working as a chemical researcher at the Institute of Chemistry, Vietnam Academy of Science and Technology, Hanoi, Vietnam. Her current work has emphasis on the isolation and structure elucidation of natural products from Vietnamese medicinal plants. Ph.D. student Linh is working on several pharmaceutical projects, and has published six scientific articles over the last two years.

Ninh The Son obtained his Ph.D. degree from Tokushima Bunri University, Tokushima, Japan, with support from the Japanese Society for the Promotion of Science (JSPS) in 2019. He is currently working at the Institute of Chemistry, Vietnam Academy of Science and Technology (VAST), as a chemistry researcher. His main research involves natural products chemistry and molecular simulation. Dr. Son received an excellence award in 2020 from VAST. He played a significant role in several projects and is an author of 72 scientific articles, among which he authored six SCI/SCIE review articles as a single author. He has also edited a book and served as a corresponding author of a book chapter. He is a member of the editorial boards of various scientific journals such as "Natural Product Research" and of the book series "Studies in Natural Products Chemistry".

Nguyen Thi Thu Ha was born in 1976. She is a researcher at the Department of Applied Biochemistry, Institute of Chemistry, Vietnam Academy of Science and Technology (VAST). She obtained a Ph.D. degree, with a major in biochemistry, at the Institute of Biotechnology, VAST in 2016. Her main research interests are in the isolation and structure determination of natural products. She is also keen on implementing and developing new biological assays and has published over 40 scientific articles.

Nguyen Thanh Tra was born in 1976. She graduated from Vietnam National University in the field of biology. She received a Ph.D. degree in biochemistry at the Institute of Biotechnology, Vietnam Academy of Science and Technology, where she has been since 2016. She has published over 40 articles and her research interests are on natural products chemistry and biological assays. Her skills are closely focused on isolating naturally occurring compounds from medicinal plants and developing bioassay methods.

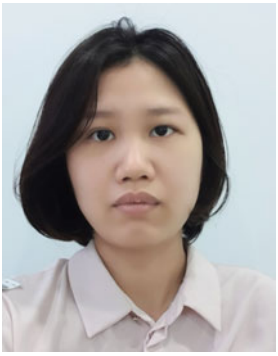

Le Thi Tu Anh was born in 1986. She received a Master's degree in Experimental Biology from Hanoi University of Science in 2013. She received a Ph.D. degree in Organic Chemistry from the University of Science and Technology, Hanoi, Vietnam, in 2019. She is currently working at the Institute of Chemistry, Vietnam Academy of Science and Technology as a biochemist. Her research interests are on natural compounds from native plants and their medical applications. She participated in many pharmaceutical research projects. She has authored more than 30 scientific articles.

Sibao Chen obtained a Ph.D. degree from the Peking Union Medical College, Beijing, China. Dr. Chen's research focuses on the discovery of pharmacologically active compounds from traditional Chinese medicine and natural products. Currently, his research aims to isolate and identify active compounds against nasopharyngeal carcinoma and triple negative breast cancer from natural products. He has co-authored over 40 peer-reviewed articles

Nguyen Van Tuyen was born in 1961. He received his Ph.D. under the supervision of Prof. Dr. P. F. Vlad in 1991. From May 1993 to October 1995, he worked as a postdoctoral fellow at the Department of Pharmacognosy, College of Pharmacy, University of Illinois at Chicago, USA under the supervision of Prof. Dr. H. S. H. Fong. From 1998 to 2003, he performed postdoctoral research at the Department of Organic Chemistry, Faculty of Bioscience Engineering, Ghent University, Belgium, under the guidance of Prof. Dr. N. De Kimpe. From 1993, he has been the Head of the Laboratory of Medicinal Chemistry at the Institute of Chemistry, Vietnam Academy of Science and Technology. He served as Deputy Director of the Institute of Chemistry during the period of 2007–2010, and Director from 2010 to now. He became a full professor in 2013, and has authored over 120 peer-reviewed articles. His research is focused on the synthesis of biologically active compounds.

Biologically Active Constituents from Plants of the Genus *Desmos*

Nguyen Thi Thuy Linh and Ninh The Son

Contents

N. T. T. Linh
Department of Chemistry, Institute of Chemistry, Graduate University of Science and Technology, Vietnam Academy of Science and Technology, 18 Hoang Quoc Viet, Caugiay, Hanoi, Vietnam
e-mail: thuylinh1992.bk@gmail.com

N. T. Son (✉)
Department of Applied Biochemistry, Institute of Chemistry, Vietnam Academy of Science and Technology, 18 Hoang Quoc Viet, Caugiay, Hanoi, Vietnam
e-mail: yamantson@mail.com

A. D. Kinghorn, H. Falk, S. Gibbons, Y. Asakawa, J.-K. Liu, V. M. Dirsch (eds.),
Progress in the Chemistry of Organic Natural Products 116,
https://doi.org/10.1007/978-3-030-80560-9_5

1 Introduction

Desmos is a genus of nearly 60 trees and shrubs in the family Annonaceae [1]. The early reports of the traditional uses of *Desmos* species centered mainly on plants found in South Asia, with species from other areas of the world gradually being investigated later [2]. *Desmos* species have a long history of medicinal applications and have been used to treat a variety of diseases. To give a typical example, *D. chinensis*, locally named "Sai-Yut" in Thailand, has been employed for the alleviation of pyretic and dysenteric diseases [3]. Furthermore, *D. dumosus* roots and leaves have been utilized traditionally for their antimalarial, insecticidal, antirheumatic, antispasmodic, and analgesic effects [4]. Flavonoids, alkaloids, miscellaneous phenolic compounds, terpenoids, phytosterols, and other types of bioactive metabolites have been found as constituents among members of the genus *Desmos*. Various sub-groups of flavonoids, in particular, have been recognized as typical constituents of *Desmos* and these exhibit a variety of bioactivities. For example, dihydrochalcones from *D. chinensis* displayed cytotoxicity against the growth of the MOLT-3, A549, HuCCA-1, and HepG2 cancer cell lines [5], while an extract of this plant promoted inhibition in a tyrosine kinase inhibitory assay [6]. Other types of biological reports of crude extracts, fractions, and secondary metabolites obtained from this genus include those of their antimicrobial, anti-HIV, antioxidative, anti-inflammatory, and aromatase inhibition effects.

Although several reports on specialized secondary metabolites from medicinal plants of genus *Desmos* have appeared in the literature, there have been no systematic reviews to provide general information about this genus. Therefore, this overview has been performed by identifying significant studies on the phytochemistry and biological properties of purified constituents of the genus *Desmos*, using international scientific sources, including The Plant List, and the Web of Science, SciFinder, Google Scholar, Scopus, Science Direct, and PubMed databases as well as journals from leading publishing companies, and also Ph.D. dissertations. The references were obtained during the period from 1982 to the present.

2 Phytochemical Investigations

The search for bioactive compounds from natural sources involves using a combination of chromatographic methods (such as the use of silica gel, Sephadex LH-20, RP-18, HPLC, GC–MS, and LC–MS) for isolation procedures and spectroscopic and spectrometric techniques (such as NMR, MS, CD, UV, and IR) for structure elucidation [7–16]. Based on the use of these well-established methods, phytochemical studies on *Desmos* species have resulted in the purification and characterization of various classes of secondary metabolites. A total of 211 constituents are summarized in Table 1 and in Figs. 2, 3, 4, 5, and 6. The names of these compounds are listed in alphabetical order. Phytochemicals derived from *Desmos* species include

Table 1 Chemical constituents of species of the genus *Desmos*

No.	Compound	Species	Ref.
Flavonoids			
Flavones			
1	Alpinetin	*D. dasymaschalus* twigs	[17]
2	Chrysin	*D. chinensis* whole plants, *D. cochinchinensis* leaves and flowers	[2, 18–20]
3	Cryptochrysin	*D. dumosus* leaves	[21]
4	Desmethoxykanugin	*D. dasymaschalus* twigs	[17]
5	Desmorostratone	*D. rostrata* stem bark	[22]
6	Desmoscochinflavone A	*D. cochinchinensis* leaves	[18]
7	Desmoscochinflavone B	*D. cochinchinensis* leaves	[18]
8	Desmosdumotin B (or Dasytrichon)	*D. dumosus* twigs and roots, *D. rostrata* stem bark	[21–23]
9	Desmosflavone (or 6,8-Dimethyl-7-methoxy-5-hydroxyflavone)	*D. chinensis* seed, *D. cochinchinesis* fruits	[24–26]
10	5,7-Dihydroxy-6-methyl-8-formylflavone	*D. dumosus* twigs	[21]
11	5,6-Dihydroxy-7-methoxyflavone	*D. chinensis* leaves	[27]

(continued)

Table 1 (continued)

No.	Compound	Species	Ref.
12	6,7-Dimethoxy-5-hydroxyflavone	*D. chinensis* leaves	[27]
13	7,8-Dimethoxy-5-hydroxyflavone	*D. dasymaschalus* twigs	[17]
14	6,8-Dimethyl-7-methoxyflavone	*D. cochinchinensis* whole plants	[26]
15	Eucryphin (or 5,7-Dihydroxy-3-(α-*O*-L-rhamnopyranosyl)-4*H*-l-benzopyran-4-one)	*D. chinensis* leaves	[28]
16	Isounonal (or 5,7-Dihydroxy-8-methyl-6-formylflavone)	*D. chinensis* leaves, stem bark and seeds, *D. cochinchinesis* fruits and roots, *D. dumosus* twigs	[5, 24, 25, 27, 29, 30]
17	Matteuorien (or 5,7-Dihydroxy-6,8-dimethylflavone)	*D. chinensis* leaves, *D. dumosus* twigs	[21, 30]
18	Mosloflavone	*D. chinensis* branches and leaves, *D. cochinchinesis* fruits, *D. dumosus* roots, *D. pedunculosus* aerial parts	[24, 28, 31–33]
19	Negletein	*D. chinensis* leaves, roots, and branches, *D. dumosus* roots, *D. pedunculosus* aerial parts	[28, 31–35]
20	Oroxylin A	*D. cochinchinesis* fruits	[24]
21	Quercitrin	*D. chinensis* leaves	[34]

(continued)

Table 1 (continued)

No.	Compound	Species	Ref.
22	Saiyunensis A (or Saiyutone A)	*D. chinensis* leaves	[3, 30]
23	Saiyunensis B (or Saiyutone B)	*D. chinensis* leaves	[3, 30]
24	Saiyunensis C (or Saiyutone C)	*D. chinensis* leaves	[3, 30]
25	Saiyunensis D (or Saiyutone D)	*D. chinensis* leaves	[3, 30]
26	Tectochrysin	*D. cochinchinensis* leaves and flowers	[18, 20]
27	Unonal (or 6-Formyl-5,7-dihydroxy-8-methylflavone)	*D. chinensis* leaves, stem bark, seeds, and roots, *D. cochinchinesis* fruits and whole plants	[5, 24–27, 30, 35]
28	Unonal-7-methyl ether	*D. chinensis* stem bark	[5]
29	Isounonal-7-methyl ether	*D. chinensis* stem bark	[5]
Flavanones			
30	Astilbin ((*2R,3R*)-3′,4′,5,7-tetrahydroxyflavanon-*3α*-L-rhamnopyranoside)	*D. chinensis* leaves	[28, 34]
31	(*S*)-5-Hydroxy-6,8,8-trimethyl-2-phenyl-2,3-dihydro-4*H*-chromene-4,7(8*H*)-dione	*D. dumosus* roots	[27]
32	Cochinine A	*D. cochinchinesis* fruits	[24]
33	Demethoxymatteucinol	*D. chinensis* roots and seeds, *D. cochinchinensis* whole plants and fruits, *D. dumosus* roots and twigs, *D. grandifolius* roots	[21, 24–26, 35–38]

(continued)

Table 1 (continued)

No.	Compound	Species	Ref.
34	Desmal (or 8-Formyl-2,5,7-trihydroxy-6-methylflavanone)	*D. chinensis* leaves and stems, *D. dumosus* twigs	[21, 30, 39]
35	Desmethoxymatteucinol-7-methyl ether (or 6,8-Dimethyl-5-hydroxy-7-methoxyflavanone)	*D. chinensis* roots, *D. cochinchinesis* roots and fruits, *D. dumosus* roots	[24, 35, 37, 40]
36	Desmosal (5,7-dihydroxy-6-formyl-8-methylflavanone)	*D. chinensis* seeds, *D. dumosus* twigs	[21, 25]
37	(–)-(2*S*)-Desmoscochinflavanone A	*D. cochinchinensis* leaves	[18]
38	(–)-(2*S*)-Desmoscochinflavanone B	*D. cochinchinensis* leaves	[18]
39	(+)-(2*S*)-Desmosdumosone	*D. dumosus* twigs	[21]
40	Desmosflavanone II (or 7-Hydroxy-5-methoxy-8-formyl-6-methyl-flavanone)	*D. cochinchinensis* roots	[41]
41	Dichamanetin	*D. cochinchinensis* leaves	[18]
42	5,6-Dihydroxy-7-methoxy-dihydroflavone	*D. chinensis* leaves, *D. cochinchinesis* fruits	[24, 34]
43	(2*S*)-5,7-Dihydroxy-8-formyl-6-methylflavanone	*D. dumosus* roots	[37]
44	(+)-(2*R*)-7,8-Dimethoxy-5-hydroxyflavanone	*D. dumosus* leaves	[21]
45	6-Formyl-2,5,7-trihydroxy-8-methylflavanone	*D. chinensis* leaves	[30]

(continued)

Table 1 (continued)

No.	Compound	Species	Ref.
46	Desmosdumotin A (5-Hydroxy-7-methoxy-8-formyl-3-benzoyl-2,6-dimethyl-2*S*,3*R*-dihydrochromone)	*D. dumosus* roots	[27, 42]
47	8-Hydroxynaringenin-4′-methyl ether	*D. dasymaschalus* twigs	[17]
48	Isochamanetin	*D. cochinchinensis* leaves	[18]
49	Isolawinal	*D. grandifolius* roots	[35]
50	Lawinal (or 7-Demethyllaridal)	*D. chinensis* stem bark and seeds, *D. cochinchinensis* roots and fruits, *D. dumosus* roots, *D. grandifolius* roots	[5, 24, 25, 27, 29, 35, 37, 38]
51	5-*O*-Methylchamanetin	*D. dumosus* leaves	[21]
52	8-Methyl-5-hydroxy-7-methoxyflavanone	*D. cochinchinesis* roots	[40]
53	(+)-(2*R*)-7-Methoxychamanetin	*D. dumosus* leaves	[21]
54	Pinocembrin	*D. cochinchinensis* leaves and flowers	[2, 18, 20]
55	Pinocembrin-7-*O*-benzoate	*D. cochinchinensis* leaves and flowers	[20]
Flavans			
56	4-*O*-Acetyldesmoflorin	*D. longiflorus* stem bark	[43]
57	Desmoflorin	*D. longiflorus* stem bark	[43]

(continued)

Table 1 (continued)

No.	Compound	Species	Ref.
58	Desmosflavan A	*D. cochinchinensis* leaves	[2]
59	Desmosflavan B	*D. cochinchinensis* leaves	[2]
60	4,7-Dihydroxyl-5-methoxyl-6-methyl-8-formylflavan	*D. chinensis* roots, *D. cochinchinensis* roots and fruits	[24, 29, 36, 40]
61	5,7-Dimethoxy-4-hydroxy-6,8-dimethylflavan	*D. cochinchinesis* roots	[40]
62	5,7-Dimethoxy-8-formyl-4-hydroxy-6-methylflavan	*D. cochinchinesis* roots	[40]
63	4,5-Dimethoxy-8-formyl-7-hydroxyflavan	*D. cochinchinesis* roots	[40]
64	4-*O*-Epidesmoflorin	*D. longiflorus* stem bark	[43]
65	8-Formyl-7-hydroxy-4α,5-dimethoxy-6-methylflavan	*D. cochinchinesis* roots and fruits	[24, 40]
66	5-Methoxy-8-formyl-4,7-dihydroxyflavan	*D. cochinchinesis* roots	[40]
Chalcones			
67	Cardamonin (or 2′,4′-Dihydroxy-6′-methoxychalcone)	*D. chinensis* whole plants, *D. cochinchinensis* leaves	[2, 19]
68	Desmosdumotin C	*D. dumosus* roots, *D. rostrata* stem bark	[4, 22]
69	2′,4′-Dihydroxy-3′-(2,6-dihydroxybenzyl)-6′-methoxychalcone	*D. chinensis* leaves	[44]
70	(2*E*)-(1-Hydroxy-3-phenylallyl)-5-methoxy-4,6,6-trimethylcyclohex-4-ene-1,3-dione	*D. dumosus* roots	[27]
71	2′-Hydroxy-4′,6′-dibenzyloxychalcone	*D. cochinchinensis* leaves and flowers	[20]

(continued)

Table 1 (continued)

No.	Compound	Species	Ref.
72	Leridal chalcone	*D. chinensis* stem bark	[5]
73	2-Methoxy-3-methyl-4,6-dihydroxy-5-(3′-hydroxy) cinnamoylbenzaldehyde	*D. dumosus* leaves and roots	[27, 33, 45]
74	3-Methyl-2,4,6-trihydroxy-5-(3′-hydroxy) cinnamoylbenzaldehyde	*D. chinensis* leaves	[27]
Dihydrochalcones			
75	Chinendihydrochalcone	*D. chinensis* stem bark	[5]
76	4,2′-Dihydroxy-3′,6′-dimethyl-4′,5′-dimethoxydihydrochalcone	*D. dunalii* leaves	[46]
77	2′,3′-Dihydroxy-4′,6′-dimethoxydihydrochalcone	*D. chinensis* leaves	[34]
78	4,2′-Dihydroxy-4′, 6′-dimethoxy-3′,5′-dimethyldihydrochalcone	*D. dunalii* leaves	[47]
79	4,2′-Dihydroxy-4′,5′,6′-trimethoxydihydrochalcone	*D. dunalii* leaves	[46, 47]
80	4,2′-Dihydroxy-4′,6′-dimethoxydihydrochalcone	*D. dunalii* leaves	[46, 47]
81	2,6-Dihydroxy-4-methoxydihydrochalcone	*D. cochinchinesis* fruits	[24]
82	2′,4′-Dihydroxy-5′-methyl-4′,6′-dimethoxydimethylchalcone	*D. dunalii* leaves	[46, 47]
Alkaloids			
Aristolactams			
83	10-Amino-3,6-dihydroxy-2,4-dimethoxyphenanthrene-1-carboxylic acid lactam	*D. dumosus* twigs	[21]
84	Aristolactam I	*D. dumosus* twigs	[21]
85	Aristolactam AII	*D. rostrata* stem bark	[1]
86	Aristolactam BII	*D. dumosus* twigs	[21]
87	Aristolactam BIII	*D. dumosus* twigs	[21]

(continued)

Table 1 (continued)

No.	Compound	Species	Ref.
88	Dasymaschalolactam A	*D. dasymaschalus* twigs	[17]
89	Dasymaschalolactam B	*D. dasymaschalus* twigs	[17]
90	Dasymaschalolactam C	*D. dasymaschalus* twigs	[17]
91	Dasymaschalolactam D	*D. dasymaschalus* twigs	[17]
92	Dasymaschalolactam E	*D. dasymaschalus* twigs	[17]
93	3,5-Dihydroxy-2,4-dimethoxyaristolactam	*D. dumosus* twigs	[21]
94	Enterocarpam-III	*D. dasymaschalus* twigs	[17]
95	Goniopedalin	*D. dasymaschalus* twigs	[17]
96	Griffithinam	*D. dasymaschalus* twigs	[17]
97	Oldhamactam	*D. dasymaschalus* twigs	[17]
98	Piperolactam D	*D. dumosus* twigs	[21]
99	Stismalactam	*D. dumosus* twigs	[21]
100	Taliscanine	*D. dasymaschalus* twigs	[17]

(continued)

Table 1 (continued)

No.	Compound	Species	Ref.
101	Velutinam	*D. dasymaschalus* twigs	[17]
Aporphines			
102	(–)-Anonaine	*D. tiebaghiensis* aerial parts	[48]
103	(–)-Asimilobine	*D. tiebaghiensis* aerial parts	[48]
104	(+)-Boldine	*D. tiebaghiensis* aerial parts	[48]
105	Dasymachaline	*D. dasymachalus* leaves	[49]
106	Desmorostratine	*D. rostrata* stem bark	[1]
107	Dicentrinone	*D. dasymachalus* leaves	[49]
108	Duguevalline	*D. dasymaschalus* twigs	[17]
109	(–)-Glaziovine	*D. tiebaghiensis* aerial parts	[48]
110	(+)-Isoboldine	*D. tiebaghiensis* aerial parts	[48]
111	(–)-Laurotetanine	*D. tiebaghiensis* aerial parts	[48]
112	Liriodenine	*D. cochinchinensis* twigs	[18]

(continued)

Table 1 (continued)

No.	Compound	Species	Ref.
113	Lysicamine	*D. cochinchinensis* twigs	[18]
114	(+)-*N*-Methyl-lauroteranine	*D. tiebaghiensis* aerial parts	[48]
115	(+)-*N*-Methylcoclaurine	*D. tiebaghiensis* aerial parts	[48]
116	(–)-Norushinsunine (Michelalbine)	*D. tiebaghiensis* aerial parts	[48]
117	Oxoanolobin	*D. chinensis* branches	[32]
118	Predicentrine	*D. rostrata* stem bark	[1]
119	(+)-Reticuline	*D. tiebaghiensis* aerial parts	[48]
120	3,9,11-Trimethoxy-1,2-methylenedioxy-oxoaporphine	*D. chinensis* branches	[32]
Protoberberines			
121	(–)-Discretarnine	*D. tiebaghiensis* aerial parts	[48]
122	Discretine	*D. rostrata* stem bark	[1]
123	Discretine *N*-oxide	*D. rostrata* stem bark	[1]
124	(–)-Stepholidine	*D. cochinchinensis* stems, *D. tiebaghiensis* aerial parts	[48, 50]
125	Dehydrodiscretine	*D. rostrata* stem bark	[1]
126	Pseudocolumbamine	*D. rostrata* stem bark	[1]
Others			
127	(–)-Pallidine	*D. tiebaghiensis* aerial parts	[48]

(continued)

Table 1 (continued)

No.	Compound	Species	Ref.
128	Desmosin	*D. dumosus* bark	[51]
Simple phenols			
Mono-hydroxy compounds			
129	Acetophenone	*D. chinensis* leaves and stem bark	[52]
130	3-Acetyl-2,4-dihydroxy-6-methoxy-5-methylbenzaldehyde	*D. chinensis* stem bark	[5]
131	Benzoic acid	*D. chinensis* roots, *D. cochinchinesis* fruits, leaves and twigs, *D. dumosus* roots, *D. grandifolius* roots	[18, 24, 35, 37, 38]
132	Benzyl alcohol	*D. chinensis* leaves and stem bark	[52]
133	4-Hydroxybenzaldehyde	*D. dasymaschalus* twigs	[17]
134	2-Hydroxybenzyl alcohol	*D. cochinchinensis* leaves	[18]
135	2-Methoxybenzoic acid	*D. chinensis* leaves	[30]
136	(2*S*,3*S*)-(3-Phenyloxiran-2-yl)methanol	*D. pedunculosus* aerial parts	[31]
Benzoate esters			
137	(2*S*,3*R*)-2-Benzoyloxy-1,3-dihydroxy-3-phenylpropane	*D. pedunculosus* aerial parts	[31]
138	(2*S*,3*R*)-3-Benzoyloxy-1,2-dihydroxy-3-phenylpropane	*D. pedunculosus* aerial parts	[31]
139	Benzyl 2,6-dihydroxybenzoate	*D. chinensis* leaves	[3]

(continued)

Table 1 (continued)

No.	Compound	Species	Ref.
140	Benzyl 2-hydroxy-5-methoxybenzoate	*D. chinensis* leaves	[3]
141	Benzyl 2-hydroxy-6-methoxybenzoate	*D. chinensis* leaves	[3]
142	Benzyl 2-hydroxybenzoate	*D. chinensis* leaves and stem bark	[3, 52]
143	Benzyl 2-methoxybenzoate	*D. chinensis* leaves sand stem bark	[5, 30]
144	Benzyl 3-hydroxybenzoate	*D. chinensis* leaves	[30]
145	Benzyl benzoate	*D. chinensis* leaves and stem bark, *D. cochinchinensis* leaves, *D. dasymaschalus* twigs, *D. dumosus* twigs, *D. pedunculosus* aerial parts	[17, 18, 21, 30, 31, 52]
146	Cinnamyl benzoate	*D. chinensis* leaves, *D. pedunculosus* aerial parts	[30, 31]
147	(2*S*,3*R*)-3-Chloro-2-hydroxy-3-phenylpropyl benzoate	*D. pedunculosus* aerial parts	[31]
148	Desmoscochin benzoate	*D. cochinchinensis* leaves	[18]
149	(2*S*,3*R*)-2-Hydroxy-3-methoxy-3-phenylpropyl benzoate	*D. pedunculosus* aerial parts	[31]

(continued)

Table 1 (continued)

No.	Compound	Species	Ref.
150	(2*S*,3*R*)-2,3-Dihydroxy-3-phenylpropyl benzoate	*D. pedunculosus* aerial parts	[31]
151	Grandiuvarone A (or 5-Acetoxy-6-benzoyloxymethyl-5*H*-oxepin-4-one)	*D. chinensis* leaves	[53]
152	Grandiuvarone B (or 5-acetoxy-3-benzoyloxymethyl-5*H*-oxepin-4-one)	*D. chinensis* leaves	[53]
153	2-Hydroxybenzyl benzoate	*D. cochinchinensis* leaves	[18]
154	2-Methoxybenzyl benzoate	*D. chinensis* leaves, *D. dasymaschalus* twigs, *D. pedunculosus* aerial parts	[17, 30, 31, 34]
155	2-Phenylethyl benzoate	*D. dasymaschalus* twigs	[17]
156	(2*S*,3*S*)-(3-Phenyloxiran-2-yl)methyl benzoate	*D. pedunculosus* aerial parts	[31]
Polyoxygenated cyclohexane and cyclohexene derivatives			
157	Desmoscochinchinene A	*D. cochinchinensis* leaves and flowers	[20]
158	Desmoscochinchinene B	*D. cochinchinensis* leaves and flowers	[20]
159	Desmoscochinchinene C	*D. cochinchinensis* leaves and flowers	[20]
160	Desmoscochinchinene D	*D. cochinchinensis* leaves and flowers	[20]
161	Desmoscochinchinene E	*D. cochinchinensis* leaves and flowers	[20]

(continued)

Table 1 (continued)

No.	Compound	Species	Ref.
162	(+)-Crotepoxide	*D. dasymaschalus* twigs	[17]
163	(1*R*,6*S*)-Cherrevenol A	*D. cochinchinensis* leaves and twigs	[20]
164	Flexuvarin B	*D. cochinchinensis* leaves and twigs	[18]
165	Flexuvarin C	*D. cochinchinensis* leaves and flowers	[20]
166	Flexuvarin D	*D. cochinchinensis* leaves and flowers, *D. dumosus* leaves	[18, 20, 21]
167	(–)-Zeylenol	*D. dasymaschalus* twigs	[17]
168	Zeylenone	*D. cochinchinensis* twigs	[18]
Terpenoids			
Sesquiterpenoids			
169	Alismoxide	*D. cochinchinensis* leaves	[54]
170	Cryptomeridiol	*D. cochinchinensis* leaves	[54]
171	4β,10α-Dihydroxy-aromadendrane	*D. cochinchinensis* leaves	[54]
172	4β,10β-Dihydroxy-aromadendrane	*D. cochinchinensis* leaves	[54]

(continued)

Table 1 (continued)

No.	Compound	Species	Ref.
173	1β,7α-Dihydroxy-eudesman-4-one	*D. cochinchinensis* leaves	[54]
174	4-Epicryptomeridiol	*D. cochinchinensis* leaves	[54]
175	α-Eudesmol	*D. chinensis* leaves and stem bark	[54]
176	β-Eudesmol	*D. chinensis* leaves and stem bark	[52]
177	11-Hydroxy-4α-methoxyselinane	*D. cochinchinensis* leaves	[54]
178	10β-Hydroxyisodauc-6-en-14-al	*D. cochinchinensis* leaves	[54]
179	5αH-Megastigm-7-ene-3α,4α,6β,9-tetrol	*D. cochinchinensis* leaves	[54]
180	Patchouli alcohol	*D. cochinchinensis* stems	[50]
181	Pipelol A	*D. cochinchinensis* leaves	[54]
182	Selin-4(15)-ene-1β,11-diol	*D. cochinchinensis* leaves	[54]
Triterpenoids			
183	Desmosinol	*D. cochinchinensis* stems	[55]
184	Heynic acid	*D. cochinchinensis* stems	[55]

(continued)

Table 1 (continued)

No.	Compound	Species	Ref.
185	15α-Hydroxy-24-methylenelanosta-7,9-(11)-dien-3-one	*D. longiflorus* stem bark	[56]
186	24-Methylene cycloartan- 3β,-21-diol	*D. cochinchinensis* stems	[55]
Diterpenoid			
187	Phytol	*D. chinensis* leaves and stem bark	[30, 52]
Phytosterols			
188	Daucosterol	*D. chinensis* seeds	[25]
189	β-Sitosterol	*D. chinensis* seeds, roots and branches, *D. cochinchinensis* whole plants, fruits, and stems, *D. dumosus* roots, *D. grandifolius* roots	[24–26, 32, 35, 37, 38, 50]
190	Stigmast-4-ene-3,6-dione	*D. dumosus* roots	[33]
191	Stigmastane-3,6-dione	*D. dumosus* roots	[33]
192	Stigmasterol	*D. chinensis* roots, *D. cochinchinesis* fruits, *D. dumosus* roots, *D. grandifolius* roots	[24, 35, 37, 38]
Oxepinones			
193	(–)-(5*R*)-Desmoscochinoxepinone A	*D. cochinchinensis* leaves and twigs	[18]
194	(–)-(5*R*)-Desmoscochinoxepinone B	*D. cochinchinensis* leaves	[18]

(continued)

Table 1 (continued)

No.	Compound	Species	Ref.
195	(–)-(5*R*)-Desmoscochinoxepinone C	*D. cochinchinensis* leaves	[18]
196	(–)-(5*R*)-Desmoscochinoxepinone D	*D. cochinchinensis* leaves	[18]
197	(–)-(5*R*)-Grandiuvarone	*D. cochinchinensis* twigs	[18]
Amides			
198	Allantoic acid	*D. chinensis* seeds	[25]
199	Desmocyclopeptide	*D. rostrata* stem bark	[22]
200	Dunaliine A	*D. dunalii* leaves	[47]
201	*N*-(*E*)-Feruloyltyramine	*D. dasymaschalus* twigs	[17]
202	Oleamide	*D. cochinchinensis* stems	[50]
203	Paprazine	*D. dasymaschalus* twigs	[17]
Fatty acid			
204	Desmosic acid	*D. cochinchinensis* stems	[50]
205	Ethyl linoleate	*D. cochinchinensis* stems	[50]

(continued)

Table 1 (continued)

No.	Compound	Species	Ref.
206	Stearic acid	*D. chinensis* seeds	[25]
207	Succinic acid	*D. chinensis* seed	[25]
Other types			
208	7-Methoxyisobenzofuran-1(3*H*)-one	*D. dasymaschalus* twigs	[17]
209	8-Methoxycoumarin	*D. dumosus* leaves	[21]
210	(+)-(1′*R*,2′*R*)-Phebalosin	*D. dumosus* leaves	[21]
211	DL-2,5,7,8-Tetramethyl-2-(4,8,12-trimethyltridecyl)-6-chromanol	*D. cochinchinensis* stems	[50]

flavonoids (**1**–**82**) (Fig. 2), alkaloids (**83**–**128**) (Fig. 3), miscellaneous phenols (**129**–**156**) (Fig. 4), polyoxygenated cyclohexane and cyclohexene derivatives (**156**–**168**) (Fig. 4), terpenoids (**169**–**187**) (Fig. 5), phytosterols (**188**–**192**) (Fig. 5), oxepinones (**193**–**197**) (Fig. 6), amides (**198**–**203**) (Fig. 6), fatty acids (**204**–**207**) (Fig. 6), and other compound types (**208**–**211**) (Fig. 6).

2.1 Flavonoids

2.1.1 Flavones

Flavonoids are the most commonly reported metabolites from *Desmos* species. Among 82 isolated compounds of this type (Table 1), 29 (**1**–**29**) may be classified in the flavone group and were found to be present in six *Desmos* species, namely, *D. chinensis* (Fig. 1a), *D. cochinchinensis* (Fig. 1b), *D. dasymaschalus*, *D. dumosus*, *D. pedunculosus*, and *D. rostrata* [2, 3, 5, 17–35]. As shown in Fig. 2, flavones from *Desmos* occur in both monomeric and dimeric forms and may be substituted by hydroxy, methyl, methoxy, glycosyl, and formyl groups. Chrysin (**2**), desmosflavone (**9**), isounonal (**16**), matteuorien (**17**), mosloflavone (**18**), negletein (**19**), and unonal (**27**) were all detected in at least two species each. Alpinetin (**1**), desmethoxykanugin (**4**), and 5,7-dihydroxy-6-methyl-8-formylflavone (**10**) are constituents observed in an EtOAc extract of the air-dried twigs of Thai *D. dasymaschalus* (syn. *Dasymascalon dasymaschalum*) [17]. Chrysin (**2**) was isolated from both *D. chinensis* whole plants and *D. cochinchinensis* leaves and flowers [2, 18–20], while its derivative cryptochrysin (**3**) was only characterized from *D. dumosus* leaves, to date [21]. Five compounds (**5**–**9**), namely, desmorostratone (**5**), desmoscochinflavones A (**6**) and B

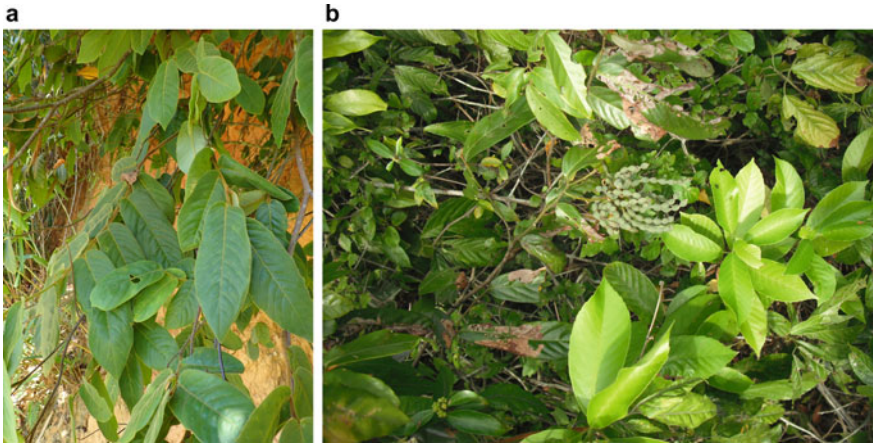

Fig. 1 Typical *Desmos* species: **a** *Desmos chinensis* and **b** *Desmos cochinchinensis*

(**7**), desmosdumotin B (**8**), and desmosflavone (**9**) were identified as new naturally occurring flavones and were isolated from *D. rostrata* stem bark, *D. cochinchinensis* leaves, *D. dumosus* roots, and *D. cochinchinesis* fruits, respectively [18, 22, 23, 26]. The leaves of *D. chinensis* proved to be a rich source of flavones, in which eight known compounds, including 5,6-dihydroxy-7-methoxyflavone (**11**), 6,7-dimethoxy-5-hydroxyflavone (**12**), eucryphin (**15**), isounonal (**16**), matteuorien

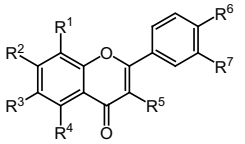

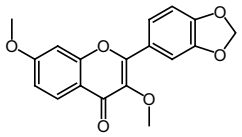

4

1 $R^1 = R^3 = R^5 = R^6 = R^7 = H$, $R^2 = OH$, $R^4 = OCH_3$
2 $R^1 = R^3 = R^5 = R^6 = R^7 = H$, $R^2 = R^4 = OH$
3 $R^1 = CH_3$, $R^2 = R^4 = OH$, $R^3 = R^5 = R^6 = R^7 = H$
6 $R^1 = X^1$, $R^2 = R^4 = OH$, $R^3 = R^5 = R^6 = R^7 = H$
7 $R^1 = X^2$, $R^2 = R^4 = OH$, $R^3 = R^5 = R^6 = R^7 = H$
9 $R^1 = R^3 = CH_3$, $R^2 = OCH_3$, $R^4 = OH$, $R^5 = R^6 = R^7 = H$
10 $R^1 = CHO$, $R^2 = R^4 = OH$, $R^3 = CH_3$, $R^5 = R^6 = R^7 = H$
11 $R^1 = R^5 = R^6 = R^7 = H$, $R^2 = OCH_3$, $R^3 = R^4 = OH$
12 $R^1 = R^5 = R^6 = R^7 = H$, $R^2 = R^3 = OCH_3$, $R^4 = OH$
13 $R^1 = R^2 = OCH_3$, $R^3 = R^5 = R^6 = R^7 = H$, $R^4 = OH$
14 $R^1 = R^3 = CH_3$, $R^2 = OCH_3$, $R^4 = R^5 = R^6 = R^7 = H$
16 $R^1 = CH_3$, $R^2 = R^4 = OH$, $R^3 = CHO$, $R^5 = R^6 = R^7 = H$
17 $R^1 = R^3 = CH_3$, $R^2 = R^4 = OH$, $R^5 = R^6 = R^7 = H$
18 $R^1 = R^5 = R^6 = R^7 = H$, $R^2 = R^3 = OCH_3$, $R^4 = OH$
19 $R^1 = R^5 = R^6 = R^7 = H$, $R^2 = OCH_3$, $R^3 = R^4 = OH$
20 $R^1 = R^5 = R^6 = R^7 = H$, $R^2 = R^4 = OH$, $R^3 = OCH_3$
21 $R^1 = R^3 = H$, $R^2 = R^4 = R^6 = R^7 = OH$, $R^5 = \alpha$-O-L-Rha
23 $R^1 = X^3$, $R^2 = X^4$, $R^3 = CH_3$, $R^4 = OH$, $R^5 = R^6 = R^7 = H$
25 $R^1 = CH_3$, $R^2 = X^4$, $R^3 = X^3$, $R^4 = OH$, $R^5 = R^6 = R^7 = H$
26 $R^1 = R^3 = R^5 = R^6 = R^7 = H$, $R^2 = OCH_3$, $R^4 = OH$
27 $R^1 = CH_3$, $R^2 = R^4 = OH$, $R^3 = CHO$, $R^5 = R^6 = R^7 = H$
28 $R^1 = CH_3$, $R^2 = OCH_3$, $R^3 = CHO$, $R^4 = OH$, $R^5 = R^6 = R^7 = H$
29 $R^1 = CHO$, $R^2 = OCH_3$, $R^3 = CH_3$, $R^4 = OH$, $R^5 = R^6 = R^7 = H$

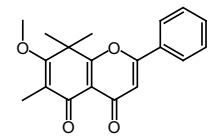

5

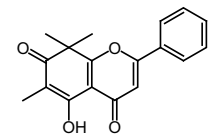

8

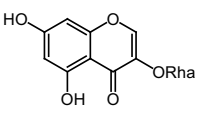

15

Rha =

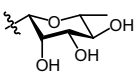

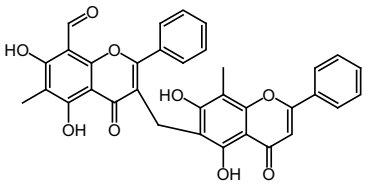

22

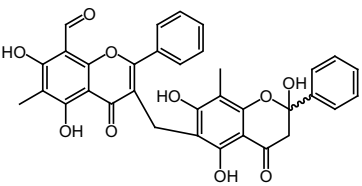

24

Fig. 2 Flavonoids from the genus *Desmos*

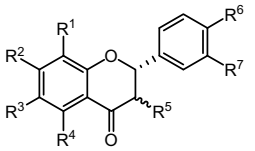

30 $R^1 = R^3 = H$, $R^2 = R^4 = R^6 = R^7 = OH$, $R^5 = \alpha$-*O*-L-Rha
32 $R^1 = CH_3$, $R^2 = OCH_3$, $R^3 = CHO$, $R^4 = OH$, $R^5 = R^6 = R^7 = H$
33 $R^1 = R^3 = CH_3$, $R^2 = R^4 = OH$, $R^5 = R^6 = R^7 = H$
35 $R^1 = R^3 = CH_3$, $R^2 = OCH_3$, $R^4 = OH$, $R^5 = R^6 = R^7 = H$
36 $R^1 = CH_3$, $R^2 = R^4 = OH$, $R^3 = CHO$, $R^5 = R^6 = R^7 = H$
37 $R^1 = R^5 = R^6 = R^7 = H$, $R^2 = R^4 = OH$, $R^3 = X^2$
38 $R^1 = R^5 = R^6 = R^7 = H$, $R^2 = R^4 = OH$, $R^3 = X^5$
40 $R^1 = CHO$, $R^2 = OH$, $R^3 = CH_3$, $R^4 = OCH_3$, $R^5 = R^6 = R^7 = H$
41 $R^1 = R^3 = X^6$, $R^2 = R^4 = OH$, $R^5 = R^6 = R^7 = H$
42 $R^1 = R^5 = R^6 = R^7 = H$, $R^2 = OCH_3$, $R^3 = R^4 = OH$
43 $R^1 = CHO$, $R^2 = R^4 = OH$, $R^3 = CH_3$, $R^5 = R^6 = R^7 = H$
47 $R^1 = R^2 = R^4 = OH$, $R^6 = OCH_3$, $R^3 = R^5 = R^7 = H$
48 $R^1 = R^5 = R^6 = R^7 = H$, $R^2 = R^4 = OH$, $R^3 = X^6$
49 $R^1 = CHO$, $R^2 = R^4 = OH$, $R^3 = CH_3$, $R^5 = R^6 = R^7 = H$
50 $R^1 = CH_3$, $R^2 = R^4 = OH$, $R^3 = CHO$, $R^5 = R^6 = R^7 = H$
51 $R^1 = X^6$, $R^2 = OH$, $R^3 = R^5 = R^6 = R^7 = H$, $R^4 = OCH_3$
52 $R^1 = CH_3$, $R^2 = OCH_3$, $R^3 = R^5 = R^6 = R^7 = H$, $R^4 = OH$
54 $R^1 = R^3 = R^5 = R^6 = R^7 = H$, $R^2 = R^4 = OH$
55 $R^1 = R^3 = R^5 = R^6 = R^7 = H$, $R^2 = BzO$, $R^4 = OH$

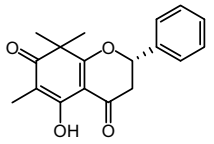

31

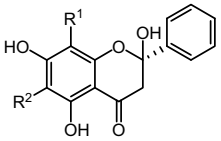

34 $R^1 = CHO$, $R^2 = CH_3$
39 $R^1 = R^2 = CH_3$
45 $R^1 = CH_3$, $R^2 = CHO$

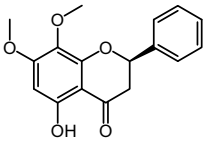

44 $R^1 = R^2 = OCH_3$, $R^3 = OH$
53 $R^1 = X^6$, $R^2 = OCH_3$, $R^3 = OH$

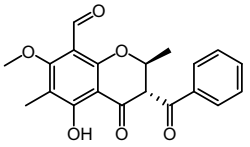

46

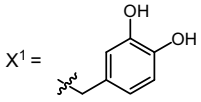

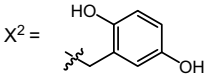

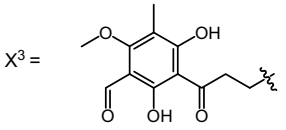

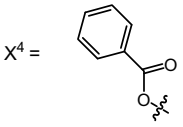

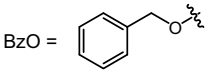

Fig. 2 (continued)

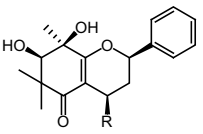

56 R = OAc
57 R = H
64 R = OH

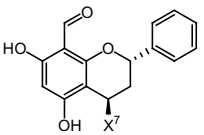

58

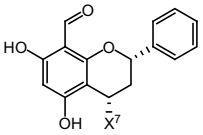

59

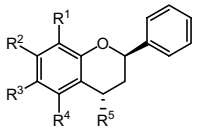

60 R^1 = CHO, R^2 = R^5 = OH, R^3 = CH_3, R^4 = OCH_3
61 R^1 = R^3 = CH_3, R^2 = R^4 = OCH_3, R^5 = OH
62 R^1 = CHO, R^2 = R^4 = OCH_3, R^3 = CH_3, R^5 = OH
63 R^1 = CHO, R^2 = OH, R^3 = H, R^4 = R^5 = OCH_3
65 R^1 = CHO, R^2 = OH, R^3 = CH_3, R^4 = R^5 = OCH_3
66 R^1 = CHO, R^2 = R^5 = OH, R^3 = H, R^4 = OCH_3

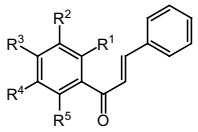

67 R^1 = R^3 = OH, R^2 = R^4 = H, R^5 = OCH_3
69 R^1 = OCH_3, R^2 = H, R^3 = R^5 = OH, R^4 = X^8
70 R^1 = R^5 = OH, R^2 = CH_3, R^3 = OCH_3, R^4 = CHO
71 R^1 = R^3 = BzO, R^2 = R^4 = H, R^5 = OH
72 R^1 = R^5 = OH, R^2 = CHO, R^3 = OCH_3, R^4 = CH_3

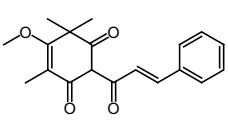

68

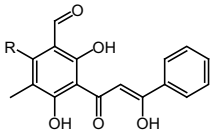

73 R = OCH_3
74 R = OH

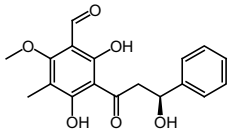

75

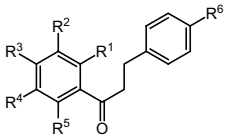

76 R^1 = R^4 = CH_3, R^2 = R^3 = OCH_3, R^5 = R^6 = OH
77 R^1 = R^3 = OCH_3, R^2 = R^6 = H, R^4 = R^5 = OH
78 R^1 = R^3 = OCH_3, R^2 = R^4 = CH_3, R^5 = R^6 = OH
79 R^1 = R^2 = R^3 = OCH_3, R^4 = H, R^5 = R^6 = OH
80 R^1 = R^3 = OCH_3, R^2 = R^4 = H, R^5 = R^6 = OH
81 R^1 = R_5 = OH, R^2 = R^4 = R^5 = H, R^3 = OCH_3, R^6 = OH
82 R^1 = R^3 = OCH_3, R^2 = CH_3, R^4 = H, R^5 = R^6 = OH

X^7 =

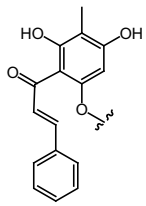

X^5 =

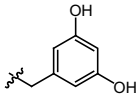

X^6 =

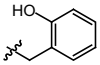

X^8 =

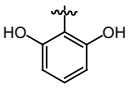

BzO =

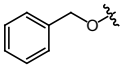

Fig. 2 (continued)

(**17**), mosloflavone (**18**), negletein (**19**), quercitrin (**21**), and unonal (**27**), were identified (Table 1). Notably, four new biflavones, saiyutones A–D (**22–25**), were isolated from a CH_2Cl_2 extract of *D. chinensis* leaves, collected in Thailand [3]. Similarly, a new derivative of compound **27**, isounonal-7-methyl ether (**29**), was precipitated from the CH_2Cl_2 extract of *D. chinensis* stem bark as a pale-yellow solid [5]. Moreover, another known compound, namely, unonal-7-methyl ether (**28**), was also detected [5].

2.1.2 Flavanones

Further to chromatographic column separation and NMR structural determination work on *Desmos* species, altogether 26 flavanones have been obtained, and these are summarized in Table 1. *Desmos* flavanones were detected in various parts of *D. chinensis*, *D. cochinchinensis*, *D. dasymaschalus*, *D. dumosus*, and *D. grandifolius* [2, 5, 18, 20, 21, 24–30, 34–40, 42]. Most of these isolated flavanones are present in the form of the 2*S*- configuration, and glycosylation occurs occasionally. Among *Desmos* flavanones, some compounds isolated have been found more frequently than others. For instance, demethoxymatteucinol (**33**) is characteristic of *D. chinensis* roots and seeds, *D. cochinchinensis* whole plants and fruits, *D. dumosus* roots and twigs, and *D. grandifolius* roots [21, 24–26, 35–38]. Also, desmethoxymatteucinol-7-methyl ether (**35**) occurs in *D. chinensis* roots, *D. cochinchinesis* roots and fruits, and *D. dumosus* roots [24, 35, 37, 40], while lawinal (**50**) was found to be present in *D. chinensis* stem bark and seeds, *D. cochinchinensis* roots and fruits, *D. dumosus* roots, and *D. grandifolius* roots [5, 24, 25, 27, 29, 37, 38]. In contrast, 13 constituents, including astilbin (**30**), (*S*)-5-hydroxy-6,8,8-trimethyl-2-phenyl-2,3-dihydro-4*H*-chromene-4,7(8*H*)-dione (**31**), cochinine A (**32**), dichamanetin (**41**), (2*S*)-5,7-dihydroxy-8-formyl-6-methylflavanone (**43**), 6-formyl-2,5,7-trihydroxy-8-methylflavanone (**45**), 8-hydroxynaringenin-4′-methyl ether (**47**), isochamanetin (**48**), isolawinal (**49**), 5-*O*-methylchamanetin (**51**), 8-methyl-5-hydroxy-7-methoxyflavanone (**52**), and pinocembrin (**53**), and its 7-*O*-benzoate (**54**), were observed in the genus *Desmos* for the first time (Table 1). Phytochemical investigations on *Desmos* species have also stimulated interest due to the characterization of new flavanones. Thus, desmal (**34**) and desmosal (**36**) are two new formyl flavanone derivatives, which were purified from the leaves and seeds of *D. chinensis*, respectively [25, 39]. Two further new flavanones, namely, (–)-(2*S*)-desmoscochinflavanones A (**37**) and B (**38**), have been purified from an EtOAc extract of Chinese *D. cochinchinensis* leaves [18], whereas desmosflavanone II (**40**), an additional new flavanone, was isolated from its roots [41]. In turn, (+)-(2*S*)-desmosdumosone (**39**) is a new flavanone obtained from Thai *D. dumosus* twigs, while two analogs with a 2*R*-configuration, (+)-(2*R*)-7,8-dimethoxy-5-hydroxyflavanone (**44**) and (+)-(2*R*)-7-methoxychamanetin (**53**), were found to be present in its leaves [21]. Desmosdumotin A (**46**) is a new flavanone isolated from an EtOH (85%) extract of Chinese *D. dumosus* roots [42]. The assignment of

compound **46** with the (2*S*,3*R*)-configuration was supported by single-crystal X-ray crystallography [42].

2.1.3 Flavans

The flavans are an additional group of flavonoids from *Desmos* species, particularly from *D. chinensis*, *D. cochinchinensis*, and *D. longiflorus*. Herein, a list of 11 isolated metabolites of this type is provided in Table 1 and Fig. 2 [2, 24, 29, 36, 40, 43]. Significantly, most of these were isolated from Nature for the first time. Desmoflorin (**57**), and its derivatives **56** and **64**, are new flavans obtained from the stem bark of *D. longiflorus* [43]. Desmosflavans A (**58**) and B (**59**), two new chalcone-flavan hybrid compounds from a CH_2Cl_2 extract of Thai *D. cochinchinensis* leaves, were assigned with (2*S*,*4S*) and (2*S*,4*R*)-configurations, respectively [2]. While searching for aromatase inhibitory agents from medicinal plants, Prachyawarakorn et al. (2013) reported the isolation and NMR determination of the four new flavans, 5,7-dimethoxy-4-hydroxy-6,8-dimethylflavan (**61**), 5,7-dimethoxy-8-formyl-4-hydroxy-6-methylflavan (**62**), 4,5-dimethoxy-8-formyl-7-hydroxyflavan (**63**), and 5-methoxy-8-formyl-4,7-dihydroxyflavan (**66**), in addition to two known analogs, 4,7-dihydroxy-5-methoxyl-6-methyl-8-formylflavan (**60**) and 8-formyl-7-hydroxy-4α,5-dimethoxy-6-methylflavan (**65**), from a CH_2Cl_2 extract of Thai *D. cochinchinensis* roots. Using a combination of the Dess-Martin periodiane reaction and ECD spectroscopy, the configurations of these newly isolated flavans were assigned as (2*S*,4*R*) at carbons C-2 and C-4 [40].

2.1.4 Chalcones and Dihydrochalcones

Among the flavonoids, the chalcone sub-group has a considerable number of biomedical and food chemistry applications [12]. Based on their structural properties, chalcones derived from *Desmos* species can be divided into two major groups, namely, chalcones **67**–**74** and the α,β-dihydroxylated type, **75**–**82** (Table 1 and Fig. 2). *Desmos chinensis*, *D. cochinchinensis*, *D. dumosus*, and *D. rostrata* are the main sources of these chalcones [2, 4, 5, 19, 20, 22, 27, 33, 44, 45], while dihydrochalcones have been found commonly in various parts of *D. chinensis*, *D. cochinchinensis*, and *D. dunalii* [5, 24, 34, 46, 47].

Both *D. chinensis* and *D. cochinchinensis* contain the chalcone cardamonin (**67**) [2, 19]. The novel cytotoxic chalcone, desmosdumotin C (**68**), was characterized from *D. dumosus* roots and was then detected in *D. rostrata* stem bark [4, 22]. Similarly, the chalcone 2′,4′-dihydroxy-3′-(2,6-dihydroxybenzyl)-6′-methoxychalcone (**68**) was isolated from *D. chinensis* leaves for the first time [44]. *Desmos dumosus* roots also contain two known chalcone derivatives, (2*E*)-(1-hydroxy-3-phenylallyl)-5-methoxy-4,6,6-trimethylcyclohex-4-ene-1,3-dione (**70**), and 2-methoxy-3-methyl-4,6-dihydroxy-5-(3′-hydroxy)cinnamoylbenzaldehyde (**73**) [27, 33]. Within the genus *Desmos*, 2′-hydroxy-4′,6′-dibenzyloxychalcone (**71**) was found only in *D.*

cochinchinensis leaves and flowers, whereas leridal chalcone (**72**) and 3-methyl-2,4,6-trihydroxy-5-(3′-hydroxy)cinnamoylbenzaldehyde (**74**) are characteristic of *D. chinensis* stem bark and leaves, respectively [5, 20, 27].

Among the dihydrochalcones, eight such constituents have been identified to date. *Desmos* dihydrochalcones are characterized by hydroxylation and/or methoxylation at the aromatic carbons (Fig. 2). Chinendihydrochalcone (**75**), with hydrogenation at carbon Cβ (δ_C 69.9 ppm in $CDCl_3$), was obtained as a new metabolite that was isolated from *D. chinensis* stem bark [5]. Abdullah and Awang (2005) reported a chromatographic separation and NMR structure elucidation procedure leading to four dihydrochalcones from a CH_2Cl_2 extract of Malaysian *D. dunalii* leaves, including 4,2′-dihydroxy-3′,6′-dimethyl-4′,5′-dimethoxydihydrochalcone (**76**), 4,2′-dihydroxy-4′,6′-dimethoxy-3′,5′-dimethyldihydrochalcone (**78**), 4,2′-dihydroxy-4′,5′,6′-trimethoxydihydrochalcone (**79**), 4,2′-dihydroxy-4′,6′-dimethoxydihydrochalcone (**80**), and 2′,4′-dihydroxy-5′-methyl-4′,6′-dimethoxydihydrochalcone (**82**) [46]. Also, 2′,3′-dihydroxy-4′,6′-dimethoxydihydrochalcone (**77**) and 2,6-dihydroxy-4-methoxydihydrochalcone (**81**) were found as typical dihydrochalcones present in Vietnamese *D. chinensis* leaves and *D. cochinchinesis* fruits, respectively [24, 34].

2.2 Alkaloids

A large number of alkaloidal constituents have been reported both from the genus *Desmos* and various other genera of the plant family Annonaceae [57]. Phytochemical investigations on *Desmos* species have resulted in the isolation and determination of 46 alkaloidal metabolites (**83**–**128**) (Table 1 and Fig. 3). *Desmos* alkaloids belong to various structural classes, but aristolactam derivatives are predominant. Aristolactam derivatives occur in *D. dasymaschalus* and *D. dumosus* as well as in *D. rostrata* [1, 17, 21]. Very recently, Suthiphasilp et al. (2021) reported that besides flavonoids, the EtOAc extract of Thai *D. dumosus* also contained seven aristolactam-type derivatives, including 10-amino-3,6-dihydroxy-2,4-dimethoxyphenanthrene-1-carboxylic acid lactam (**83**), aristolactam I (**84**), aristolactam BII (**86**), aristolactam BIII (**87**), 3,5-dihydroxy-2,4-dimethoxyaristolactam (**93**), piperolactam D (**98**), and stismalactam (**99**). Significantly, an α-glucosidase inhibitory EtOAc extract of Thai *D. dasymaschalus* twigs was found to contain five new aristolactams, dasymaschalolactams A–E (**88–92**), in addition to six known analogs, enterocarpam-III (**94**), goniopedalin (**95**), griffithinam (**96**), oldhamactam (**97**), taliscanine (**100**), and velutinam (**101**) [21].

Aporphines **102**–**120** are a second class of alkaloids found among *Desmos* species [1, 17, 18, 32, 48, 49]. *Desmos tiebaghiensis* is thought to be a main source of these derivatives. Leboeuf et al. (1982) applied an acid–base extraction method on *D. tiebaghiensis* aerial parts that led to the isolation of ten aporphines, consisting of (−)-anonaine (**102**), (−)-asimilobine (**103**), (+)-boldine (**104**), (−)-glaziovine (**109**), (+)-isoboldine (**110**), (–)-laurotetanine (**111**), (+)-*N*-methyl lauroteranine (**114**), (+)-*N*-methylcoclaurine (**115**), (−)-norushinsunine (**116**), and (+)-reticuline (**119**), with

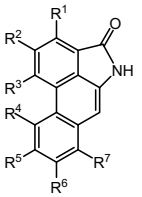

83 $R^1 = R^3 = OCH_3$, $R^2 = R^5 = OH$, $R^4 = R^6 = R^7 = H$
86 $R^1 = R^4 = R^5 = R^6 = R^7 = H$, $R^2 = R^3 = OCH_3$
87 $R^1 = R^4 = R^6 = R^7 = H$, $R^2 = R^3 = R^5 = OCH_3$
88 $R^1 = R^2 = R^3 = R^7 = OCH_3$, $R^4 = R^5 = R^6 = H$
89 $R^1 = R^2 = R^3 = R^4 = OCH_3$, $R^5 = R^6 = R^7 = H$
90 $R^1 = R^2 = R^3 = OCH_3$, $R^4 = OH$, $R^5 = R^6 = R^7 = H$
91 $R^1 = R^2 = R^4 = OCH_3$, $R^3 = OH$, $R^5 = R^6 = R^7 = H$
92 $R^1 = R^4 = R^7 = H$, $R^2 = OH$, $R^3 = R^5 = R^6 = OCH_3$
93 $R^1 = R^3 = OCH_3$, $R^2 = R^4 = OH$, $R^5 = R^6 = R^7 = H$
94 $R^1 = R^4 = R^6 = H$, $R^2 = OH$, $R^3 = R^5 = R^7 = OCH_3$
95 $R^1 = R^3 = OCH_3$, $R^2 = OH$, $R^4 = R^5 = R^6 = R^7 = H$
96 $R^1 = R^4 = R^5 = R^6 = H$, $R^2 = R^7 = OCH_3$, $R^3 = OH$,
97 $R^1 = R^2 = R^3 = OCH_3$, $R^4 = R^5 = R^6 = H$, $R^7 = OH$
98 $R^1 = OH$, $R^2 = OCH_3$, $R^3 = R^4 = R^5 = R^6 = R^7 = H$
99 $R^1 = R^2 = R^3 = OCH_3$, $R^5 = OH$, $R^4 = R^6 = R^7 = H$
100 $R^1 = R^4 = R^5 = R^6 = H$, $R^2 = R^3 = R^7 = OCH_3$
101 $R^1 = R^4 = R^5 = R^6 = H$, $R^2 = R^3 = OCH_3$, $R^7 = OH$

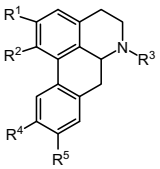

103 $R^1 = OH$, $R^2 = OCH_3$, $R^3 = R^4 = R^5 = H$
104 $R^1 = OH$, $R^2 = OCH_3$, $R^3 = CH_3$, $R^4 = R^5 = H$
110 $R^1 = R^4 = OCH_3$, $R^2 = R^5 = OH$, $R^3 = CH_3$
111 $R^1 = R^2 = R^4 = OCH_3$, $R^3 = H$, $R^5 = OH$
113 $R^1 = OH$, $R^2 = R^4 = R^5 = OCH_3$, $R^3 = CH_3$
120 $R^1 = R^2 = R^4 = OCH_3$, $R^3 = CH_3$, $R^5 = OH$

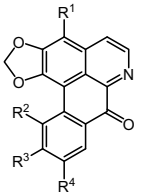

107 $R^1 = R^2 = H$, $R^3 = R^4 = OCH_3$,
108 $R^1 = R^2 = R^4 = OCH_3$, $R^3 = H$
112 $R^1 = R^2 = R^3 = R^4 = H$
117 $R^1 = R^2 = R^3 = H$, $R^4 = OH$

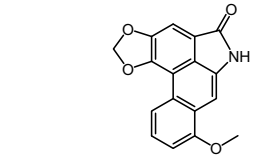

84

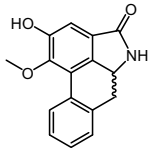

85

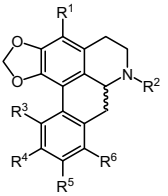

102 $R^1 = R^2 = R^3 = R^4 = R^5 = R^6 = H$
106 $R^1 = R^5 = R^6 = OCH_3$, $R^2 = R^3 = R^4 = H$
114 $R^1 = R^3 = R^5 = OCH_3$, $R^2 = R^4 = R^6 = H$

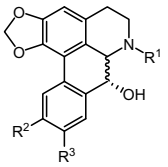

105 $R^1 = CH_3$, $R^2 = R^3 = OCH_3$
116 $R^1 = R^2 = R^3 = H$

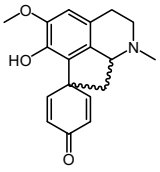

109

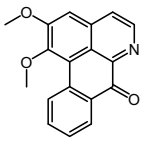

118

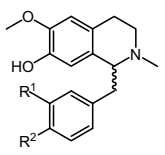

115 $R^1 = H$, $R^2 = OH$
119 $R^1 = OH$, $R^2 = OCH_3$

Fig. 3 Alkaloids from the genus *Desmos*

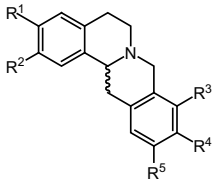

121 R^1 = OH, R^2 = OCH_3, R^3 = OCH_3, R^4 = OH, R^5 = H
122 R^1 = OH, R^2 = OCH_3, R^3 = H, R^4 = OCH_3, R^5= OCH_3
124 R^1 = R^3 = OCH_3, R^2 = R^4 = OH, R^5 = H

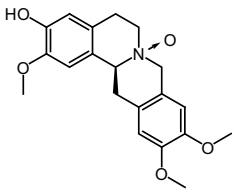

123

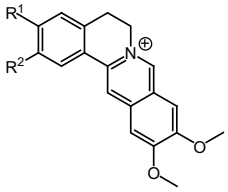

125 R^1 = OH, R^2 = OCH_3
126 R^1 = OCH_3, R^2 = OH

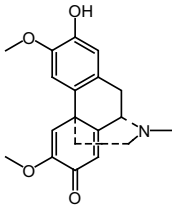

127

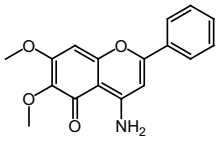

128

Fig. 3 (continued)

all of these alkaloids obtained from the genus *Desmos* for the first time [48]. The new derivative, dasymachaline (**105**), and the known compound, dicentrinone (**107**), were separated from *D. dasymachalus* leaves, while another known analog, duguevalline (**108**), was isolated from its twigs [17, 49]. Nguyen et al. (2008) isolated the new aporphine, desmorostratine (**106**), together with the known analog, predicentrine (**118**), from the stem bark of Vietnamese *D. rostrata* [1]. *Desmos cochinchinensis* twigs have been shown to contain the two aporphine alkaloids liriodenine (**112**) and lysicamine (**113**) [18]. Along with the known compound, oxoanolobin (**117**), 3,9,11-trimethoxy-1,2-methylenedioxyloxoaporphine (**120**) is a new metabolite found in *D. chinensis* branches [32].

Other types of alkaloids present in *Desmos* species include five protoberberines (**112–116**) [1, 48, 50], a morphinandienone (**127**) [48], and a flavanone-type alkaloid (**128**) [51]. Among them, discretine *N*-oxide (**123**) and desmosin (**128**) were obtained as two new compounds from *D. rostrata* stem bark and *D. dumosus* bark, respectively [1, 51]. However, metabolite **128** is likely to be an artifact produced during the isolation process [51].

2.3 Miscellaneous Phenols

Aromatic compounds bearing oxygen functionalities are a class of compounds that are particularly important among metabolites of plants. Oxyfunctionalized aromatic

compounds found in *Desmos* can be divided into two groups: simple phenols **129**–**136** and benzoic acid esters **137**–**156** (Table 1 and Fig. 4).

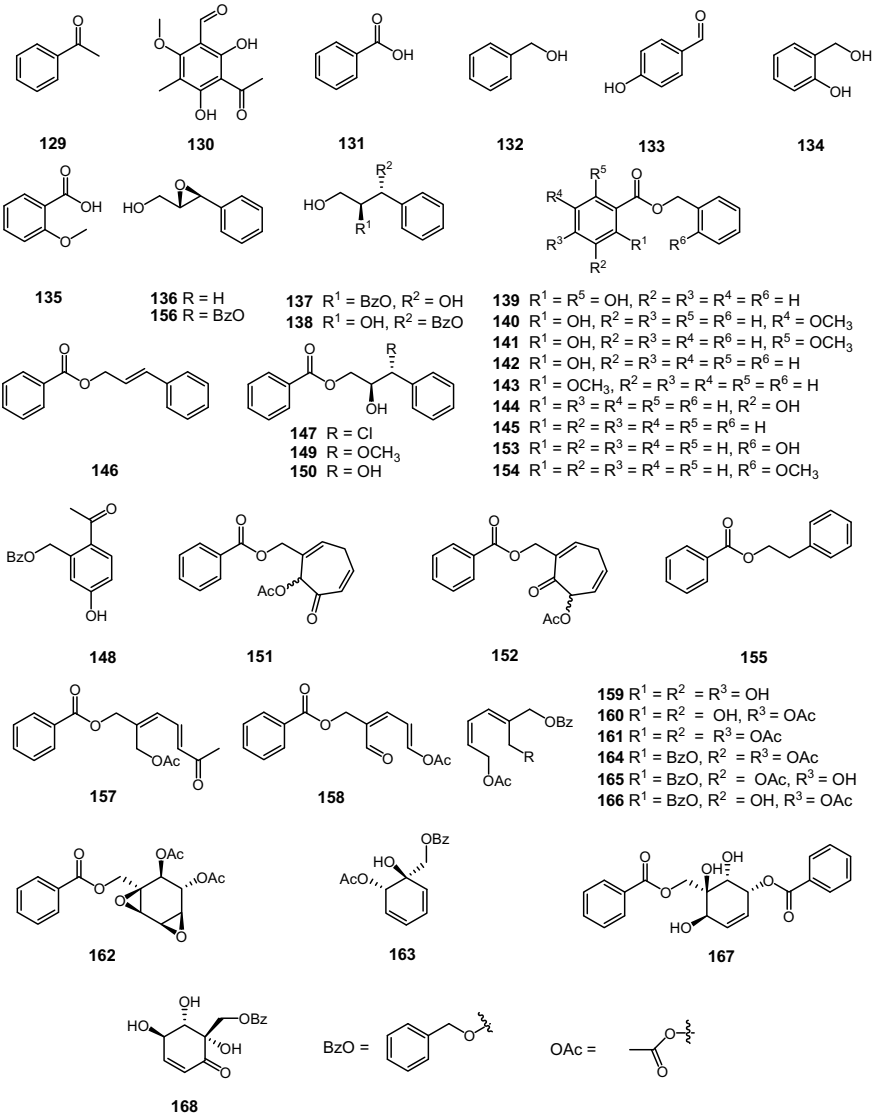

Fig. 4 Miscellaneous phenols and polyoxygenated cyclohexane and cyclohexene derivatives from the genus *Desmos*

2.3.1 Simple Phenols

Simple phenolic derivatives have been obtained mostly from *D. chinensis*, *D. cochinchinensis*, *D. dasymaschalus*, *D. dumosus*, *D. grandifolius*, and *D. pedunculosus* [5, 17, 18, 24, 30, 31, 35, 37, 38, 40]. Benzoic acid (**131**) has been observed in *D. chinensis* roots, *D. cochinchinesis* fruits, leaves and twigs, *D. dumosus* roots, *D. grandifolius* roots [5, 17, 18, 24, 30, 31, 35, 37, 38], whereas the remaining derivatives were isolated from the genus *Desmos* only on one occasion each. Thus, acetophenone (**129**), 3-acetyl-2,4-dihydroxy-6-methoxy-5-methylbenzaldehyde (**130**), benzyl alcohol (**132**), and 2-methoxybenzoic acid (**135**) were reported in various plant parts of *D. chinensis* [5, 30, 52], while 4-hydroxybenzaldehyde (**133**), 2-hydroxybenzyl alcohol (**134**), and (2*S*,3*S*)-3-(phenyloxiran-2-yl)methanol (**136**) were detected in *D. dasymaschalus* twigs, *D. cochinchinensis* leaves, and *D. pedunculosus* aerial parts, respectively [17, 18, 31].

2.3.2 Benzoic Acid Esters

Compounds derived from *Desmos* species are also present in form of benzoic acid esters. As tabulated in Table 1, this compound type has been isolated from *D. chinensis*, *D. cochinchinensis*, *D. dasymaschalus*, *D. dumosus*, and *D. pedunculosus* [3, 5, 17, 18, 21, 30, 31, 34, 53, 58]. The most abundant derivative, benzyl benzoate (**145**) is known to accumulate in *D. chinensis* leaves and stem bark, *D. cochinchinensis* leaves, *D. dasymaschalus* twigs, *D. dumosus* twigs, and *D. pedunculosus* aerial parts [17, 18, 21, 30, 31, 52], while 2-methoxybenzyl benzoate (**154**) is a constituent of *D. chinensis* leaves, *D. dasymaschalus* twigs, and *D. pedunculosus* aerial parts [17, 30, 31, 34]. Phytochemical studies conducted by Clement et al. (2017) led to the isolation and identification of six benzoates from of a 90% aqueous methanol extract of the aerial parts of the Vietnamese *D. pedunculosus* including (2*S*,3*R*)-2-benzoyloxy-1,3-dihydroxy-3-phenylpropane (**137**), (2*S*,3*R*)-3-benzoyloxy-1,2-dihydroxy-3-phenylpropane (**138**), (2*S*,3*R*)-3-chloro-2-hydroxy-3-phenylpropyl benzoate (**147**), (2*S*,3*R*)-2-hydroxy-3-methoxy-3-phenylpropyl benzoate (**149**), (2*S*,3*R*)-2,3-dihydroxy-3-phenylpropyl benzoate (**150**), and (2*S*,3*S*)-3-phenyloxiran-2-yl)methyl benzoate (**156**). Among them, compounds **147**, **149**, and **150** have not been characterized as natural products previously [31]. The leaves and stem bark of *D. chinensis* was found to contain a large number of benzoates, i.e., eight metabolites of this type (**139**–**146**) were found in the leaves, with compounds **142** and **143** detected in the both leaves and stem bark. While grandiuvarone A (**151**) is a known benzoate, but grandiuvarone B (**152**) has been determined as a new analog, and both two compounds **151** and **152** were obtained from a methanol extract of *D. chinensis* leaves [53]. Benzoates were further observed in other *Desmos* species, such as 2-phenylethyl benzoate (**155**) in *D. dasymaschalus* twigs [17]. Together with the known compound 2-hydroxybenzyl benzoate (**153**), desmoscochin benzoate (**148**) was obtained as a new compound isolated from *D. cochinchinensis* leaves [18].

2.4 Polyoxygenated Derivatives

Utilizing phytochemical and NMR structural procedures, polyoxygenated open-chain and cyclic derivatives were determined as being present in certain *Desmos* species. By applying quick column chromatography, a phytochemical study on the MeOH and EtOAc extracts of Thai *D. cochinchinensis* leaves and flowers resulted in the isolation and NMR spectroscopic elucidation of the five new compounds, desmoscochinchinenes A–E (**157**–**161**), and the three known analogs, (1*R*,6*S*)-herrevenol A (**163**), and flexuvarins C (**165**) and D (**166**) [20]. Furthermore, flexuvarin B (**164**) was found in both *D. cochinchinensis* leaves and twigs, but zeylenone (**168**) was detected only in the twigs [18]. Besides aristolactam derivatives, an α-glucosidase inhibitory extract of *D. dasymaschalus* twigs proved to contain one cyclohexane, (+)-crotepoxide (**162**), and one cyclohexene, (–)-zeylenol (**167**) [17].

2.5 Terpenoids

2.5.1 Sesquiterpenoids

Terpenoid derivatives (isoprenoids) are the most numerous and diverse class of chemical compounds produced by plants. *Desmos* species are characterized by a high proportion of this class that are sesquiterpenoids (Table 1 and Fig. 5). Two new sesquiterpenoids, along with nine known analogs were isolated from a MeOH extract of the Taiwanese *D. cochinchinensis* leaves [54]. Their structures were elucidated by means of spectroscopic analysis as alismoxide (**169**), cryptomeridiol (**170**), 4β,10α-dihydroxyaromadendrane (**171**), 4β,10β-dihydroxyaromadendrane (**172**), 1β,7α-dihydroxyeudesman-4-one (**173**, new), 4-epicryptomeridiol (**174**), 11-hydroxy-4α-methoxyselinane (**177**), 10β-hydroxyisodauc-6-en-14-al (**178**), 5αH-megastigm-7-ene-3α,4α,6β,9-tetrol (**179**, new), pipelol A (**181**), and selin-4(15)-ene-1β,11-diol (**182**) [54]. The sesquiterpenoid patchouli alcohol (**180**) is a key material in certain perfumes and is also a sesquiterpenoid found in the stems of *D. cochinchinensis* [50]. α-Eudesmol (**175**) and its β-form **176** have been recorded to occur in *D. chinensis* leaves and stem bark [52].

2.5.2 Triterpenoids and a Diterpenoid

A total of four triterpenoids including desmosinol (**183**), heynic acid (**184**), 15α-hydroxy-24-methylenelanosta-7,9-(11)-dien-3-one (**185**), and 24-methylene cycloartan-3β,-21-diol (**186**), were isolated from *Desmos* species (Table 1). Compounds **183** and **185** were reported as new compounds and were obtained from *D. cochinchinensis* stems and *D. longiflorus* stem bark, respectively [55, 56]. Phytol

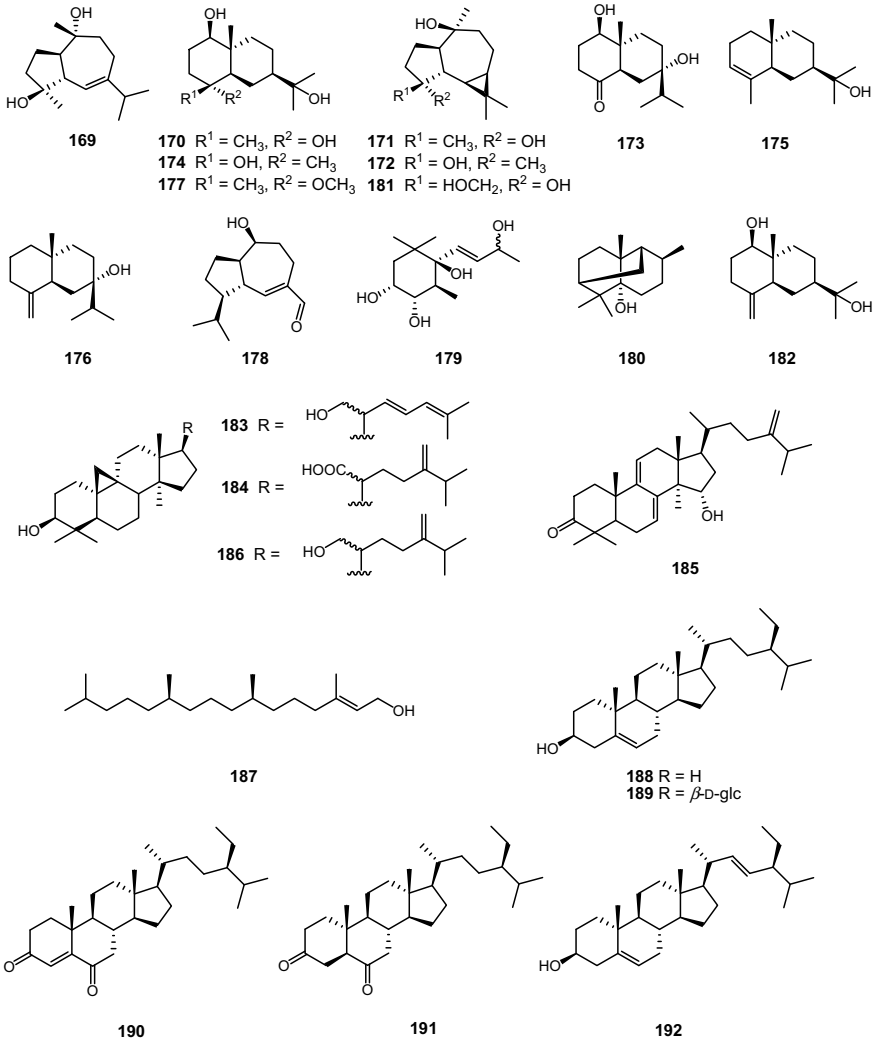

Fig. 5 Terpenoids and steroids from the genus *Desmos*

(**187**) was sourced from *D. chinensis* leaves and stem bark and is the only diterpenoid found thus far in the genus *Desmos* [30, 52].

2.6 Phytosterols

Phytosterols are also common chemical constituents of *Desmos* species (Table 1 and Fig. 5). β-Sitosterol (**189**) is highly abundant in the plant kingdom and occurs in

D. chinensis seeds, roots, and branches, *D. cochinchinensis* whole plants, fruits, and stems, *D. dumosus* roots, and *D. grandifolius* roots [24–26, 32, 37, 38, 50]. Moreover, another common sterol, stigmasterol (**192**), could be purified from the extracts of *D. chinensis* roots, *D. cochinchinesis* fruits, *D. dumosus* roots, and *D. grandifolius* roots [24, 35, 37, 38]. The β-glucosylated form of compound **189**, namely, daucosterol (**188**), has been reported as being present in *D. chinensis* seeds [25]. Within this compound class, stigmast-4-ene-3,6-dione (**190**) and stigmastane-3,6-dione (**191**) were isolated as constituents of *D. dumosus* roots [33].

2.7 Oxepinones, Amides, Fatty Acids, and Other Compounds

The oxepinones that have been isolated from *Desmos* species are a rarely encountered chemical class of compounds within the family Annonaceae. Hence, four new derivatives, (–)-(5*R*)-desmoscochinoxepinones A–D (**193**–**196**), were characterized from *D. cochinchinensis* leaves, and the new analog, (–)-(5*R*)-grandiuvarone (**197**), was observed in its twigs (Table 1 and Fig. 6) [18]. These metabolites contain a seven-membered ring and share the same (5*R*)-configuration. Therefore, oxepinones may have significance as chemotaxonomic indicators for the genus *Desmos*.

Additional phytochemical studies on *Desmos* species have led to reports of six amides (**198**–**203**), four fatty acids (**204**–**207**), an isobenzofuran (**208**), two coumarins (**209** and **210**), and a chromanol (**211**) (Table 1 and Fig. 6). All of these metabolites have been purified in a species in the genus *Desmos* for the first time. Among the group of amides, desmocyclopeptide (**199**) was determined structurally as a novel cyclic peptide, and this originated from a MeOH extract of the stem bark of the Vietnamese *D. rostrata* [22]. In addition, another new compound, dunaliine A (**200**), was obtained in the form of a precipitate from a CH_2Cl_2 extract of Malaysian *D. dunalii* leaves [47]. However, according to the investigators involved, this compound is an artifact of compound **78** [47]. Among compounds **204**–**207**, desmosic acid (**204**) from *D. cochinchinensis* stems was new when first isolated and, using spectroscopic methods, was determined to contain a *cis*-double bond between carbons C-7 and C-8 [50]. Of the remaining compounds (**208**–**211**), isobenzofuran 7-methoxyisobenzofuran-1(3*H*)-one (**208**) was present in *D. dasymaschalus* twigs, while the two coumarins 8-methoxycoumarin (**209**) and (+)-(1′*R*,2′*R*)-phebalosin (**210**) were purified from *D. dumosus* leaves, and the chromanol DL-2,5,7,8-tetramethyl-2-(4,8,12-trimethyltridecyl)-6-chromanol (**211**) was separated from *D. cochinchinensis* stems [17, 21, 50]. In particular, compound **210** was elucidated as a new coumarin with a 1′*R*,2′*R*-configuration and with epoxidation evident in the side chain.

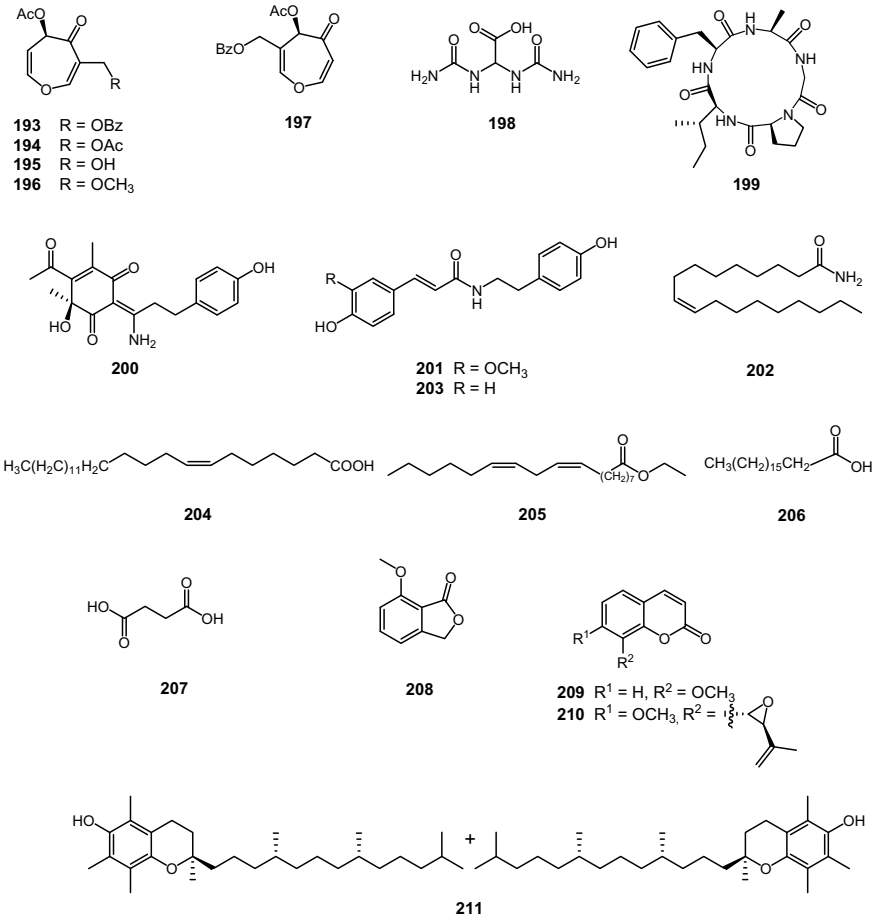

Fig. 6 Oxepinones, amides, fatty acids, and others from the genus *Desmos*

2.8 Essential Oil Components

Plant-derived essential oils are comprised of many active volatile small-organic molecule components and may have commercial use in pharmaceuticals, foods, and beverages, and household cleaning products [14, 59]. Aromatic plants are recognized as rich sources of essential oils, and those from *Desmos* species have attracted some attention. Table 2 and Fig. 7 summarize the GC–MS results for the major components in some *Desmos* species essential oils, with monoterpenes and sesquiterpenes being the main components that occur. Eugenol (**212**) (31.3%) and α-cyperone (**213**) (10.5%) were found as the principal components in the essential oil of the leaves of Indian *D. chinensis*, but the monoterpenoids limonene (**214**) (11.8%), germacrene D (**215**) (11.5%), and α-pinene (**216**) (11.3%) were characteristic of the same species

Table 2 Essential oil components from representative *Desmos* species

Species	Collection	Parts used	Main constituents	Ref.
D. chinensis	South India	Leaves	Eugenol (**212**) (31.3%), α-cyperone (**213**) (10.5%)	[61]
	Hatinh, Vietnam	Leaves	Limonene (**214**) (11.8%), germacrene D (**215**) (11.5%), α-pinene (**216**) (11.3%)	[64]
D. cochinchinensis	Hatinh, Vietnam	Leaves	β-Caryophyllene (**217**) (26.3%), germacrene D (**215**) (14.6%), α-pinene (**216**) (11.5%)	[60]
	Nghean, Vietnam	Stems	*β*-Caryophyllene (**217**) (16.9%), bicyclogermacrene (**218**) (11.6%)	[65]
		Fruits	β-Caryophyllene (**217**) (20.9%), limonene (**214**) (15.9%), germacrene D (**215**) (12.5%)	
D. dumosus	Hatinh, Vietnam	Leaves	β-Caryophyllene (**217**) (20.4%), germacrene D (**215**) (15.1%), α-pinene (**216**) (9.5%)	[60]
D. goezeanus	Malanda, Australia	Leaves	Benzyl benzoate (**219**) (40.1%), benzyl salicylate (**220**) (15.3%), bicyclogermacrene (**218**) (10.0%)	[63]
	Wongabel, Australia	Leaves	Benzyl salicylate (**220**) (45.2%), benzyl benzoate (**219**) (18.6%)	[63]
D. penduculosus	Hatinh, Vietnam	Leaves	β-Elemene (**221**) (39.5%), β-caryophyllene (**217**) (13.9%), germacrene D (**215**) (9.9%)	[60]
D. wardianus	Tolga, Australia	Leaves	α-Pinene (**216**) (36.9%)	[63]

grown in Vietnam [60, 61]. Dai et al. (2012, 2014) determined that germacrene D (**215**) (9.9–15.1%) and β-caryophyllene (**217**) (13.9–26.3%) were the most abundant compounds present in the essential oils of the Vietnamese plants *D. cochinchinensis*, *D. dumosus*, and *D. penduculosus* [60, 62]. α-Pinene (**214**) reached up to 36.9% in the leaf essential oil of a Tolga, Australia sample of *D. wardianus*, while benzyl benzoate (**219**) (18.6–40.1%) and benzyl salicylate (**220**) (15.3–45.2%) were obtained as the main compounds in *D. goezeanus* leaves collected from Malanda and Wongabel in Australia [63].

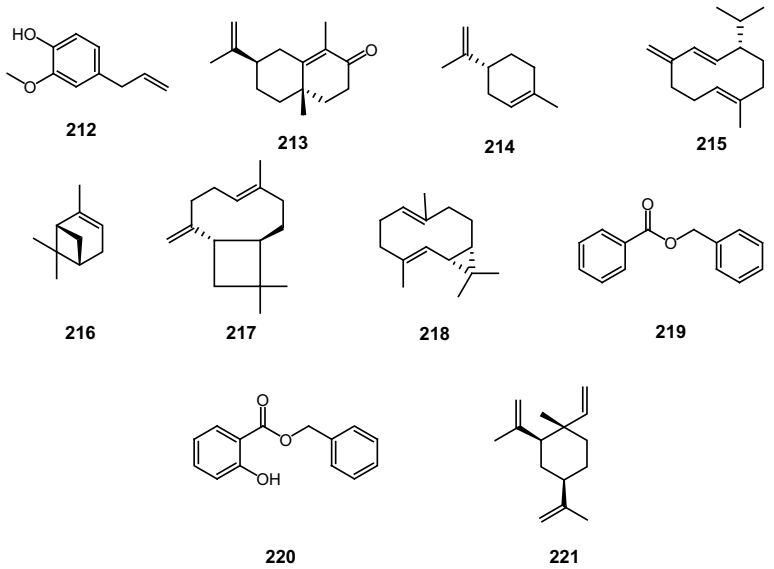

Fig. 7 Major components of *Desmos* spp. essential oils

3 Biosynthesis and Synthesis Aspects

As stated earlier in this chapter, flavonoids are the predominant *Desmos* specialized metabolites and as a group have a wide spectrum of bioactivities. Therefore, proposed biosynthesis routes and synthesis procedures of *Desmos* flavonoids have been documented.

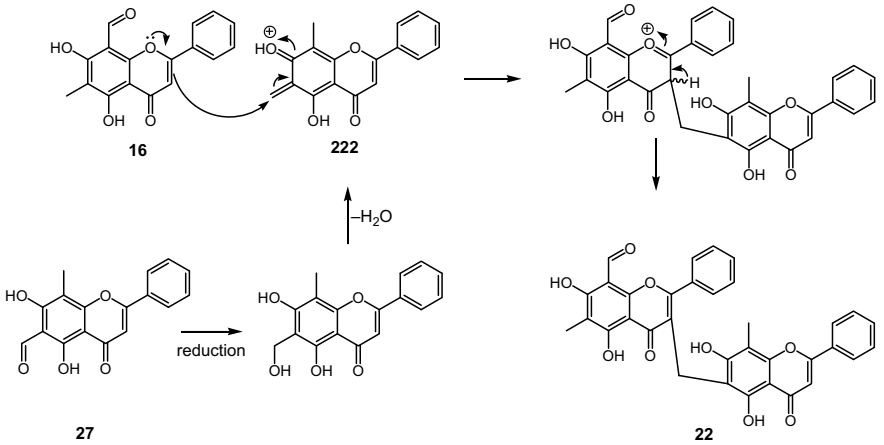

Fig. 8 Biosynthesis scheme for saiyutone A (**22**)

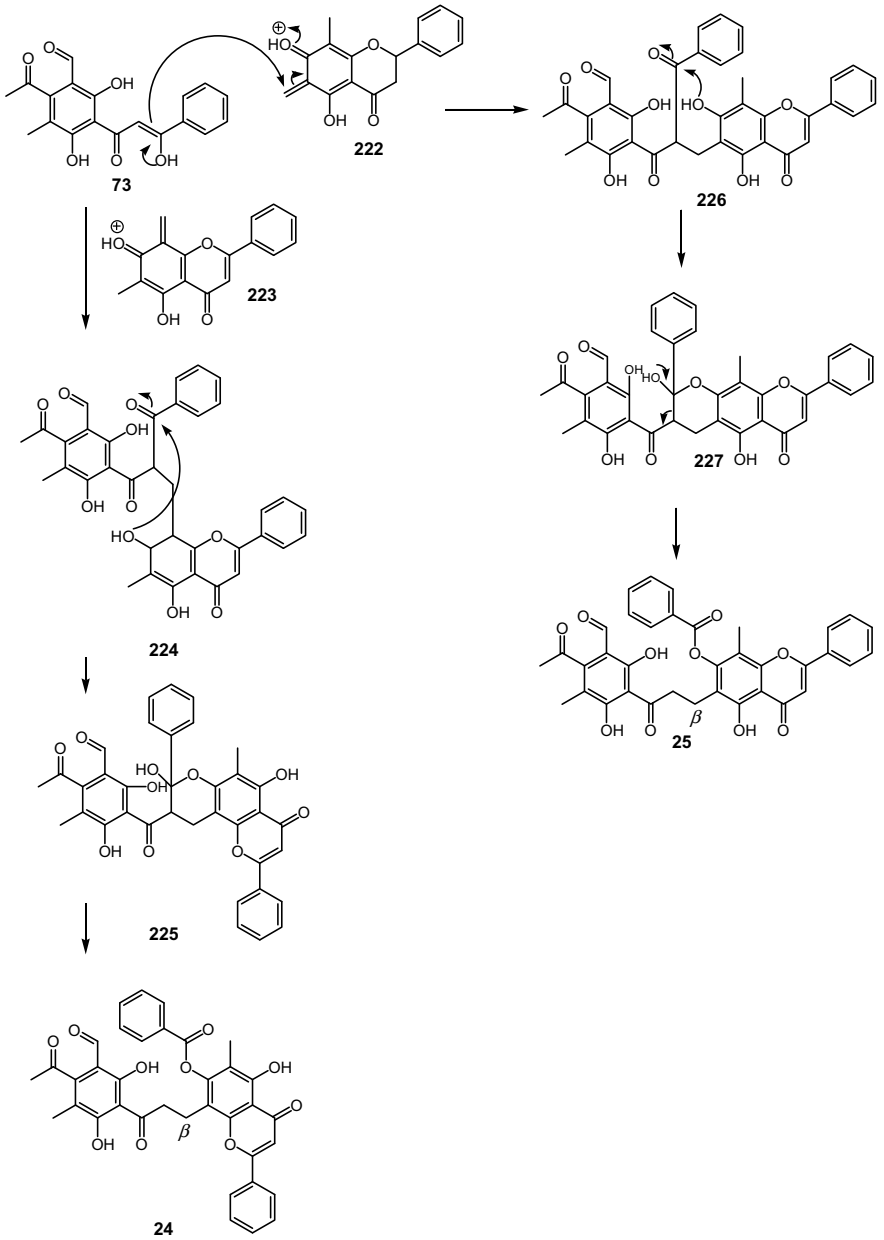

Fig. 9 Biosynthesis scheme for saiyutone C (**24**) and saiyutone D (**25**)

The biosynthesis routes for the three new unusual flavonoids **22**, **24**, and **25** from *D. chinensis* leaves were proposed by Ritiwong et al. (2011), as shown in Figs. 8 and 9 [3]. Thus, a newly identified biflavone with a 3–6″ linkage through a methylene group in (**22**) could be obtained from a combination of isounonal (**16**) and the *o*-quinomethine of unonal (**222**) via nucleophilic addition and aromatization [3].

For the biosynthesis of the unusual structures saiyutone C (**24**) and saiyutone D (**25**), an electrophilic addition may occur between 3-formyl-2,6-dihydroxy-4-methoxy-5-methyldibenzoyl-methane (**73**) and the *o*-quinomethine of isounonal (**223**) or unonal (**222**), respectively. The intermediates **224** and **226** could form the respective key cyclic hemiketals **225** and **227**, which then lead to **24** and **25** after ring-opening. The process is outlined in Fig. 9 [3].

Desmosdumotin C (**68**) has been found in both *D. dumosu*s roots and *D. rostrata* stem bark and showed low micromolar growth inhibition of several different cancer cell lines [27]. The synthesis of compound **68** starting from 2,4,6-trihydroxyacetophenone (**228**) was carried out through three short simple steps [22]. The first step was methylation of **228** with MeI in the presence of *tert*-BuOK to give compound **229** (72%). Then, the hydroxy group in **229** was replaced by a methoxy group and reacted with trimethylsilyl diazomethane to produce compound **230** (60%). Chalcone **68** was obtained in good yield (91%) after condensation of **230** with benzaldehyde. After this, the flavonoids desmorostratone (**5**) and desmosdumotin B (**8**) were synthesized from **68** with only one step each in yields of 65% and 71%, respectively. Desmorostratone (**5**) was obtained by treatment **68** with SeO_2 in dimethyl sulfate while the oxidative cyclization of **68** by DMSO/I_2 in the presence of a small amount of H_2SO_4 produced compound (**8**) as represented in Fig. 10 [22].

The potent anti-HIV chalcone, 2-methoxy-3-methyl-4,6-dihydroxy-5-(3′-hydroxy) cinnamoylbenzaldehyde (**73**), was prepared by a synthesis route involving

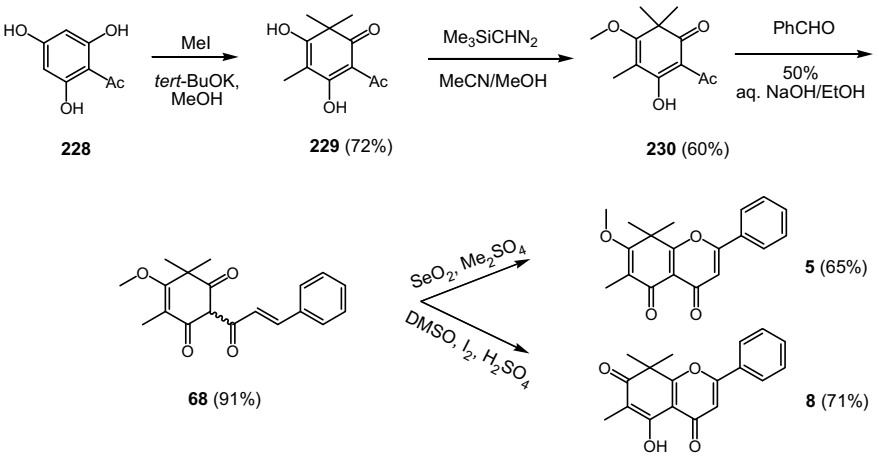

Fig. 10 Synthesis of desmorostratone (**5**), desmosdumotin B (**8**), and desmosmoduntin C (**68**)

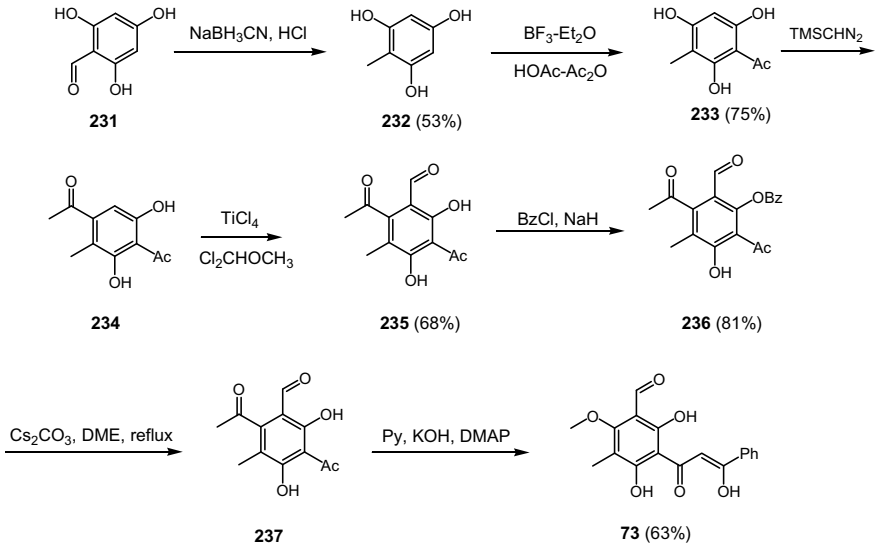

Fig. 11 Synthesis of 2-methoxy-3-methyl-4,6-dihydroxy-5-(3′-hydroxy) cinnamoylbenzaldehyde (**73**)

seven steps without the use of any protecting groups. The process started with 2,4,6-trihydroxybenzaldehyde (**231**) as outlined in Fig. 11. Under acidic conditions, this compound easily converted to 2,4,6-trihydroxytoluene (**232**), which then was acetylated using acetic acid to form **233**. Compounds **234** and **235** were synthesized as intermediate substances to produce compound **236**. After removing one benzoyl group in **236**, the obtained key compound **237** was then treated with KOH/DMAP in pyridine followed by a Baker-Venkataraman transformation [66] to yield chalcone **73** (63%) [45].

4 Biological Activities

4.1 Cytotoxic Activity

Cytotoxic assays using cancer cell lines have been the most frequently performed type of biological testing on purified constituents of *Desmos* species. A cytotoxic evaluation conducted by Wu et al. (2002) indicated that the ED_{50} values obtained for the new chalcone desmosdumotin C (**68**) against the growth of cancer cell lines were in the order: HOS (ED_{50} 2.5 μg/cm^3) < MCF-7 (3.8 μg/cm^3) < 1A9 (4.0 μg/cm^3) < HCT-8 (5.0 μg/cm^3) < vincristine-resistant KB (5.6 μg/cm^3) < epidermoid nasopharyngeal carcinoma KB (6.5 μg/cm^3) [4]. In another biological assessment, the new hybrid flavan-chalcone, desmosflavan A (**58**), inhibited the growth of the HuC-CA-1,

HepG2, A549, and MOLT-3 cancer cell lines with IC_{50} values in the range 0.29–3.75 μg/cm^3, in comparison to the chalcone cardamonin (**67**) (IC_{50} range 1.62–27.0 μg/cm^3), the new hybrid flavan-chalcone desmosflavan B (**59**) (IC_{50} range 1.71–27.0 μg/cm^3), the flavone chrysin (**2**) (IC_{50} range 7.2–9.7 μg/cm^3), and the flavanone pinocembrin (**54**) (inactive) [2]. In the same manner, the *D. chinensis* flavonoids **16**, **27**, **28**, **29**, **50**, and **75** were also investigated for their antiproliferative ability against the MOLT-3, A549, HuCCA-1, and HepG2 cancer cell lines. From the data obtained, unonal-7-methyl ether (**28**) showed the most potent effect for the MOLT-3 cell line, with an IC_{50} value of 7.16 μg/cm^3 [5]. The new dihydrochalcone **75** exhibited moderate effects against the MOLT-3, HuCCA-1, and HepG2 cancer cell lines, having IC_{50} values of 7.16–34.00 μg/cm^3, respectively, but phenols **143** and **145** were inactive in this regard [5].

Other phytochemical classes of *Desmos* compounds such as triterpenoids, alkaloids, and fatty acids were also evaluated for their cytotoxic activities [1, 50, 55]. As a representative example, a triterpenoid from *D. cochinchinensis* stems, heynic acid (**184**), displayed significant cytotoxic effects against the A549, MCF-7, and HT-29 cancer cell lines with ED_{50} values of 0.4, 0.4, and 3.0 μg/cm^3, respectively [55]. Similarly, triterpenoid **186** showed positive data against the HT-29 and RPMI7951 cancer cell lines, with ED_{50} values of 3.0 and 4.0 μg/cm^3, respectively [55]. In a search for tumor inhibitors from *D. cochinchinensis,* it was noted that the new fatty acid, desmosic acid (**204**), exhibited cytotoxic activity for the HT-29 human colon cell line with an ED_{50} value of 4.0 μg/cm^3 [50]. Desmorostratine (**106**), isolated from *D. rostrata* stem bark, was moderately cytotoxic to the KB cancer cell line (IC_{50} of 2.4 μM), in comparison with the positive control Taxotere (IC_{50} of 0.0002 μM), but the other alkaloidal analogs tested (**85**, **118**, **122**, **123**, and **125**) were all inactive [1].

4.2 Antimicrobial Activity

Using agar disk diffusion and agar dilution methods, a chloroform extract of *Desmos chinensis* leaves was evaluated for antibacterial activity against the Gram-positive bacteria *Staphylococcus aureus, Staphylococcus epidermidis*, and *Bacillus subtilis* and gave *MIC* values of 500–1000 μg/cm^3. However, this extract inhibited the dermatophytic fungi *Trichophyton rubrum, Trichophyton mentagrophytes*, and *Microsporum gypseum* more effectively and gave *MIC* values of 31.25–62.50 μg/cm^3. In comparison, the hexane extract of the leaves of *D. chinensis* also exhibited in vitro growth-inhibitory effects on the above-mentioned fungi, but the methanol and water extracts failed to control the growth of the test microbial species used [67]. The antifungal activity was studied further on this plant, and its leaf dichloromethane extract possessed effects on the growth of the fungi *Bipolaris oryzae, Pyricularia oryzae,* and *Sclerotium rolfsii*, with respective *MIC* values of 31.2, 3.9, and 15.6 μg/cm^3. The positive control compound propiconazole gave *MIC* values of 0.2 to 1.9 μg/cm^3 against these same fungi [58].

Apart from cytotoxic activity, compound **75** has demonstrated antifungal activity against *P. oryzae* and *Rhizoctonia solani*, with *MIC* values of 15.6 and 31.2 μg/cm^3, respectively. Compounds **16** and **27** both possess a similar antifungal effect to **75** on *P. oryzae* but failed to affect the growth of *R. solani* [5]. Several structural analogs of benzoate esters have been employed as fungicides, due to their influence on the sporulation process and mycelial growth [68]. Likewise, the newly obtained natural benzoate ester, grandiuvarone B (**152**), showed potent antifungal activity on *Aspergillus flavus* growth, with a *MIC* value of 0.01 μg/cm^3, which was closely comparable to compound **151** (*MIC* 0.02 μg/cm^3). Moreover, compound **152** was also reported to suppress the growth of the pathogenic bacterial strain *Ralstonia solanacearum* [53].

4.3 Anti-HIV Activity

Certain chalcones have been recognized previously as being promising bioactive agents, with anti-inflammatory, antihistaminic, antioxidant, and cytotoxic effects [69]. In work performed by Wu et al. (2003), a number of *Desmos* chalcones were evaluated for their anti-HIV activities. Among 16 tested compounds, chalcone **73** was found to be comparable in potency to the positive control azidothymidine (EC_{50} 0.022 μg/cm^3) against HIV-1 replication in the H9 lymphocytic cell line. This positive result can be explained by the presence of the C-2 methoxy group in the chalcone skeleton in **73** when compared with inactive compound **74**. Flavanone **33**, with an EC_{50} value of 4.97 μg/cm^3, showed a somewhat lesser anti-HIV potency than flavanone **50** (EC_{50} 2.30 μg/cm^3) [27]. It has been suggested that the presence of a formyl group may be preferential for this type of antiviral activity when compared to a methyl group.

4.4 Aromatase Inhibitory Activity

An increase of estrogen levels in certain tissues may cause breast cancer, and this pathological factor accounts for 75% of all breast cancer cases found in women [70]. The aromatase enzyme is important in the aromatization process of androgens to biosynthesize estrogens. Therefore, the reduction of estrogen levels by inhibiting aromatase activity is regarded as a promising therapeutic approach for breast cancer treatment [71]. From an investigation on aromatase inhibitors present in *Desmos* plants, five flavonoid derivatives, **2**, **54**, **58**, **5**9, and **67**, were subjected to testing in an aromatase inhibition assay. Except for the inactive cardamonin (**67**), the remaining four compounds gave IC_{50} values ranging from 0.8 to 3.3 μ*M* [2]. Other flavonoids also demonstrated aromatase inhibitory activity, according to a report by Prachyawarakorn et al. performed in 2013 [40]. Among eight compounds tested, flavans **60**, **63**, and **66** inhibited the aromatase enzyme with respective IC_{50} values

of 80, 90, and 40 nM, in comparison with the reference compound, letrozole (IC_{50} 1.1 nM) [40].

4.5 α-Glucosidase Inhibition Activity

Flavonoids and oxepinones derived from *Desmos* species have been shown as the main constituents of this genus that are able to inhibit α-glucosidase. The flavanone dichamanetin (**41**) is a promising agent in this regard and gave an IC_{50} value of 0.2 μM, while the two new flavones desmoscochinflavones A (**6**) and B (**7**) displayed the same IC_{50} value of 0.9 μM, and oxepinone **197** was also active (IC_{50} 3.1 μM). Flavonoids **2**, **26**, **48**, and **54** and oxepinones **193–196**, with IC_{50} values ranging from 2.9 to 158.2 μM, were more potent as α-glucosidase inhibitors than the positive control used, acarbose (IC_{50} 170.7 μM) [18]. Furthermore, two derivatives, *N-trans*-feruloyltyramine (**201**) and paprazine (**203**), have shown good α-glucosidase inhibitory activities, with the respective IC_{50} values of 24.7 and 4.5 μM, as compared with that of the positive control acarbose (IC_{50} 73.7 μM) [17].

4.6 Other Bioactivities

The oxygen radical absorbance capacity (ORAC) assay is a well-known and widely used tool for determining the antioxidant capacity of natural product test samples. Flavonoids **2** and **67** gave responses of 12.2 and 15.0 ORAC units in an antioxidative assay, respectively [2]. In an in vitro anti-inflammatory activity test, metabolites **9**, **27**, **32**, **33**, **50**, and **65** from *D. cochinchinensis* fruits exhibited nitric oxide (NO) inhibition, with IC_{50} values ranging from 23.9 to 82.4 μM, for which the most potent of these IC_{50} values was demonstrated for desmosflavone (**9**) [24]. Following testing in a tyrosine kinase inhibition assay, a chloroform extract of *D. chinensis* leaves showed a 34.3% inhibition at the concentration level used [6], and the pure compound desmal (**34**) was found to be active in this same bioassay system with an IC_{50} value of 2.5 μg/cm^3 [39].

The nuclear factor of activated T cells (NFAT) transcription factor plays an important role in immunopathological reactions including autoimmunity, transplant rejection, and inflammation [72]. Therefore, compounds showing inhibition of NFAT transcription factor could be useful in the treatment of immune diseases. Thus, six constituents of *D. chinensis* leaves were also investigated for their potential inhibitory activities against NFAT transcription. Among them, flavone **19**, with an IC_{50} value of 3.89 μM, showed the most potent inhibitory effect, while flavone **42** was inactive in this test system ($IC_{50} > 50$ μM). The phenolic compounds **77** and **154**, having respective IC_{50} values of 9.77 and 28.4 μM, showed more moderately potent NFAT transcription inhibition [34].

In terms of its potential antimalarial activity, an alkaloidal fraction of the entire plant of *D. rostrata*, at a dose of 10 μg/cm^3, induced 40% inhibition against a *Plasmodium falciparum* strain, whereas its constituents **122**, **123**, and **125** notably showed potent effects with the IC_{50} values of 1.6, 0.9, and 4.2 μM, respectively [1]. An alkaloid constituent, desmorostratin (**106**), also caused the inhibition of *P. falciparum* growth (IC_{50} 3.6 μM) (Table 3) [1].

Table 3 Biological activities of isolated compounds and plant extracts from the genus *Desmos*

Compound/Extract	Model	Effect	Ref.
Cancer cell line cytotoxic activity			
2	In vitro	IC_{50} = 7.2–9.7 μg/cm^3, HuCCA-1 cells, HepG2, A549, and MOLT-3 cells	[2]
28	In vitro	IC_{50} = 7.16 μg/cm^3, MOLT-3 cells	[2]
54	In vitro	IC_{50} = 22.8 μg/cm^3, MOLT-3 cells IC_{50} > 50 μg/cm^3, HuCCA-1 cells, HepG2, and A549 cells	[2]
58	In vitro	IC_{50} = 0.29–3.75 μg/cm^3, HuCCA-1 cells, HepG2, A549, and MOLT-3 cells	[2]
59	In vitro	IC_{50} = 1.71–27.0 μg/cm^3, HuCCA-1 cells, HepG2, A549, and MOLT-3 cells	[2]
67	In vitro	IC_{50} = 1.62–27.0 μg/cm^3, HuCCA-1 cells, HepG2, A549, and MOLT-3 cells	[2]
68	In vitro	ED_{50} = 2.5 μg/cm^3, HOS cells ED_{50} = 3.8 μg/cm^3, MCF-7 cells ED_{50} = 4.0 μg/cm^3, 1A9 cells ED_{50} = 5.0 μg/cm^3, HCT-8 cells ED_{50} = 5.6 μg/cm^3, vincristine-resistant KB cells ED_{50} = 6.5 μg/cm^3, epidermoid nasopharyngeal carcinoma KB cells	[4]
75	In vitro	IC_{50} = 7.16–34.00 μg/cm^3, MOLT-3, HuCCA-1, and HepG2 cells	[5]
85	In vitro	Inactive (IC_{50} > 37 μM), KB cells	[1]
106	In vitro	IC_{50} = 2.4 μM, KB cells	[1]
118, 122, and **125**	In vitro	Inactive (IC_{50} > 29 μM), KB cells	[1]

(continued)

Table 3 (continued)

Compound/Extract	Model	Effect	Ref.
123	In vitro	Inactive ($IC_{50} > 28\ \mu M$), KB cells	[1]
143 and **145**	In vitro	$IC_{50} > 50\ \mu g/cm^3$, MOLT-3, HuCCA-1, and HepG2 cells	[5]
184	In vitro	$ED_{50} = 0.4\ \mu g/cm^3$, A549 cells $ED_{50} = 0.4\ \mu g/cm^3$, MCF-7 cells $ED_{50} = 3.0\ \mu g/cm^3$, HT-29 cells	[55]
186	In vitro	$ED_{50} = 3.0\ \mu g/cm^3$, HT-29 cells $ED_{50} = 4.0\ \mu g/cm^3$, RPMI7951 cells	[55]
204	In vitro	$ED_{50} = 4.0\ \mu g/cm^3$, HT-29 cells	[50]
Antimicrobial activity			
16 and **27**	In vitro	$MIC = 15.6\ \mu g/cm^3$, *P. oryzae* $MIC = 125\ \mu g/cm^3$ (inactive), *R. solani*	[5]
75	In vitro	$MIC = 15.6\ \mu g/cm^3$, *P. oryzae* $MIC = 31.2\ \mu g/cm^3$, *R. solani*	[5]
151	In vitro	$MIC = 0.02\ \mu g/cm^3$, *A. flavus*	[53]
152	In vitro	$MIC = 0.01\ \mu g/cm^3$, *A. flavus*	[53]
Anti-HIV activity			
33	In vitro	$EC_{50} = 4.97\ \mu g/cm^3$, H9 lymphocytic cells	[27]
50	In vitro	$EC_{50} = 2.30\ \mu g/cm^3$, H9 lymphocytic cells	[27]
73	In vitro	$EC_{50} = 0.022\ \mu g/cm^3$, H9 lymphocytic cells	[27]
74	In vitro	Inactive in anti-HIV testing	[27]
Aromatase inhibition activity			
2, **54**, **58**, and **59**	In vitro	$IC_{50} = 0.8–3.3\ \mu M$, aromatase inhibition	[2]
60	In vitro	$IC_{50} = 80\ nM$, aromatase inhibition	[40]
63	In vitro	$IC_{50} = 90\ nM$, aromatase inhibition	[40]
66	In vitro	$IC_{50} = 40\ nM$, aromatase inhibition	[40]
67	In vitro	Showed no effect on aromatase inhibition activity	[2]

(continued)

Table 3 (continued)

Compound/Extract	Model	Effect	Ref.
α-Glucosidase inhibition activity			
2, **26**, **48**, **54**, and **193–196**	In vitro	$IC_{50} = 2.9–158.2\ \mu M$, α-glucosidase inhibition	[18]
6 and **7**	In vitro	$IC_{50} = 0.9\ \mu M$, α-glucosidase inhibition	[18]
41	In vitro	$IC_{50} = 0.2\ \mu M$, α-glucosidase inhibition	[18]
201	In vitro	$IC_{50} = 24.7\ \mu M$ α-glucosidase inhibition	[17]
203	In vitro	$IC_{50} = 4.5\ \mu M$, α-glucosidase inhibition	[17]
Other bioactivities			
2	In vitro	ORAC units = 12.2, antioxidative activity	[2]
9, **27**, **32**, **33**, **50**, and **65**	In vitro	$IC_{50} = 23.9–82.4\ \mu M$, NO inhibition	[24]
19	In vitro	$IC_{50} = 3.89\ \mu M$, inhibition of NFAT transcription factor	[34]
34	in vitro	$IC_{50} = 2.5\ \mu g/cm^3$, tyrosine kinase inhibition	[39]
42	in vitro	$IC_{50} > 50\ \mu M$, inhibition of NFAT transcription factor	[34]
67	In vitro	ORAC units = 15.0, antioxidative activity	[2]
77	In vitro	$IC_{50} = 9.77\ \mu M$, inhibition of NFAT transcription factor	[34]
106	In vitro	$IC_{50} = 3.6\ \mu M$, antiplasmodial activity	[1]
122	In vitro	$IC_{50} = 1.6\ \mu M$, antiplasmodial activity	[1]
123	In vitro	$IC_{50} = 0.9\ \mu M$, antiplasmodial activity	[1]
125	In vitro	$IC_{50} = 4.2\ \mu M$, antiplasmodial activity	[1]
154	In vitro	$IC_{50} = 28.4\ \mu M$, inhibition of NFAT transcription factor	[34]
Pharmacological activities of extracts			
Chloroform extract of *D. chinensis* leaves (3.9–2000 $\mu g/cm^3$)	In vitro antimicrobial activity	$MIC = 500–1000\ \mu g/cm^3$ against *S. aureus, S. epidermidis*, and *B. subtilis* $MIC = 31.25–62.50\ \mu g/cm^3$ against *T. rubrum, T. mentagrophytes*, and *M. gypseum*	[67]

(continued)

Table 3 (continued)

Compound/Extract	Model	Effect	Ref.
n-Hexane extract of *D. chinensis* leaves (3.9–2000 μg/cm^3)	In vitro antimicrobial activity	*MIC* = 31.25–62.50 μg/cm^3 against *T. rubrum, T. mentagrophytes*, and *M. gypseum*	[67]
Methanol and water extracts of *D. chinensis* leaves (3.9–2000 μg/cm^3)	In vitro antimicrobial activity	Showed no activity against any of *S. aureus, S. epidermidis*, *B. subtilis, T. rubrum, T. mentagrophytes*, and *M. gypseum*	[67]
Dichloromethane extract of *D. chinensis* leaves (200 μg/cm^3)	In vitro antifungal activity	*MIC* = 31.2 μg/cm^3 against *B. oryzae* *MIC* = 3.9 μg/cm^3 against *P. oryzae* *MIC* = 15.6 μg/cm^3 against *S. rolfsii*	[58]
Chloroform extract of *D. chinensis* leaves (20 μg/cm^3)	In vitro antityrosinase activity	Showed 34.3% of tyrosinase inhibition	[6]
Alkaloidal fraction of *D. rostrata* plants (10 μg/cm^3)	In vitro antiplasmodial activity	Showed 40% inhibition against *P. falciparum* strain	[1]

5 Conclusions

This contribution has provided an overview of work performed on the phytochemistry and biological evaluation of the plant genus *Desmos* (family Annonaceae) for the first time. Altogether, 211 isolated compounds have been documented, with flavonoids, alkaloids, and miscellaneous phenolic compounds found to occur in plants of this genus most frequently. Thus, 82 *Desmos* flavonoids have been isolated, and these are representative of diverse chemical subtypes and include flavones, flavanones, chalcones, and dihydrochalcones. Oxepinones are an unusual chemical class of isolated compounds that have been isolated from certain *Desmos* species and previously have been found only rarely in the family Annonaceae.

Sesquiterpenes seem to be the main compounds in *Desmos* species essential oils sourced in Vietnam, but phenolic compounds and monoterpenes have been recorded in volatile oil samples from species in this genus collected from different locations in Australia. The purified constituents of *Desmos* species have shown a wide spectrum of biological activities, such as cytotoxic, antimicrobial, anti-HIV, antioxidative, anti-inflammatory, and aromatase inhibition effects. Despite numerous promising in vitro biological studies conducted to date on these compounds, cellular mechanistic investigations using purified *Desmos* constituents are yet to be performed.

Acknowledgments The compilation of information described in this chapter was supported by the Vietnam Academy of Science and Technology, Vietnam-2021.

References

1. Nguyen NT, Pham VC, Litaudon M, Guéritte F, Grellier P, Nguyen VT, Nguyen VH (2008) Antiplasmodial alkaloids from *Desmos rostrata*. J Nat Prod 71:2057
2. Bajgai SP, Prachyawarakorn V, Mahidol C, Ruchirawat S, Kittakoop P (2011) Hybrid flavan-chalcones, aromatase and lipoxygenase inhibitors, from *Desmos cochinchinensis*. Phytochemistry 72:2062
3. Rittiwong T, Mutarapat T, Ponglimanont C, Mahabusarakam W, Chakthong S (2011) Saiyutones A-D: four new unusual biflavones from *Desmos chinensis*. Tetrahedron 67:5444
4. Wu JH, McPhail AT, Bastow KF, Shiraki H, Ito J, Lee KH (2002) Desmosdumotin C, a novel cytotoxic principle from *Desmos dumosus*. Tetrahedron 43:1391
5. Tuntipaleepu M, Chakthong S, Ponglimanont C, Plodpai P, Voravuthikuncha SP (2012) Anti-fungal and cytotoxic substances from the stem barks of *Desmos chinensis*. Chin Chem Lett 23:587
6. Dej-adisai S, Meechai I, Puripattanavong J, Kummee S (2014) Antityrosinase and antimicrobial activities from Thai medicinal plants. Arch Pharmacal Res 37:473
7. Linh NTT, Ha NTT, Tra NTT, Anh LTT, Tuyen NV, Son NT (2021) Medicinal plant *Centipeda minima*: a resource of bioactive compounds. Mini Rev Med Chem 21:273
8. Son NT, Elshamy AI (2021) Flavonoids and other non-alkaloidal constituents of genus *Erythrina*: phytochemical review. Comb Chem High Throughput Screen 24:20
9. Son NT (2017) An overview of the genus *Prismatomeris*: phytochemistry and biological activity. Bull Fac Pharm Cairo Univ 55:11
10. Son NT (2017) A review on the medicinal plant *Dalbergia odorifera* species: phytochemistry and biological activity. Evid-Based Compl Alt Med 2017, ID 7142370
11. Son NT (2018) Notes on the genus *Paramignya*: phytochemistry and biological activity. Bull Fac Pharm Cairo Univ 56:1
12. Son NT (2019) Genus *Miliusa*: a review of phytochemistry and pharmacology. Evid-Based Compl Alt Med 2019, ID 8314693
13. Son NT (2019) Genus *Erythrophleum*: botanical description, traditional use, phytochemistry and pharmacology. Phytochem Rev 18:571
14. Son NT (2019) Secondary metabolites of genus *Pandanus*-an aspect of phytochemistry. Mini Rev Org Chem 16:689
15. Son NT (2020) A mini-review of the tropical plant *Cratoxylum fomosum* ssp. *pruniflorum*: phytochemical and pharmacological aspects. Lett Org Chem 17:327
16. Son NT, Linh NTT, Tra NT, Ha NTT, Anh LTT, Cham BT, Anh DTT, Tuyen NV (2021) Genus *Styrax*: a resource of bioactive compounds. Stud Nat Prod Chem 69:299
17. Suthiphasilp V, Maneerat W, Andersen RJ, Phukhatmuen P, Pyne SG, Laphookhieo S (2019) Dasymaschalolactams A-E, aristolactams from a twig extract of *Dasymaschalon dasymaschalum*. J Nat Prod 82:3176
18. Meesakul P, Richardson C, Pyne SG, Laphookhieo S (2019) α-Glucosidase inhibitory flavonoids and oxepinones from the leaf and twig extracts of *Desmos cochinchinensis*. J Nat Prod 82:741
19. Qais N, Rahman MM, Rashid MA, Koshino H, Nagasawa K, Nakata T (1996) Antibacterial flavonoids from *Desmos chinensis*. Fitoterapia 67:554
20. Suthiphasilp V, Maneerat T, Duangyod T, Charoensup R, Raymond JA, Stephen GP, Laphookhieo S (2020) Polyoxygenated *seco*-cyclohexenes derivatives from flower and leaf extracts of *Desmos cochinchinensis* and their α-glucosidase inhibitory activity. Heliyon 6:e05791
21. Suthiphasilp V, Maneerat T, Raymond JA, Brian OP, Stephen GP, Surat L (2021) α-Glucosidase inhibitory activity of compounds isolated from the twig and leaf extracts of *Desmos dumosus*. Heliyon 7:e06180
22. Nguyen NT, Pham VC, Litaudon M, Guéritte F, Bodo B, Nguyen VT, Nguyen VH (2009) Novel cyclopeptide and unique flavone from *Desmos rostrata*. Total synthesis of desmorostratone. Tetrahedron 65:7171

23. Wu JH, Mao SL, Liao SX, Yi YH, Lan CQ, Su ZW (2001) Desmosdumotin B: a new special flavone from *Desmos dumosus* Chin Chem Lett 12:49
24. Kuo PC, Tran DT, Huang GJ, Huang BS, Le TMH, Yang ML, Wu TS (2015) Flavonoids from the fruits of *Desmos cochinchinesis* var. *fulvescens* and their inhibitory effects on NO production. Chem Nat Compd 51:1
25. Ju J, Yu J (1999) Studies on chemical constituents of seeds of *Desmos chinensis* Lour. China J Chin Mater Med 24:418
26. Wu JH, Liao SX, Liang HQ, Mao SL (1994) Isolation and identification of flavones from *Desmos cochinchinensis* Lour. Acta Pharm Sin B 29:621
27. Wu JH, Wang XH, Yi YH, Lee KH (2003) Anti-AIDS agents 54. A potent anti-HIV chalcone and flavonoids from genus *Desmos.* Bioorg Med Chem Lett 13:1813
28. Shi M, Pan Q, Min Z (2003) Study on chemical constituents from leaves of *Desmos chinensis* Lour. Zhongguo Yaoke Daxue Xuebao 34:503
29. Liao SX, Han GY, Zhang YR, Zheng QT, He CH (1989) Chemical constituents of the root of *Desmos cochinchinensis* Lour. Acta Pharm Sin B 24:110
30. Rittiwong T (2010) Chemical constituents from the leaves of *Desmos chinensis* Lour. MS thesis, Prince of Songkla University, Hat Yai, Thailand
31. Clement JA, Ondeyka JG, Goetz MA (2017) Benzoate esters and flavonoids from *Desmos pedunculosus.* Phytochem Lett 22:117
32. Liu XT, Zhang Q, Liang JY, Min ZD (2004) A new oxoaporphine from *Desmos chinensis* Lour. Chin J Nat Med 2:205
33. Wu JH, Liao SX, Mao SL, Yi Y, Takeya K, Su Z, Lan C (1999) Studies on chemical constituents from *Desmos dumosus* Saff. Acta Pharm Sin B 34:682
34. Kiem PV, Minh CV, Huong HT, Lee JJ, Lee IS, Kim YH (2005) Phenolic constituents with inhibitory activity against NFAT transcription from *Desmos chinensis.* Arch Pharm Res 28:1345
35. Wu JH, Lan C, Mao SL, Liao SX, Su Z (2000) Chemical constituents from the root of *Desmos chinensis.* Chin Tradit Herbal Drugs 31:567
36. Jin Z (1992) Chemical constituents on the roots of *Desmos chinensis.* Yunnan Zhiwu Yanjiu 14:97
37. Liao SX, Mi HM, Yang GJ, Su ZW (1997) Isolation and identification of constituents from *Desmos dumosus.* Chin Trad Herbal Drugs 28:515
38. Wu JH, Mao SL, Liao SX, Shi WH, Su ZW, Lan CQ (2000) Studies on chemical constituents in the root of *Desmos grandifolius* (I). China J Chin Mater Med 25:419
39. Kakeya H, Imoto M, Tabata Y, Iwami J, Matsumoto H, Nakamura K, Koyano T, Tadano K, Umezawa K (1993) Isolation of a novel substrate-competitive tyrosine kinase inhibitor, desmal, from the plant *Desmos chinensis.* FEBS Lett 320:169
40. Prachyawarakorn V, Sangpetsiripan S, Surawatanawong P, Mahidol C, Ruchirawatacd S, Kittakoop P (2013) Flavans from *Desmos cochinchinensis* as potent aromatase inhibitors. Med Chem Commun 4:1590
41. Wu JH, Liao SX, Mao SL, Liang HQ, Wang YL, Su ZW (1997) Desmosflavanone II: a new flavanone from *Desmos cochinchinensis* Lour. J Chin Pharm Sci 6:119
42. Wu JH, Mao SL, Liao SX, Yi YH, Su ZW (2001) Desmosdumotin A, a new compound from *Desmos dumosus.* J Chin Pharm Sci 10:1
43. Connolly JD, Dagli S, Haque ME (2005) Constituents of the Annonaceae species *Miliusa velutina* and *Desmos longiflorus.* J Indian Chem Soc 80:1169
44. Rahman MM, Qais N, Rashid MA (2003) A new C-benzylated chalcone from *Desmos chinensis.* Fitoterapia 74:511
45. Nakagawa-Goto K, Lee KH (2006) Anti-AIDS agents 68. The first total synthesis of a unique potent anti-HIV chalcone from the genus *Desmos.* Tetrahedron Lett 47:8263
46. Abdullah Z, Awang K (2005) Chemical constituents of *Desmos dunalii* (Hk. f. et. Th.) Sanfford. Mal J Sci 24:267
47. Chan KC, Ton HT (1986) 7-Hydroxyaporphine alkaloid from *Desmos dasymachalus.* Phytochemistry 25:1999

48. Leboeuf M, Cavé A, Tohami ME, Pusset J, Forgacs P, Provost J (1982) Alkaloids of Annonaceae. XXXV. Alkaloids of *Desmos tiebaghiensis.* J Nat Prod 45:617
49. Awang K, Abdullah Z, Mukhtar MR, Litaudon M, Jaafar FM, Hadi HAA, Thomas NF (2009) Dunaliine A, a new amino diketone from *Desmos dunalii* (Annonaceae). Nat Prod Res 23:652
50. Sun NJ, Ho DK, Hu XE, Sneddon JM, Stephens RE, Cassady JM (1995) New cytotoxic fatty acid from *Desmos cochinchinensis* (Annonaceae). Nat Prod Lett 7:35
51. Sulaiman M, Martin MT, Pas M, Hadi AHA, Awang K (1998) Desmosine, an artefact alkaloid from *Desmos dumosus.* Phytochemistry 49:2191
52. Plodpai P, Chuenchitt S, Petcharat V, Chakthong S, Voravuthikunchai S (2013) Anti-*Rhizoctonia solani* activity by *Desmos chinensis* extracts and its mechanism of action. J Crop Prot 43:65
53. Zhi QQ, Yan QH, Wang Q, Sun PF, Zhou HY, He ZM (2020) Purification and characterization of two grandiuvarones from *Desmos chinensis* leaves and their antimicrobial activities. Nat Prod Res 34:1105
54. Wu TY, Cheng YB, Cheng FT, Hsu YM, Dinh TT, Chang FR, Wu YC (2014) Chemical constituents of the leaves of *Desmos cochinchinensis* var. *fulvescens* Ban. Helv Chim Acta 97:1714
55. Sun NJ, Ho DK, Sneddon JM, Stephens RE, Cassady JM (1992) New cytotoxic cycloartane triterpenoids from *Desmos cochinchinensis* (Annonaceae). Nat Prod Lett 1:109
56. Connolly JD, Haque MDE, Hasan CM, Hossain MS (1994) l5α-Hydroxy-24-methylenelanosta-7,9(1l)-dien-3-one from the stem bark of *Desmos longiflorus.* Phytochemistry 36:1337
57. Silva GND, Dutra LM, Lorenzo VP, Silva GD (2021) Phytochemicals and biological properties of *Annona coriacea* Mart. (Annonaceae): a systematic review from 1971 to 2020. Chem Biol Interact 336:109390
58. Plodpai P, Petcharat V, Chuenchit S, Chakthong S, Joycharat N, Voravuthikunchai S (2013) *Desmos chinensis*: a new candidate as natural antifungicide to control rice diseases. Ind Crops Prod 42:324
59. Son NT, Anh LT, Thuy DTT, Luyen ND, Tuyen TT (2021) Essential oils of *Polythia suberosa* leaf and twig and their cytotoxic and anti-microbial activities. Chem Biodivers 18:e21000284
60. Dai DN, Hoi TM, Thang TD, Ogunwande IA (2012) The leaf essential oils of five Vietnamese *Desmos* species (Annonaceae). Nat Prod Commun 7:231
61. Hisham A, Rameshkumar KB, Sherwani N, Al-Saidi S, Al-Kindy S (2012) The composition and antimicrobial activities of *Cyperus conglomeratus*, *Desmos chinensis* var. *lawii* and *Cyathocalyx zeylanicus* essential oils. Nat Prod Commun 7:663
62. Dai DN, Thanh BV, Thang TD, Ogunwande IA (2014) Identification of volatile constituents of the stem bark and fruits of *Desmos cochinchinensis* Lour. Am J Essent Oil 1:20
63. Brophy JJ, Goldsack RJ, Forster PI (2002) The leaf essential oils of the Australian species of *Desmos* (Annonaceae). J Essent Oil Res 14:298
64. Dai DN, Thang TD (2012) Chemical composition of the leaf essential oil of *Desmos chinensis* Lour. (Annonaceae) from Vietnam. J Essent Oil Bear Plants 15:1044
65. Dai DN, Hoi TM, Thang TD, Ogunwande IA (2014) Analysis of essential oil constituentsof three *Dasymaschalon* species (Annonaceae) from Vietnam. Nat Prod Res 28:156
66. Wang Z (2010) Baker-Venkataraman rearrangement. Comprehensive organic name reactions and reagents. Part 1. Wiley, Hoboken NJ, USA, p 168
67. Kummee S, Intaraksa N (2008) Antimicrobial activity of *Desmos chinensis* leaf and *Maclura cochinchinensis* wood extracts. Songklanakarin J Sci Technol 30:635
68. Kim JH, Campbell BC, Mahoney N, Chan KL, Molyneux RJ, Balajee A (2010) Augmenting the activity of antifungal agents against aspergilli using structural analogues of benzoic acid as chemosensitizing agents. Fungal Biol 114:817
69. Batovsk D, Todorova I (2010) Trends in utilization of the pharmacological potential of chalcones. Curr Clin Pharmacol 5:1
70. Grodin JM, Siiteri PK, Macdonald PC (1973) Source of estrogen production in postmenopausal women. J Clin Endocrinol Metab 36:207

71. Ghosh D, Lo J, Morton D, Valette D, Xi J, Griswold J, Davies HML (2012) Novel aromatase inhibitors by structure-guided design. J Med Chem 55:8464
72. Abbas AK, Lichtman AH, Pober JS (1997) Cellular and molecular immunology, 3rd ed. WB Saunders, Philadelphia, USA, p 315

Nguyen Thi Thuy Linh obtained her Master's degree in the field of organic chemistry at Irkutsk National Research Technical University, Russia. She was then appointed as a Ph.D. student at the Graduate University of Science and Technology, Hanoi, Vietnam in 2019. From 2018, she started working as a chemical researcher at the Institute of Chemistry, Vietnam Academy of Science and Technology. Her current work has emphasis on the isolation and structure elucidation of natural products from Vietnamese medicinal plants. Ph.D. student Linh is participating in several pharmaceutical projects, and has published six scientific articles over the last two years.

Ninh The Son obtained his Ph.D. degree from Tokushima Bunri University, Tokushima, Japan, with support from the Japanese Society for the Promotion of Science (JSPS) in 2019. He is currently working at the Institute of Chemistry, Vietnam Academy of Science and Technology (VAST), as a chemistry researcher. His main research involves natural products chemistry and molecular simulation. Dr. Son received an excellence award-2020 from VAST. He played a significant role in several projects and is an author of 72 scientific articles, among which he authored six SCI/SCIE review articles as a single author. He has also edited a book and served as a corresponding author of a book chapter. He is a member of the editorial boards of various scientific journals such as "Natural Product Research" and of the book series "Studies in Natural Products Chemistry".